Numerical modeling of high-pressure phase-equilibria data using neural networks

by

Annelette Coetzee

Dissertation submitted in the partial fulfilment

of the requirements for the qualification

of

MASTER OF ENGINEERING
(CHEMICAL ENGINEERING)

in the

Faculty of Engineering at Stellenbosch University

Supervisor

Prof. C.E. Schwarz

Co-supervisor

Prof. J.H. Knoetze

December 2020

DECLARATION

By submitting this dissertation electronically, I declare that the entirety of the work contained therein is my own, original work, that I am the sole author thereof (save to the extent explicitly otherwise stated), that reproduction and publication thereof by Stellenbosch University will not infringe any third party rights and that I have not previously in its entirety or in part submitted it for obtaining any qualification.

Date: *14 September 2020*

PLAGIARISM DECLARATION

1. Plagiarism is the use of ideas, material and other intellectual property of another's work and to present it as my own.
2. I agree that plagiarism is a punishable offence because it constitutes theft.
3. I also understand that direct translations are plagiarism.
4. Accordingly, all quotations and contributions from any source whatsoever (including the internet) have been cited fully. I understand that the reproduction of text without quotation marks (even when the source is cited) is plagiarism.
5. I declare that the work contained in this dissertation, except where otherwise stated, is my original work and that I have not previously (in its entirety or in part) submitted it for grading in this module/assignment or another module/assignment.

Student number:

……..

Initials and surname:

……..

Signature:

……..

Date:

……..

ACKNOWLEDGEMENTS

I would like to thank the following people for supporting me during the execution of my project:

- My supervisors, Prof Schwarz and Prof Knoetze for their valuable knowledge and guidance.
- Prof Auret, Dr Louw and Prof Aldrich for helping me by responding to questions and giving me invaluable insight.
- My family (my mom, dad, and sister) for their motivation, patience and advice throughout my project, and giving me the “dit wat jy nou insit is nie verniet nie” speech, every time.
- Lian, for supporting, accepting and sometimes debating about relevant and irrelevant topics.

ABSTRACT

The design of process systems is greatly dependent on phase behaviour data, which can be predicted using equations of state (EOSs). These models, however, often fail to predict the behaviour near the mixture critical region. A more accurate and reliable method for predicting thermodynamic behaviour in the vicinity of the mixture critical region is therefore required.

The aim of this project was to model the vapour-liquid equilibrium of binary systems containing supercritical CO_2 and hydrocarbons using Artificial Neural Networks (ANNs). The bubble and dew point pressures were predicted as a function of functional group, acentric factor, critical temperature and pressure of the hydrocarbon, system temperature and CO_2 composition of the liquid and vapour phases.

The ability of ANNs to predict the vapour-liquid phase equilibrium of binary systems was evaluated by modelling different systems and comparing the results to experimental data and EOS models. Case study 1 considered binary systems containing only CO_2 and alkanes. Case study 2 considered binary systems of CO_2 and various hydrocarbons, increasing the complexity by adding various functional groups. The hydrocarbons included alkanes, alcohols and carboxylic acids. The modelled results from case study 1 and 2 showed that the phase equilibrium of both simple and complex binary systems can be modelled using ANNs. After investigating the structure of the neural networks, the chain length and critical pressure of the hydrocarbon were eliminated as input parameters for case studies 1 and 2. The system temperature and liquid and vapour compositions of CO_2 were relatively more important compared to other input parameters for case study 1 where the critical and system temperatures and CO_2 composition of the vapour phase had a higher relative importance for case study 2. Using a feedforward neural network with two hidden layers and the log-sigmoid transfer function resulted in the optimum results for both these studies. Case study 1 and 2 resulted in acceptable R^2 and $AAD\%$ values for the training and testing data over the entire range. R^2 was 0.992 and 0.991 for case study 1 and 0.949 and 0.995 for case study 2 for the training and testing data sets. $AAD\%$ was 9.7% and 5.6% for case study 1 and 16.4% and 7.1% for case study 2 for the training and testing data sets. The ANN models were able to predict the phase behaviour over the entire range of compositions including the mixture critical region, whereas the EOS correlation models (the RK-Aspen EOS) failed to converge in the mixture critical region.

Case study 3 considered the optimisation of ANNs as used in published articles by using the methodology and outcomes as used and concluded in case studies 1 and 2. The main difference in the methodology was the way the validation and test sets were divided: these sets consisted of complete binary systems instead of single data points extracted from binary systems. Although worse results

were obtained using this methodology, the results were still acceptable. Using two hidden layers improved the accuracy of the results obtained by case study 3.

OPSOMMING

Prosesstelsels se ontwerp is grootliks afhanklik van fasegedragsdata, wat voorspel kan word deur toestandsvergelykings (EOSs) te gebruik. Hierdie modelle misluk egter dikwels om die gedrag na aan die kritiese mengbaarheidsgebiede te voorspel. ’n Meer akkurate en betroubare metode om die termodinamiese gedrag naby die kritiese mengbaarheidsgebied te voorspel, word dus benodig.

Hierdie studie se doel is om binêre stelsels se verdampingsvloeistof-ewewigsdata, wat superkritiese CO_2 en koolwaterstowwe bevat, te moduleer deur kunsmatige neurale netwerke (ANNs) te gebruik. Die borrel- en doupuntdrukke word voorspel as ’n funksie van ’n funksionele groep, aksentriese faktor en kritiese temperatuur en druk van die koolwaterstof, stelseltemperatuur en die vloeistof- en verdampingsfases se CO_2-komposisies.

ANNs se vermoë om binêre stelsels se verdampingsvloeistoffase-ewewigsdata te voorspel, is geëvalueer deur verskillende stelsels te moduleer en die resultate met eksperimentele data en EOS-modelle te vergelyk. Gevallestudie 1 oorweeg binêre stelsels wat slegs CO_2 en alkane bevat. Gevallestudie 2 oorweeg binêre stelsels van CO_2 en verskeie koolwaterstowwe waarvan die kompleksiteit verhoog word deur verskeie funksionele groepe by te voeg. Die koolwaterstowwe sluit alkane, alkohol en karboksielsuur in. Gevallestudie 1 en 2 se gemoduleerde resultate toon dat die eenvoudige en komplekse binêre stelsels se fase-ewewigsdata gemoduleer kan word deur ANNs te gebruik. Nadat die neurale netwerke se struktuur ondersoek is, is die kettinglengte en kritiese druk vir gevallestudie 1 en 2 as invoer-veranderlikes geklimatiseer. CO_2 se stelseltemperatuur en vloeistof- en verdampingskomposisies is relatief belangriker as ander invoer-veranderlikes vir gevallestudie 1. Daarenteen het die kritiese en stelseltemperatuur en die verdampingsfase se CO_2-komposisie ’n hoër relatiewe belangrikheid vir gevallestudie 2. Deur ’n voorwaartsvoerende neurale netwerk met twee versteekte lae en die houtsigmoïed-oordragsfunksie te gebruik, lei tot optimum-resultate vir albei studies. Gevallestudie 1 en 2 bied aanvaarbare R^2- en $AAD\%$-waardes vir die opleiding- en toetsdata oor die hele reeks. R^2 is 0,992 en 0,991 vir gevallestudie 1 en 0,949 en 0,995 vir gevallestudie 2 vir die opleiding- en toetsdatastelle. $AAD\%$ is 9,7% en 5,6% vir gevallestudie 1 en 16,4% en 7,1% vir gevallestudie 2 vir die opleiding- en toetsdatastelle. Die ANN-modelle kan die fasegedrag oor die komposisies se hele reeks voorspel, insluitend die kritiese mengbaarheidsgebied, terwyl die EOS-korrelasiemodelle (die RK-Aspen EOS) misluk om die kritiese mengbaarheidsgebied te konvergeer.

Gevallestudie 3 oorweeg die optimisasie van ANNs, soos dit in gepubliseerde artikels gebruik word, deur die metodiek en uitkomste te gebruik soos dit in gevallestudie 1 en 2 gebruik en afgesluit is. Die hoofverskil in die metodiek is die wyse waarop die validasie- en toetsstelle verdeel is: hierdie stelle bestaan uit volledige binêre stelsels in plaas van enkeldatapunte wat uit binêre stelsels onttrek is.

Alhoewel swakker resultate verkry is deur hierdie metodiek te gebruik, is die resultate steeds aanvaarbaar. Deur twee versteekte lae te gebruik, is die akkuraatheid van gevallestudie 3 se resultate verbeter.

TABLE OF CONTENTS

NOMENCLATURE

Symbol	Matrix size	Description
a	1×1	Energy parameter of the Redlich-Kwong EOS
$\propto_{\mathrm{m}}$	1×1	Additional constant to the RK-Aspen model
a_m and a_n	1×1	Pure component energy parameters of component a and b for the Redlich-Kwong EOS
$a_{node,j}$	1×1	Activation of a node in the neural network
α^k	1×1	Learning rate for iteration k
b	1×1	Co-volume parameter of the Redlich-Kwong EOS
b_i^k	1×1	Bias to each node i in each column k
b_m and b_n	1×1	Co-volume parameters of component a and b for the Redlich-Kwong EOS
$\boldsymbol{b_{hidden}}$	$S \times S$	Bias matrix for the hidden layer in the neural network
$\boldsymbol{b_{input}}$	$S \times I$	Bias matrix for the input layer in the neural network
$\boldsymbol{b_{output}}$	$Q \times S$	Bias matrix for the output layer in the neural network
C	1×1	Number of components present in a system
c_i and d_i	1×1	Modified parameters for the Mathias-Boston alpha function
E	1×1	Error function used for training a neural network
f	1×1	Transfer function in neural networks
F	1×1	Number of intensive variables that can be varied independently
f_m	1×1	Characteristic constant for the RK-Aspen model
g^k	1×1	Current gradient for iteration k
H	1×1	Number of phases present in a system
I	1×1	Number of inputs to the neural network
i	1×1	Node number for the starting point of a connection in a weight matrix of a neural network
j	1×1	Node number for the end point of a connection in a weight matrix of a neural network
k	1×1	Column number in a vector
$k_{a,mn}$ and $k_{b,mn}$	1×1	Temperature dependant interaction parameters for a and b of component m and n for the Redlich-Kwong EOS
$k^0_{a,mn}$ and $k^0_{b,mn}$	1×1	Binary interaction parameters for a and b in the temperature dependent interaction parameter equation for the Redlich-Kwong EOS

Symbol	Matrix size	Description
$k^1_{a,mn}$ and $k^1_{b,mn}$	1×1	Binary interaction parameters for a and b in the temperature dependent interaction parameter equation for the Redlich-Kwong EOS
L	1×1	Number of hidden layers in a neural network
N	1×1	Number of data points obtained to train, test and validate a neural network
η_m	1×1	Polar factor for pure component m for the RK-Aspen model
N_b	1×1	Number of data points in each binary system
N_{sample}	1×1	Number of samples used in the uncertainty equation
P	1×1	System pressure (MPa)
P_c	1×1	Critical pressure (MPa)
P_{c_m}	1×1	Critical pressure of component m
$\boldsymbol{p_{train}}$	$I \times ND_{train}$	Input vector of the training data used in a neural network
$\boldsymbol{p_{test}}$	$I \times ND_{test}$	Input vector of the testing data used in a neural network
$\boldsymbol{p_{validate}}$	$I \times ND_{validate}$	Input vector of the validation data used in a neural network
Q	1×1	Number of outputs in a neural network
R	1×1	Universal gas constant
R^2	1×1	Coefficient of determination
$\boldsymbol{RI_i}$	$I \times 1$	Relative importance of input i (%)
S	1×1	Number of nodes in each hidden layer in a neural network
s_y	1×1	Standard deviation of a specific variable
T	1×1	System temperature (K)
$\boldsymbol{t}$	$Q \times N$	Target vector in a neural network
T_c	1×1	Critical temperature (K)
T_{c_m}	1×1	Critical temperature of component m
t_N	1×1	Student's t statistic for N_{sample} number of samples
$T_{r,m}$	1×1	Reduced temperature of component m
$\boldsymbol{t_{train}}$	$Q \times ND_{train}$	Target vector of the training data used in a neural network
$\boldsymbol{t_{test}}$	$Q \times ND_{test}$	Target vector of the testing data used in a neural network
$\boldsymbol{t_{validate}}$	$Q \times ND_{validate}$	Target vector of the validation data used in a neural network
U	1×1	Uncertainty for a small sample size
V_m	1×1	Specific volume of compound m
$\boldsymbol{w_{hidden}}$	$S \times S$	Weight matrix for the hidden layer in the neural network
$\boldsymbol{w_{input}}$	$S \times I$	Weight matrix for the input layer in the neural network

Symbol	Matrix size	Description
$\boldsymbol{w_{output}}$	$Q \times S$	Weight matrix for the output layer in the neural network
$w_{i,j}^{k}$	1×1	Weight connected to node i from node j of column k in a neural network
$\boldsymbol{X}$	$I \times 1$	Product of between the input, hidden layers and output layer weights in a neural network
x, y		Composition range of CO_2 (mole fraction)
x_i	1×1	Input node of node i in a neural network
x_m and x_n	1×1	Mass fractions of components m and n
y_b	1×1	Bubble point pressure predicted by the neural network
y_d	1×1	Dew point pressure predicted by the neural network
y_L	1×1	Linear output from a node in a neural network
$\boldsymbol{y}$	$Q \times N$	Output vector of a neural network
$\boldsymbol{y_{train}}$	$Q \times ND_{train}$	Output vector of the training data used in a neural network
$\boldsymbol{y_{test}}$	$Q \times ND_{test}$	Output vector of the testing data used in a neural network
$\boldsymbol{y_{validate}}$	$Q \times ND_{validate}$	Output vector of the validation data used in a neural network
$\boldsymbol{z_i}$	1×1	Output node of node j used in a neural network

ACRONYMS

Acronym	Description
$AAD\%$	Average absolute deviation percentage
$AARD\%$	Average absolute relative deviation percentage
ANN	Artificial neural network
ANN_{P_c}	Artificial neural network without the critical pressure of the hydrocarbon as input
$ANN_{P_c\&CL}$	Artificial neural network without the critical pressure and chain length of the hydrocarbon as input
ANN_w	Artificial neural network without the acentric factor of the hydrocarbon as input
AI	Artificial intelligence
BIP	Binary interaction parameter
CL	Chain length
CNN	Convolutional neural network
CO_2	Carbon dioxide
EOS	Equation of state
Exp	Experimental data
HFC-134a	1,1,1,2-tetrafluoro-ethane
LCEP	Lower critical end point
LL	Liquid-liquid
MAE	Mean absolute error
MLP	Multilayer perception
MM	Molecular mass
MSE	Mean squared error
NIST	National Institute of Standards and Technology
PR	Peng-Robinson
R227ea	1,1,1,2,3,3,3,-heptafluoropropane
R30	Dichloro-methane
R32	Difluoromethane
R610	Decafluoro-butane
RI	Relative importance
RK	Redlich-Kwong
RK-Aspen	Redlich-Kwong-Soave with Mathias mixing rules
RNN	Recurrent neural network

Acronym	Description
SMILES	Simplified molecular-input line entry system
SRK	Soav-Redlich-Kwong
SSE	Sum squared error
UCEP	Upper critical end point
VLE	Vapour-liquid equilibrium

1. Introduction

1.1. Background

Thermodynamic data such as vapour-liquid equilibria (VLEs) play an important role in the synthesis, separation, design, optimisation and control of processing systems. Most industrial designs are based on equations of state (EOSs), but these equations become limited when processes are performed at high pressures, and are often insufficient for modelling the critical region (Ferreira, 2018; Fourie et al., 2018; Zamudio et al., 2013). In the proximity of the critical point, the liquid and vapour densities are very similar, which complicates the modelling thereof (Fourie et al., 2018). Since the algorithms fail in modelling in the mixture critical region, it is important to find an accurate method to predict thermodynamic data in the mixture critical region.

Instead of developing a model from first principles and making assumptions regarding the nature of the parameters, artificial neural networks (ANNs) use examples and learn by observing data (Nielsen, 2019), as illustrated in Figure 1-1. Each example from literature contains input and target values. The inputs from each example are fed into the ANN to predict the output(s), where the outputs of the ANN are compared to the target values (Bishop, 2006). The error between the outputs from the ANN and the target values are minimised by training the ANN and adjusting the weights to each node in the ANN. Each neural network has three types of layer: an input layer, a hidden layer(s) and an output layer.

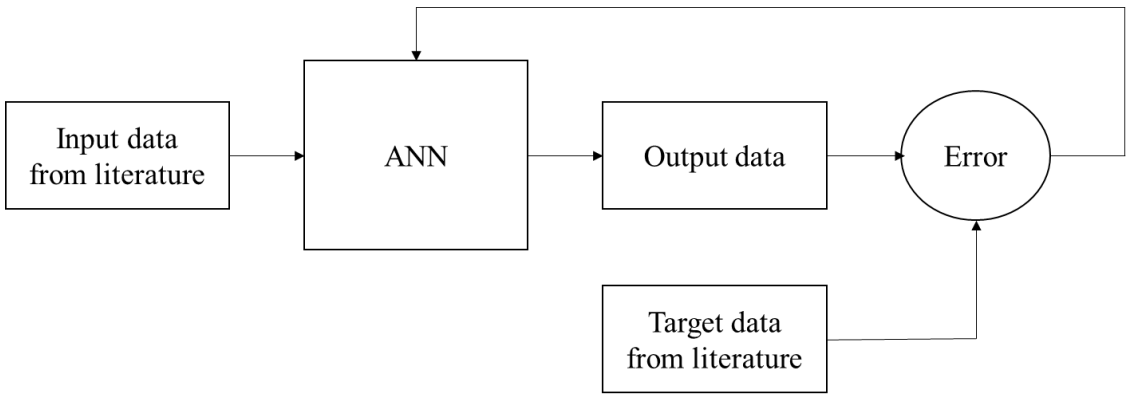

Figure 1-1: Simplified schematic diagram of an ANN

As evident in Figure 1-2, ANNs consist of nodes in the input layer, hidden layer(s) and an output layer with connection weights connecting the nodes between each layer, which is referred to as the structure of the neural network (Aggarwal, 2018). Each node in the input layer represents an input variable and each node in the output layer represents an output variable (Bishop, 2006).

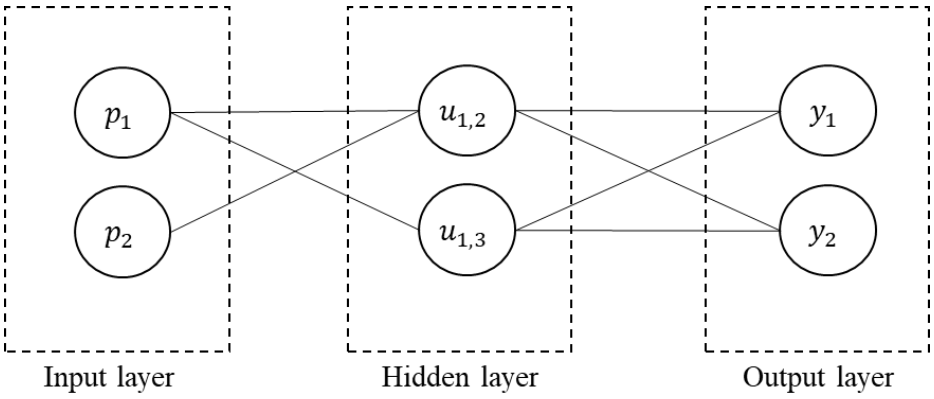

Figure 1-2: Simplified schematic of the structure of an ANN

To train a neural network, the hyperparameters need to be specified. The hyperparameters in a neural network are parameters for which the values are chosen before the training procedure starts (Demuth & Beale, 2004). For this study, the hyperparameters include the type of neural network (dependent on connections between each node), the number of hidden layers, the number of nodes in each hidden layer and the transfer function. A transfer function is used to map a node's input to its output, as discussed in more detail in Section 2.2.2.

The advantages of thermodynamic predictions using ANNs include increased accuracy relative to EOSs, lower costs than for experimental work, and time efficiency (Bishop, 2006).

1.2. Aim and objectives

The aim of this project is to model the phase behaviour of binary systems containing supercritical carbon dioxide (CO_2) and hydrocarbons by predicting the bubble and dew point pressures as a function of molecular characteristics, system temperature and CO_2 content in the different phases by using ANNs.

This aim will be addressed by the following objectives:

1) to investigate the structure of a neural network used to model high-pressure phase equilibria for three data sets: (1) CO_2 and alkanes referred to as case study 1; (2) CO_2 and various hydrocarbons containing alkanes, alcohols and carboxylic acid, respectively, referred to as case study 2; as well as (3) data obtained from published articles using neural networks to model high-pressure phase equilibria;
2) to determine the optimal hyperparameters of the neural networks to model high-pressure phase equilibria for case studies 1 to 3; and
3) to compare the results obtained for case studies 1 and 2 with traditional modelling methods.

1.3. Approach

After obtaining binary phase equilibrium data of CO_2 and hydrocarbons, the objectives as stated in Section 1.2 will be addressed as follows:

1) investigate the structure of the neural network by considering the following parameters: (1) input parameters to be used in the neural network and (2) the relative importance (RI) of the input variables;
2) determine the optimal hyperparameters of the neural network by considering different neural network types. Determine whether one or two hidden layers are required, find the optimal number of nodes in each hidden layer by maximizing the coefficient of determination (R^2) and minimizing the geometric distance and average absolute deviation ($AAD\%$, as discussed in Section 2.3) and evaluate the form of the P-xy graphs obtained from the results; and
3) compare the ANN P-xy predictions with correlations using the RK-Aspen model (see section 2.1.4 for a detailed discussion) to evaluate whether ANNs can be used as an alternative to traditional modelling methods.

Figure 1-3 illustrates the structure of this study. A literature review was performed to evaluate the possibility of modelling high-pressure phase equilibrium using neural networks. Data considered were binary systems containing CO_2 and alkanes, CO_2 and alcohols, and CO_2 and carboxylic acids with temperature ranges between 200 and 400 K where the chain lengths (CLs) of the alkanes, alcohols and carboxylic acids ranged between 5 and 20, 4 and 18, and 3 and 18, respectively. In the methodology chapter it is explained how each objective was achieved. Through the application of the discussed methods, isothermal VLE was modelled using ANNs for case studies 1 and 2: (1) CO_2 and alkanes; and (2) CO_2 and various hydrocarbons containing alkanes, alcohols and carboxylic acids respectively. Thereafter a third case study was used to evaluate two methods to divide the training, testing and validation data. Furthermore, for case study 3, the use of two hidden layers (as concluded from case studies 1 and 2) was compared to using only one hidden layer (according to published articles).

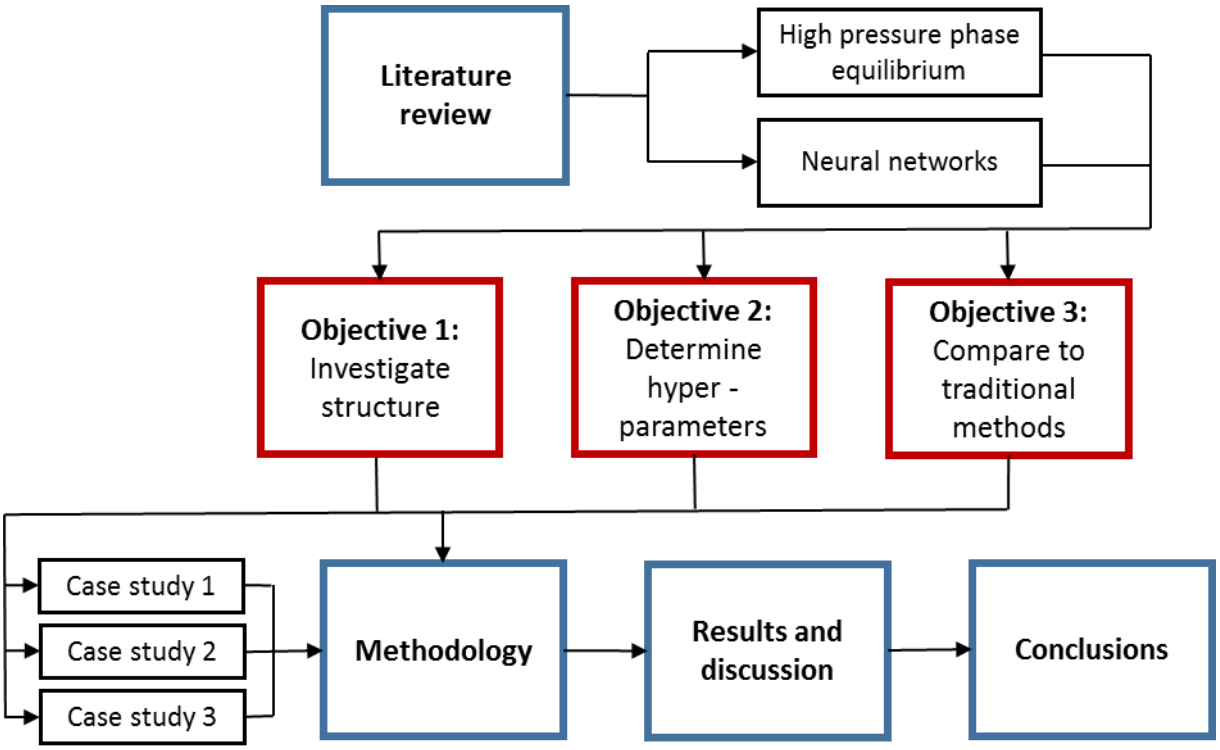

Figure 1-3: Structure of the study

2. Literature Review

In this section, high-pressure phase equilibrium will be investigated by reviewing traditional modelling and measuring methods, available high-pressure VLE data and types of phase behaviour. Neural networks will be proposed and discussed as an alternative modelling method to model thermodynamic data.

2.1. High-pressure phase equilibrium

A good understanding of high-pressure phase equilibrium behaviour and the ability to predict it is important for the design and optimisation of supercritical separation processes. Supercritical fluid extraction is an eco-friendly process relative to many other separation technologies and can be used for the purification of hydrocarbons and in biochemical processes (Hosseini & Pazuki, 2014). Hydrocarbon and alcohol mixtures are highly relevant in processes that produce natural gas and biodiesel (Peters et al., 1995) and carboxylic acids are used as raw materials in pharmaceutical, food and detergent processes (Bharath et al., 1993). CO_2 is often used as a near-critical solvent because it has high reaction and mass transfer rates, and it is inexpensive, non-toxic, non-flammable and non-polar (Heo, et al., 2001). It is also hydrophobic, where light non-polar molecules dissolve relatively easily in supercritical CO_2, and polar heavy molecules have low solubility in this solvent (Gupta & Shim, 2007). Supercritical hydrocarbon and CO_2 mixtures are specifically relevant in organic Rankine cycles to produce power (Feng et al, 2017). In sugar fermentation, sugars are converted to alcohols where supercritical alcohol and CO_2 phase behaviour is important for the distillation of crude alcohol mixtures (Inomata et al, 2005). Supercritical carboxylic acid and CO_2 phase behaviour is important when designing processes contain enzymic reactions (Heo, et al., 2001).

In order to predict phase equilibrium, specific inputs are needed to determine the outputs and to fully define a phase boundary. The Gibbs phase rule and the Duhem theorem can be used to determine the number of input variables required to determine the output variables, as discussed below. The Gibbs phase rule determines the number of intensive variables that can be varied independently, assuming that the system is non-reacting and that all phases are in equilibrium (Sandler, 2006). The number of intensive variables (F) can be determined by the following equation (Sandler, 2006):

$$F = 2 + C - H \qquad [2\text{-}1]$$

where C is the number of components present and H is the number of phases present. The Duhem theorem states that for a closed system (given the mass and composition of the chemical species), the equilibrium state is determined completely when any two independent variables are fixed (Smith, 2005). As stated above, the Gibbs phase rule and the Duhem theorem can only be used to determine

the number of input variables required to determine the output variables in order to fully define a phase boundary. To obtain phase equilibrium data, different measuring methods are available, as discussed in Section 2.1.1.

2.1.1. Experimental methods to determine binary phase behaviour

In order to determine phase equilibria, the temperature, pressure and composition of the coexisting phases of the phase boundary should be known. Various experimental methods and techniques can be used to determine the phase equilibria at high pressures (Dohrn et al., 2010).

There are two main types of experimental methods that are defined by the way in which the compositions in the different equilibrium phases are measured: analytically or synthetically (Dohrn et al., 2010). The synthetic method uses a prepared mixture with a known overall composition of the components to determine the temperature and pressure, whereas the analytical method requires measurements of the composition of the coexisting phases to determine the phase boundary (Dohrn et al., 2010).

Each method can be further categorised as illustrated in Figure 2-1, redrawn from Dohrn et al. (2010).

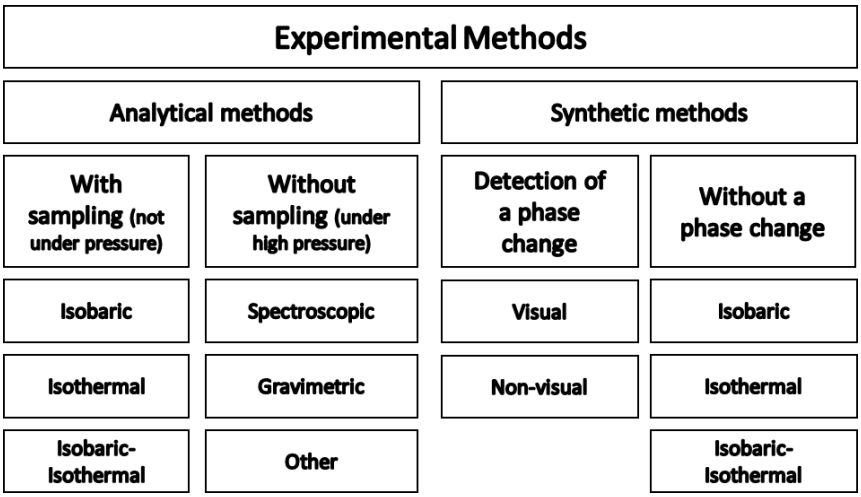

Figure 2-1: Experimental methods redrawn from Dohrn et al. (2010)

For the analytical method (as seen from Figure 2-1), the composition of the equilibrium phases can be analysed either with or without sampling (Dohrn et al., 2010). Equilibrium phases can either be measured outside the equilibrium cell at ambient pressures which requires sampling of the equilibrium phases, or inside the equilibrium cell under high pressure where no sampling is required (Dohrn et al., 2010). When sampling of the equilibrium phases is required, it can be measured statically (with isothermal or isobaric measurement) or dynamically, where fluid streams are continuously pumped into an equilibrium cell at a constant pressure (Dohrn et al., 2010). If the

equilibrium phases cannot be measured due to reacting systems, spectroscopic or gravimetric methods can be used.

As seen in Figure 2-1 and discussed by Dohrn et al. (2010), for the synthetic method detection can be performed with or without a phase change. For detection with a phase change, the temperature and pressure are adjusted until a single phase exists. Then, either the temperature or the pressure is adjusted until a second phase is observed. Visual or non-visual methods can further be used to determine exactly when the second phase appears. For synthetic methods without a phase change, equilibrium properties (temperature, pressure, volume and density) are measured and the compositions of the equilibrium phases are calculated using material balances. This method can further be divided into isothermal, isobaric or other methods (Dohrn et al., 2010).

According to Raeissi et al. (2010) the most influential factor for inconsistensies in data measured at the same conditions, is different measuring methods. It is therefore important to note the measurement methods that were used when comparing data from literature.

2.1.2. Evaluation of available data for CO_2 and hydrocarbons

For any modelling method, experimental data are required. In this study, phase equilibrium of CO_2 and hydrocarbons will be investigated. Available data from literature are listed in Table 2-1 (for CO_2 and alkanes), Table 2-2 (for CO_2 and alcohols) and Table 2-3 (for CO_2 and carboxylic acids). Each table lists the CL of the hydrocarbon at a specific temperature (T), pressure range (P), composition range in mole fractions (x, y) and the number of data points in each binary system (N_b).It should be noted that an additional dimension would be added if T-xy data were used. Neural networks are trained by following a trend. If enough data points were added to complete the additional dimension, T-xy data could be considered.

Table 2-1: Binary system for CO_2 and alkanes

Alkane chain length	T (K)	P (MPa)	x, y (mole fraction)	N_b	Reference
5	311	0.41 - 7.14	0.037 - 0.97	28	Cheng et al. (1989)
5	344	0.469 - 9.1	0.0144 - 0.886	28	Cheng et al. (1989)
5	378	0.786 - 9.62	0.0103 - 0.786	26	Cheng et al. (1989)
5	394	0.986 - 9.14	0.0062 - 0.719	23	Cheng et al. (1989)
6	313	0.779 - 7.48	0.080 - 0.981	20	Li et al. (1981)
6	353	0.862 - 10.7	0.052 - 0.886	28	Li et al. (1981)
6	393	0.896 - 11.6	0.028 - 0.793	30	Li et al. (1981)
7	311	0.186 - 7.56	0.022 - 0.950	46	Kalra et al. (1978)
7	353	0.424 - 11.6	0.031 - 0.905	34	Kalra et al. (1978)
7	394	1.13 - 13.3	0.073 - 0.882	34	Kalra et al. (1978)
8	313	1.50 - 7.55	0.143 - 0.992	12	Weng & Lee (1992)
8	328	2.0 - 9.50	0.174 - 0.974	12	Weng & Lee (1992)
8	348	2.0 - 11.4	0.145 - 0.958	16	Weng & Lee (1992)
8	313	1.15 - 7.85	0.110 - 0.945	18	Yu et al. (2006)
8	333	1.70 - 10.5	0.157 - 0.936	20	Yu et al. (2006)
8	353	1.70 - 12.3	0.145 - 0.915	20	Yu et al. (2006)
8	373	1.85 - 13.9	0.217 - 0.902	16	Yu et al. (2006)
8	393	1.11 - 14.4	0.156 - 0.873	20	Yu et al. (2006)
8	322	2.01 - 8.53	0.178 - 0.986	14	Jime´nez - Gallegos et al. (2006)
8	348	2.08 - 11.5	0.142 - 0.958	18	Jime´nez - Gallegos et al. (2006)
8	373	3.15 - 13.8	0.185 - 0.908	24	Jime´nez - Gallegos et al. (2006)
9	343	3.73 - 11.8	0.296 - 0.967	12	Jennings & Schucker (1996)
9	315	2.03 - 8.03	0.221 - 0.996	16	Camacho - Camacho et al. (2007)
9	345	2.11 - 12.0	0.178 - 0.964	16	Camacho - Camacho et al. (2007)
9	373	2.06 - 15.0	0.147 - 0.919	22	Camacho - Camacho et al. (2007)
10	313	1.43 - 7.84	0.147 - 0.997	10	Adams et al. (1988)
10	344	6.38 - 12.7	0.457 - 0.935	40	Nagarajan & Robinson (1986)
10	378	10.3 - 16.5	0.565 - 0.922	46	Nagarajan & Robinson (1986)
10	344	4.33 - 11.9	0.338 - 0.984	12	Jennings & Schucker (1996)
10	311	4.55 - 6.86	0.446 - 0.999	10	Iwai et al. (1994)
10	344	5.51 - 11.9	0.383 - 0.988	10	Iwai et al. (1994)
10	278	0.345 - 3.91	0.0545 - 1.00	24	Reamer & Sage (1963)
10	311	0.689 - 7.46	0.073 - 0.995	24	Reamer & Sage (1963)
10	344	1.38 - 12.8	0.112 - 0.948	18	Reamer & Sage (1963)
10	378	1.38 - 16.5	0.0931 - 0.905	22	Reamer & Sage (1963)
10	319	3.49 - 8.9	0.340 - 0.987	16	Jime´nez - Gallegos et al. (2006)
10	345	4.59 - 12.7	0.342 - 0.968	16	Jime´nez - Gallegos et al. (2006)
10	373	3.24 - 16.1	0.215 - 0.927	26	Jime´nez - Gallegos et al. (2006)
11	315	2.37 - 8.29	0.243 - 0.993	18	Camacho - Camacho et al. (2007)

Table 2-1 continued

Alkane chain length	T (K)	P range (MPa)	x, y (mole fraction)	N_b	Reference
11	344	2.56 - 13.4	0.185 - 0.952	18	Camacho - Camacho et al. (2007)
11	373	3.47 - 17.1	0.225 - 0.932	20	Camacho - Camacho et al. (2007)
12	318	0.95 - 8.94	0.114 - 0.985	20	Gardeler et al. (2002)
15	292	4.57 - 19.5	0.620 - 0.935	21	Scheidgen (1997)
15	298	4.74 - 13.4	0.623 - 0.929	15	Scheidgen (1997)
15	316	7.29 - 13.2	0.642 - 0.928	19	Scheidgen (1997)
16	323	10.0 - 16.4	0.703 - 0.954	10	Pohler (1994)
16	353	10.0 - 20.0	0.604 - 0.936	14	Kordikowski & Schneider (1993)
16	393	10.1 - 25.6	0.497 - 0.920	30	Spee & Schneider (1991)
16	314	13.6 - 8.07	0.871 - 0.997	12	D'Souza. et al. (1988)
16	333	14.9 - 7.69	0.823 - 0.998	12	D'Souza. et al. (1988)
16	353	16.1 - 11.2	0.809 - 0.998	10	D'Souza. et al. (1988)
16	353	10.0 - 20.0	0.678 - 0.936	14	Kordikowski & Schneider (1993)
17	323	10.0 - 22.2	0.612 - 0.931	12	Pohler (1994)
17	333	10.0 - 21.3	0.639 - 0.930	12	Pohler (1994)
17	353	10.0 - 23.1	0.592 - 0.931	12	Pohler (1994)
17	373	10.0 - 25.3	0.56 - 0.929	14	Pohler (1994)
17	393	10.0 - 27.3	0.545 - 0.923	16	Pohler (1994)
18	323	10.0 - 25.0	0.759 - 0.999	12	Pohler (1994)
18	333	10.0 - 24.0	0.649 - 0.941	12	Pohler (1994)
18	353	10.0 - 25.0	0.635 - 0.94	12	Pohler (1994)
18	373	10.0 - 26.6	0.574 - 0.936	14	Pohler (1994)
18	393	10.0 - 28.7	0.540 - 0.929	16	Pohler (1994)
19	318	10.0 - 45.5	0.639 - 0.922	10	Pohler (1994)
19	323	10.0 - 33.5	0.683 - 0.918	10	Pohler (1994)
19	333	10.0 - 28.6	0.626 - 0.931	10	Pohler (1994)
19	343	10.0 - 27.7	0.573 - 0.934	18	Pohler (1994)
19	348	10.0 - 27.5	0.571 - 0.937	14	Pohler (1994)
19	353	10.0 - 27.5	0.536 - 0.919	10	Kordikowski & Schneider (1993)
19	393	10.0 - 30.3	0.468 - 0.931	14	Kordikowski & Schneider (1993)
19	353	10.0 - 27.5	0.536 - 0.919	10	Kordikowski (1992)
19	393	10.0 - 30.3	0.468 - 0.931	14	Kordikowski (1992)
20	323	0.992 - 5.01	0.114 - 0.446	10	Huang et al. (1988)
20	373	1.02 - 5.06	0.0842 - 0.342	10	Huang et al. (1988)
20	353	10.0 - 30.2	0.517 - 0.916	14	Kordikowski & Schneider (1993)
20	393	10.0 - 32.0	0.464 - 0.934	16	Kordikowski & Schneider (1993)
20	353	10.0 - 30.2	0.517 - 0.916	14	Kordikowski (1992)
20	393	10.0 - 32.0	0.464 - 0.934	16	Kordikowski (1992)

Table 2-2: Binary system for CO_2 and alcohols

Alcohol chain length	T (K)	P range (MPa)	x, y (mole fraction)	N_b	Reference
3	345	11.5 - 12.3	0.600 - 0.889	10	Elizalde - Solis et al. (2007)
3	373	12.1 - 15.0	0.493 - 0.821	14	Elizalde - Solis et al. (2007)
3	397	12.3 - 15.8	0.417 - 0.781	10	Elizalde - Solis et al. (2007)
4	313	4.38 - 8.31	0.290 - 0.991	19	Byun & Kwak (2002)
4	333	5.59 - 10.6	0.290 - 0.980	17	Byun & Kwak (2002)
4	353	6.38 - 11.7	0.290 - 0.980	17	Byun & Kwak (2002)
4	373	6.93 - 10.9	0.290 - 0.980	17	Byun & Kwak (2002)
4	393	7.62 - 15.1	0.290 - 0.937	15	Byun & Kwak (2002)
4	354	2.07 - 13.0	0.096 - 0.951	18	Elizalde - Solis et al. (2007)
4	399	2.13 - 15.5	0.080 - 0.909	20	Elizalde - Solis et al. (2007)
6	303	0.77 - 7.96	0.051 - 0.82	22	Beier et al. (2003)
6	313	0.53 - 9.82	0.028 - 0.872	20	Beier et al. (2003)
6	325	8.02 - 9.19	0.548 - 0.992	10	Elizalde - Solis et al. (2003)
6	354	11.5 - 16.0	0.604 - 0.929	12	Elizalde - Solis et al. (2003)
6	398	7.06 - 19.6	0.305 - 0.887	25	Elizalde - Solis et al. (2003)
7	316	7.09 - 12.5	0.364 - 0.909	17	Scheidgen (1997)
7	393	10.1 - 20.2	0.421 - 0.937	11	Scheidgen (1997)
7	375	4.04 - 14.6	0.217 - 0.990	16	Elizalde - Solis et al. (2003)
7	303	0.58 - 6.51	0.0464 - 0.995	16	Secuianu et al. (2008)
7	313	1.68 - 11.6	0.136 - 0.903	28	Secuianu et al. (2008)
7	333	1.14 - 14.0	0.0723 - 0.952	24	Secuianu et al. (2008)
7	353	1.54 - 10.2	0.0871 - 0.997	20	Secuianu et al. (2008)
8	328	3.0 - 13.3	0.182 - 0.976	12	Hwu et al. (2004)
8	348	1.0 - 5.0	0.0478 - 0.999	10	Lee & Chen (1994)
8	313	4.0 - 15.5	0.270 - 0.920	14	Lee & Chen (1994)
8	328	4.0 - 17.0	0.241 - 0.919	14	Lee & Chen (1994)
8	348	4.0 - 19.0	0.205 - 0.933	14	Lee & Chen (1994)
8	313	3.25 - 9.56	0.216 - 0.984	17	Chiu et al. (2008)
8	328	3.92 - 12.2	0.229 - 0.984	16	Chiu et al. (2008)
8	348	4.86 - 14.8	0.229 - 0.984	16	Chiu et al. (2008)
8	328	3.0 - 13.4	0.169 - 0.973	12	Feng et al. (2001)
8	308	1.51 - 7.74	0.108 - 0.993	24	Chieming et al. (1998)
8	318	2.17 - 9.78	0.134 - 0.993	18	Chieming et al. (1998)
8	328	2.89 - 15.1	0.176 - 0.942	32	Chieming et al. (1998)
8	313	0.5 - 15.2	0.046 - 0.924	26	Chrisochoou et al. (1997)
8	313	2.93 - 12.4	0.220 - 0.965	11	Byun & Kwak (2002)
8	333	3.62 - 14.9	0.220 - 0.965	11	Byun & Kwak (2002)
8	353	4.17 - 17.5	0.220 - 0.965	11	Byun & Kwak (2002)
8	373	4.41 - 19.1	0.220 - 0.965	11	Byun & Kwak (2002)

Table 2-2 continued

Alcohol chain length	T (K)	P range (MPa)	x, y (mole fraction)	N_b	Reference
8	393	4.66 - 20.0	0.220 - 0.965	11	Byun & Kwak (2002)
9	308	2.23 - 7.91	0.162 - 0.991	18	Chieming et al. (1998)
9	318	2.52 - 10.4	0.165 - 0.985	20	Chieming et al. (1998)
9	328	2.86 - 15.6	0.179 - 0.974	30	Chieming et al. (1998)
9	303	11.3 - 34.0	0.652 - 0.896	14	Pfohl et al. (1999)
9	308	1.76 - 7.02	0.142 - 0.998	14	Secuicano et al. (2010)
9	313	1.15 - 7.44	0.0896 - 0.998	12	Secuicano et al. (2010)
9	333	1.15 - 8.94	0.00752 - 0.997	20	Secuicano et al. (2010)
9	353	1.15 - 10.3	0.0675 - 0.997	20	Secuicano et al. (2010)
10	313	12.1 - 32.3	0.600 - 0.887	14	Pohler (1994)
10	323	12.4 - 24.4	0.536 - 0.895	14	Pohler (1994)
10	333	10.0 - 21.6	0.603 - 0.902	12	Pohler (1994)
10	353	10.0 - 21.9	0.562 - 0.897	12	Pohler (1994)
10	373	10.3 - 23.5	0.469 - 0.899	12	Pohler (1994)
10	393	10.0 - 24.8	0.446 - 0.898	14	Pohler (1994)
10	303	1.85 - 15.1	0.201 - 0.630	13	Ioniţă et al. (2013)
10	308	1.68 - 5.56	0.115 - 0.405	11	Ioniţă et al. (2013)
10	323	2.36 - 12.1	0.164 - 0.66	11	Ioniţă et al. (2013)
10	333	2.3 - 13.3	0.142 - 0.65	14	Ioniţă et al. (2013)
10	343	1.92 - 12.6	0.125 - 0.607	11	Ioniţă et al. (2013)
10	348	1.0 - 5.0	0.0502 - 1.00	10	Lee & Chen (1994)
10	308	2.23 - 7.75	0.162 - 0.997	18	Chieming et al. (1998)
10	318	2.18 - 10.5	0.152 - 0.992	18	Chieming et al. (1998)
10	328	2.89 - 15.2	0.181 - 0.978	26	Chieming et al. (1998)
10	348	7.0 - 19.0	0.367 - 0.970	16	Weng et al. (1994)
12	313	1.09 - 6.82	0.0922 - 0.997	16	Secuianu et al. (2016)
12	333	1.0 - 8.29	0.098 - 0.998	18	Secuianu et al. (2016)
12	353	1.04 - 9.36	0.0712 - 0.999	18	Secuianu et al. (2016)
12	353	10.0 - 25.2	0.463 - 0.904	12	Kordikowski & Schneider (1993)
12	393	10.0 - 27.5	0.422 - 0.886	18	Spee & Schneider (1991)
12	375	22.2 - 26.1	0.790 - 0.940	10	Scheidgen (1997)
12	333	10.0 - 28.7	0.567 - 0.934	20	Holsher (1988)
12	393	10.3 - 27.3	0.437 - 0.92	20	Holsher (1988)
12	393	10.0 - 27.5	0.422 - 0.886	18	Spee (1990)
14	373	1.01 - 5.07	0.995 - 0.270	10	Jan et al. (1994)
16	373	1.01 - 5.07	0.0635 - 0.998	10	Jan et al. (1994)
16	393	10.4 - 32.3	0.452 - 0.939	20	Holsher (1988)
18	373	1.01 - 5.07	0.0721 - 1.00	10	Jan et al. (1994)

Table 2-3: Binary system for CO_2 and carboxylic acid

Acid chain length	T (K)	P range (MPa)	x, y (mole fraction)	N_b	Reference
4	313	3.03 - 8.74	0.25 - 0.999	16	Byun et al. (2000)
4	333	3.72 - 11.0	0.25 - 0.991	14	Byun et al. (2000)
4	353	4.51 - 12.2	0.25 - 0.983	13	Byun et al. (2000)
4	373	5.37 - 11.3	0.25 - 0.983	13	Byun et al. (2000)
4	393	6.31 - 9.61	0.25 - 0.979	12	Byun et al. (2000)
5	313	2.58 - 8.48	0.212 - 0.997	19	Byun et al. (2000)
5	333	3.27 - 12.0	0.212 - 0.982	16	Byun et al. (2000)
5	353	3.96 - 14.5	0.212 - 0.982	16	Byun et al. (2000)
5	373	4.79 - 17.1	0.212 - 0.948	14	Byun et al. (2000)
5	393	5.34 - 19.2	0.212 - 0.932	12	Byun et al. (2000)
6	313	2.76 - 8.46	0.319 - 0.999	10	Bharath et al. (1993)
6	353	2.72 - 15.9	0.171 - 0.964	11	Bharath et al. (1993)
6	308	2.53 - 7.0	0.249 - 0.997	21	Byun et al. (2000)
6	328	3.27 - 10.1	0.249 - 0.997	20	Byun et al. (2000)
6	348	4.05 - 12.3	0.249 - 0.994	18	Byun et al. (2000)
6	373	5.15 - 10.1	0.249 - 0.997	19	Byun et al. (2000)
8	313	10.4 - 5.89	0.908 - 0.546	10	Heo et al. (2001)
8	323	13.2 - 6.83	0.908 - 0.546	10	Heo et al. (2001)
8	333	15.9 - 7.47	0.908 - 0.546	10	Heo et al. (2001)
8	343	18.4 - 8.49	0.908 - 0.546	10	Heo et al. (2001)
8	353	20.6 - 9.52	0.908 - 0.546	10	Heo et al. (2001)
8	308	2.33 - 7.62	0.241 - 0.999	22	Byun et al. (2000)
8	328	2.95 - 10.9	0.241 - 0.998	20	Byun et al. (2000)
8	348	3.74 - 12.2	0.241 - 0.998	19	Byun et al. (2000)
8	373	4.52 - 16.7	0.241 - 0.994	16	Byun et al. (2000)
9	313	1.9 - 10.5	0.214 - 0.839	10	Schieman et al. (1993)
9	333	2.05 - 13	0.181 - 0.745	10	Schieman et al. (1993)
9	353	2.0 - 14.3	0.156 - 0.670	10	Schieman et al. (1993)
9	373	1.0.1 - 23	0.072 - 0.790	10	Schieman et al. (1993)
9	393	20.0 - 201	0.100 - 0.679	10	Schieman et al. (1993)
10	313	13.8 - 2.2	0.898 - 0.393	10	Heo et al. (2001)
10	323	16.8 - 2.85	0.898 - 0.393	10	Heo et al. (2001)
10	333	19.4 - 3.81	0.898 - 0.393	10	Heo et al. (2001)
10	343	21.6 - 4.45	0.898 - 0.393	10	Heo et al. (2001)
10	353	23.8 - 5.07	0.898 - 0.393	10	Heo et al. (2001)
10	323	10.0 - 16.4	0.677 - 0.948	10	Pohler (1994)
10	353	10.0 - 22.9	0.612 - 0.943	14	Pohler (1994)
10	393	10.0 - 28.7	0.479 - 0.928	16	Pohler (1994)
12	318	10.0 - 24.3	0.695 - 0.915	14	Pohler (1994)

Table 2-3 continued

Acid chain length	T (K)	P range (MPa)	x, y (mole fraction)	N_b	Reference
12	323	10.0 - 23.6	0.584 - 0.917	10	Pohler (1994)
12	333	10.0 - 24.9	0.571 - 0.917	12	Pohler (1994)
12	343	10.0 - 26.5	0.461 - 0.916	14	Pohler (1994)
12	348	10.0 - 27.9	0.550 - 0.920	14	Pohler (1994)
12	353	10.0 - 28.4	0.523 - 0.915	16	Pohler (1994)
12	373	10.0 - 30.7	0.488 - 0.902	12	Pohler (1994)
12	333	2.57 - 24.6	0.247 - 0.959	18	Bharath et al. (1993)
12	353	5.33 - 27.7	0.351 - 0.969	12	Bharath et al. (1993)
12	373	1.01 - 5.07	0.0657 - 1.00	10	Yau et al. (1992)
12	393	10.0 - 32.6	0.419 - 0.928	14	Kordikowski (1992)
14	328	10.0 - 36.2	0.696 - 0.931	16	Pohler (1994)
14	333	10.0 - 35.5	0.718 - 0.941	14	Pohler (1994)
14	343	10.0 - 34.7	0.617 - 0.934	14	Pohler (1994)
14	353	10.0 - 35	0.536 - 0.941	16	Pohler (1994)
14	373	10.0 - 36	0.559 - 0.940	18	Pohler (1994)
14	393	10.0 - 37.5	0.501 - 0.934	24	Pohler (1994)
18	353	2.15 - 25.8	0.199 - 0.778	10	Schiemann et al. (1993)
18	373	2.5 - 26.0	0.212 - 0.761	10	Schiemann et al. (1993)
18	393	2.7 - 26.2	0.185 - 0.737	10	Schiemann et al. (1993)

As seen in Table 2-1 to Table 2-3, a large quantity of data are available for CO_2 and various hydrocarbons, including more binary systems at shorter CLs. For CO_2 and alkanes more data points and the largest range of CL data are available. Since the National Institute of Standard Technology was used to collect data, it should be noted that not all available published data are listed in the tables above.

Figure 2-2, 2-3 and Figure 2-4 illustrate the relationship between CL, bubble point pressure and mass fraction of CO_2 for CO_2 and alkanes (with data from Yu et al., (2006), Camacho-Camacho et al. (2007) and Pohler (1994)), CO_2 and alcohols (with data from Elizalde-Solis et al. (2007), Byun and Kwak (2002) and Pohler (1994)), and CO_2 and carboxylic acids (with data from Byun and Kwak (2000) and Yau et al. (1992)), respectively.

As seen in Figure 2-2, the bubble point pressures increase as the CL of the alkanes increase. For high pressures and high mass fractions, the CLs of alkanes increase as the bubble point pressure increases. For mass fractions below 0.4, the pressures seems to drop for chain lengths of 17 to 22. This is

expected since the same behaviour was found by Ting *et al.* (2003) where hexane and alkanes of different chain lengths were compared.

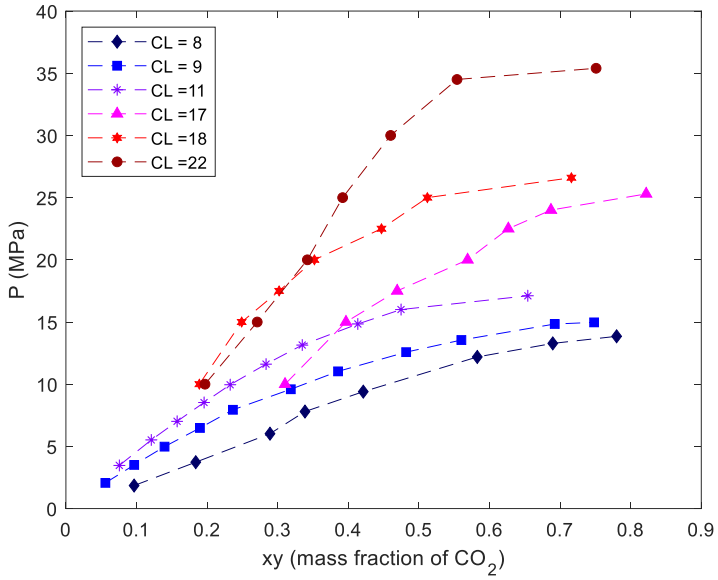

Figure 2-2: Relationship between chain length, bubble point pressure and mass fraction for CO_2 and alkanes at 373 K – data from Yu et al. (2006), Camacho-Camacho et al. (2007) and Pohler (1994)

As for alkanes, the bubble point pressures for CO_2 and alcohols increase as the CL of the alcohol increase for mass fractions of CO_2 above 0.5 (Fig. 2-3). For mass fractions of CO_2 below 0.5, a pressure drop occurs for CL larger than 10. This could be because of shorter molecules being more polar, and having a lower vapour pressure and therefore a higher bubble point pressure (Ferreira, 2018).

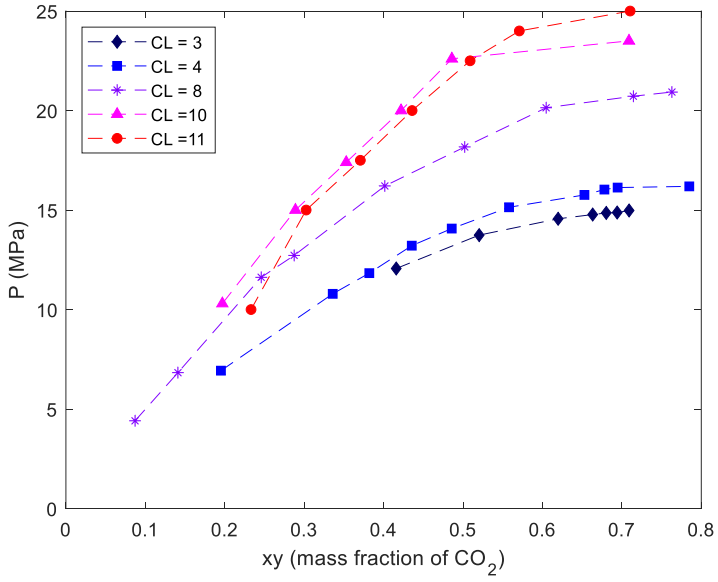

Figure 2-3: Relationship between chain length, bubble point pressure and mole fraction for CO_2 and alcohols at 373 K from Elizalde-Solis et al. (2007), *Byun and Kwak* (2002) *and Pohler* (1994)

The same observations can be made for CO_2 and carboxylic acids (as for CO_2 and alkanes and CO_2 and alcohols discussed above), as seen in Figure 2-4. The pressure increases as the CL and mass fraction of CO_2 increase at high pressures and high mass fractions of CO_2. The pressure drop for this functional group occurs for CL longer than 7 with mass fractions below 0.4.

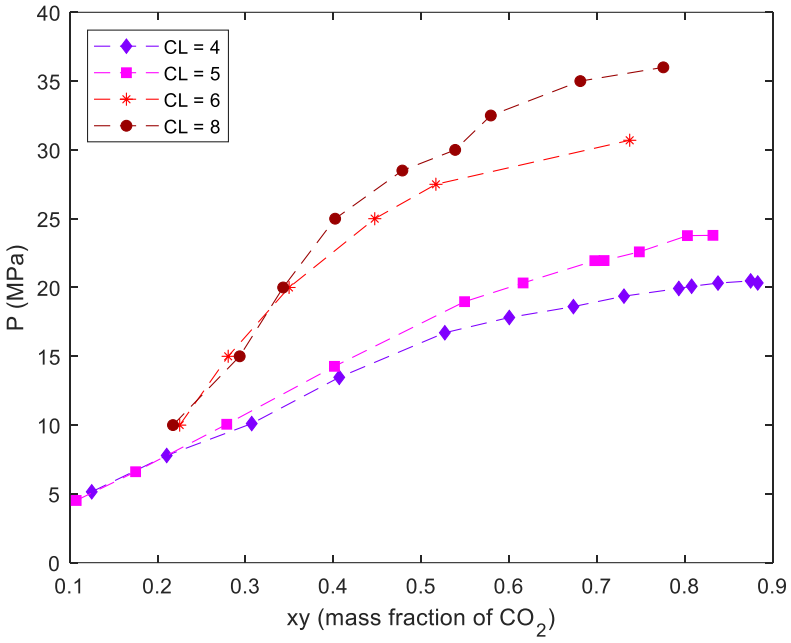

Figure 2-4: Relationship between chain length, bubble point pressure and mass fraction for CO_2 and carboxylic acids at 373 K– from Byun and Kwak (2000) and Yau et al. (1992)

The behaviours at high CL and low mass fractions observed in Figure 2-2 to Figure 2-4 could be explained by the presence of a temperature inversion (Zamudio, 2014), if the temperatures were close to the critical temperature of CO_2.. Temperature inversions contradicts the common behaviour where the phase transition pressure increases with an increase in temperature, which could have an effect on the separation processes (Zamudio, 2014). Since the temperatures of the binary systems used in the figures above are significantly higher than the critical temperature of CO_2, it is unlikely for a temperature inversion to cause the behaviour as observed in these figures.

According to van Konynenburg and Scott (1980) and Peters and Gauter (1999), binary phase behaviour can be classified into six different types, as discussed in Section 2.1.3.

2.1.3. Types of phase behaviour for binary mixtures

When working with supercritical fluid processes, it is important to avoid multiple phase regions. It is highly likely for a second liquid phase to occur in processes comprising dissimilar molecules (Peters & Gauter, 1999). Binary phase behaviour can be classified into three main groups (classes 1 to 3) (van Konynenburg & Scott, 1980) that can be subdivided into six types (type I to VI) (Peters &

Gauter, 1999). The groups describe the manner in which the mixture curves are connected, whereas the types are used to classify behaviours according to their temperature-pressure projections (van Konynenburg & Scott, 1980). Mixture curves represent the space where two phases become identical in density and composition at specific pressures and temperatures (van Konynenburg & Scott, 1980).

Class 1 describes two component mixtures with comparable gas-liquid critical properties, interaction strengths and molecular sizes (McHuge & Krukonis, 1994) where class 2 describes two-component mixtures with very distinctive gas-liquid critical properties, interaction strengths and molecular sizes (van Konynenburg & Scott, 1980). Class 3 describes complex mixtures, which falls outside the scope of this study. In class 1 the critical points of the pure components (C_1 for the light component and C_2 for the heavy component) are continuously connected by the mixture curve (types I, II and VI as discussed below), whereas in class 2 there is no continuous connection between these two points (types III, IV and V as discussed below) (van Konynenburg & Scott, 1980). Continuous connecting points for class 2 typically fall between the limiting upper critical solution point (C_∞) and the upper or lower critical endpoints (UCEPs and LCEPs). C_∞ describes the critical point at infinite pressure (van Konynenburg & Scott, 1980), whereas UCEP and LCEP describe the upper and lower points where two liquid phases are critical in the presence of a vapour phase (Ferreira, 2018).

The classes and types of phase behaviour discussed above are summarised in Table 2-2. Type I entails the simplest form of phase behaviour, where only VLE occurs. Three-phase equilibrium occurs at lower temperatures for types II, VI, III and IV and at higher temperatures and pressures for type V.

Table 2-4: Mixture curves for different groups and types of binary phase equilibrium (van Konynenburg & Scott, 1980)

Class	Type	Mixture description of components	Connecting points for mixture curve in the TP-projections
Class 1	Type I	Similar molecular sizes and interaction strengths.	A single mixture curve: 1. C_1 and C_2 (VL)
	Type II	Non-ideal mixtures with partial miscibility at subcritical temperatures.	Two mixture curves: 1. C_1 to C_2 (VL) 2. C_∞ to UCEP (LL)
	Type VI	Non-ideal mixtures. Similar to type I, but with a closed loop immiscibility at specific regions.	Two mixture curves: 1. C_1 and C_2 (VL) 2. UCEP to LCEP
Class 2	Type III	Non-ideal liquid mixtures at high pressures and temperatures where the two liquids become immiscible near T_c of the more volatile component.	Two mixture curves: 1. C_1 to UCEP (VL) 2. C_∞ to C_2 (LL to VL)

	Type IV	Non-ideal mixtures where the two liquids are immiscible at medium temperatures.	Three mixture curves: 1. C_1 to UCEP (VL) 2. LCEP to C_2 (LL to VL) 3. C_∞ to UCEP (LL)
	Type V	Near-ideal system with dissimilar molecular sizes of components. Components are miscible at low temperatures.	Two mixture curves: 1. C_1 to UCEP (VL) 2. LCEP to C_2 (LL to VL)

According to Peters and Gauter (1999), binary systems containing CO_2 and alkanes with CLs of up to 12 have a type II phase behaviour, whereas for a CL of 13, type IV phase behaviour occurs and for CLs longer than 13, type III phase behaviour occurs. For binary systems containing CO_2 and alcohols, type II phase behaviour occurs for CLs up to 5, whereas type III phase behaviour occurs for CLs of 6 and higher (Peters & Gauter, 1999).

2.1.4. Traditional thermodynamic modelling methods

Traditional thermodynamic modelling methods such as EOSs are currently used to predict and correlate phase behaviour to model phase equilibrium data, by using specific input variables to predict specific output variables. These models usually require experimental data to regress the modelling method parameters. Cubic EOSs such as the Peng-Robinson (PR) equation (Peng & Robinson, 1976) and the Redlich-Kwong (RK) equation (Redlich & Kwong, 1979) are typically used to model systems containing (among others) hydrocarbons and CO_2 (Hussain & Ahsan, 2018). The problem with both of these equations is that the shape of the molecule or the polar forces are not considered. The RK-Aspen model, suitable for asymmetric and polar molecules, was used and proposed by Lombard (2015), (binary systems containing hydrocarbons), Zamudio et al. (2013) (binary systems containing alkanes and alcohols in supercritical CO_2), Fourie et al. (2018) (binary systems containing alcohols and alkanes) and Ferreira (2018) (ternary systems containing CO_2, decanol and tetradecane). This model is an extension of the Soave-Redlich-Kwong (SRK) EOS, which can be described by the following equation:

$$P = \frac{RT}{V-b} - \frac{a}{V(V+b)} \qquad [2\text{-}2]$$

where P is the pressure, V is the specific molar volume, R is the universal gas constant, T is temperature, a is the energy parameter and b is the co-volume parameter.

The energy parameter (a) and the co-volume parameter (b) can be determined by using the following equations (Zamudio et al., 2013):

$$a = \sum_m \sum_n x_m x_n (a_m a_n)^{0.5} (1 - k_{a,mn}) \qquad [2\text{-}3]$$

$$b = \sum_m \sum_n x_m x_n \frac{b_m + b_n}{2} (1 - k_{b,mn}) \quad [2\text{-}4]$$

where $k_{a,mn}$ and $k_{b,mn}$ are the temperature dependant interaction parameters for a and b respectively, x_m and x_n are the mass fractions, a_m and a_n, are the pure component energy parameters, and b_m and b_n are the pure component co-volume parameters of components m and n.

The temperature-dependent interaction parameters can be determined with the following equations:

$$k_{a,mn} = k^0_{a,mn} + k^1_{a,mn} \frac{T}{1000} \quad [2\text{-}5]$$

$$k_{a,mn} = k^0_{b,mn} + k^1_{b,mn} \frac{T}{1000} \quad [2\text{-}6]$$

where $k^0_{a,mn}$, $k^1_{a,mn}$, $k^0_{b,mn}$ and $k^1_{b,mn}$ are the binary interaction parameters (BIPs) which can be determined using regression applied on experimental binary phase equilibrium data (Zamudio et al., 2013).

The SRK EOS with an additional modification to the energy parameter (as seen using Equation 2-3) was derived by Mathias (1983), resulting in more accurate results when polar compounds are used.

$$a_m = \propto_m 0.42747 \frac{R^2 T^2_{c,m}}{P_{c,m}} \quad [2\text{-}7]$$

The pure component co-volume parameter remains the same, and is calculated as follows (Mathias, 1983):

$$b_m = 0.08664 \frac{R T_{c,m}}{P_{c,m}} \quad [2\text{-}8]$$

where $T_{c,m}$ and $P_{c,m}$ are the critical temperature and pressure of component m.

The additional constant to the RK-Aspen model ($\propto_m$) can be calculated in two ways: with the Mathias alpha function (Mathias, 1983) or with the Boston-Mathias alpha function (Boston & Mathias, 1980). The Mathias alpha function is used when the reduced temperature of component m ($T_{r,m}$) is smaller than 1 (subcritical components), as shown in Equation *2*-9, whereas the Boston-Mathias alpha function is used when $T_{r,m}$ is larger than one (supercritical components), as shown in Equation 2-10.

$$\propto_m = \left[1 + f_m\left(1 - \sqrt{T_{r,m}}\right) - \eta_m\left(1 - T_{r,m}\right)\left(0.7 - T_{r,m}\right)\right]^2 \quad [2\text{-}9]$$

$$\propto_m = \left(exp\left(c_m\left(1 - T^{d_m}_{r,m}\right)\right)\right) \quad [2\text{-}10]$$

where $T_{r,m}$ is the reduced temperature of component m, f_m is the characteristic constant for the Mathias alpha function (a function of the acentric factor of component m), η_m is the polar factor for pure component m for the Mathias alpha function, and d_m and c_m are the modified parameters for the Mathias-Boston alpha function.

f_m, d_m and c_m can be determined using the following equations:

$$f_m = 0.48508 + 1.55171w_m - 0.15613w_m^2 \quad [2\text{-}11]$$

$$d_m = 1 + \frac{f_m}{2} + 0.3\eta_m \quad [2\text{-}12]$$

$$c_m = 1 - \frac{1}{d_m} \quad [2\text{-}13]$$

Therefore, four pure component parameters ($T_{c,m}$, $P_{c,m}$, $w_{c,m}$ and η_m) and four binary interaction parameters ($k^0_{a,mn}$, $k^1_{a,mn}$, $k^0_{b,mn}$ and $k^1_{b,mn}$) are required to model thermodynamic data using the RK-Aspen model. The polar factor for each pure component can be determined by regression, using correlated pure component vapour pressure data.

Figure 2-5 illustrates the experimental data (Cheng et al., 1989) and RK-Aspen correlations of CO_2 and pentane at 311 K obtained using Aspen Plus. The Antoine parameters used to determine the vapour pressure of pentane are listed in Table E-1 in Appendix E. In addition, the polar factor is listed in Table E-2, regressed by using vapour pressure data within a temperature range of 268.8 K to 341.4 K. The binary interaction parameters, regressed (using Aspen Plus) using VLE data of pentane at 311 K as listed in Table A-1, are listed in Table E-2.

As seen in Figure 2-5, the EOS is relatively accurate in predicted phase behaviour at low pressures, but is unable to predict phase behaviour in the critical region of the mixture. According to Ferreira (2018), Latsky (2019) and Zamudio et al. (2013), this is due to numerical methods failing near the mixture critical point, because of phase transition pressure that cannot be correlated.

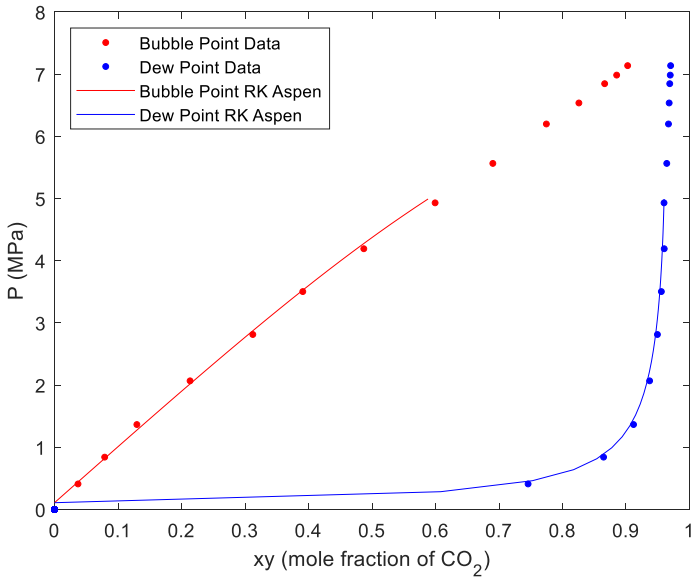

Figure 2-5: Experimental data (Cheng et al., 1989) and RK-Aspen prediction (with η_m, $k^0_{a,mn}$ and $k^0_{b,mn}$ values of 0.1024, 0.1344 and -0.00476) of CO_2 and pentane at 311 K

The aim of this subsection was to evaluate high-pressure phase equilibria by investigating traditional modelling methods and measuring methods (Section 2.1.1) and sourcing available high-pressure VLE data (Section 2.1.2). Since there are enough data available (as discussed in Section 2.1.2) and EOSs fail near the critical region, it is therefore proposed to use ANNs as an alternative method, as discussed in Section 2.2.

2.2. Neural networks

According to the three scientists who won the Turning Award in 2018 for laying the foundation of the artificial intelligence (AI) revolution (Geoffrey Hilton, Yoshua Bengio and Yann LeCun), the most powerful pattern recognition tool is the human brain (Hoffmann, 2019). These scientists developed AI techniques such as neural networks in the 1990s to mimic the functioning of the human brain, but the techniques only recently became popular, due to the large amounts of data and storage capacity that they require (Vincent, 2019).

Phillips et al. (2018) used convolutional neural network (CNN)-gated recurrent unit networks using simplified molecular-input line entry systems (SMILES) strings as inputs to predict the chemical solubility. Goh et al. (2018) used deep recurrent neural networks (RNNs) and Goh et al. (2017) used deep CNNs to predict toxicity, activity, solubility and solvation energy using SMILES strings as inputs.

Several studies used ANNs to predict VLE: Hoskins et al. (1991) and Aldrich and Slater (2001) did fault diagnoses in complex chemical plants and predicted liquid-liquid (LL) equilibrium; Parinet et al. (2015) predicted the equilibrium vapour pressure isotope effect of organic compounds (including alcohols, acids, alkanes, alkenes and aromatics) using molecular descriptions as input variables at intermediate temperatures; Eze and Masuku (2018) predicted liquid and vapour compositions of synthesis gas using pressure and temperature as input parameters; and Ghanadzadeh and Ahmadifar (2008) predicted bubble point temperature of *tert*-butanol + 2-ethyl-1-hexanol and *n*-butanol + 2-ethyl-1-hexanol using the pressure and composition of the liquid and vapour phase, respectively.

2.2.1. Artificial neural networks

Neural networks consist of different layers (an input layer, hidden layer(s) and an output layer), where each layer consists of a vector of nodes operating in parallel (Demuth & Beale, 2004). Figure 2-6 illustrates a neural network with two input variables (p_1 and p_2), two hidden layers (u_1 and u_2), three nodes in each hidden layer, and two output variables (y_1 and y_2). The nodes in each vector are connected by weights (solid lines) forming weight matrixes for the input ($\boldsymbol{w_{input}}$), hidden ($\boldsymbol{w_{hidden}}$) and output ($\boldsymbol{w_{output}}$) layers, respectively. A weight matrix contains strengths (numerical values that

are an indication of the importance of the connection) from one layer to the next where each connection is represented by a specific weight ($w_{i,j}^{k}$) and where k is the layer number, i is the node number for the starting point of the connection in a specific layer and j is the end point of the connection for a specific layer (Demuth & Beale, 2004). The biases (dashed lines) with values of b_i^k are connected to each node in each layer used to shift the transfer function (Jabbar & Khan, 2015) forming bias matrixes for the input ($\boldsymbol{b}_{input}$), hidden ($\boldsymbol{b}_{hidden}$) and output ($\boldsymbol{b}_{output}$) layers respectively. The input and output vectors are interconnected with a hidden layer vector ($\boldsymbol{u}$ with a size of $L \times S$ where L is the number of the hidden layers and S is the number of nodes in a specific hidden layer) (Demuth & Beale, 2004). Note that each hidden layer in the hidden layer vector counts as a separate layer (k). The number of hidden layers and nodes in each hidden layer is dependent on the complexity of the system, whereas the optimum number of hidden layers is determined iteratively for each specific case, as discussed in Section 2.3.

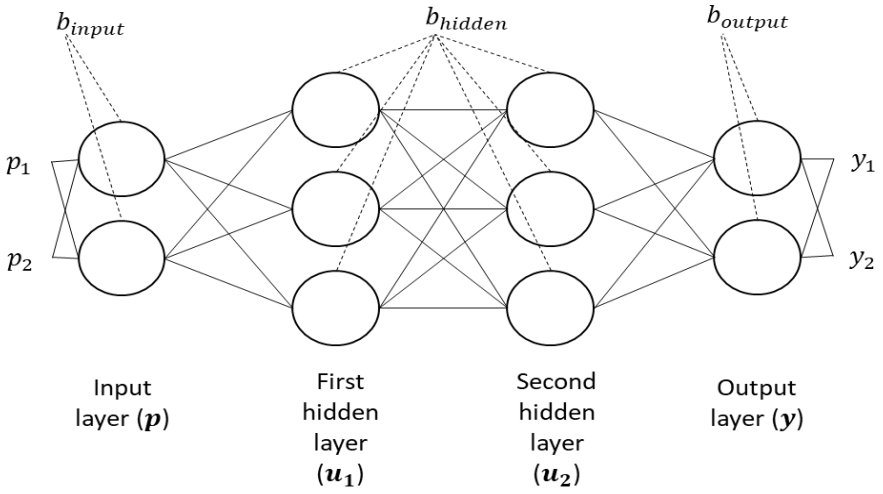

Figure 2-6: Simplified schematic diagram of a neural network

There are two main pattern recognition methods that are applied to neural networks: classification and regression (Bishop, 1995). Classification problems assign new input variables to different classes, whereas regression problems assign specific values to the output variables (Bishop, 1995).

When referring to ANNs, different kinds exist, including multilayer perceptions (MLPs), CNNs and RNNs (Nielsen, 2019). MLPs are the simplest form of ANNs and consist of an input and output layer with one or more hidden layers (Figure 2-6). CNNs were developed for image analysis where the images are analysed using exemplified functions to map features (Bishop, 1995). RNNs are used for sequence prediction including numerical time series data, stock markets, rainfall measurements and text and speech recognition using the Markov model (Bishop, 2006).

For this study, the MLP using the regression pattern recognition method was used, since the data obtained are not images and do not require sequential prediction. MLPs can further be classified into subtypes based on the construction of the connections between the nodes in the neural network.

The most common approach for constructing connections between the nodes of a neural network is the fully connected neural network (Bishop, 2006), as seen in Figure 2-6. For a fully connected ANN with two hidden layers (Figure 2-6), each input node in the input layer is connected to each node in the first hidden layer, each node in the first hidden layer is connected to each node in the second hidden layer, and each node in the second hidden layer is connected to each output node in the output layer. The structure of the neural network can change if the connections between the nodes change (Bishop, 2006). Other connection approaches such as the skip-layer network and the sparse network are also commonly used (Bishop, 2006). The skip-layer network is a network where some of the connections skip a layer. For example, the input connection skips the first hidden layer and goes straight to the second hidden layer. There are two types of skip layer neural networks, the first is an addition of connections to an existing neural network where the second method is used in densely connected architectures, typically CNNs. The sparse network is a network where not all the connections are present (Bishop, 2006). This occurs when some of the connection weights are less important, as discussed in Sections 2.2.5 and 2.2.7.

The most common types of neural networks used in previous studies modelling VLE are the feedforward neural network (Lashkarbolooki et al., 2011; Vaferi et al., 2013; Vaferi et al., 2018) and the cascade feedforward backpropagation neural network (Lashkarbolooki and Vaferi *et al.*, 2013; Lashkarbolooki and Shafipour et al., 2013). The cascade-feedforward backpropagation network is an example of the skip-layer network where each layer in the network has a weight originating from the input layer (Demuth & Beale, 2004). It should be noted that the cascade-feedforward neural networks are similar to the feed forward networks, but include a connection from the input and every previous layer to the following layers.

The strengths of ANN models are that it does not require relationships between the input and output information and assumptions about the nature of parameters can be avoided (Bishop, 2006). The weaknesses of an ANN model are that it is very dependent on the input data, it can be time-consuming to determine the weights and biases for large systems, and it is also mainly used for interpolation and becomes inaccurate when used for extrapolation (Demuth & Beale, 2004).

Neural networks are trained by adjusting the weight and bias matrixes so that a specific input vector ($\boldsymbol{p}$ with a size of $I \times N$ with I inputs and N data points) predicts a specific output vector ($\boldsymbol{y}$ with a size of $Q \times N$ where Q is the number of output variables) (Demuth & Beale, 2004), as illustrated in Figure 2-7 redrawn and adjusted from Demuth & Beale (2004). Training of a neural network is

terminated when the error between the target vector ($\boldsymbol{t}$ with a size of $Q \times N$) and the output vector is minimized (Demuth & Beale, 2004), as discussed in more detail in Section 2.2.3.

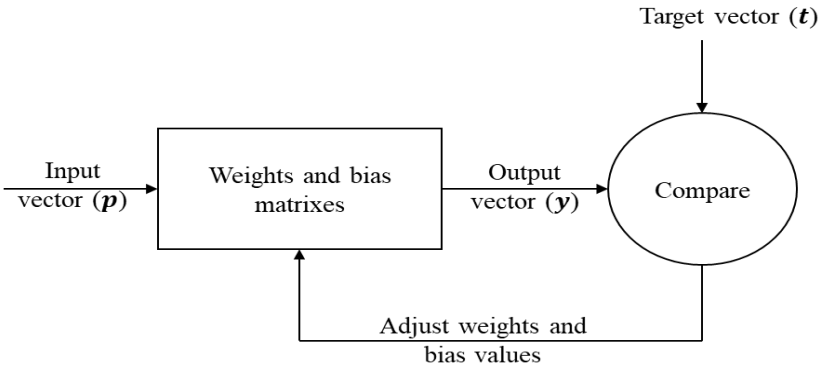

Figure 2-7: Illustrating how a neural network is trained – redrawn and adjusted from Demuth & Beale (2004)

To determine the output of each node, the weighted sum of the inputs into the node is determined as shown in the following equation (Bishop, 2006):

$$z_j = f\left(a_{node,j}\right) = f\left(\sum_{i=1}^{I} w_{ij}^{k} x_i + b_i^k\right) \qquad [2\text{-}14]$$

where z_j is the output of node j, f is the transfer function, a_j is the activation, x_i is the input to node, w_{ij}^k is the weight between each node, i and b_i^k is the bias to each node (i) and each layer (k) respectively. A bias value is summed to a node's weighted inputs to shift the transfer function to determine a node's output (Demuth & Beale, 2004). High bias values are an indication of overfitting, whereas low bias values are an indication that the model is fitted well (Jabbar & Khan, 2015).

2.2.2. Transfer functions

Transfer functions such as linear transfer functions and non-linear transfer functions can be used, where non-linear transfer functions include threshold functions, log-sigmoid functions and hyperbolic-tangent functions (Abdi et al., 2011). Typically, the nodes in the hidden layers of a neural network consist of non-linear transfer functions, followed by linear transfer functions for the nodes in the output layer (Demuth & Beale, 2004).

The threshold transfer function is a very simple transfer function, where only two outputs exist: either 0 or 1, where 0 results in an inactive input, and 1 results in an active input to the next node (Abdi, Valentin, & Edelman, 2011). As seen in Figure 2-8, if the input is smaller or equal to 0, the output will be 0. If the input is larger than 0, the output will be 1. The threshold transfer function is typically used in perception (networks used for simple problems) and classification (typically used for decision boundaries) neural networks (Demuth & Beale, 2004). Since a regression model was used for this study, it is expected that this transfer function will not be suitable.

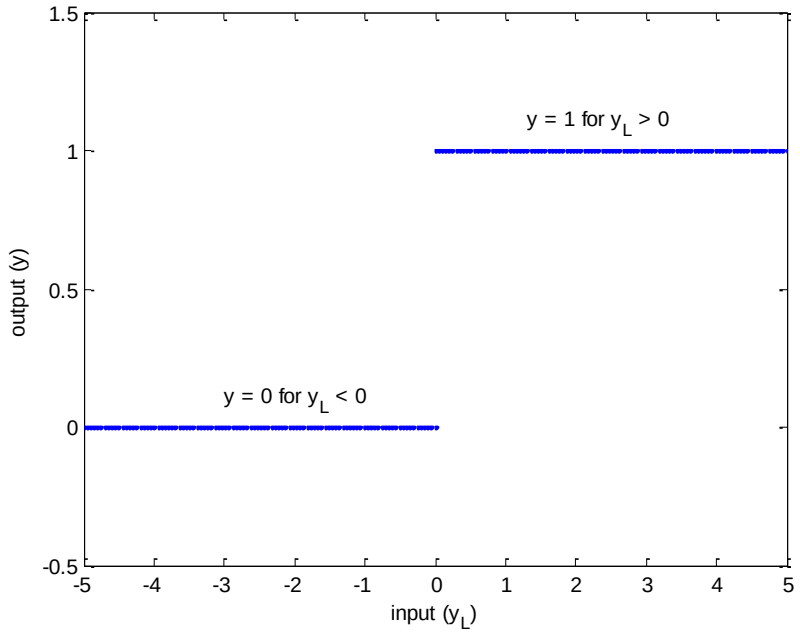

Figure 2-8: Threshold transfer function (Demuth & Beale, 2004)

The most popular transfer function, the log-sigmoid function, normalises the inputs to the transfer function to an interval of [0 1] (Lashkarbolooki, Vaferi et al., 2013), as seen in Figure 2-9. This transfer function is typically used in backpropagation networks (as discussed in Section 2.2.3) (Demuth & Beale, 2004).

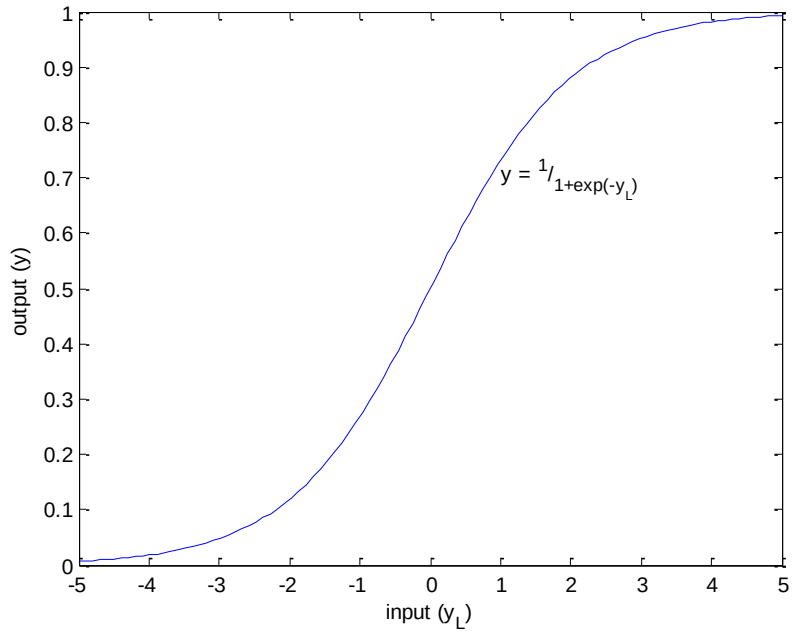

Figure 2-9: Log-sigmoid transfer function (Demuth & Beale, 2004)

The hyperbolic-tangent transfer function is similar to the log-sigmoid transfer function, normalising the inputs to the transfer function to an interval of [-1 1], as seen in Figure 2-10 (Abdi, *et al.*, 2011).

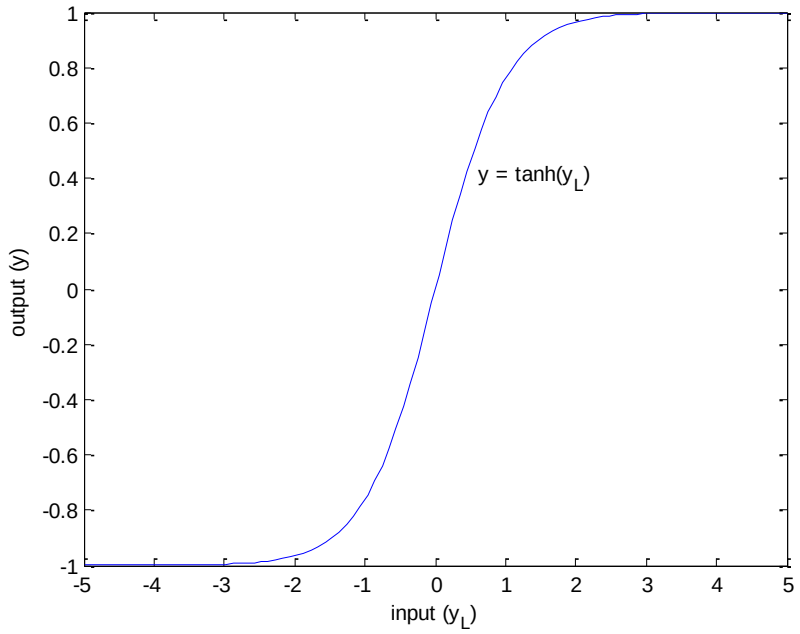

Figure 2-10: Hyperbolic-tangent transfer function (Abdi, et al., *2011)*

The linear transfer function determines the linear output by adding all the weighted activation values to a specific node. The first node in the first hidden layer will be used as an illustrative example, as seen in Figure 2-11, redrawn and adjusted from Demuth & Beale (2004). Linear transfer functions are typically used for linear approximations (Demuth & Beale, 2004).

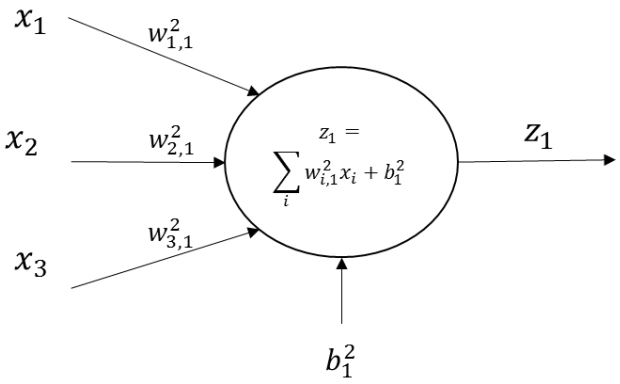

Figure 2-11: Visualisation of a linear node (Demuth & Beale, 2004)

If the node is non-linear, the output of the node is determined by a non-linear transfer function $f(y_L)$ where y_L is the linear output (Figure 2-11), and also the input to the transfer function, as shown in Figure 2-12, redrawn and adjusted from Demuth & Beale (2004).

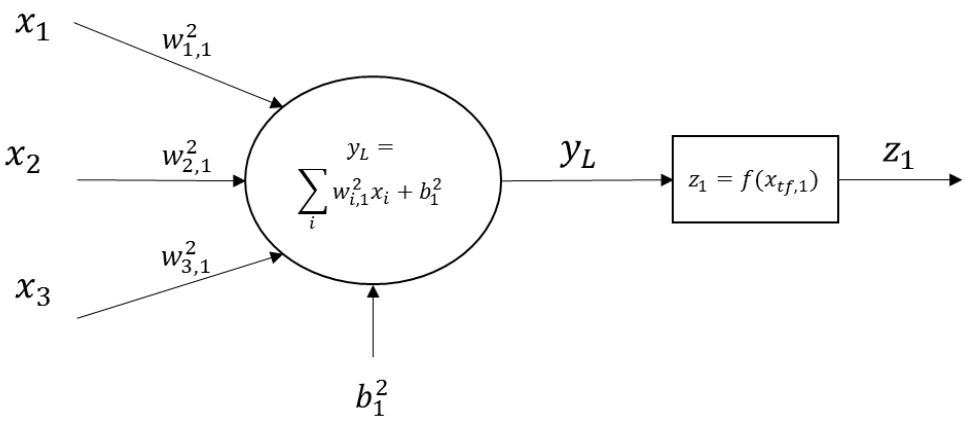

Figure 2-12: Visualization of a non-linear node (Demuth & Beale, 2004)

Since this study used a regression approximation with backpropagation, it is expected that the log-sigmoid or hyperbolic tangent transfer function will be used in the hidden layers and the linear transfer function will be used in the output layer.

After determining the initial structure of the neural network (number of inputs, hidden layers, nodes in each hidden layer, outputs and transfer functions), the network can be trained. The network is trained by either minimising the performance function (as discussed in the next section) or by maximising the likelihood function (Bishop, 2006). The likelihood function expresses how likely the observed data is for different values in the weight matrix (Bishop, 2006). The likelihood function requires independent input variables (Bishop, 2006) and was therefore not used in this study.

2.2.3. Backpropagation

Many variations of backpropagation exist, such as gradient descent, momentum, quasi-Newton and Levenberg-Marquardt methods as discussed throughout this section. Gradient decent will be used to explain backpropagation, where the variations of backpropagation will be discussed at the end of this section.

The simplest form of backpropagation (gradient descent) is an iterative approach where the weights and bias vectors are updated in the direction that the performance function decreases the most (Demuth & Beale, 2004). The performance function minimises the error between the output and target vector. Each iteration is referred to as an epoch, the presentation of a set of training vectors to a network and the calculation of a new set of weight and bias values (Demuth & Beale, 2004). Two stages are involved in each iteration. In the first stage, the derivatives of the performance function (as discussed below) with respect to the weights are determined and evaluated (Bishop, 2006). In the second stage, the weights and bias vectors are adjusted according to the derivatives calculated (Bishop, 2006), and can be written as (Demuth & Beale, 2004):

$$w_{i,j}^{k+1} = w_{i,j}^{k} - \alpha^{k} g^{k} \quad [2\text{-}15]$$

where α is the learning rate and g is the current gradient for each iteration k.

Different performance functions can be used such as the sum squared error (SSE), mean absolute error (MAE) or mean squared error (MSE) (Demuth & Beale, 2004). SSE is the simplest performance function measuring performance according to the SSE, as seen in Equation 2-16. MAE is used when the output data are Gaussian with some outliers, which measure the data according to the MAE, as seen in Equation 2-17. MSE, which is the most frequently used performance function, is used when the distribution of the output data are Gaussian, as seen in Equation 2-18 (Demuth & Beale, 2004). The performance functions listed above for multiple outputs can be calculated as follows (Demuth & Beale, 2004):

$$SSE = \sum_{n=1}^{N} \left(y_{nq} - t_{nq}\right)^2 \quad [2\text{-}16]$$

$$MAE = \frac{\sum_{n=1}^{N} |y_{nq} - t_{nq}|}{N} \quad [2\text{-}17]$$

$$MSE = \frac{\frac{1}{2}\sum_{n=1}^{N}\sum_{k=1}^{K} \left(y_{nq} - t_{nq}\right)^2}{NQ} \quad [2\text{-}18]$$

where y_{nq} and t_{nq} are q^{th} actual and target output for the n^{th} example respectively.

To minimise the performance function, the optimum weight to each node resulting in the minimum error is a prerequisite, as illustrated in Figure 2-13, redrawn and adjusted from Bishop (2006).

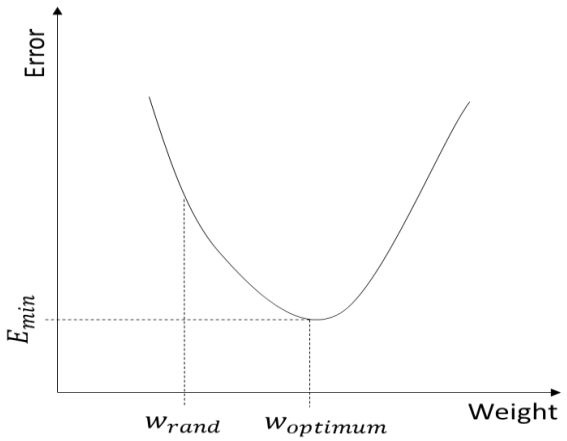

Figure 2-13: Error surface redrawn from Bishop (2006)

As seen in Figure 2-13, a random weight is initially selected. To decrease the error, the gradient, which is the derivative of the error with respect to the weight $\left(\frac{dE}{dw}\right)$ is determined, which is the first step of backpropagation. The weights are then adjusted in the direction in which the gradient decreases, the second step of backpropagation. This technique is repeated with the new weight until the minimum error is found (Bishop, 2006).

Gradient descent can be implemented in two ways: in incremental or batch mode (Demuth & Beale, 2004). For incremental mode, both steps of backpropagation are determined by using a single data point in the training set for each epoch (Demuth & Beale, 2004). For batch training, the first step of backpropagation is determined after each data point, and averaged to determine the weights and biases, which is used to update the weights and biases after each training set, the second step of backpropagation (Demuth & Beale, 2004).

Although the gradient descent method is a reasonable approach, Bishop (2006) states that it is a poor algorithm. As seen in Equation 2-15, the learning rate is a fixed value that can be hard to determine. A large learning rate (α, Equation 2-15) results in a larger change in weight values which could result in an unstable algorithm where the error could increase and the minimum error will not be obtained, where a small learning rate results in slow training of the neural network (Demuth & Beale, 2004).

Since non-linearities in the network sometimes result in a nonconvex performance function, error surfaces sometimes result in more than one minimum (Bishop, 2006). If this is the case, the gradient descent method would not be preferable since a shallow local minimum could be selected instead of the global minimum. By combining the gradient decent and momentum methods, and adapting the learning rate after each epoch, the optimum weight with the global minimum will be obtained faster.

The gradient descent and the momentum methods are generally very slow and are only used when incremental training is desired (Demuth & Beale, 2004). Newton's method was proposed for faster training and more accurate results near the minimum error (Figure 2-13) as seen using the following equation (Demuth & Beale, 2004):

$$\left(\boldsymbol{w}_{i,j}^{k}\right)^{c} = \left(\boldsymbol{w}_{i,j}^{k}\right)^{c} - (\boldsymbol{A}^{c})^{-1}\boldsymbol{g}^{c} \qquad [2\text{-}19]$$

where $\boldsymbol{A^c}$ is the Hessian matrix of the performance function for iteration c. This method is not often used since it is expensive (long calculation times) to determine the Hessian matrix (Demuth & Beale, 2004).

The Levenberg-Marquardt training method ($trainlm$) is therefore proposed for small to medium training sets, where the Hessian matrix (Equation 2-20) and the gradient (Equation 2-21) can be determined as (Demuth & Beale, 2004):

$$\boldsymbol{A} = \boldsymbol{J}^{T}\boldsymbol{J} \qquad [2\text{-}20]$$

$$\boldsymbol{g} = \boldsymbol{J}^{T}\boldsymbol{e} \qquad [2\text{-}21]$$

and the Levenberg-Marquardt method as (Demuth & Beale, 2004):

$$\left(\boldsymbol{w}_{i,j}^{k+1}\right)^{c} = \left(\boldsymbol{w}_{i,j}^{k}\right)^{c} - (\boldsymbol{A}^{c} + \mu\boldsymbol{I})^{-1}\boldsymbol{J}^{T}\boldsymbol{e} \qquad [2\text{-}22]$$

where **J** is the Jacobian matrix, $\boldsymbol{e}$ is the performance function matrix, μ is an added term in the Levenberg-Marquardt method and **I** is the identity matrix. Equations 2-19 and 2-22 are similar when

μ is zero, resulting in an approximation of Newton's method (Demuth & Beale, 2004). Comparing Equations 2-19 and 2-22, the gradient descent method with a small learning rate value is followed when μ becomes larger (Demuth & Beale, 2004). The value of μ changes throughout the training procedure, increasing near the local/global minimum and decreasing after each iteration (Demuth & Beale, 2004).

The Levenberg-Marquardt method was used by Lashkarbolooki and Shafipour et al. (2013), Lashkarbolooki and Vaferi et al. (2011), Vaferi and Rahnama et al. (2013) and Vaferi and Lashkarbolooki et al. (2018) to model VLE and it is therefore expected to be sufficient for this study.

Training a neural network is important for finding the optimal weight and bias matrixes, but it is also important to terminate training when the neural network's predictions are accurate enough and to test the neural network after training.

2.2.4. Training, testing and validation of neural networks

After obtaining a sufficient number of data points, the data are split into training ($\boldsymbol{p}_{train}$ and $\boldsymbol{t}_{train}$), testing ($\boldsymbol{p}_{test}$ and $\boldsymbol{t}_{test}$) and validation ($\boldsymbol{p}_{valitate}$ and $\boldsymbol{t}_{validate}$) sets where the fractions of data to each set is typically $D_{train} = 0.75$ for the training set and $D_{test} + D_{valiate} = 0.25$ for the testing and validation sets (Lashkarbolooki and Vaferi et al., 2013). The training data are used to determine the weights and the bias vectors of the neural network, wheras the validation data are used for early stopping (a regularization method) in the training phase, and the testing data are used to test the results of unseen data after the neural network was trained (Demuth & Beale, 2004). The error on the validation data (validation error) is monitored during training of the neural network, where training is terminated when a certain point is reached, referred to as early stopping (Demuth & Beale, 2004). The validation error will typically decrease during the training phase and will increase when the model begins to overfit the data (Demuth & Beale, 2004). Early stopping will occur just before the validation error increases (Demuth & Beale, 2004).

For a neural network to be trained, the structure and hyperparameters of the neural network should be defined. Determining the structure and hyperparameters of a neural network is an iterative approach. Therefore, several neural networks should be trained in order to optimise the neural network. The structure of a neural network is defined by the layers (input, hidden and output layers), the nodes in each layer, and the connection weights between each node (Aggarwal, 2018). For this study, the hyperparameters include the type of neural network, the number of hidden layers, the number of nodes in each hidden layer and the transfer function used. Determination of the input parameters are discussed in Sections 2.2.5 and 2.2.6, the connection weights between each node are

discussed in Section 2.2.7, and the determination of the type of neural network, number of hidden layers and the number of nodes in each hidden layer are discussed in Section 2.3.

2.2.5. Randomising input parameters

To determine the importance of the input variables, a sensitivity analysis can be performed by randomising each input variable across the entire input range, while keeping all other inputs constant. Olden and Jackson (2002) used the randomisation test to remove connection weights with a small influence on the outputs of the neural network. This test can also be used to eliminate insignificant input variables to the neural network. The randomisation of each input independently will determine whether a specific input has a significant effect on the neural network.

An illustrative example is presented in Figure 2-14 to explain the randomisation test. As seen in this figure, an MLP with p_1 to p_3 as input variables and y_1 and y_2 as output variables will be used.

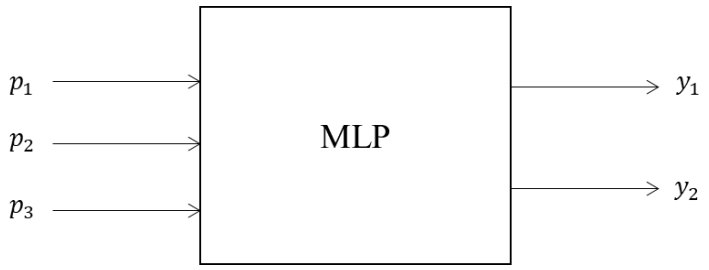

Figure 2-14: Illustration of input randomization approach

After obtaining training data, as listed in Table 2-5 (four data points a_p to d_p for each input p), p_1 will be randomised, where p_2 and p_3 will be kept constant. This input data will then be used to train an MLP where the trained MLP will be used to determine the output variables, y_1 and y_2. The output variables will then be compared to the target variables and the $AAD\%$ (or the average absolute relative deviation percentage ($AARD\%$) as discussed in Section 2.3 using Equations 2-26 and 2-27) will be determined.

Table 2-5: Example of input randomization approach

Input	**Data points for each input before randomization**				**Data points for each input after randomization**			
p_1	a_1	b_1	c_1	d_1	b_1	d_1	a_1	c_1
p_2	a_2	b_2	c_2	d_2	a_2	b_2	c_2	d_2
p_3	a_3	b_3	c_3	d_3	a_3	b_3	c_3	d_3

The same approach will be followed for randomising p_2 and p_3. After randomising each input, the $AAD\%$ will be obtained by randomising each input. To determine the normal condition, the $AAD\%$ should be determined using a trained MLP where no inputs are randomised to use as a reference state. If the $AAD\%$ of the randomised inputs are smaller than the normal condition $AAD\%$, the randomised

input has an insignificant effect on the neural network and should be eliminated as input variable. According to Olden and Jackson's (2002) methodology, it is not necessary to determine new hyperparameters for the neural network after each elimination of an input.

2.2.6. Categorical input variables

Outputs of neural networks are determined based on the magnitude of each weight and bias value. These weight and bias values are determined based on the numerical value of the input and target values, as discussed in Section 2.2.3. The inputs to a neural network should therefore be proposed as numerical values (Aggarwal, 2018). Some input variables are defined in terms of words, for example the name of a functional group, the day of the week or the colour of a flower. Label encoding can be used to assign a numerical value to each category (Aggarwal, 2018). Using functional groups as an example, a label can be assigned to each functional group, as seen in Table 2-6. Here, alkanes, alcohols and carboxylic acids are described by the numerical values of 1, 2 and 3, respectively.

Table 2-6: Illustrative example of label encoding

Functional group	**Numerical label**
Alkane	1
Alcohol	2
Carboxylic acid	3

Since the weight and bias values are determined based on average values of data points (as discussed in Section 2.2.3), problems such as halfway predictions between categories or higher numerical values that are being favoured can occur (Aggarwal, 2018). It is therefore proposed to use one-hot encoding (Aggarwal, 2018). One-hot encoding represents each categorical variable as a separate input to the neural network (Aggarwal, 2018), as illustrated using Table 2-7. Here, alkanes, alcohols and carboxylic acids are described by vectors [1; 0], [0; 1] and [0; 0], respectively.

Table 2-7: Illustrative example of one-hot encoding

Functional group	**Numerical label for first input**	**Numerical label for second input**
Alkane	1	0
Alcohol	0	1
Carboxylic acid	0	0

After determining the inputs (as discussed in Section 2.2.5) and the outputs (as discussed in this section) of the neural network, the weights and bias vectors of the neural network can be determined, as discussed in Section 2.2.4. By implementing the weights, the relative importance (RI) of the input variables can be determined, as discussed in Section 2.2.7.

2.2.7. Connection weight approach

The connection weight approach can be used not only to determine the input parameters to the neural network, but also to determine the relative importance of each input for each neural network (Olden et al., 2004). As discussed using Figure 2-6 in Section 2.2.1, the links between the input and output variables are the weights between each node (including the hidden layer nodes) and are therefore important to interpret (Olden & Jackson, 2002). The magnitude of the connection weights is directly proportional to the impact of that weight on the neural network (Olden & Jackson, 2002).

To determine the impact of each input variable on each output variable, the connection weight approach (Olden & Jackson, 2002) will be used. This approach calculates the product between the input, hidden and output nodes, and determines the relative importance of each input relative to each output (Olden et al., 2004).

Equation 2-23 determines the product ($\boldsymbol{X}$) between the layers where Equation 2-24 calculates the relative importance ($\boldsymbol{RI}_i$) of each input i:

$$\boldsymbol{X} = \boldsymbol{w}_{input} \times \boldsymbol{w}_{hidden} \times \boldsymbol{w}_{output} \qquad [2\text{-}23]$$

$$\boldsymbol{RI}_i = \frac{|\boldsymbol{X}_i|}{\sum \boldsymbol{X}} \times 100 \qquad [2\text{-}24]$$

where $\boldsymbol{w}_{input}$ of size $I \times S$ is the connection weight matrix between the input and first hidden layer, $\boldsymbol{w}_{hidden}$ of size $S \times S$ is the connection weight matrix between the two hidden layers and $\boldsymbol{w}_{output}$ of size S$\times$ Q is the connection weight matrix between the second hidden layer and the output layer, as discussed in Section 2.2.1.

Since different results will be obtained after training each neural network (because of random initial weight and bias vectors), it leads to a significant amount of uncertainty in the results obtained by neural networks. In the next section, the uncertainty of neural networks will be discussed.

2.2.8. Uncertainty of neural networks

When neural networks are trained, random weight and bias values are initially selected for the first iteration, as mentioned in Section 2.2.3. It is therefore unlikely that the same optimum weight and bias matrixes will be obtained after training a neural network. To determine the uncertainty of a neural network, it is proposed to train multiple neural networks and to determine the average of the predictions made from the network with uncertainty when the structure of the neural network is determined. The uncertainty for a small sample size can be determined as follows (Lindberg, 2000):

$$U = t_N \times \frac{s_y}{\sqrt{N_{sample}}} \qquad [2\text{-}25]$$

where u is the uncertainty parameter, t_N is the student's t statistic for N_{sample} number of samples and s_y is the standard deviation of a specific variable.

After investigating artificial neural networks, neural networks used for thermodynamic modelling will be discussed in Section 2.3.

2.3. Neural networks for thermodynamic modelling

Since the results from EOSs become unreliable at high pressures (Figure 2-5), neural networks can be used as an alternative method to determine the phase behaviour of binary systems. Previous studies on modelling thermodynamic data using neural networks include binary systems containing CO_2 and cyclic compound mixtures (Lashkarbolooki, Vaferi et al., 2013), hydrocarbons (Lashkarbolooki, Shafipour, *et al.*, 2013) and refrigerants (Vaferi et al., 2018). For all of these studies, the reduced temperature of the system, the critical pressure, the acentric factor of the cyclic compounds, hydrocarbons and refrigerants respectively, and the composition of CO_2 in the vapour and liquid phases were used as inputs, and the bubble and dew point pressures were predicted. Vaferi et al. (2013) and Lashkarbolooki, *et al.* (2011) used the same approach as the previous studies, using binary systems containing CO_2 and ethanol and CO_2 and hydrocarbons, respectively, but they used other input and output variables. Vaferi et al. (2013) used the liquid composition of ethanol, the temperature, boiling temperature, critical temperature, critical pressure and acentric factor to predict the bubble point pressure and vapour composition, whereas Lashkarbolooki et al. (2011) used the critical pressure, critical temperature and acentric factor of the hydrocarbons and system pressure and system temperature to predict the solubility. The log-sigmoid transfer function was used in all these studies. The minimum amount of data points used to model thermodynamic data with six different binary systems was 271 VLE points (Lashkarbolooki and Vaferi et al., 2013) and the maximum amount of data points used for a binary system modelling nine different binary systems was 970 (Lashkarbolooki et al., 2011). A single hidden layer was used in all these studies.

High-pressure binary phase equilibrium and/or binary phase transition data containing CO_2 and hydrocarbons such as alkanes, alcohols and carboxylic acid were required to train the required neural networks in this study. According to the Gibbs phase rule (Equation 2-1, Section 2.1.1), the number of intensive variables that can be varied independently is two. Therefore, isothermal data were collected where the pressure and the composition were varied independently.

Suitable input parameters such as the functional group, CL, molecular mass (MM) and the critical temperature and pressure of the hydrocarbon, the system temperature, and the composition in the vapour and liquid phase of CO_2 were considered in order to determine the desired output parameters.

The target vector ($\boldsymbol{t}$) will have the same size as the desired output vector containing the bubble ($\boldsymbol{y_b}$) and the dew point pressures ($\boldsymbol{y_d}$).

Since an average of the data points were used to determine the weight and bias matrixes (as discussed in Section 2.2.3), more data points in a specific region could result in inaccurate predictions. For example, if VLE data were collected for binary systems containing CO_2 and alkanes, alcohols and carboxylic acid respectively, and more data were available for the alkane functional group, the results predicting VLE containing alkanes would have been be favoured. This problem can be solved by duplicating the alcohol and carboxylic acid VLE data until an equal number of data points for all functional groups are used (Jothilakshmi & Gudivada, 2016). The same problem can arise with the data available for a specific CL of the hydrocarbon (for example more data are available for short CL hydrocarbons), the number of binary systems available per CL of the hydrocarbon, and the number of data points in each binary system. The advantage of duplicating data points is that the bias towards regions with more data points are removed where the disadvantage with duplication of data points is overfitting during the training phase.

The binary systems used in this study containing CO_2 and a specific hydrocarbon are listed in Table 2-1 to Table 2-3 and the phase equilibrium data are listed in Tables A-1 to A-3 for alkanes, alcohols and carboxylic acid as the hydrocarbons.

As discussed in Section 2.2.4, data should be divided into training, testing and validation sets. The data can either be divided by separating each binary system and testing individual data points extracted from each system as done by Lashkarbolooki and Vaferi et al. (2013), Vaferi et al. (2018), Vaferi et al. (2013) and Lashkarbolooki et al. (2011), or ccomplete binary systems at a specific temperature can be used as training, testing and validation sets. In this study, the latter approach was applied since the former approach interpolates between data points.

The hyperparameters in a neural network are parameters for which the values are chosen before the training procedure starts (Demuth & Beale, 2004). The hyperparameters for this study include the type of neural network, the number of hidden layers, the number of nodes in each hidden layer, and the transfer function. The type of neural network, the number of hidden layers and the transfer function will be determined by considering different possibilities as discussed in previous sections, whereas the number of nodes in each hidden layer will be determined by minimising the $AAD\%$ (Equation 2-26) or the $AARD\%$ (Equation 2-27), maximising R^2 (Equation 2-28; Lashkarbolooki and Vaferi et al., 2013) and minimising the geometric distance between the training and the testing data (Demuth & Beale, 2004). The geometric distance for this study is the distance between the training and testing R^2, $AAD\%$ or $AARD\%$ respectively (Kubat, 2017):

$$AAD\% = \frac{1}{N}\sum_{i=1}^{N}\left(\left|\frac{{p_i}^{exp} - {p_i}^{predict}}{{p_i}^{exp}}\right|\right) \times 100 \quad [2\text{-}26]$$

$$AARD\% = \frac{1}{N}\sum_{i=1}^{N}\left(\left|\frac{{p_i}^{exp} - {p_i}^{predict}}{{p_i}^{predict}}\right|\right) \times 100 \quad [2\text{-}27]$$

$$R^2 = \frac{\sum_{i=1}^{N}({p_i}^{exp} - p_{average})^2 - \sum_{i=1}^{N}({p_i}^{exp} - {p_i}^{predict})^2}{\sum_{i=1}^{N}({p_i}^{exp} - p_{average})^2} \quad [2\text{-}28]$$

It is also possible to use hybrid schemes, as proposed by Eikens et al. (2001), Greaves et al. (2001) and Meleiro et al. (2001). Hybrid schemes analyse and combine the knowledge as derived from first principles and neural networks (Eikens et al., 2001)). Kamali and Mousavi (2008) and Bravo-Sa´nchez et al. (2002) used hybrid modelling for phase equilibrium where they combined ANNs with PR EOSs and the Back Equation of State respectively. Kamali and Mousavi (2008) used a simple additional equation to combine these two methods. Hybrid modelling was, however, not investigated in this study, since the scope is to investigate whether neural networks are an alternative to EOSs.

The aim of the literature review was to investigate the possibility of modelling thermodynamic data using neural networks. In achieving the aim of this chapter, a simple neural network containing VLE data with CO_2 and alkanes (case study 1) were be trained to test the possibility of modelling thermodynamic data using neural networks. The neural network was trained after the structure and hyperparameters were determined, and the results will be compared to traditional modelling methods.

Since viable results were obtained by training a simple neural network (case study 1), a second case study was performed following the same approach, where data were added to increase the complexity of the neural network by adding different functional groups, and therefore more data. In case study 2, a neural network containing VLE data with CO_2 and various hydrocarbons (alkanes, alcohols and carboxylic acid) were trained. These case studies will be described in more detail in Section 3.

As discussed earlier in this section, training, testing and validation data can be divided by separating each binary system, therefore validating and testing individual data points of a binary system. The second option is to use a complete binary system as testing and validation sets. A third case study were performed based on published articles and by comparing the results using the first and second options for dividing data sets. Since only a single hidden layer was used for all of the studies listed earlier in this chapter, using two hidden layers were also be investigated in case study 3.

To achieve the outcomes of each case study, the structure of the neural network in each case study were investigated, including the determination of inputs to the neural networks (objective 1). After determining the inputs to the neural networks in each case study, the hyperparameters were optimised (objective 2). After optimising each neural network, the results will be compared to traditional modelling methods in order to determine whether neural networks are a comparing alternative to model high-pressure phase equilibrium (objective 3).

3. Methodology

In this chapter, the methodology that was applied in order to achieve all objectives of this study, will be discussed. The aim of case study 1 was to evaluate the possibility of modelling high-pressure phase equilibrium using neural networks. The aim of case study 2 was to evaluate a neural network with more data and more functional groups than case study 1, thereby increasing the complexity of the neural network. Case study 3 was used to evaluate the effect of using two hidden layers instead of a single one and also to evaluate different approaches to dividing the training, testing and validation data. The data used for the neural networks, initial input variables and output variables for each case study are listed in Table 3-1.

Table 3-1: Summary of differences between case studies

	Case study 1	**Case study 2**	**Case study 3**
Data used for the neural network	82 binary systems containing CO_2 and alkanes using 1382 data points	238 binary systems containing CO_2 and hydrocarbons (alkanes, alcohols and carboxylic acid) using 3731 data points	Six binary systems containing CO_2 and cyclic compounds (271 data points) as selected by Lashkarbolooki & Vaferi, et al. (2013) and also nine binary systems containing CO_2 and refrigerants (503 data points) as selected by Vaferi, et al. (2018)
Initial system inputs	Acentric factor (w), critical temperature (T_c), critical pressure (P_c), chain length (CL) and molecular mass (MM) of the alkane	Functional group (FG_1 and FG_2), acentric factor (w), critical temperature (T_c), critical pressure (P_c), chain length (CL) and molecular mass (MM) of the hydrocarbon	Critical pressure, reduced temperature and acentric factor of the cyclic compound
Initial data point inputs	System temperature (T), liquid-vapour-distinction (x/y), liquid (x) and vapour (y) composition of CO_2	system temperature (T), liquid-vapour-distinction (x/y), liquid composition (x) and vapour composition (y) of CO_2	CO_2 composition
Output variables	Bubble and dew point pressure	Bubble and dew point pressure	Bubble and dew point pressure

The objectives for each case study are illustrated in Figure 3-1 and discussed in Sections 3.1 to 3.5.

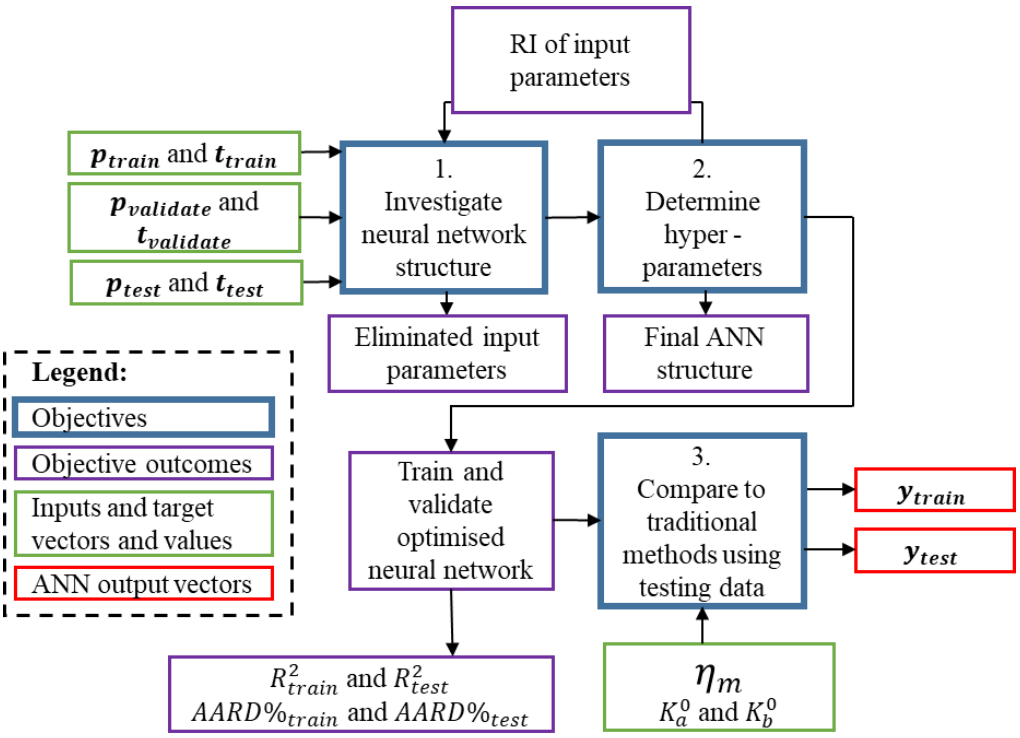

Figure 3-1: Experimental plan

3.1. Data collection and preparation

In order to predict binary phase behaviour with the use of neural networks, data are required. Binary phase equilibrium data used for case studies 1, 2 and 3 are listed in Tables A-1 to A-3 in Appendix A. The critical temperature, critical pressure and acentric factors for the hydrocarbons are listed in Tables A-4 to A-6. Since the composition of CO_2 in the liquid and vapour phases were considered as individual inputs, and the bubble and dew point pressures were considered as individual outputs, the vapour composition and dew point pressure were set to zero if values were assigned to the liquid composition and bubble point pressures. If values were assigned to the vapour composition and dew point pressure, the liquid composition and bubble point pressure were set to zero.

After obtaining enough data for the neural networks used in case studies 1 and 2, the data set were divided into training, testing and validating sets. The training and testing data sets can be divided by using two methodologies (as discussed in Section 2.3): either by separating each binary system, and testing individual data points from each system, or complete binary systems can be split up by testing and validating specific binary systems. The former option results in very accurate results, as obtained by previous studies, since neural networks interpolate data very well. For case studies 1 and 2, the latter were applied since it is more likely for a whole data system to be unavailable in practice. For case study 3, data from published articles were used and were divided by using the latter approach. The results as obtained in case study 3 were then compared to the results obtained in the published articles. The data were therefore divided by selecting a whole binary system with approximate ratios

of 10%, 15% and 75% for testing, validation and training data respectively for case studies 1 and 2. The verification data were selected using the *linspace* function but the testing data weren't. Only binary systems where EOS predictions were made were considered as testing data, since the results were compared to EOS. For case study 3, the same ratios were used as used in the publications. To divide data in the MATLAB Toolbox, the $net.divideFcn$ was used selecting the $divideblock$ option. This function was used to divide the training separate validation data where the testing data was unseen by the network which was used after training.

After dividing the data into training, testing and validation sets, data were further prepared. If less data points were available in a specific region (as discussed in Section 2.3) according to the functional group, CL and data points per binary system, data points were duplicated for the training data set as follows:

1. Determine which binary system contains the most data points at a specific temperature ($N_{b,max}$).
2. Add data points to each binary data set until all data sets have $N_{b,max}$ number of data points. Use the *linspace* function in MATLAB, to generate linear spaces between data points. For example, if three data points should be added, the first, the middle and the last data points will be duplicated. The *linspace* function ensures that data over the entire range are selected, opposed to selecting random data points which may result in clusters of data in the same area.
3. Determine the CL with the most binary system data sets ($N_{CL,max}$).
4. Add data sets to each CL until all CL categories have $N_{CL,max}$ number of data sets.
5. Determine the functional group with the most CL data sets ($N_{FG,max}$).
6. Add data sets to each functional group until all functional group categories have $N_{FG,max}$ number of data sets.

3.2. Determination of input variables

Initial system inputs included the functional group (alkanes, alcohols and carboxylic acids), acentric factor, critical temperature and pressure, CL and MM of the hydrocarbon, and the initial data point inputs included the system temperature and the liquid and vapour composition of CO_2, as listed in Table 3-1. The system inputs are considered to be model parameters where the data point inputs adhere to the Duhem Theorem, as discussed in Section 2.1.

Additional inputs for the functional group were used with one-hot encoding as discussed in Section 2.2.6, therefore, two input nodes were assigned to the functional group (FG_1 and FG_2). Since the liquid and vapour compositions are dependent variables, an additional input was added called the

vapour-liquid distinction to distinguish (x/y) whether the phase was in liquid or vapour form, using 0 or 1 notation.

To determine the input variables of the neural network, a preliminary feedforward neural network (Vaferi et al., 2018) with one hidden layer was used. The feedforward neural network is the most used ANN used by various authors (Lashkarbolooki & Shafipour et al., 2013; Lashkarbolooki et al., 2011; Vaferi et al., 2013; Vaferi et al., 2018). The Levenberg-Marquardt training algorithm and the MSE, as used by Lashkarbolooki & Vaferi et al. (2013), were used to adjust the weights and biases in order to minimise the error between the target vector and the output vector, as discussed in Section 2.2.4. Early stopping of the training phase occurred by using the validation set, preventing overfitting of the network. The number of nodes in each hidden layer was determined by maximising R^2 and minimizing $AAD\%$ of the training and testing data and minimising the geometric distance between the training and testing data of the R^2 and $AAD\%$ values. After determining the number of nodes per hidden layer, the P-xy results of a binary system from the testing set were used to justify the choice.

To determine the significant inputs of the neural network, a sensitivity analysis was performed where each input variable was randomised across the entire input range while all other inputs were kept constant as discussed in Section 2.2.5.

After data were obtained and divided into training, testing and validation sets using the preliminary neural network, the following steps were taken to determine the input variables to the neural network:

1. Train and test the preliminary neural network using the parameters as discussed above and the neural network toolbox in MATLAB (as discussed in Appendix B) without randomising any input variables, to obtain the normal condition as a reference state. Save the $AAD\%$ of the test set.
2. Randomise the first input variable of the preliminary neural network while keeping all other input variables constant. Train and test this neural network using the neural network toolbox in MATLAB. Save the $AAD\%$ of the test set where the first input of the neural network was randomised.
3. Repeat step 2, randomising all input variables respectively.
4. Repeat steps 2 and 3 five times to determine the uncertainty of the $AAD\%$, as discussed in Section 2.2.8.
5. Compare all $AAD\%$ of the test sets using a bar chart.
6. If there are input variables with $AAD\%$ values lower than the normal condition, the input variable with the lowest $AAD\%$ should be eliminated.

7. If an input variable was eliminated, repeat steps 1 to 5 without the input variables eliminated in step 6.
8. If there are input variables with $AAD\%$ values lower than the normal condition, compare these $AAD\%$ with the current normal condition and the normal condition obtained by the previous bar chart. If there are no input variables with $AAD\%$ values lower than the normal condition, continue to step 12.
9. If the $AAD\%$ of the input variables with $AAD\%$ values lower than the normal condition are significantly higher than the $AAD\%$ with the current normal condition and the normal condition obtained by the previous bar chart, continue to step 12.
10. If the $AAD\%$ of the input variables with $AAD\%$ values lower than the normal condition are relatively the same or lower than the $AAD\%$ with the current normal condition and the normal condition obtained by the previous bar chart, this input variable should be eliminated.
11. Repeat steps 7 to 10.
12. No inputs should further be eliminated.
13. Plot and compare the VLE results of each removed input to ensure that the best results are obtained.

After the input variables to the neural network were determined, the hyperparameters needed to be determined.

3.3. Determination of hyperparameters

The hyperparameters of neural networks in this study include the type of neural network, the number of hidden layers, the number of nodes in each hidden layer and the transfer function, as discussed in Section 2.3. The neural network types considered were a feedforward neural network and a cascade feedforward backpropagation neural network. The cascade feedforward backpropagation is similar to the feedforward neural network, with additional weights from each layer to the input layer, as discussed in Section 2.2.1. The number of hidden layers considered were a single hidden layer and two hidden layers. The functions from the neural network toolbox are listed and discussed in Appendix B. The range of nodes per hidden layer were 0 to 30. The threshold, linear, log-sigmoid and hyperbolic tangent transfer functions were considered as transfer functions.

To determine the type of neural network, the number of hidden layers, and the number of nodes in each hidden layer, R^2 was maximised and $AAD\%$ was minimised for both the training and testing data and the geometric distance (as discussed in Section 2.3). For each iteration, five values of R^2 and $AAD\%$ were determined in order to calculate the uncertainty, as discussed in Section 2.2.8. The

range of nodes per hidden layer were increased if the R^2 values increased significantly and the $AAD\%$ values decreased significantly at the end of the range.

To determine the transfer function, the $AAD\%$ of the training data was minimised, where each iteration was repeated five times to determine the uncertainty, as discussed in Section 2.2.8. After minimising R^2, maximising $AAD\%$ and minimising the geometric distance between the training and testing data, randomly selected P-xy plots of the training data and all of the testing data were evaluated.

3.4. Implementation of weights

Equations 2-23 and 2-24 were used to determine the relative importance of the input variables, as listed in Section 2.2.7. The inputs with the lowest relative importance had the lowest effect on the output variables.

3.5. Comparison of results to traditional modelling methods

After obtaining the optimum neural network for case studies 1 and 2, the bubble and dew point pressures are determined using the weight and bias vectors (for each case study respectively) where these results were compared to RK-Aspen models.

The RK-Aspen models can be determined by using Equations 2-2 to 2-13 as listed in Section 2.1.4 and Aspen Plus. As mentioned in Section 2.1.4, the polar factor and the BIP can be determined with regression.

Using the built-in data regression function in Aspen Plus and vapour pressures of the pure components (with Antoine parameters as listed in Table D-1), η_m were regressed using the following objective function which employs the Britt-Luecke minimisation procedure (Lombard, 2015):

$$OF = \sum_{m=1}^{N_{data}} \frac{P_{sat,m}^{exp} - P_{sat,m}^{calc}}{\left(P_{sat,m}^{exp}\right)^2} \qquad [3\text{-}1]$$

where N_{data} is the number of data points. Using the built-in data regression function in Aspen Plus, the pure component parameters as listed in Tables A-4 to A-6 and the VLE data listed in Tables A-1 to A-3, the BIP were regressed using the following objective function, performing a maximum likelihood estimation (also employed using the Britt Luecke minimisation procedure) (Lombard, 2015):

$$OF = \sum_{i=1}^{N_{group}} W_i \sum_{j=1}^{N_{data}} \left(\left(\frac{T_{exp} - T_{calc}}{\sigma_{T,j}} \right)^2 + \left(\frac{P_{exp} - P_{calc}}{\sigma_{P,j}} \right)^2 + \sum_{m=1}^{NC-1} \left(\frac{x_{exp} - x_{calc}}{\sigma_{x,j,m}} \right)^2 + \sum_{m=1}^{NC-1} \left(\frac{y_{exp} - y_{calc}}{\sigma_{y,j,m}} \right)^2 \right) \qquad [3\text{-}2]$$

where N_{group} is the number of data groups, N_{comp} is the number of components, W_i is the weights for each data group, and σ is the standard deviation for T, P, x, and y respectively. The regressed polar factors and BIPs are listed in Table E-2.

The results that were obtained after implementation of methods discussed in this chapter, are presented and discussed in Chapters 4 to 6 for case studies 1 to 3, respectively.

4. Results and discussion of case study 1: Neural network predicting binary phase behaviour of CO_2 and alkanes

For case study 1, VLE data containing CO_2 and alkanes were used to model high-pressure phase equilibria by training a simple neural network. The method (as discussed in Section 3) were followed to achieve the objectives. The structure of the neural network were investigated (objective 1) by determining the significant inputs using the randomisation approach (as discussed in Section 4.2), determining the relative importance of the input variables (as discussed in Section 4.4) and evaluating a neural network without the acentric factor as input variable (Section 4.5). The second objective were achieved by determining the hyperparameters (Section 4.3), and the results were compared to traditional modelling methods, as discussed in Section 4.6 (objective 3).

4.1. Collection and preparation of data

After obtaining data, as listed in Tables A-1 (VLE data) and A-4 (pure component data) in Appendix A, data points were added to distribute the data evenly, as discussed in Section 3.1. The number of data points available in each binary system at a specific temperature (N_b) and the number of binary systems available for each CL (N_{CL}) are listed in Table 4-1. As seen in this table, the maximum N_b is 46 and the maximum N_{CL} is 14. Therefore, data points were duplicated until there were 46 data points in each binary system at a specific temperature, and binary systems were duplicated until there were 14 binary systems for each CL. As mentioned in Section 3.1, the *linspace* function in MATLAB was used to duplicate data with linear spaces. Therefore, if for example data points with a CL of 8 are duplicated until 14 binary systems are present for each CL, the duplicated data systems will be at temperatures of 313 K, 348 K (Weng & Lee, 1992) and 393 K (Yu, *et al.*, 2006).

Table 4-1: Number of data points available for a specific chain length and temperature for alkanes

Chain length	N_{CL}	T (K)	N_b	Reference
5	4	311	28	Cheng et al. (1989)
		344	28	Cheng et al. (1989)
		378	26	Cheng et al. (1989)
		394	23	Cheng et al. (1989)

Table 4-1 *continued*

Chain length	N_{CL}	T (K)	N_b	Reference
6	3	313	20	Li et al. (1981)
		353	28	Li et al. (1981)
		393	30	Li et al. (1981)
7	3	311	46	Kalra et al. (1978)
		353	34	Kalra et al. (1978)
		394	34	Kalra et al. (1978)
8	11	313	12	Weng & Lee (1992)
		313	18	Yu et al. (2006)
		322	14	Jime´nez-Gallegos et al. (2006)
		328	12	Weng & Lee (1992)
		333	20	Yu et al. (2006)
		348	16	Weng & Lee (1992)
		348	18	Jime´nez-Gallegos et al. (2006)
		353	20	Yu et al. (2006)
		373	16	Yu et al. (2006)
		373	24	Jime´nez-Gallegos et al. (2006)
		393	20	Yu et al. (2006)
9	4	343	12	Jennings & Schucker (1996)
		315	16	Camacho-Camacho et al. (2007)
		345	16	Camacho-Camacho et al. (2007)
		373	22	Camacho-Camacho et al. (2007)
10	14	278	24	Reamer & Sage (1963)
		311	10	Iwai et al. (1994)
		311	24	Reamer & Sage (1963)
		313	10	Adams et al. (1988)
		319	16	Jime´nez-Gallegos et al. (2006)
		344	40	Nagarajan & Robinson (1986)
		344	12	Jennings & Schucker (1996)
		344	10	Iwai et al. (1994)
		344	18	Reamer & Sage (1963)
10	14	345	16	Jime´nez-Gallegos et al. (2006)
		373	26	Jime´nez-Gallegos et al. (2006)
		378	46	Nagarajan & Robinson (1986)
		378	22	Reamer & Sage (1963)
11	3	315	18	Camacho-Camacho et al. (2007)
		344	18	Camacho-Camacho et al. (2007)
		373	20	Camacho-Camacho et al. (2007)
12	1	318	20	Gardeler et al. (2002)
15	3	292	21	Scheidgen (1997)
		298	15	Scheidgen (1997)
		316	19	Scheidgen (1997)

Table 4-1 *continued*

Chain length	N_{CL}	T (K)	N_b	Reference
16	7	314	12	D'Souza et al. (1988)
		323	10	Pohler (1994)
		333	12	D'Souza et al. (1988)
		353	14	Kordikowski & Schneider (1993)
		353	10	D'Souza et al. (1988)
		353	14	Kordikowski & Schneider (1993)
		393	30	Spee & Schneider (1991)
17	5	323	12	Pohler (1994)
		333	12	Pohler (1994)
		353	12	Pohler (1994)
		373	14	Pohler (1994)
		393	16	Pohler (1994)
18	5	323	12	Pohler (1994)
		333	12	Pohler (1994)
		353	12	Pohler (1994)
		373	14	Pohler (1994)
		393	16	Pohler (1994)
19	9	318	10	Pohler (1994)
		323	10	Pohler (1994)
		333	10	Pohler (1994)
		343	18	Pohler (1994)
		348	14	Pohler (1994)
		353	10	Kordikowski & Schneider (1993)
19	9	353	10	Kordikowski (1992)
		393	14	Kordikowski & Schneider (1993)
		393	14	Kordikowski (1992)
20	6	323	10	Huang et al. (1988)
		353	14	Kordikowski & Schneider (1993)
		353	14	Kordikowski (1992)
		373	10	Huang et al. (1988)
		393	16	Kordikowski & Schneider (1993)
		393	16	Kordikowski (1992)

After obtaining data, the structure of the neural network was determined. The inputs of a neural network form part of the structure, and will be discussed in Section 4.2.

4.2. Determination of significant inputs of the neural network

To determine the inputs of a neural network, a preliminary neural network is required. For a first iteration, a feedforward neural network with one hidden layer using the log-sigmoid transfer function was used as discussed in Section 3.2. The number of nodes in each hidden layer was determined by maximising R^2 and minimising $AAD\%$ and the geometric distance between the training and testing data of both R^2 and $AAD\%$ values (as discussed in Section 2.3, illustrated in Figure 4-1 and listed in Table C-1, Appendix C). The geometric distance is the difference between the training and the testing data for the R^2 and *AAD%* values, respectively. For each iteration, five neural networks were train to determine five values of the R^2 and $AAD\%$ values. The uncertainty of each iteration was determined using Equation 2.25 as listed in Section 2.2.8.

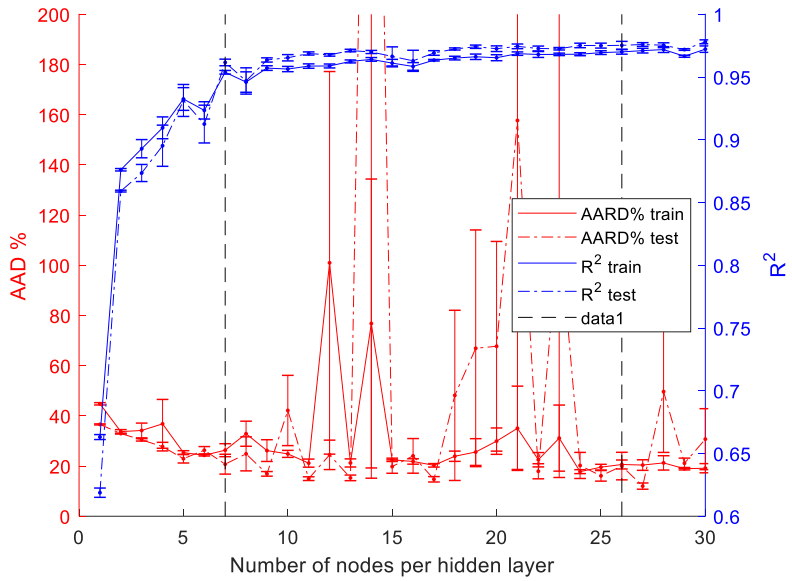

Figure 4-1: Preliminary AAD % and R^2 results of neural networks using a range of number of nodes per hidden layer using binary system data containing CO_2 and alkanes

As seen in Figure 4-1, the overall trend of the $AAD\%$ values decrease as the number of nodes in each hidden layer increase. The $AAD\%$ values start to oscillate more rapidly at 7 nodes for the training and testing data, where at 26 nodes the $AAD\%$ and geometric distance are minimised. The values of the R^2, *AAD%* and geometric distances are listed in Table C-1, Appendix C.

Overall, R^2 increases as the number of nodes increases in each hidden layer. The geometric distances of the R^2 values for 9 to 30 nodes are approximately the same, where the maximum R^2 values range between 21 and 28 nodes.

As concluded from Figure 4-1, since at 7 nodes per hidden layer the $AAD\%$ values start to oscillate more rapidly and the R^2 values increase less gradually, 7 nodes per hidden layer is the minimum number of nodes required. At 26 nodes, $AAD\%$ is minimised and R^2 is maximised.

Thee P-xy results obtained from the testing data for pentane at 311 K using 7 and 26 nodes are compared to experimental results as obtained by Cheng, et al. (1989) in Figure 4-2.

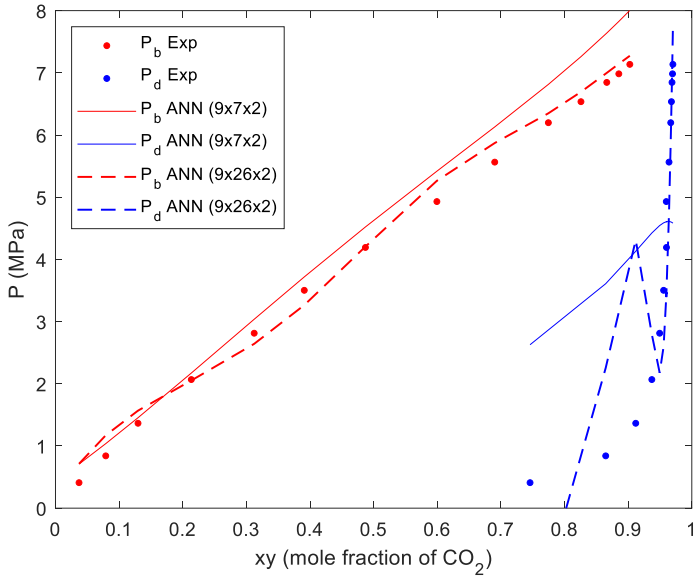

Figure 4-2: Bubble and dew point pressures of a binary system with CO_2 and pentane at 311 K obtained from experimental data (Cheng et al., 1989), an ANN with a size of $(9 \times 7 \times 2)$ and an ANN with a size of $(9 \times 26 \times 2)$ using CO_2 and alkanes as testing data

As seen in this figure, the neural network with 26 nodes resulted in better predictions for the bubble (P_b) and dew point (P_d) pressures. At low pressures, the neural network with 26 nodes oscillates, but still provides better predictions than the neural network with 7 nodes. Therefore, a neural network with one hidden layer and 26 nodes in the hidden layer was used to determine the significant inputs to the neural network for case study 1.

To determine the significant inputs to the neural network, the effect of randomising data points of all input variables respectively was measured using the $AAD\%$ of the testing data, as discussed in Sections 2.2.5 and 3.2 and illustrated in Figure 4-3. For case study 1, acentric factor (w), critical temperature (T_c) and pressure (P_c) of the alkane, system temperature (T), chain length (CL) and molecular mass (MM) of the alkane, vapour-liquid distinction (x/y) and the liquid and vapour composition of CO_2 were considered as initial inputs. To determine the normal condition, no inputs were randomised and were used as a reference (step 1, Section 3.2). To determine the $AAD\%$ after randomising each input variable, steps 2 to 4 were performed, as discussed in Section 3.2.

As seen in Figure 4-3, all $AAD\%$ values obtained by randomising a specific input to the neural network have values (26.99%, 19.54%, 51.09%, 19.96%, 37.81%, 31.37% and 25.12% for T_c, T, CL, MM, x/y, x and y) higher than the normal condition (14.96%), except for P_c (13.19%) and w (14.28%).

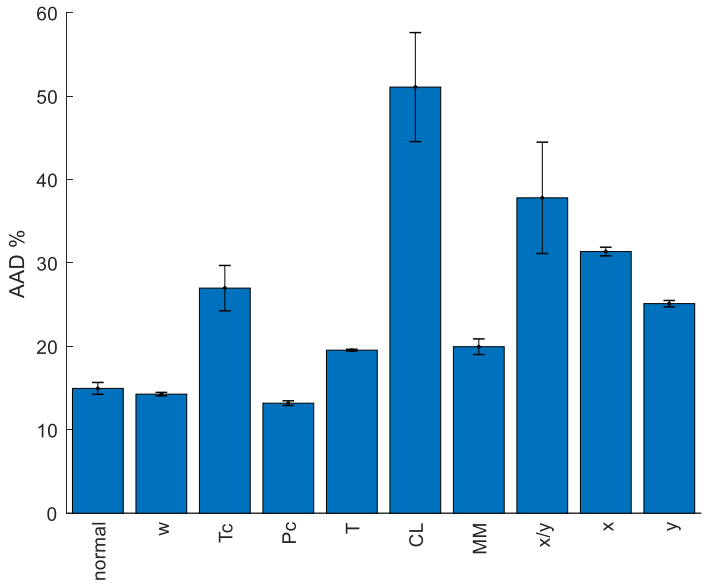

Figure 4-3: The AAD % of the testing data to determine the significant inputs using all input variables for binary system containing CO_2 and alkanes

P_c were therefore eliminated as input to the neural network (as discussed in step 6, Section 3.2), as illustrated in Figure 4-4.

Although the $AAD\%$ of the normal condition increased from 14.96% to 18.98% by eliminating P_c as input variable, the $AAD\%$ randomising CL (15.89%) remained approximately the same as the previous normal condition of 14.96% (Figure 4-4). Furthermore, all $AAD\%$ values obtained by randomising a specific input to the neural network have values (24.55%, 32.73%, 18.94%, 21.45%, 21.75%, 31.67% and 26.89% for w, T_c, T, MM, x/y, x and y) that are relatively the same or higher than the current normal condition, except for CL, as mentioned above. Therefore, CL were removed as input.

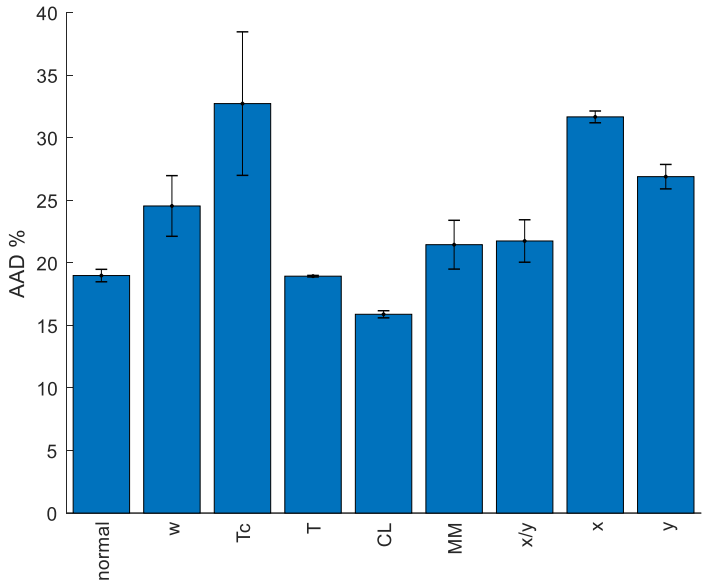

Figure 4-4: The AAD % of the testing data to determine the significant inputs where the critical pressure is eliminated as input using binary system data containing CO_2 and alkanes

Figure 4-5 illustrates the $AAD\%$ of the testing data (randomising each input respectively) where P_c and CL were eliminated as input variables. As seen in this figure, all $AAD\%$ have values relatively the same or larger than the normal condition. Therefore, no further inputs were removed.

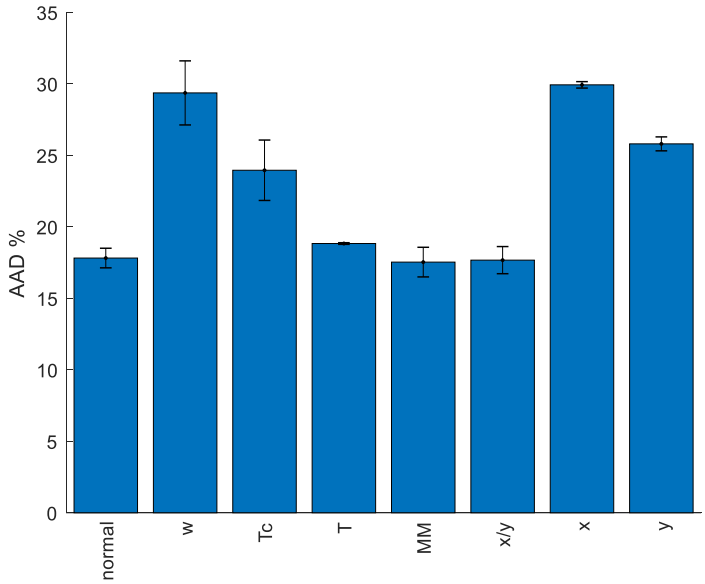

Figure 4-5: The AAD % of the testing data to determine the significant inputs where the chain length and critical pressure are eliminated as inputs using binary system data containing CO_2 and alkanes

Evaluating the results as obtained in this section, Figure 4-6 illustrates the P-xy results (Cheng et al., 1989) from the testing set comparing a neural network where no inputs were removed (ANN), where P_c was removed as input (ANN_{P_c}) (Figure 4-3) and a neural network where P_c and CL were removed

as inputs ($ANN_{P_{c\&CL}}$) (Figure 4-4). As seen in this figure, $ANN_{P_c\&CL}$ resulted in accurate results for the whole pressure range for the bubble and dew point pressures. ANN oscillates at low pressures for dew point predictions and through the whole pressure range for bubble point predictions. ANN_{P_c} resulted in relatively accurate results, but were over predicted at high bubble point pressures and under predicted at low dew point pressures. It is clear from Figure 4-6 that $ANN_{P_c\&CL}$ resulted in better predictions.

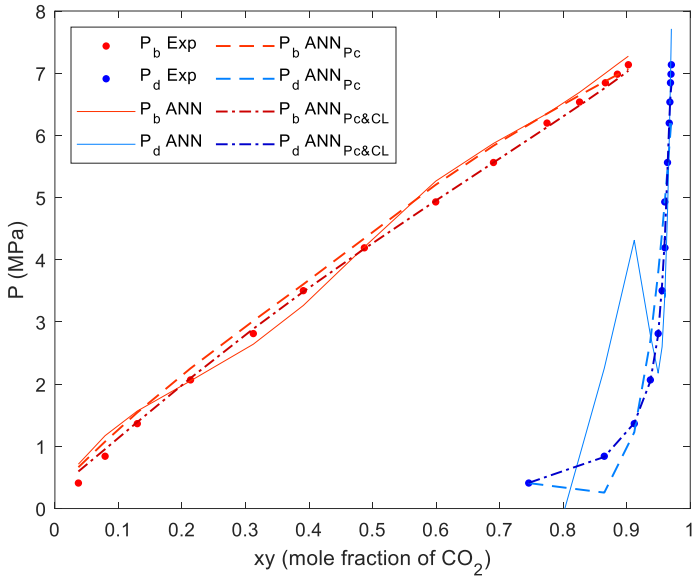

Figure 4-6: Bubble and dew point pressures of a binary system with CO_2 and pentane at 311 K obtained from experimental data (Cheng et al., 1989), an ANN where no inputs were removed, an ANN with Pc removed as input and an ANN with Pc and CL removed as input using CO_2 and alkanes as testing data

The significant inputs to the neural network for case study 1 were therefore acentric factor (w), critical temperature (T_c) of the alkane, system temperature (T), molecular mass (MM) of the alkane, vapour-liquid distinction (x/y) and the liquid (x) and vapour (y) composition of CO_2. Using these inputs to the neural network, the hyperparameters were determined, as discussed in the next section.

4.3. Determination of hyperparameters

The hyperparameters of the neural network were determined by using the determined inputs as calculated in Section 4.2, and will be discussed in this section. The hyperparameters include the type of neural network, number of hidden layers, number of nodes in each hidden layer and the transfer functions. A feedforward neural network and a cascade feedforward backpropagation neural network were considered, as proposed by Lashkarbolooki, Vaferi et al. (2013), Lashkarbolooki, Shafipour et al. (2013), Vaferi et al. (2013), Vaferi et al. (2018), and Lashkarbolooki et al. (2011). The type of neural network, the number of hidden layers and the number of nodes in each hidden layer were

determined by maximising R^2 and minimising $AAD\%$ and the geometric distance between the training and testing data of the R^2 and $AAD\%$ values, as discussed in Section 2.3. As mentioned earlier, the geometric distance is the difference between the training and testing results for R^2 and $AAD\%$ respectively. The threshold, linear, log-sigmoid and hyperbolic tangent transfer functions were considered, as described in Section 2.2.2. The transfer function was selected based on the $AAD\%$ of the testing data. The optimum hyperparameters were evaluated using P-xy plots of the testing data before finalising the hyperparameters.

Figure 4-7 to Figure 4-8 and Figure 4-10 to Figure 4-11 illustrate the results of the R^2 and $AAD\%$ values for the training and testing data using different types of neural networks and numbers of hidden layers. The R^2 and $AAD\%$ values of the training and testing data and the geometric distances of these values (as used in Figure 4-7 to Figure 4-8 and Figure 4-10 to Figure 4-11 are listed in Tables C-2 to C-5 in Appendix C.

Figure 4-7 and Figure 4-8 illustrate the results of the R^2 and $AAD\%$ values for the training and testing data using a feedforward neural network with one and two hidden layers respectively with the number of nodes in each hidden layer ranging from 0 to 30, whereas **Error! Reference source not found.** depicts the P-xy results of the considered hyperparameters for the feedforward neural networks.

As seen in Figure 4-7, R^2 sharply increases and *AAD%* sharply decreases between 1 and 4. Both R^2 and $AAD\%$ oscillate between 4 and 8 nodes per hidden layer. After 8 nodes per hidden layer, the R^2 and $AAD\%$ values stabilise with small oscillations. At 20 nodes per hidden layer, the values and geometric distances of $AAD\%$ are relatively small, and will therefore be selected for the feedforward neural network with one hidden layer resulting in R^2 and $AAD\%$ of 0.964 and 19.72% for the training data and 0.972 and 20.41% for the testing data, respectively.

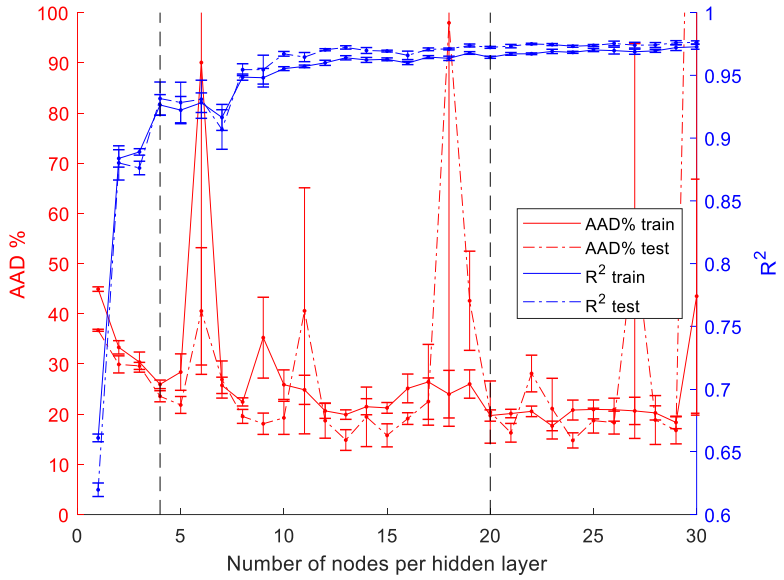

Figure 4-7: R^2 and AAD % values for the training and testing data using a feedforward neural network and one hidden layer using binary system data containing CO_2 and alkanes

It should be noted that the testing statistics are lower than the training statistics, and could be explained by the test sets being too small or that the binary systems selected for the test set might be easier to fit compared to the training sets since test sets were selected based on which binary systems were available that was also modelled using EOS. This problem could be resolved by increasing the size of the test set. Since the results were compared to EOS, randomly selecting test sets were not possible, therefore limiting the process where test sets were selected.

As seen in Figure 4-8, for two hidden layers, the R^2 values sharply increase between 1 and 6 nodes per hidden layer, and stabilise after 6 nodes per hidden layer. The $AAD\%$ values gradually decrease as the number of nodes per hidden layer increases, reaching an average minimum (between the training and testing data) at 26 nodes per hidden layer. At 26 nodes per hidden layer, R^2 is maximised and $AAD\%$ is minimised, with relatively small geometric distance values. Therefore, 26 nodes in each hidden layer were considered to be the optimum size for a feedforward neural network with two hidden layers resulting in R^2 and $AAD\%$ of 0.992 and 9.67% for the training data and 0.991 and 5.62% for the testing data.

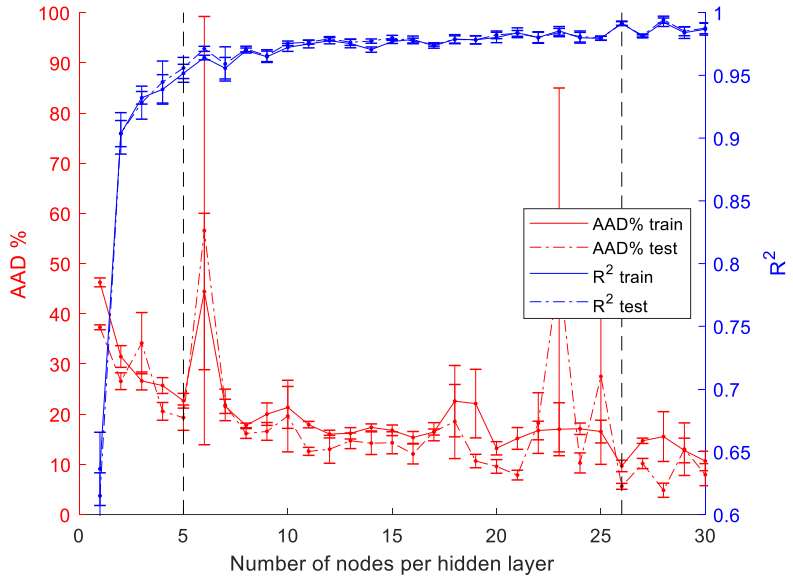

Figure 4-8: R^2 and AAD % values for the training and testing data using a feedforward neural network and two hidden layers using binary system data containing CO_2 and alkanes

When comparing Figure 4-7 and Figure 4-8, the R^2 values of the ANN with two hidden layers stabilises faster, compared to the ANN with one hidden layer. Since the geometric distances were minimised for both the R^2 and *AAD%* values while maximising and minimising these values, a higher number of nodes in the hidden layers were selected to optimise all these parameters.

As concluded from Figure 4-7 and Figure 4-8, there is a point where the R^2 and $AAD\%$ values start to oscillate, and a point where the maximum R^2 and minimum $AAD\%$ and geometric distance values are reached. **Error! Reference source not found.** compares experimental measurements obtained by Cheng et al. (1989) with these two points obtained by each type of neural network presented in Figure 4-7 (resulting in a $7 \times 4 \times 2$ and a $7 \times 20 \times 2$ neural network) and Figure 4-8 (resulting in a $7 \times 5 \times 5 \times 2$ and a $7 \times 26 \times 26 \times 2$ neural network). As seen in **Error! Reference source not found.**, for the bubble point pressures the $7 \times 4 \times 2$ and $7 \times 20 \times 2$ neural networks under and over predicted at low pressures and over and under predicted at high pressures, forming second order polynomial curves for predictions from both neural networks, which do not agree with the form of experimental data, forming a logarithmic curve. The predicted dew point values for the $7 \times 4 \times 2$ and $7 \times 20 \times 2$ neural networks formed a near linear line, predicting poorly at high and low pressures. For both the $7 \times 5 \times 5 \times 2$ and $7 \times 26 \times 26 \times 2$ neural networks, similar forms for the bubble point pressures were obtained as for the experimental data. The $7 \times 5 \times 5 \times 2$ neural network predicted dew point pressures poorly. Overall, the $7 \times 26 \times 26 \times 2$ neural network made good predictions for bubble and dew point pressures.

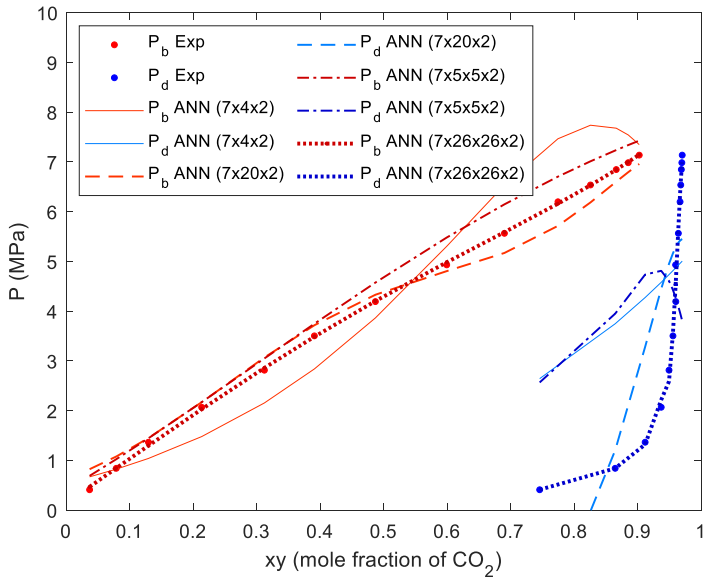

Figure 4-9:Bubble and dew point pressures of a binary system with CO_2 and pentane at 311 K obtained from experimental data (Cheng et al., 1989) and ANNs using a feedforward neural network with sizes of $7 \times 4 \times 2$, $7 \times 20 \times 2$, $7 \times 5 \times 5 \times 2$*and* $7 \times 26 \times 26 \times 2$ *respectively containing CO_2 and alkanes as testing data*

In conclusion, for the feedforward neural network, a neural network with two hidden layers and 26 nodes in each layer resulted in the best predictions.

Figure 4-10 and Figure 4-11 illustrate the $AAD\%$ and R^2 values for the training and testing data of a cascade feedforward backpropagation neural network for one and two hidden layers respectively with a range of 0 to 30 nodes in each hidden layer, whereas Figure 4-12 compares the P-xy results of the considered hyperparameters using a cascade feedforward backpropagation neural network.

As seen in Figure 4-10, R^2 increases as the nodes in each hidden layer increase where the R^2 values and geometric distances start to stabilise (with a slight increase) at 9 nodes per hidden layer. At 17, 25 and 29 nodes per hidden layer, peaks occur for the R^2 values. $AAD\%$ decreases as the number of nodes per hidden layer increases. At 4 nodes per hidden layer, $AAD\%$ starts to stabilise with some oscillation. Comparing the results at 25 and 29 nodes per hidden layer, the geometric distance for the $AAD\%$ values at 25 nodes is smaller. Therefore, 25 nodes per hidden layer were selected for a cascade feedforward backpropagation neural network with one hidden layer resulting in R^2 and $AAD\%$ values of 0.972 and 19.54% for the training data and 0.976 and 15.42% for the testing data respectively.

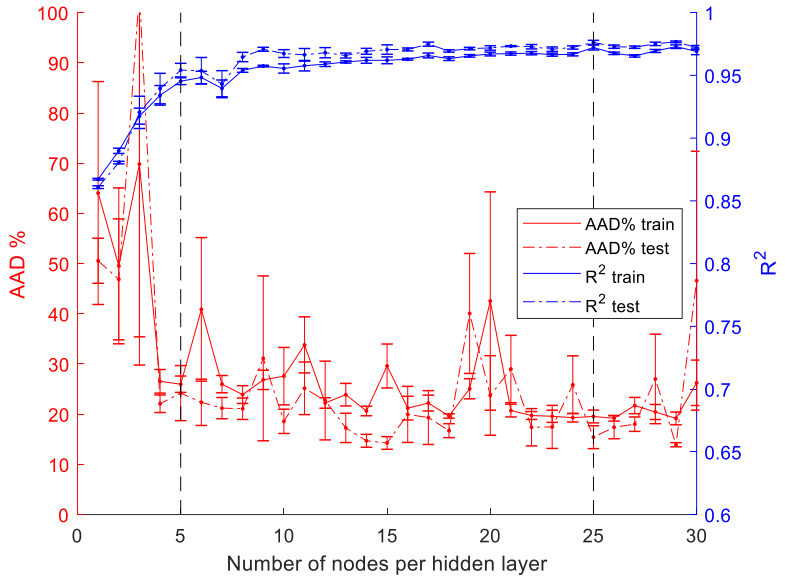

Figure 4-10: R^2 and AAD % values for the training and testing data using a cascade feedforward backpropagation neural network and one hidden layer using binary system data containing CO_2 and alkanes

As seen in Figure 4-11, R^2 increases and $AAD\%$ decreases as the number of nodes per hidden layer increases. At 9 nodes per hidden layer, both the R^2 and $AAD\%$ values start to stabelize. R^2 is at a maximum and $AAD\%$ is at a minimum at 22 nodes per hidden layer with small geometric distances relative to the other values. Therefore, 22 nodes per hidden layer was selected for a cascade feedforward backpropagation neural network with two hidden layers with R^2 and $AAD\%$ values of 0.966 and 25.45% for the training data and 0.944 and 17.64% for the testing data respectively.

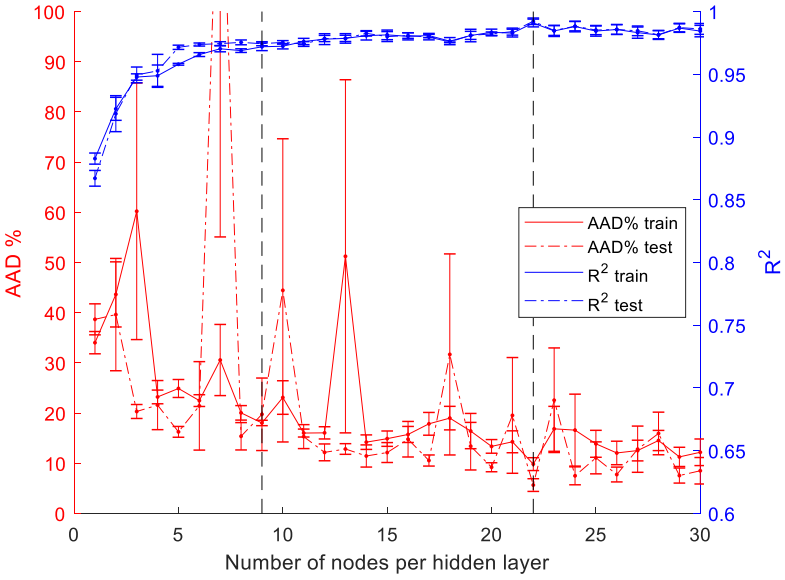

Figure 4-11: R^2 and AAD % values for the training and testing data using a cascade feedforward backpropagation neural network and two hidden layers using binary system data containing CO_2 and alkanes

As seen in Figure 4-10 and Figure 4-11 (and **Error! Reference source not found.**), there is a point where the R^2 and $AAD\%$ values start to oscillate, and a point where the maximum R^2 and minimum $AAD\%$ and geometric distance values are reached. In Figure 4-12, the results from Figure 4-10 ($7 \times 5 \times 2$ and $7 \times 25 \times 2$ neural networks) and Figure 4-11 ($7 \times 9 \times 9 \times 2$ and $7 \times 22 \times 22 \times 2$ neural networks) are compared with experimental results obtained by Cheng et al. (1989). As seen in this figure, the $7 \times 5 \times 2$ neural network under predicts at medium to high pressures and over predicts at low pressures for the bubble point pressure predictions, where for dew point pressures, the $7 \times 5 \times 2$ neural network made an approximate linear prediction, over predicting at low pressures and under predicting at high pressures. The $7 \times 25 \times 2$, $7 \times 9 \times 9 \times 2$ and $7 \times 22 \times 22 \times 2$ neural networks predict the dew point pressures well at high pressures, where bubble point predictions are relatively accurate. Although the $7 \times 22 \times 22 \times 2$ seems to fit experimental data better for both the bubble and dew point predictions, the $7 \times 9 \times 9 \times 2$ neural network curves make a better fit compared with the experimental data curve.

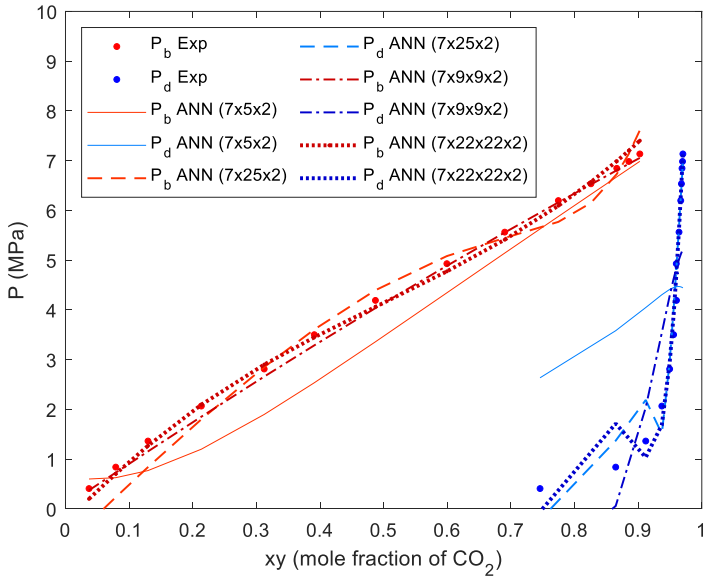

Figure 4-12: Bubble and dew point pressures of a binary system with CO_2 and pentane at 311 K obtained from experimental data (Cheng, et al., 1989) and ANNs using a cascade feedforward neural network with sizes of $7 \times 5 \times 2$, $7 \times 25 \times 2$, $7 \times 9 \times 9 \times 2$ and $7 \times 22 \times 22 \times 2$ respectively containing CO_2 and alkanes as testing data

When comparing results presented in **Error! Reference source not found.** and Figure 4-12 (using the optimal nodes presented in Figure 4-7, Figure 4-8, Figure 4-10 and Figure 4-11), a feedforward neural network with 2 hidden layers and 26 nodes in each layer resulted in the best predictions.

The R^2 and $AAD\%$ values for the neural networks are listed in Table 4-2 where the R^2 and AAD% values start to oscillate and the optimised point, as obtained in Figure 4-7, Figure 4-8, Figure 4-10 and Figure 4-11. As seen in Table 4-2, the neural networks with two hidden layers performed better than the neural networks with only one hidden layer. When comparing the types of neural networks, the feedforward neural network is slightly better than the cascade feedforward backpropagation network.

Table 4-2: Optimal R^2 and AAD % to determine the neural network structure using binary system data containing CO_2 and alkanes

Neural network type		**Start of oscillations**			**Optimal point**		
		Training	**Testing**	**Neural network structure ($N_{HL} \times N_{nodes}$)**	**Training**	**Testing**	**Neural network structure ($N_{HL} \times N_{nodes}$)**
Feedforward	R^2	0.926	0.932	$7 \times 4 \times 2$	0.964	0.972	$7 \times 20 \times 2$
	AAD %	25.9	23.6		19.7	20.4	
Feedforward	R^2	0.952	0.956	$7 \times 5 \times 5 \times 2$	0.992	0.991	$7 \times 26 \times 26 \times 2$
	AAD %	22.7	19.3		9.7	5.6	
Cascade feedforward backpropagation	R^2	0.945	0.954	$7 \times 5 \times 2$	0.972	0.976	$7 \times 25 \times 2$
	AAD %	26.0	24.2		19.5	15.4	
Cascade feedforward backpropagation	R^2	0.972	0.974	$7 \times 9 \times 9 \times 2$	0.991	0.992	$7 \times 22 \times 22 \times 2$
	AAD %	18.0	19.8		9.8	5.7	

As summarised from Figure 5-9 and Figure 5-12, the optimal structures for a feedforward and a cascade feedforward backpropagation neural network are $7 \times 26 \times 26 \times 2$ and $7 \times 9 \times 9 \times 2$, respectively. When comparing these two figures, the feedforward neural network with a size of $7 \times 26 \times 26 \times 2$ resulted in better predictions. This result is in agreement with the results presented in Table 4-2 and were therefore used for further optimisation of selecting a transfer function. It should be noted that the number of adjustable parameters are a lot compared to the number of data points, but smaller neural networks were considered in this sections where the hyperparameters were determined, but the larger neural networks resulted in better results. The trade-off was between larger neural networks possibly being slightly overfitted.

Figure 4-13 illustrates the $AAD\%$ of the testing data for a feedforward neural network with a size of $7 \times 26 \times 26 \times 2$ using the threshold, linear, log-sigmoid and hyperbolic tangent transfer function respectively. As seen from this figure, the $AAD\%$ of the testing data using the threshold, linear, log-sigmoid and hyperbolic tangent transfer functions were 39.89%, 45.32%, 8.97% and 12.65%, respectively. The log-sigmoid transfer function resulted in the lowest $AAD\%$ of the testing data. This is in agreement with Lashkarbolooki & Shafipour et al. (2013), Lashkarbolooki & Vaferi et al. (2013), Vaferi et al. (2018) and Vaferi et al. (2013), since they also used the log-sigmoid transfer function modelling VLE data using neural networks.

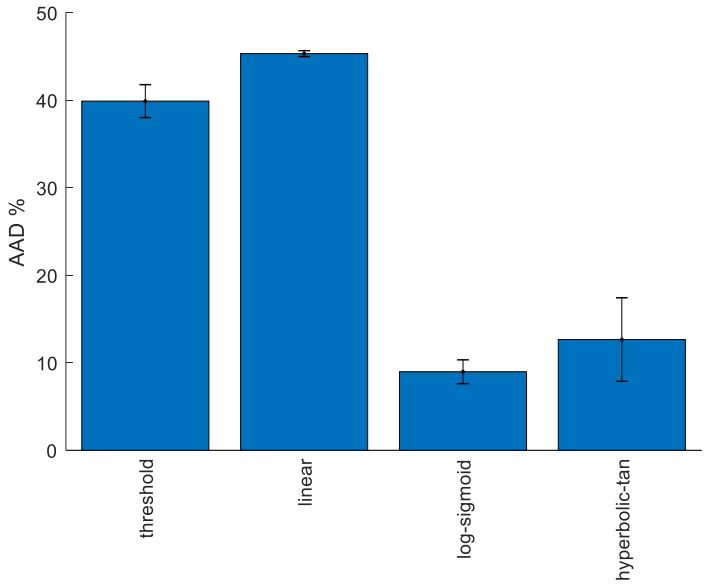

Figure 4-13: The AAD % values for the testing data using a feedforward neural network with a threshold, linear, log-sigmoid and hyperbolic tangent transfer function respectively using binary system data containing CO_2 and alkanes

The optimised hyperparameters for a neural network predicting the bubble and dew point pressures using CO_2 and alkanes data are a feedforward neural network with two hidden layers, 26 nodes in each hidden layer using the log-sigmoid function as transfer function.

Figure 4-14 compares the experimental results of the binary systems (as illustrated and discussed in Section 2.1.2 using Figure 2-2) with the ANN results with optimised hyperparameters as determined in this section. The AAD% of the ANN results deviating from the experimental data (Exp) of the binary systems as illustrated in this figure are 15.68%, 2.51%, 0.75%, 1.18% and 0.97% for the CO_2 and octane (Yu, et al., 2006), CO_2 and nonane (Camacho-Camacho, et al., 2007), CO_2 and undecane (Camacho-Camacho, et al., 2007), CO_2 and heptadecane (Pholer, 1994) and CO_2 and octadecane (Pholer, 1994) systems respectively at 373 K. As seen in this figure and as indicated by the AAD% values, overall, the AAD% decreases as the chain length increases. As further observed from these

figure, the lower chain length binary systems predicts the bubble point pressures better at high pressures compared to low pressures. This is interesting since EOS predicts these pressures better at low pressures but are unable to make predictions in the supercritical region for certain binary systems.

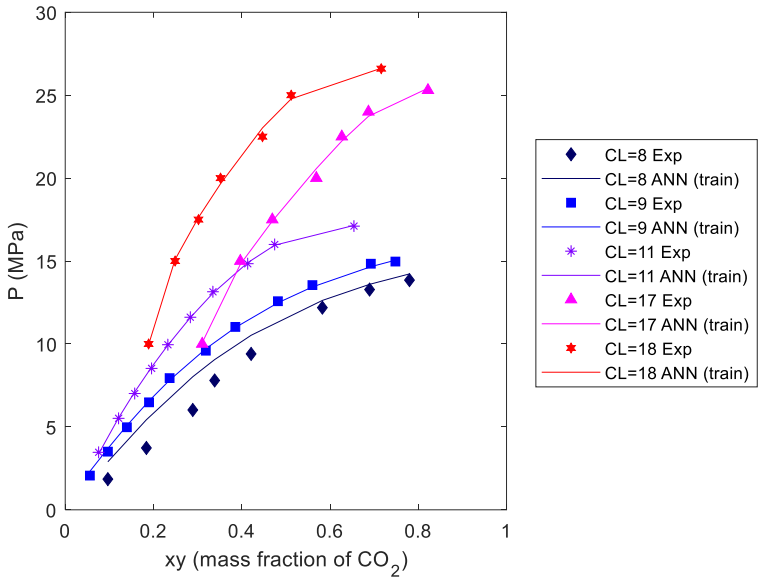

Figure 4-14: ANN results comparing the chain length, bubble point pressure and mass fraction for CO_2 of alkanes at 373 K – data from Yu et al. (2006), Camacho-Camacho et al. (2007) and Pohler (1994)

Figure 4-15 illustrates the results of the ANN compared to with experimental results of CO_2 and decane at different temperatures (Reamer & Sage, 1963). The AAD% of the binary systems at 227 K, 310 K, 344 K and 377 K are 24.70%, 23.22%, 32.16% and 0.81% respectively. It should be noted that the binary system at 344 K is part of the testing data, therefore resulting in the poorest predictions with an $ADD\%$ of 32.16%. Overall, as seen from this figure and as observed from the ADD% values, the accuracy of the predictions increases as the temperature increases.

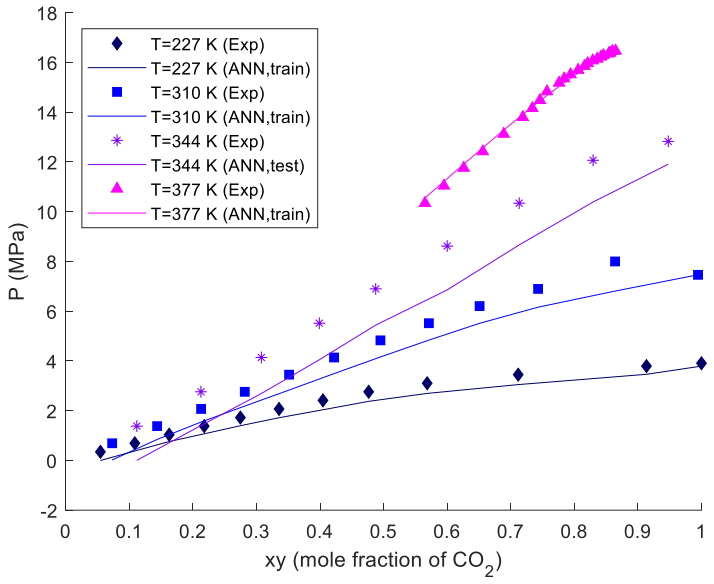

Figure 4-15: ANN predictions of the bubble point pressures compared to experimental results from (Reamer & Sage (1963) for case study 1

4.4. Relative importance of the input variables

As discussed in Sections 2.2.7 and 3.4, the weights can be implemented using the connection weight approach. Tables D-1 to D-3 in Appendix D list the connection weights and biasses of the neural network for case study 1 as determined in Sections 4.1 to 4.3. As seen in these tables, the bias values are in the same order as the connection weighs, indicating that the model is not overfitted, as discussed in Section 2.2.1. Further, as observed in these tables, some of the connection weight values are close to zero, indicating that the connection weight plays a small role determining the outputs of the neural network. These connection weights with small magnitudes will be outlined using the connection weight approach.

Using the connection weights, as listed in Tables D-1 to Table D-3, the relative importance of the input variables can be determined using the connection weight approach (Equations 2-23 and 2-24), as discussed in Sections 2.2.7 and 3.4. Figure 4-16 illustrates the relative importance of the inputs relative to each output variable (the bubble and dew point pressures). For the bubble point pressure output, the relative importance of the inputs relative to the first output is 16.9%, 4.3%, 24.5%, 12.3%, 12.2%, 22.1%, and 7.6% for w, T_c, T, MM, x/y, x and y respectively. The relative importance of the inputs relative to the second output is 17.7%, 10.9%, 22.5%, 19.6%, 6.5%, 2.6% and 20.3% w, T_c, T, MM, x/y, x and y respectively.

The system temperature (T) is the most important input variable, when determining the relative importance for both the bubble and dew point pressures. It is interesting that the liquid composition

of CO_2 (x) and the vapour composition of CO_2 (y) are high when determining the relative importance of the bubble point pressure and the dew point pressure, respectively. These are the data point inputs, as listed in Table 3-1 required to specify the phase boundary.

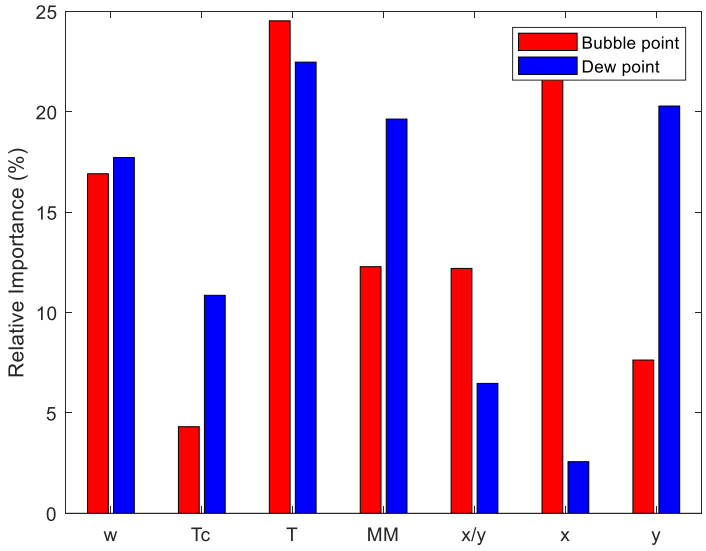

Figure 4-16: Relative importance of the input variables relative to the output variables (bubble point and dew point pressure pressures) of the neural network for case study 1

As mentioned in section 2.1.4, the parameters required for the RK-Aspen EOS are the pure component parameters ($T_{c,m}$, $P_{c,m}$, $w_{c,m}$ and η_m) and the binary interaction parameters ($k^0_{a,mn}$, $k^1_{a,mn}$, $k^0_{b,mn}$ and $k^1_{b,mn}$). To determine η_m, additional vapour pressure data for the pure component are required, whereas for the BIPs, additional phase equilibrium data are required. Table 4-3 compares the parameters used for the ANN and the RK-Aspen EOS. As seen in this table, the contrasting parameters are the vapour pressure data and the critical pressure used for the RK Aspen EOS and the molecular mass used in the ANN.

Table 4-3: Comparison between the parameters required for the ANN and the RK Aspen EOS

	Parameters required for RK Aspen EOS	**Parameters required for ANN**
Identical parameters for the models	Phase equilibrium data, w, T_c	Phase equilibrium data, w, T_c
Contrasting parameters for the models	Vapour pressure data, P_c	MM

The acentric factor is important for determining both output variables, as seen in Figure 4-16 (and Table 4-3). Since the acentric factor is relatively important as input variable, predictions for some hydrocarbons will be less accurate because the acentric factor is not available (although it is possible

to calculate) for some pure components (for example hydrocarbons with long CLs). In the next section, a neural network without the acentric factor will be evaluated if future work requires modelling of compounds where the acentric factor is not available.

4.5. Neural networks without the acentric factor as input variable

In this section, a feedforward neural network with two hidden layers and the log-sigmoid transfer function (as determined in Section 4.3) without the acentric factor will be discussed and the impact on the results will be depicted using a P-xy diagram with pentane at 311 K comparing results obtained by Cheng, *et al*. (1989) and neural network predictions.

Using a feedforward neural network with two hidden layers, the number of nodes per hidden layer was determined, as illustrated in Figure 4-17. As determined in the previous sections, R^2 was maximised and $AAD\%$ and the geometric distance were minimised. As seen in this figure, the optimum number of nodes per hidden layer is 29 nodes resulting in R^2 values of 0.989 and 0.988 and $AAD\%$ values of 10.5% and 6.4% for the training and testing data.

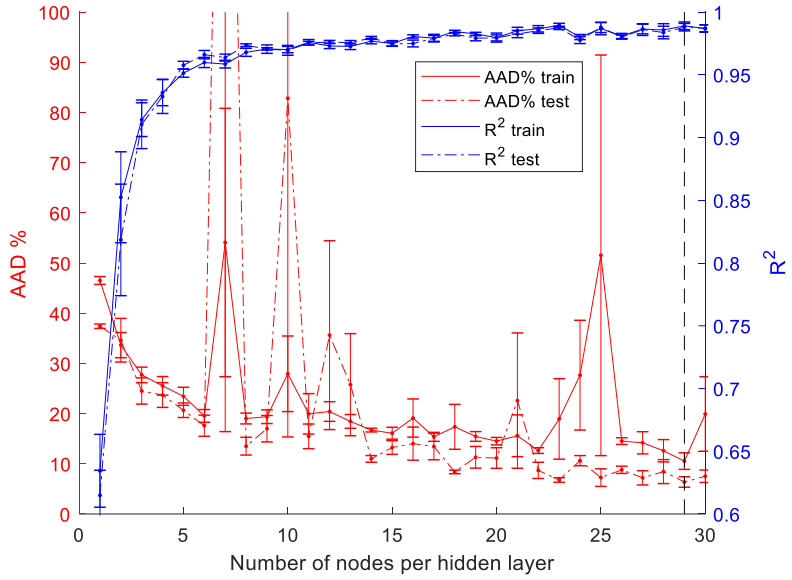

Figure 4-17: R^2 and AAD % values for the training and testing data using a feedforward neural network without the acentric factor as input containing CO_2 and alkanes as training data

Figure 4-18 provides the P-xy results of pentane and CO_2 comparing an ANN without the acentric factor as presented in Figure 4-17 (ANN_w) with experimental data (Cheng et al., 1989) and an ANN with the acentric factor (ANN) (as determined in Sections 4.2 to 4.3). It is expected that the neural network without the acentric factor would perform worse than the other networks. As seen in this figure, the bubble point prediction for the neural network without the acentric factor as input is accurate relative to the experimental results and the results obtained by previous sections with slight

under predictions at high pressures. Since the dew point region at high pressure is important when determining the feasibility of a process, it is interesting to note that the dew point pressures resulted in relatively accurate predictions at high pressures, where predictions at medium and low pressures are slightly over and under predicted at medium and low pressures with approximately 1 MPa and 2 MPa.

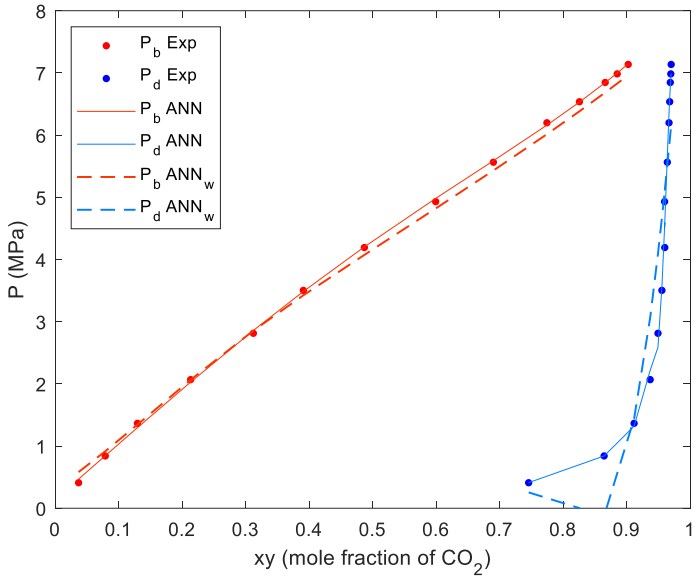

Figure 4-18:Bubble and dew point pressures comparing binary system with CO_2 and pentane at 311 K obtained from experimental data (Cheng et al., 1989, an ANN with the acentric factor as input and an ANN without the acentric factor as input containing CO_2 and alkanes as testing data

Although it is more favourable to use the acentric factor when predicting high-pressure phase equilibria, a network without the acentric factor made accurate predictions, especially at high pressures.

For the final objective, the neural network, determined in Section 4.2 and 4.3 will be compared to traditional modelling methods in the following section.

4.6. Neural networks relative to traditional modelling methods

In this section, a neural network with optimised hyperparameters as calculated in Sections 4.2 and 4.3 will be compared to traditional modelling methods.

Figure 4-19 depicts the regression plot of the optimised neural network (as determined in Sections 4.2 and 4.3) for the training and validation (with combined R^2 and $AAD\%$ values of 0.995 and 24.1%) and testing data (with R^2 and $AAD\%$ values of 0.995 and 4.4%) of the bubble and dew point pressures. For the training data, bubble and dew point pressures are accurate within 10% (as indicated by the dashed lines) for pressures above 12 MPa (for bubble point pressures) and 20 MPa (for dew

point pressures) where the maximum pressure deviations are within 4.4 MPa and 6.3 MPa, respectively. For the testing data, bubble and dew point pressures are accurate within 10% for pressures above 0.5 MPa and 7.5 MPa, respectively, whereas the maximum pressure deviations are within 0.05 MPa and 3.2 MPa, respectively. For the validation data, bubble and dew point pressures are accurate within 10% for pressures above 0.5 MPa and 10.6 MPa, respectively, whereas the maximum pressure deviations are within 0.05 MPa and 2.7 MPa, respectively.

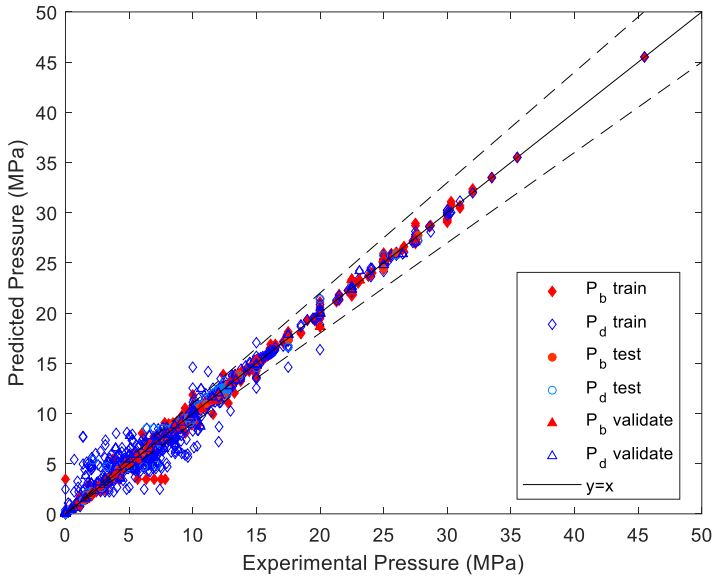

Figure 4-19: Predicted pressure vs experimental pressure using the training, testing and validation data using the optimised hyperparameters for case study 1

Figure 4-20 and Figure 4-21 illustrates the comparison of the P-xy diagrams of the binary systems containing CO_2 and pentane and decane, respectively, that were obtained by using testing data from the optimised neural network with RK-Aspen models. Figure 4-22 compares the results obtained from training the optimised neural network with the PR EOS, redrawn from D'souza, et al. (1988). As seen in these figures, the dots illustrate the experimental data points obtained by Cheng, et al. (1989), Nagarajan & Robinson (1986) and D'souza, et al. (1988), the solid lines illustrate the RK-Aspen correlations, and the dotted lines depict the neural network predictions.

The RK-Aspen correlations were determined as discussed in Section 2.1.4 and 3.5. Since the scope of this study is not focussed on thermodynamic modelling using EOSs, and only temperature independent BIPs were regressed for the RK-Aspen models, additional EOSs were compared to the ANNs. As seen in Figure 4-20 and Figure 4-21, the RK-Aspen model correlates the experimental data well, but are unable to make predictions at high pressures. This is not a model problem, but a simulation problem, since Aspen Plus cannot model the fugacities due to similar densities.

Figure 4-20 illustrates the P-xy diagram for CO_2 + pentane at 311 K, a type I system where only VLE occurs, as discussed in Section 2.1.3. As seen in this figure, the RK-Aspen and the PR (Vitu et al., 2008) EOSs are depicted. Comparing the two EOSs, the correlations are very similar at low pressures, but the RK-Aspen model was unable to make correlations above 4.3 MPa. At high pressures, the PR EOS slightly under predicts bubble point pressures and slightly over predicts dew point pressures. This binary system was extracted from the testing set for the ANN predictions. Predictions were accurate with a maximum pressure deviation of 0.06 MPa for the bubble point predictions and 0.4 MPa for the dew point predictions. The EOSs and the neural network models resulted in accurate correlations and predictions at low to medium pressures. The neural network performs better than the RK-Aspen model, since pressure predictions are accurate and are able to make predictions through the whole pressure range.

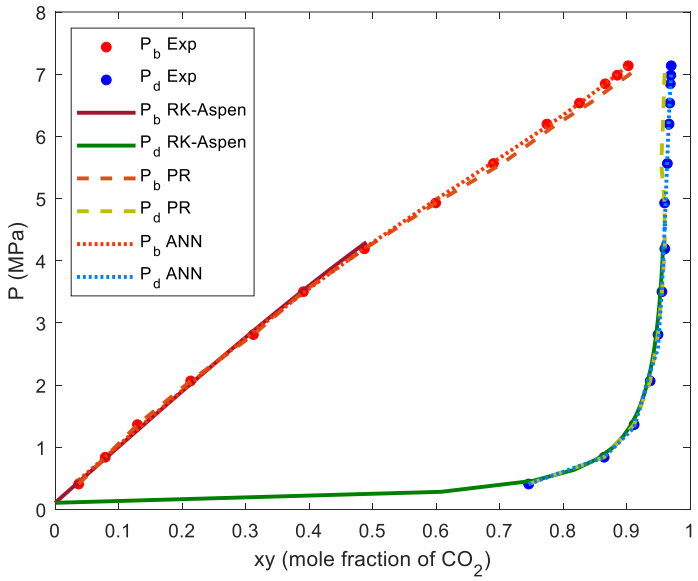

Figure 4-20: Bubble and dew point pressures of a binary system with CO_2 and pentane at 311 K obtained from experimental data (Cheng, et al., 1989), an RK-Aspen mode (with η_m, $k^0_{a,mn}$ and $k^0_{b,mn}$ values of 0.1024, 0.1344 and -0.00476), a PR model (Vitu, Privat, Jaubert, & Mutelet, 2008) and the attained ANN using CO_2 and alkanes as testing data

The P-xy results of experimental data and two different models for CO_2 and decane, as stated above, using the testing data from the optimised neural network, are compared in Figure 4-21. For a binary system containing CO_2 and decane, it is expected that type I phase behaviour occurs at supercritical temperatures and that type II phase behaviour occurs at subcritical temperatures, as discussed in Section 2.1.3. Since this binary system is at supercritical conditions (since $T_{r,CO_2} > 1$), it is expected that type I phase behaviour occurs, therefore expecting only VLE. As seen in this figure, the RK-Aspen model is only able to correlate pressures up to approximately 11 MPa where the PR EOS,

redrawn from Kian and Scurto (2018) can predict up to approximately 12 MPa. The neural network can predict pressures in the mixture critical region. All models slightly under predicts the bubble point pressures. For the dew point pressured predictions for the ANN above 12 MPa, a pressure maximum (opposed to the experimental data) occurs at 12.4 MPa and then the pressure decreases as the mole fraction of CO_2 decreases. The maximum errors as predicted by the neural network for this system are 0.05 MPa for the bubble point pressures and 2.1 MPa for the dew point pressures. The bubble point pressures are accurate throughout the whole pressure range with a maximum error of 0.05 kPa, where the dew point pressures are accurate for pressures up to 12 MPa, where the maximum error is 2.1 MPa for pressures above 12 MPa.

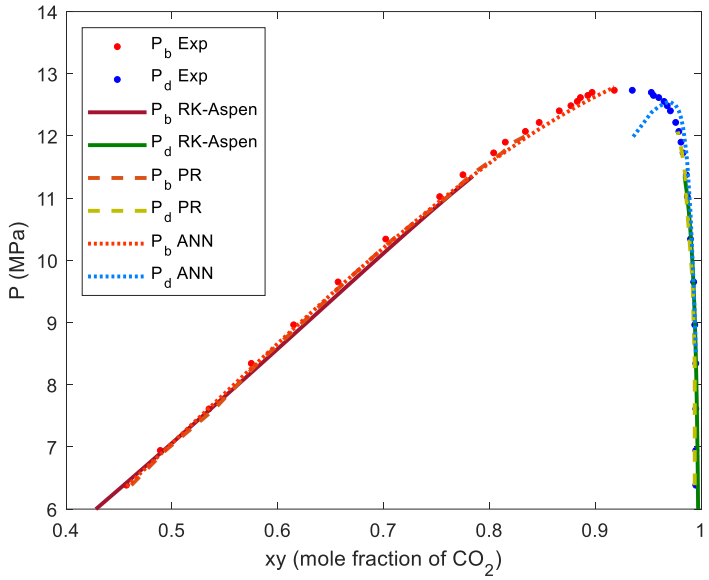

Figure 4-21: Bubble and dew point pressures of a binary system with CO_2 and decane at 344 K obtained from experimental data (Nagarajan & Robinson, 1986), an RK-Aspen model (with η_m, $k^0_{a,mn}$ and $k^0_{b,mn}$ values of 0.0497, 0.1015 and -0.02771), a PR model (Kian & Scurto, 2018) and the attained ANN using CO_2 and alkanes as training data

Since the methodology of this study minimized the geometric distance between R^2 and $AAD\%$, it is possible that the model is overfitted, explaining the oscillations either at high or low pressure predictions.

The training data obtained from the optimised neural network are compared with experimental data (D'Souza et al., 1988) and the PR EOS (only modelling the bubble point pressures), redrawn from D'souza et al., (1988) in Figure 4-22. This figure depicts the results for a binary system containing CO_2 and hexadecane, a type III classification according to Van Konynenburg and Scott (1980), as discussed in Section 2.1.3. For type III phase behaviour, it is expected that three-phase equilibrium

occurs at low temperatures. This system is considered to be at supercritical conditions, since T_{r,CO_2} is larger than one with a value of 1.03. It is therefore unlikely for a third phase to form.

It is evident that the neural network makes better predictions than the PR model at high pressure with pressure deviations of 0.3 MPa and 0.7 MPa at a liquid CO_2 composition of 0.8, respectively. At medium pressures, the performance of the two models are similar. At low pressures, the neural network performed better than the PR model with pressure deviations of 0.1 MPa and 0.5 MPa at a liquid CO_2 composition of 0.5, respectively. Overall, as observed in this figure, the neural network performed better than the PR EOS.

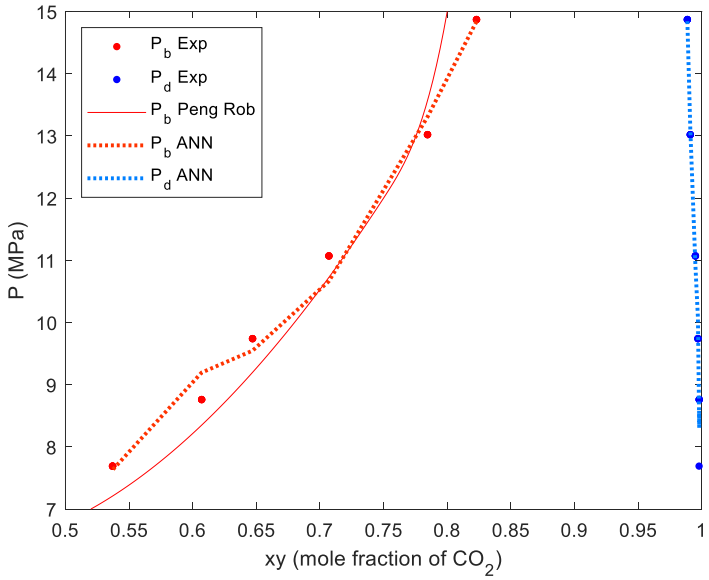

Figure 4-22: Bubble and dew point pressures of a binary system with CO_2 and hexadecane at 333 K obtained from experimental data (D'souza, et al., 1988), an Peng Robinson model redrawn from D'souza , et al., (1988) and the attained ANN using CO_2 and alkanes as training data

The aim of this section was to evaluate the possibility of using neural networks to model high-pressure phase equilibrium. As observed and concluded from Figure 4-20 to Figure 4-22, the neural network performed better than the EOS. Therefore, a neural network with more data and more functional groups will be evaluated in the next section.

5. Results and discussion of case study 2: Neural network predicting binary phase behaviour of CO_2 and hydrocarbons

As concluded from case study 1, a neural network containing VLE data with CO_2 and alkanes makes accurate predictions at high pressures. For case study 2, more functional groups and therefore more data were added to make the model more complex. Data containing CO_2 and hydrocarbons including alkanes, alcohols and carboxylic acids were used. The same methodology was used to achieve the objectives as used in case study 1 and discussed in Section 3. For the first objective, the structure of the neural network was investigated by determining the significant inputs using the randomisation approach (as discussed in Section 5.2) and the relative importance of the input variables (as discussed in Section 5.4). The second objective was achieved by determining the hyperparameters (Section 5.3). The results will be compared to traditional modelling methods as discussed in Section 5.5 (objective 3).

5.1. Collection and preparation of data

After data were collected, as listed in Tables A-1 to A-3 (VLE data) and Table A-4 to Table A-6 (pure component data) in Appendix A, data points were added to distribute the data evenly according to the functional group, chain length and number of data points in each binary system, as discussed in Section 3.1. The number of data points available in each binary system at a specific temperature (N_b), the number of binary systems available for each chain length (N_{CL}) and the number of binary systems for each functional group (N_{FG}) are listed in Table 5-1. As seen in this table, the maximum N_b, N_{CL} and N_{FG} is 80, 18 and 87, respectively. Data points were duplicated until there were 80 data points in each binary system at a specific temperature, and binary systems were duplicated until there were 18 binary systems for each CL and were further duplicated until there were 87 binary systems for each functional group.

Table 5-1: Number of data points available for a specific functional group, chain length and temperature for various hydrocarbons

Functional group of hydrocarbons		**Chain length of hydrocarbon**		**Binary system at specific temperature**		**Reference**
Functional group	N_{FG}	**Chain length**	N_{CL}	**T (K)**	N_b	
Alkanes	87	5	4	311	28	Cheng et al. (1989)
				344	28	Cheng et al. (1989)
				378	26	Cheng et al. (1989)
				394	23	Cheng et al. (1989)
		6	3	313	20	Li et al. (1981)
				353	28	Li et al. (1981)
				393	30	Li et al. (1981)
		7	3	311	46	Kalra et al. (1978)
				353	34	Kalra et al. (1978)
				394	34	Kalra et al. (1978)
		8	11	313	12	Weng & Lee (1992)
				313	18	Yu et al. (2006)
				322	14	Jime´nez-Gallegos et al. (2006)
				328	12	Weng & Lee (1992)
				333	20	Yu et al. (2006)
				348	16	Weng & Lee (1992)
				348	18	Jime´nez-Gallegos et al. (2006)
				353	20	Yu et al. (2006)
				373	16	Yu et al. (2006)
				373	24	Jime´nez-Gallegos et al. (2006)
				393	20	Yu et al. (2006)
		9	4	343	12	Jennings & Schucker (1996)
				315	16	Camacho-Camacho et al. (2007)
				345	16	Camacho-Camacho et al. (2007)
				373	22	Camacho-Camacho et al. (2007)
		10	14	278	24	Reamer & Sage (1963)
				311	10	Iwai et al. (1994)
				311	24	Reamer & Sage (1963)
				313	10	Adams et al. (1988)
				319	16	Jime´nez-Gallegos et al. (2006)
				344	40	Nagarajan & Robinson (1986)
				344	12	Jennings & Schucker (1996)
				344	10	Iwai et al. (1994)
				344	18	Reamer & Sage (1963)

Table 5-1 continued

Functional group of hydrocarbons		Chain length of hydrocarbon		Binary system at specific temperature		Reference
Functional group	N_{FG}	**Chain length**	N_{CL}	**T (K)**	N_b	
Alkanes	87	10	14	345	16	Jime´nez-Gallegos et al. (2006)
				373	26	Jime´nez-Gallegos et al. (2006)
				378	46	Nagarajan & Robinson (1986)
				378	22	Reamer & Sage (1963)
		11	3	315	18	Camacho-Camacho et al. (2007)
				344	18	Camacho-Camacho et al. (2007)
				373	20	Camacho-Camacho et al. (2007)
		12	1	318	20	Gardeler et al. (2002)
		15	3	292	21	Scheidgen (1997)
				298	15	Scheidgen (1997)
				316	19	Scheidgen (1997)
		16	7	314	12	D'Souza et al. (1988)
				323	10	Pohler (1994)
				333	12	D'Souza et al. (1988)
				353	14	Kordikowski & Schneider (1993)
				353	10	D'Souza et al. (1988)
				353	14	Kordikowski & Schneider (1993)
				393	30	Spee & Schneider (1991)
		17	5	323	12	Pohler (1994)
				333	12	Pohler (1994)
				353	12	Pohler (1994)
				373	14	Pohler (1994)
				393	16	Pohler (1994)
		18	5	323	12	Pohler (1994)
				333	12	Pohler (1994)
				353	12	Pohler (1994)
				373	14	Pohler (1994)
				393	16	Pohler (1994)
		19	9	318	10	Pohler (1994)
				323	10	Pohler (1994)
				333	10	Pohler (1994)
				343	18	Pohler (1994)
				348	14	Pohler (1994)
				353	10	Kordikowski & Schneider (1993)
		19	9	353	10	Kordikowski (1992)
				393	14	Kordikowski & Schneider (1993)
				393	14	Kordikowski (1992)

Table 5-1 continued

Functional group of hydrocarbons		Chain length of hydrocarbon		Binary system at specific temperature		Reference
Functional group	N_{FG}	**Chain length**	N_{CL}	**T (K)**	N_b	
Alkanes	87	20	6	323	10	Huang et al. (1988)
				353	14	Kordikowski & Schneider (1993)
				353	14	Kordikowski (1992)
				373	10	Huang *et al.* (1988)
				393	16	Kordikowski & Schneider (1993)
				393	16	Kordikowski (1992)
Alcohols	86	3	3	345	10	Elizalde-Solis et al. (2007)
				373	14	Elizalde-Solis et al. (2007)
				397	10	Elizalde-Solis et al. (2007)
		4	7	313	19	Byun & Kwak (2002)
				333	17	Byun & Kwak (2002)
				353	17	Byun & Kwak (2002)
				373	17	Byun & Kwak (2002)
				393	15	Byun & Kwak (2002)
				354	18	Elizalde-Solis et al. (2007)
				399	20	Elizalde-Solis et al. (2007)
		6	5	303	22	Beier et al. (2003)
				313	20	Beier et al. (2003)
				325	10	Elizalde-Solis et al. (2003)
				354	12	Elizalde-Solis et al. (2003)
				398	25	Elizalde-Solis et al. (2003)
		7	7	316	17	Scheidgen (1997)
				393	11	Scheidgen (1997)
				375	16	Elizalde-Solis et al. (2003)
				303	16	Secuianu et al. (2008)
				313	28	Secuianu et al. (2008)
				333	24	Secuianu et al. (2008)
				353	20	Secuianu et al. (2008)

Table 5-1 continued

Functional group of hydrocarbons		Chain length of hydrocarbon		Binary system at specific temperature		Reference
Functional group	N_{FG}	**Chain length**	N_{CL}	**T (K)**	N_b	
Alcohols	86	8	18	328	12	Hwu et al. (2004)
				348	10	Lee & Chen (1994)
				313	14	Lee & Chen (1994)
				328	14	Lee & Chen (1994)
				348	14	Lee & Chen (1994)
				313	17	Chiu et al. (2008)
				328	16	Chiu et al. (2008)
				348	16	Chiu et al. (2008)
				328	12	Feng et al. (2001)
				308	24	Chieming et al. (1998)
				318	18	Chieming et al. (1998)
				328	32	Chieming et al. (1998)
				313	26	Chrisochoou et al. (1997)
				313	11	Byun & Kwak (2002)
				333	11	Byun & Kwak (2002)
				353	11	Byun & Kwak (2002)
				373	11	Byun & Kwak (2002)
				393	11	Byun & Kwak (2002)
		9	8	308	18	Chieming et al. (1998)
				318	20	Chieming et al. (1998)
				328	30	Chieming et al. (1998)
				303	14	Pfohl et al. (1999)
				308	14	Secuianu et al. (2010)
				313	12	Secuianu et al. (2010)
				333	20	Secuianu et al. (2010)
				353	20	Secuianu et al. (2010)

Table 5-1 continued

Functional group of hydrocarbons		**Chain length of hydrocarbon**		**Binary system at specific temperature**		**Reference**
Functional group	N_{FG}	**Chain length**	N_{CL}	**T (K)**	N_b	
Alcohols	86	10	16	313	14	Pohler (1994)
				323	14	Pohler (1994)
				333	12	Pohler (1994)
				353	12	Pohler (1994)
				373	12	Pohler (1994)
				393	14	Pohler (1994)
				303	13	Ioniţă et al. (2013)
				308	11	Ioniţă et al. (2013)
				323	11	Ioniţă et al. (2013)
				333	14	Ioniţă *et al.* (2013)
				343	11	Ioniţă et al. (2013)
				348	10	Lee & Chen (1994)
				308	18	Chieming et al. (1998)
				318	18	Chieming et al. (1998)
				328	26	Chieming et al. (1998)
				348	16	Weng et al. (1994)
		12	9	313	16	Secuianu et al. (2016)
				333	18	Secuianu et al. (2016)
				353	18	Secuianu et al. (2016)
				353	12	Kordikowski & Schneider (1993)
				393	18	Spee & Schneider (1991)
				375	10	Scheidgen (1997)
		12	9	333	20	Holsher (1988)
				393	20	Holsher (1988)
				393	18	Spee (1990)
		14	1	373	10	Jan et al. (1994)
		16	2	373	10	Jan et al. (1994)
				393	20	Holsher (1988)
		18	1	373	10	Jan et al. (1994)

Table 5-1 continued

Functional group of hydrocarbons		Chain length of hydrocarbon		Binary system at specific temperature		Reference
Functional group	N_{FG}	**Chain length**	N_{CL}	**T (K)**	N_b	
Carboxylic acid	59	4	5	313	16	Byun et al. (2000)
				333	14	Byun et al. (2000)
				353	13	Byun et al. (2000)
				373	13	Byun et al. (2000)
				393	12	Byun et al. (2000)
		5	5	313	19	Byun et al. (2000)
				333	16	Byun et al. (2000)
				353	16	Byun et al. (2000)
				373	14	Byun et al. (2000)
				393	12	Byun et al. (2000)
		6	6	313	10	Bharath et al. (1993)
				353	11	Bharath et al. (1993)
				308	21	Byun et al. (2000)
				328	20	Byun et al. (2000)
				348	18	Byun et al. (2000)
				373	19	Byun et al. (2000)
		8	9	313	10	Heo et al. (2001)
				323	10	Heo et al. (2001)
				333	10	Heo et al. (2001)
				343	10	Heo et al. (2001)
				353	10	Heo et al. (2001)
		8	9	308	22	Byun et al. (2000)
				328	20	Byun et al. (2000)
				348	19	Byun et al. (2000)
				373	16	Byun et al. (2000)
		9	5	313	10	Schieman et al. (1993)
				333	10	Schieman et al. (1993)
				353	10	Schieman et al. (1993)
				373	10	Schieman et al. (1993)
				393	10	Schieman et al. (1993)
		10	8	313	10	Heo et al. (2001)
				323	10	Heo et al. (2001)
				333	10	Heo et al. (2001)
				343	10	Heo et al. (2001)

Table 5-1 continued

Functional group of hydrocarbons		Chain length of hydrocarbon		Binary system at specific temperature		Reference
Functional group	N_{FG}	**Chain length**	N_{CL}	**T (K)**	N_b	
Carboxylic acid	59	10	8	353	10	Heo et al. (2001)
				323	10	Pohler (1994)
				353	14	Pohler (1994)
				393	16	Pohler (1994)
		12	11	318	14	Pohler (1994)
				323	10	Pohler (1994)
				333	12	Pohler (1994)
				343	14	Pohler (1994)
				348	14	Pohler (1994)
				353	16	Pohler (1994)
				373	12	Pohler (1994)
				333	18	Bharath et al. (1993)
				353	12	Bharath et al. (1993)
				373	10	Yau et al. (1992)
				393	14	Kordikowski (1992)
		14	6	328	16	Pohler (1994)
				333	14	Pohler (1994)
				343	14	Pohler (1994)
				353	16	Pohler (1994)
				373	18	Pohler (1994)
				393	24	Pohler (1994)
		18	3	353	10	Schiemann et al. (1993)
				373	10	Schiemann et al. (1993)
				393	10	Schiemann et al. (1993)
		22	1	373	10	Yau et al. (1992)

After obtaining data to train, test and validate the neural network, the structure and hyperparameters of the neural network were determined, as discussed in the following sections.

5.2. Determination of the significant inputs of the neural network

In this section, the significant inputs of the neural network used for case study 2 that were determined, are discussed. For a first iteration, a feedforward neural network with one hidden layer was used, as for case study 1. The number of nodes in each hidden layer was determined by maximising R^2 and minimising $AAD\%$ and the geometric distance between the training and testing data of both R^2 and $AAD\%$ values, as illustrated in Figure 5-1 and listed in Table C-6, Appendix C.

As seen in Figure 5-1, R^2 increases and $AAD\%$ decreases more rapidly between 1 and 8 nodes per hidden layer, as the number of nodes in each hidden layer increases. The values and geometric distance of $AAD\%$ and R^2 are relatively low at 23 nodes (for AAD%) and between 18 and 23 nodes (for R^2) in each hidden layer. A feedforward neural network with a size $11 \times 8 \times 2$ and $11 \times 23 \times 2$ will therefore be considered to determine the significant inputs of the neural network.

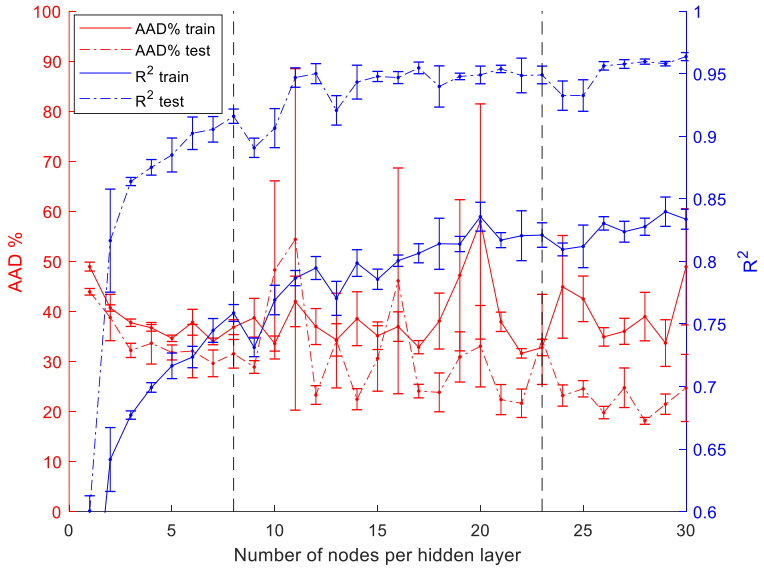

Figure 5-1: Preliminary AAD % and R^2 results of neural networks using a range of number of nodes per hidden layer using binary system data containing CO_2 and hydrocarbons.

Using Figure 5-2, the P-xy results obtained from the testing data for pentane at 311 K using 8 and 23 nodes per hidden layer were compared to experimental results obtained by Cheng et al. (1989). As seen from this figure, for bubble point predictions, $11 \times 23 \times 2$ resulted in better predictions relative to the $11 \times 8 \times 2$ neural network since pressure deviations for the latter network were higher. For dew point pressures, the form of the $11 \times 23 \times 2$ network is better especially when extrapolation at higher pressures are required.Overall, the $11 \times 23 \times 2$ neural network performed better. Therefore, a neural network with one hidden layer and 23 nodes in the hidden layer were used to determine the significant inputs to the neural network for case study 2.

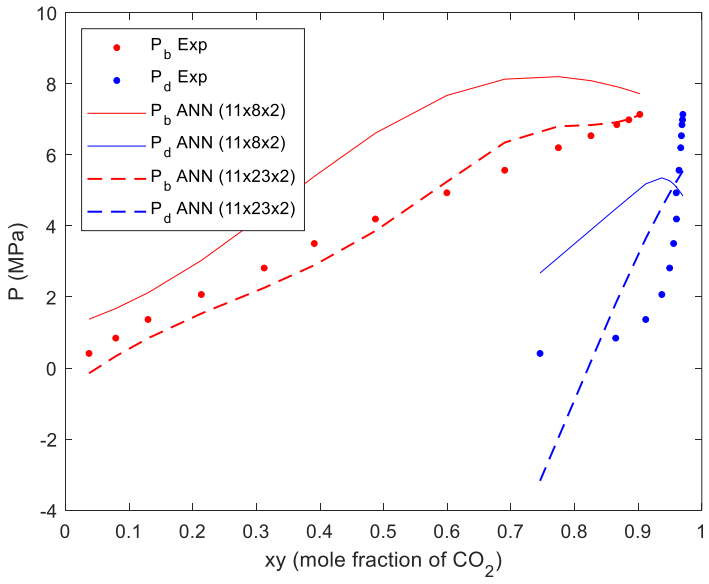

Figure 5-2: Bubble and dew point pressures of a binary system with CO_2 and pentane at 311 K obtained from experimental data (Cheng et al., 1989), an ANN with a size of $(11 \times 8 \times 2)$ and an ANN with a size of $(11 \times 23 \times 2)$ using CO_2 and hydrocarbons as testing data

The same approach to determine the significant inputs to the neural network that was used for case study 1, was used in this case study. For case study 2, the functional group (FG_1 and FG_2), acentric factor (w), critical temperature (T_c) and critical pressure (P_c) of the hydrocarbon, system temperature (T), chain length (CL) and molecular mass (MM) of the hydrocarbon, liquid and vapour distinction (x/y), and the composition of CO_2 in the liquid (x) and vapour (y) phases were considered as initial inputs to the neural network.

Figure 5-3 illustrates the $AAD\%$ values obtained by randomising a specific input to the neural network, as discussed in Section 3.2. As seen in this figure, all $ADD\%$ values (27.82%, 21.61%, 30.19%, 22.66%, 21.07%, 22.27%, 19.86%, 27.30%, 34.51% and 29.67% for FG_1, FG2, w, T_c, T, CL, MM, x/y, x and y) are larger than the normal condition (20.70%), except for P_c (18.91%).

Comparing Figure 4-3 used for case study 1 with Figure 5-3, for both case studies, T_c is more important than P_c and CL is more important than MM. As observed in the RK-Aspen EOS equations, the modified energy parameter (Equation 2-7) and the co-volume parameter (Equation 2-8) are both functions of P_c and T_c where the alpha functions (Equations 2-9 and 2-10, an additional parameter to account for polar compounds) are only a function of T_c. It therefore makes sense that T_C was not removed using the ANN, since polar molecules are present in the data sets. Although P_c is required to determine the energy parameter and the co-volume parameter for the RK-Aspen EOS, using T_c and MM (opposed to using P_c as well) seems to be sufficient for the ANN.

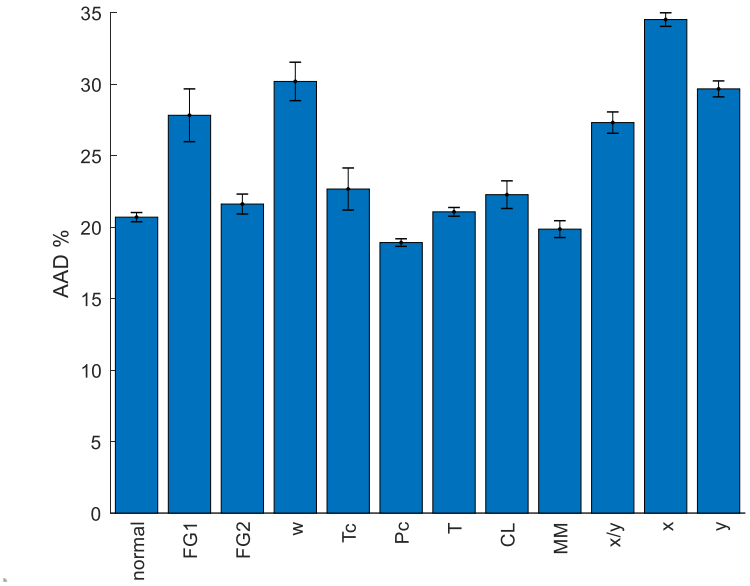

Figure 5-3: The AAD % of the testing data to determine the significant inputs using all input variables for binary system containing CO_2 and various hydrocarbons

P_c was therefore eliminated as input to the neural network, where the normal condition of the following neural network will be without P_c as input, as illustrated in Figure 5-4.

Removing the critical pressure of the hydrocarbon as input to the neural network, Figure 5-4 illustrates the $AAD\%$ of the testing data obtained by randomising a specific input to the neural network.

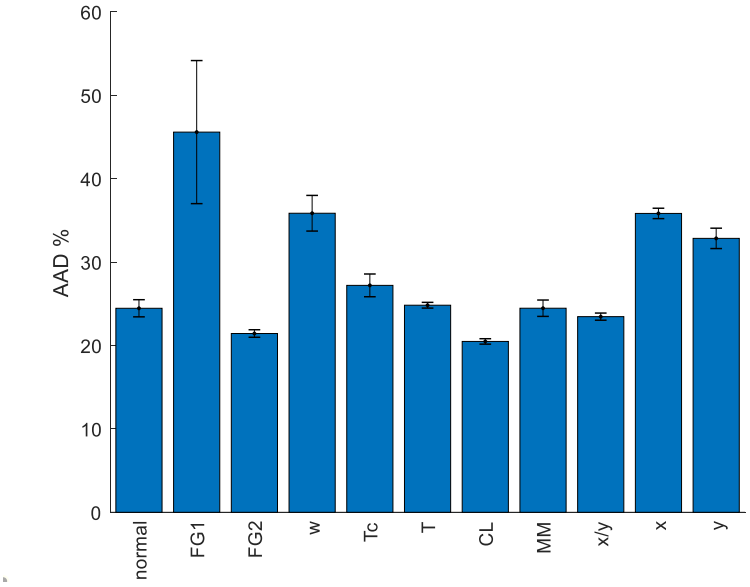

Figure 5-4: The AARD% of the testing data to determine the significant inputs with the critical pressure of the hydrocarbon eliminated using binary system data containing CO_2 and hydrocarbons

As seen in this figure, the $AAD\%$ values of FG_2 (21.43%) and CL (20.49%) have smaller values than the normal condition (24.46%). All other $AAD\%$ are larger than the normal condition with values of 45.58%, 35.85%, 27.21%, 24.83%, 24.47%, 23.46%, 35.84% and 32.84% for FG_1, w, T_c, T, MM, x/y, x and y. Since FG_1 and FG_2 are used in combination, and since the $AAD\%$ of randomising CL resulted in the smallest $AAD\%$ (smaller than the current normal condition and the previous normal condition as presented in Figure 5-3), only CL was removed as input.

After removing CL and P_c as input variables, Figure 5-5 illustrates the $AAD\%$ values of randomising each input variable respectively. As seen in this figure, all $AAD\%$ have values (13.13%, 20.59%, 13.92%, 17.67%, 20.21%, 15.38%, 21.03% and 31.68% for FG_1, FG_2, w, T_c, T, MM, x/y, x and y respectively) relatively the same or larger than the normal condition (13.25%). Therefore, no further inputs were removed.

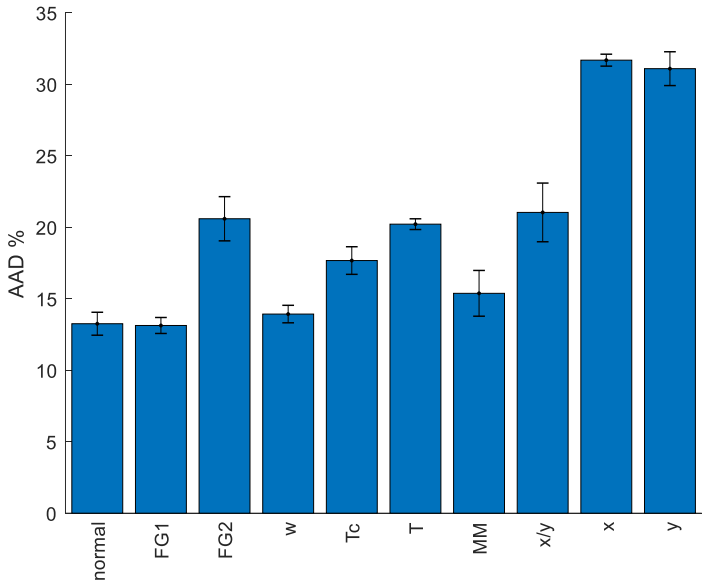

Figure 5-5: The AARD% of the testing data to determine the significant inputs with the critical pressure chain length of the hydrocarbon eliminated using binary system data containing CO_2 and hydrocarbons

As seen in Table 2-7 in Section 2.2.6, FG_1 and FG_2 in combination defines the alkane, alcohol and carboxylic functional groups with vectors [1; 0], [0; 1] and [0; 0], respectively. As observed from Figure 5-3 to Figure 5-5, either the $AAD\%$ of FG_1 (Figure 5-3 and Figure 5-4) or the $AAD\%$ of FG_2 (Figure 5-5) is high. Since both input variables FG_1 and FG_2 are required to define the functional group, neither of these input variables were removed.

In Figure 5-6, the P-xy results are compared after removing none of the inputs (ANN), removing only P_c (ANN_{P_c}), and removing P_c and CL ($ANN_{P_{c\&}\&CL}$) as input variables to the neural network to evaluate the results obtained in this section. As seen in this figure, $ANN_{P_{c\&}\&CL}$ resulted in accurate

results for the bubble point pressures, whereas for dew point pressures, pressures were slightly over predicted and under predicted at medium and low pressures. For ANN, the dew point pressure resulted in a linear prediction where the bubble point predictions oscillated over the entire pressure range. For ANN_{P_c}, fairly accurate results were obtained, however, small fluctuations occured over the entire pressure range.

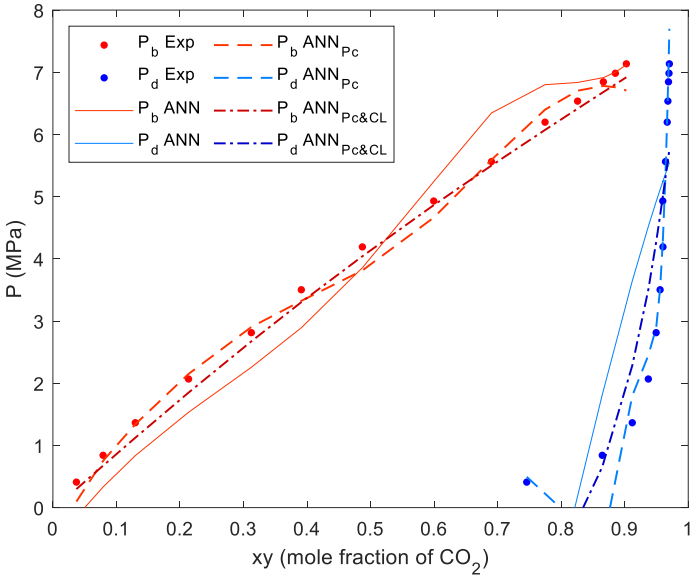

Figure 5-6: Bubble and dew point pressures of a binary system with CO_2 and pentane at 311 K obtained from experimental data (Cheng et al., 1989), an ANN where no inputs were removed, an ANN with Pc removed as input and an ANN with Pc and CL removed as input using CO_2 and hydrocarbons as testing data

The significant inputs to the neural network for case study 2 are therefore functional group (FG_1 and FG_2), acentric factor (w), critical temperature (T_c) and molecular mass (MM) of the hydrocarbon, system temperature (T), liquid-vapour-distinction (x/y), liquid composition (x) and vapour composition (y) of CO2. Using these inputs to the neural network, the hyperparameters were determined and will be discussed in Section 5.3.

5.3. Determination of hyperparameters

Following the same approach as used for case study 1 and using the inputs as determined in Section 5.2, the hyperparameters and the transfer functions were determined, as disscussed in this section.

Figure 5-7, Figure 5-8, Figure 5-10 and Figure 5-11 illustrate the results of the R^2 and $AAD\%$ values for the training and testing data using different types of neural networks and the number of hidden layers, whereas Figure 5-13 illustrates the $AAD\%$ of different transfer functions. The R^2 and $AAD\%$ values of the training and testing data of these figures are provided in Tables C-7 to C-10 in Appendix C.

The same approach was used to determine the optimum number of nodes in each hidden layer as used for case study 1, where the R^2 values were maximized and the $AAD\%$ and the geometric distances were minimized.

Figure 5-7 illustrates the R^2 and $AAD\%$ results for the training and testing data for a range of 0 to 60 nodes per hidden layer using a feedforward neural network with one hidden layer containing CO_2 and various hydrocarbons as training data.

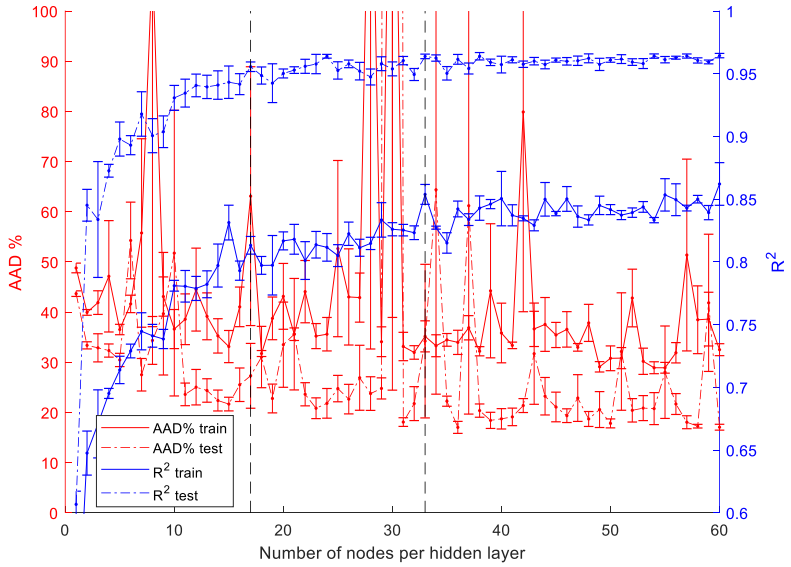

Figure 5-7: R^2 and AAD % values for the training and testing data using a feedforward neural network and one hidden layer using binary system data containing CO_2 and various hydrocarbons

As seen in Figure 5-7, overall, R^2 increases and $AAD\%$ decreases as the number of nodes per hidden layer increases for a range of 0 to 50 nodes per hidden layer. At 17 nodes per hidden layer, the R^2 values for the testing data stabilise with small fluctuations where the R^2 values for the training data increase less gradually compared to the values with lower nodes per hidden layer. The $AAD\%$ values oscillates throughout the whole range, decreasing more rapidly for a range of 0 to 17 nodes per hidden layer. At 33 nodes per hidden layer, the geometric distances for both R^2 and $AAD\%$ are relatively small, R^2 values are relatively large (0.854 and 0.964 for the training and testing data respectively) and $AAD\%$ values are relatively small (35.1% and 34.2% for the training and testing data respectively) for both the training and testing data.

Figure 5-8 illustrates the R^2 and $AAD\%$ results after training neural networks for a range of 0 to 50 nodes per hidden layer using a feedforward neural network with two hidden layers containing CO_2 and various hydrocarbons as training data.

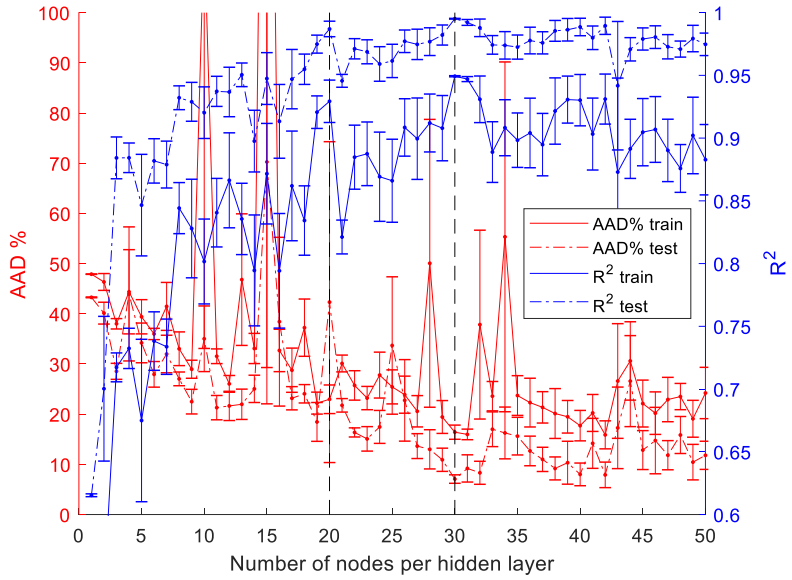

Figure 5-8: R^2 and AAD % values for the training and testing data using a feedforward neural network and two hidden layers using binary system data containing CO_2 and various hydrocarbons

As seen in this figure, R^2 increases and $AAD\%$ decreases as the number of nodes per hidden layer increases for a range of 0 to 30 nodes per hidden layer. R^2 reaches a local maximum at 20 nodes per hidden layer where R^2 and $AAD\%$ reach a global maximum and minimum respectively at 30 nodes per hidden layer with values of R^2 values of 0.949 and 0.995 and $AAD\%$ values of 16.41% and 7.07% for the training and testing data respectively. The geometric distances at both these nodes are relatively small for R^2 and $AAD\%$.

As concluded from Figure 5-7 and Figure 5-8, there is a point where the R^2 and $AAD\%$ values start to increase less rapidly, and a point where the R^2, $AAD\%$ and geometric distance values are optimised. In Figure 5-9, the experimental results obtained by Cheng, *et al*. (1989) are compared to the AAN predictions as presented in Figure 5-7 and Figure 5-8 at the two points mentioned above. As seen in this figure, the bubble point predictions oscillate rapidly for both the $9 \times 26 \times 2$ and $9 \times 50 \times 2$ neural networks. For these networks with one hidden layer, the maximum dew point pressure predictions are approximately 4 MPa where predictions oscillate at low pressures. The predictions for the $9 \times 20 \times 20 \times 2$ and $9 \times 30 \times 30 \times 2$ neural networks are very similar, where the $9 \times 20 \times 20 \times 2$ neural network is slightly more accurate at high pressures for the bubble point predictions and the $9 \times 30 \times 30 \times 2$ neural network is slightly more accurate at low bubble point predictions, and predicting the dew point pressures over the entire range. Therefore, the feedforward neural network with a size of $9 \times 30 \times 30 \times 2$ was considered for further optimisation.

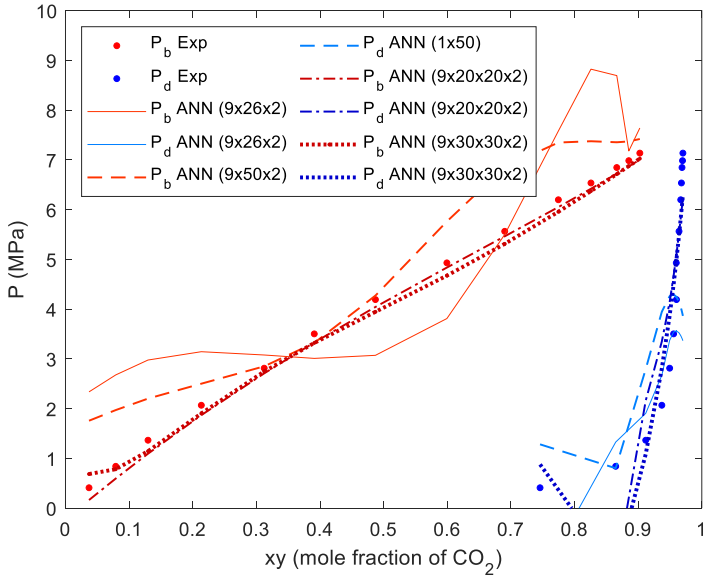

Figure 5-9: Bubble and dew point pressures of a binary system with CO_2 and pentane at 311 K obtained from experimental data (Cheng et al., 1989) and ANNs using a feedforward neural network with sizes of $9 \times 26 \times 2$, $9 \times 50 \times 2$, $9 \times 20 \times 20 \times 2$ *and* $9 \times 30 \times 30 \times 2$ *respectively containing CO_2 and hydrocarbons as testing data*

Figure 5-10 illustrates the R^2 and $AAD\%$ results for the training and testing data for a range of 0 to 60 nodes per hidden layer using a cascade feedforward backpropagation neural network with one hidden layer containing CO_2 and various hydrocarbons as training data.

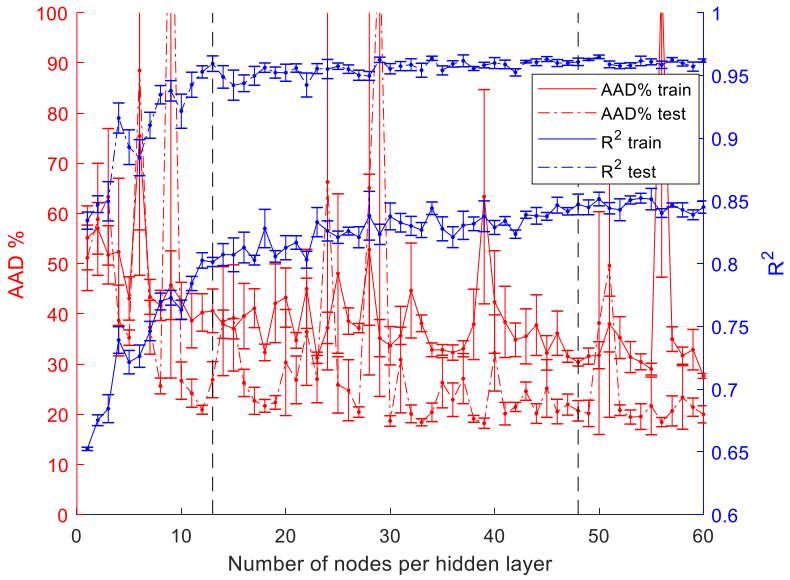

Figure 5-10: R^2 and AAD % values for the training and testing data using a cascade feedforward neural network and one hidden layer using binary system data containing CO_2 and various hydrocarbons

As seen in this figure, R^2 increases and $AAD\%$ decreases rapidly as the nodes per hidden layer increase for a range of 0 to 13 nodes per hidden layer. For a range of 14 to 50 nodes per hidden layer,

R^2 increases and $AAD\%$ decreases slightly as the nodes per hidden layer increase for the training and testing data. At 48 nodes per hidden layer, R^2 (0.847 and 0.961 for the training and testing data) is relatively high and the $AAD\%$ (30.4% and 20.7% for the training and testing data) and the geometric distances are relatively low, as seen in Table C-9 listed in Appendix C.

Figure 5-11 illustrates the R^2 and $AAD\%$ results for the training and testing data for a range of 0 to 50 nodes per hidden layer using a cascade feedforward backpropagation neural network with two hidden layers containing CO_2 and various hydrocarbons as training data. As seen in this figure, R^2 increases and $AAD\%$ decreases rapidly as the number of nodes per hidden layer increases for 0 to 23 nodes per hidden layer for both the training and testing data. For a range of approximately 24 to 50 nodes per hidden layer, R^2 increases slightly and $AAD\%$ decreases slightly with oscillation as the number of nodes per hidden layer increase. At 46 nodes per hidden layer, the R^2 (0.952 and0.996 for the training and testing data) values are relatively large and the $AAD\%$ (13.7% and 4.9% for the training and testing data) and geometric distances values are relatively small for both the training and testing data.

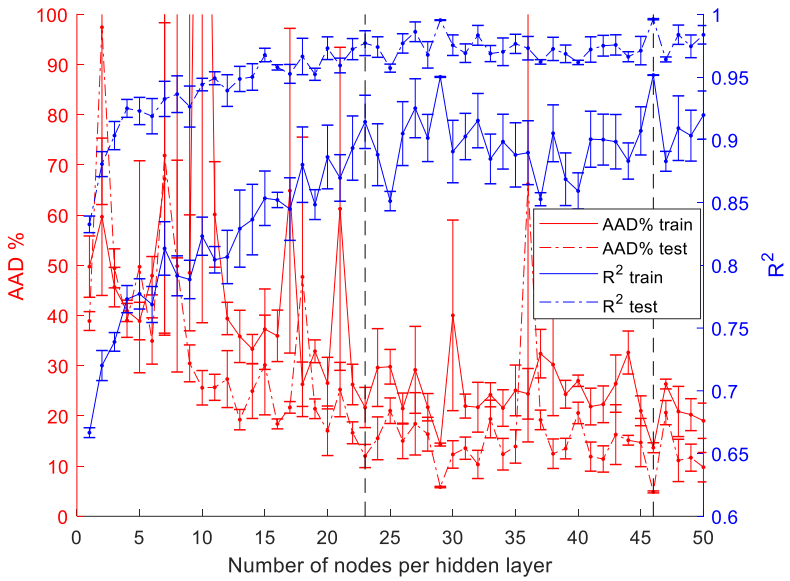

Figure 5-11: R^2 and AAD % values for the training and testing data using a cascade feedforward neural network and two hidden layers using binary system data containing CO_2 and various hydrocarbons

As concluded from Figure 5-10 and Figure 5-11, the points where R^2 and $AAD\%$ start to increase less rapidly at neural network sizes of $9 \times 13 \times 2$ and $9 \times 23 \times 23 \times 2$ and the points where R^2, $AAD\%$ and geometric distance values are optimised are at neural network sizes of 1x48 and $9 \times 46 \times 46 \times 2$. In Figure 5-12, these neural networks are compared with the experimental results obtained by Cheng et al. (1989) for a VLE system containing pentane and CO_2 at 311 K.

As seen in Figure 5-12, the form of the dew point pressure curves for the $9 \times 13 \times 2$ and $9 \times 23 \times 23 \times 2$ neural networks increases exponentially, reaches maximum pressures at approximately 4.4 MPa and 5.5 MPa, respectively, and then decreases, resulting in unreliable predictions. The bubble point pressure predictions for the $9 \times 13 \times 2$ neural network oscillates through the entire pressure range. The $9 \times 48 \times 2$ bubble point pressures are accurate at high pressures and under predicted by approximately 1.5 MPa at medium and low pressures. The $9 \times 23 \times 23 \times 2$ bubble point pressures are accurate at medium pressures but under predict at low pressures by approximately 1.4 MPa and over predict at high pressures by approximately 0.7 MPa. The $9 \times 46 \times 46 \times 2$ network is relatively accurate predicting high and low bubble point pressures over, where at medium pressures, predictions are over predicting by approximately 1 MPa. The $9 \times 46 \times 46 \times 2$ network makes relatively accurate predictions, where pressures are under predicted at low pressures and over predicted at medium pressures. At high pressures, the optimal network for predicting bubble point pressures is $9 \times 48 \times 2$ where the $9 \times 46 \times 46 \times 2$ network predicts dew point pressure well.

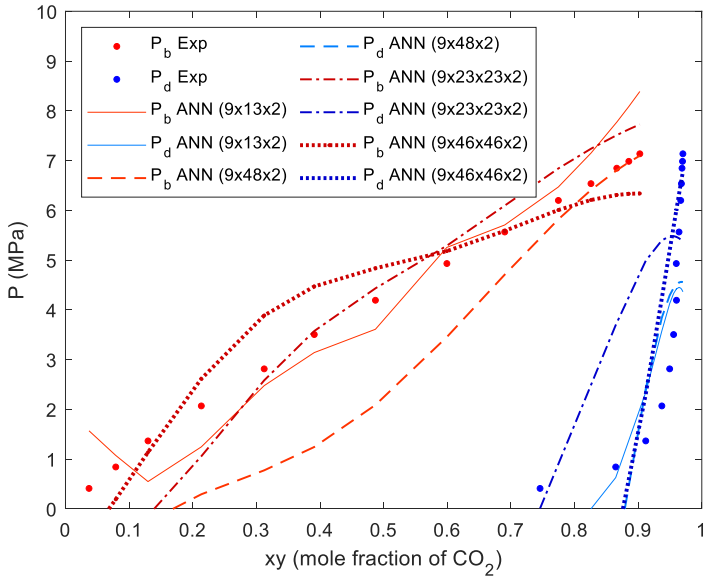

Figure 5-12: Bubble and dew point pressures of a binary system with CO_2 and pentane at 311 K obtained from experimental data (Cheng et al., 1989) and ANNs using a cascade feedforward backpropagation neural network with sizes of $9 \times 13 \times 2$, $9 \times 48 \times 2$, $9 \times 23 \times 2$ *and* $9 \times 46 \times 46 \times 2$ *respectively containing CO_2 and hydrocarbons as testing data*

Table 5-2 lists the R^2 and $AAD\%$ values for the neural networks as presented in Figure 5-9 and Figure 5-12, obtained using Figure 5-7, Figure 5-8, Figure 5-10 and Figure 5-11. A seen in this table, the neural networks with two hidden layers performed better than the neural networks with a single hidden layer. Comparing the types of neural networks, the cascade feedforward backpropagation

neural network obtained slightly better R^2 and $AAD\%$ values compared to the feedforward neural network. When comparing Figure 5-9 and Figure 5-12 (the P-xy results comparing testing data with experimental data), the feedforward neural network with a size of $9 \times 30 \times 30 \times 2$ performed better than the cascade feedforward backpropagation neural network with a size of $9 \times 46 \times 46 \times 2$. Therefore, statistically, the cascade feedforward backpropagation neural network performed better when all training and testing data are compared, but comparing the P-xy plot, the feedforward neural network performed better.

Table 5-2: R^2 and AAD% values at the start of oscillation and the optimal points to determine the neural network structure using binary system data containing CO_2 and various hydrocarbons

Neural network type		**Start of oscillations**			**Optimal point**		
		Training	**Testing**	**Neural network structure ($N_{HL} \times N_{nodes}$)**	**Training**	**Testing**	**Neural network structure ($N_{HL} \times N_{nodes}$)**
Feedforward	R^2	0.822	0.958	$9 \times 26 \times 2$	0.854	0.964	$9 \times 33 \times 2$
	AAD %	43.1	22.7		35.2	34.2	
Feedforward	R^2	0.929	0.987	$9 \times 20 \times 20 \times 2$	0.949	0.995	$9 \times 30 \times 30 \times 2$
	AAD %	23.0	42.3		16.4	7.1	
Cascade feedforward backpropagation	R^2	0.801	0.960	$9 \times 13 \times 2$	0.847	0.961	$9 \times 48 \times 2$
	AAD %	40.6	26.9		30.4	20.7	
Cascade feedforward backpropagation	R^2	0.914	0.977	$9 \times 23 \times 23 \times 2$	0.952	0.996	$9 \times 46 \times 46 \times 2$
	AAD %	21.7	12.0		13.7	4.9	

Using a feedforward neural network with a size of $9 \times 30 \times 30 \times 2$, a comparison of the $AAD\%$ of the testing data using the threshold, linear, log-sigmoid and hyperbolic tangent transfer function respectively (as explained in Section 2.2.2) is presented in Figure 5-13. As seen from this figure, the $AAD\%$ of the testing data using the threshold, linear, log-sigmoid and hyperbolic tangent transfer functions in decreasing order were 57.2%, 38.1%, 11.9% and 10.2% respectively. It is clear that the hyperbolic-tangent transfer resulted in lower $AAD\%$. Since the data used to train the networks are highly non-linear, it was likely that the threshold and linear transfer functions would not work. It was further expected that the log-sigmoid transfer function would perform better, since this transfer function was used by Lashkarbolooki & Shafipour et al. (2013), Lashkarbolooki & Vaferi et al. (2013) and Vaferi et al. (2018). The log-sigmoid and hyperbolic tangent transfer functions are very similar, where the normalszation range differs being 0 to 1 for the log-sigmoid function and -1 to 1 for the hyperbolic tangent-function, making both transfer functions acceptable for MLPs.

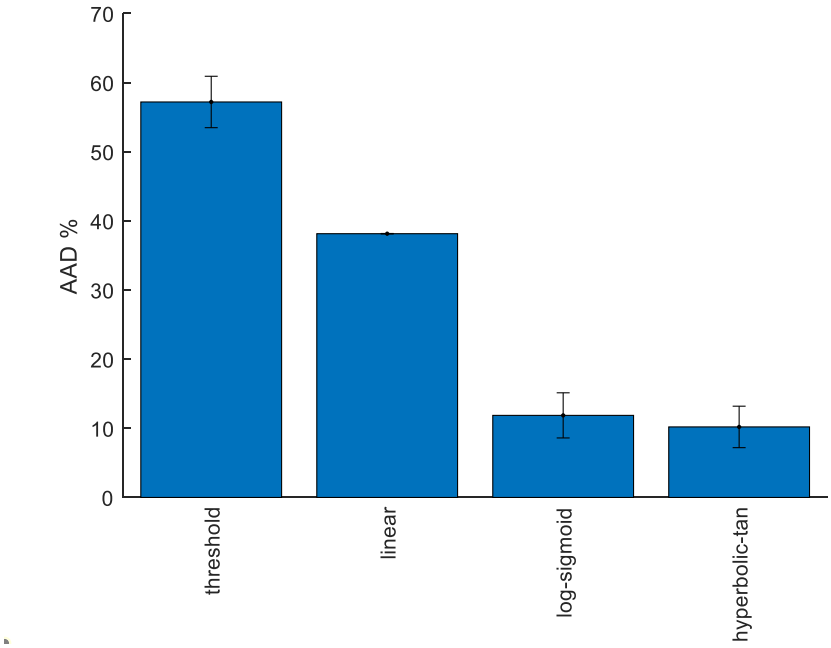

Figure 5-13: The AAD % values for the testing data using a feedforward neural network with a threshold, linear, log-sigmoid and hyperbolic tangent transfer function respectively using binary system data containing CO_2 and hydrocarbons

In Figure 5-14, a comparison of the P-xy results obtained by experimental data obtained by Cheng et al. (1989) and the neural networks with different transfer functions (as discussed using Figure 5-13) is presented.

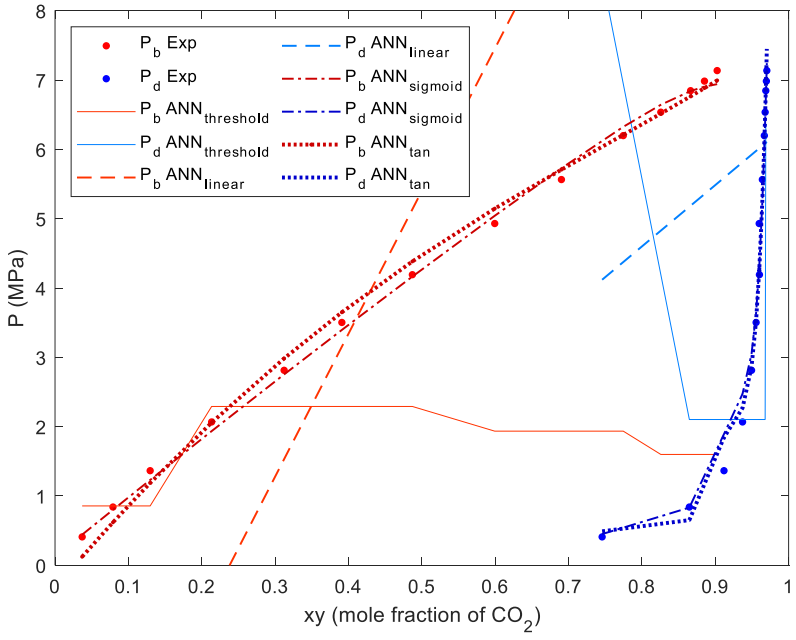

Figure 5-14: Bubble and dew point pressures of a binary system with CO_2 and pentane at 311 K obtained from experimental data (Cheng et al., 1989) and ANNs using a cascade feedforward backpropagation neural

network with the threshold, linear, log-sigmoid and hyperbolic-tangent transfer functions containing CO_2 and hydrocarbons as testing data

As seen from this figure, the threshold function only works at high pressures predicting the dew point pressures. The linear transfer function makes linear predictions, as expected, which is not suited for this data since non-linear predictions are required. The log-sigmoid and hyperbolic-tangent predictions are very similar, as expected since the transfer functions are very similar. The hyperbolic-tangent function slightly over predicts at medium bubble point pressures and under predicts at low dew point pressures. The log-sigmoid transfer function performs slightly worse at high bubble point pressures and medium dew point pressures. Overall, the log-sigmoid transfer function performs better.

As concluded from this section, a feedforward neural network with a size of $9 \times 30 \times 30 \times 2$ and a log-sigmoid transfer function were selected as hyperparameters for case study 2.

Figure 5-15 to Figure 5-17 compares experimental data with the ANN predictions using the optimised hyperparameters as determined in this section with experimental data at different chain lengths (as discussed using Figure 2-2 to Figure 2-4 in Section 2.1.2).

Comparing the $AAD\%$ of the binary systems containing CO_2 and alkanes at different chain lengths plotted using Figure 4-14 (obtained from case study 1) with Figure 5-15 (as obtained from case study 2), the $AAD\%$ values of case study 2 is higher compared to case study 1. This is expected since the neural network used in this case study is more complex.

Table 5-3: Comparing the AAD% values of case studies 1 and 2 for binary systems containing CO_2 and alkanes at different chain lengths

Binary system	***AAD*% for case study 1**	***AAD*% for case study 2**	**Reference for experimental data**
CO_2 and octane	15.68%	17.94%	Yu, et al. (2006)
CO_2 and nonane	2.51%	10.23%	Camacho-Camacho, et al. (2007)
CO_2 and undecane	0.75%	4.25%	Camacho-Camacho, et al. (2007)
CO_2 and heptadecane	1.18%	2.28%	Pholer (1994)
CO_2 and octadecane	0.97%	3.84%	Pholer (1994)

As observed from Figure 5-15 and as indicated by the $AAD\%$ values as listed in Table 5-3, the accuracy of the predictions made by the ANN increases as the chain length of the hydrocarbon increases, which is the same occurrence as obtained from case study 1.

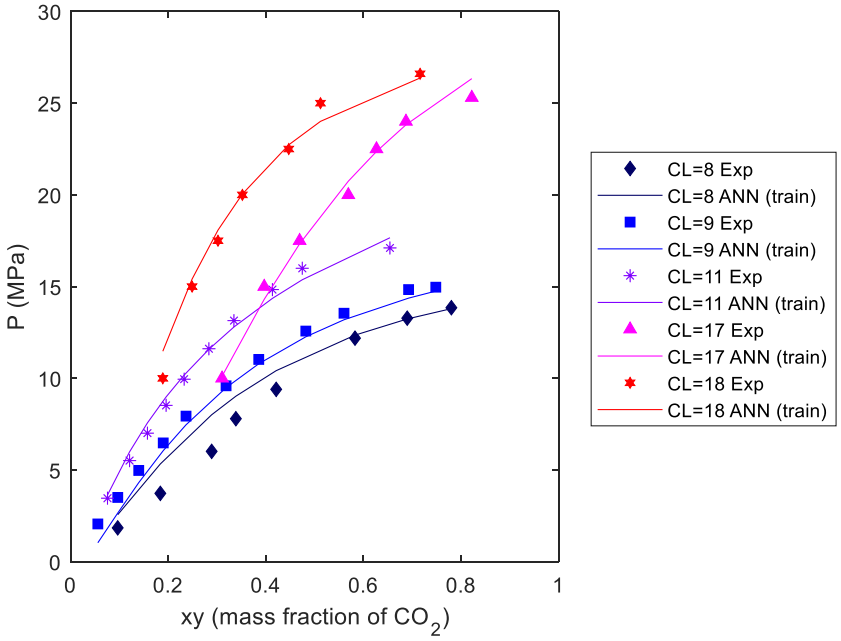

Figure 5-15: ANN results comparing the chain length, bubble point pressure and mass fraction for CO_2 of alkanes at 373 K – data from Yu et al. (2006), Camacho-Camacho et al. (2007) and Pohler (1994)

Figure 5-16 illustrates the ANN results for binary systems containing CO_2 and alcohols with experimental data as obtained from Elizalde-Solis et al. (2007) (CO_2 and propanol), Byun and Kwak (2002) (CO_2 and butanol and octanol respectively), and Pohler (1994) (CO_2 and decanol) resulting in $ADD\%$ values of 0.28%, 3.75%, 3.14% and 4.64% respectively. It should be noted that the CO2 and propanol system is a validation set.

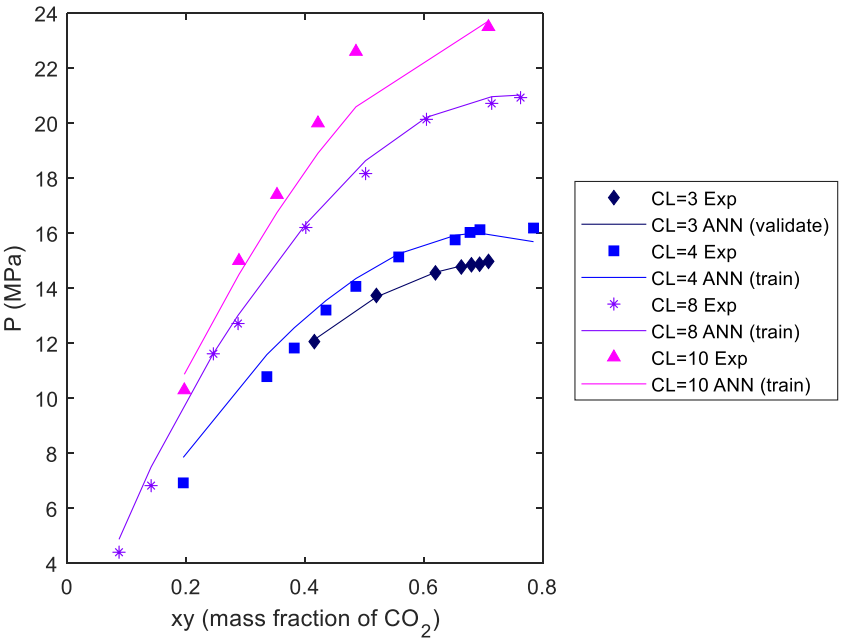

Figure 5-16: ANN results comparing the chain length, bubble point pressure and mass fraction for CO_2 of alcohols at 373 K – data from Elizalde-Solis et al. (2007), Byun and Kwak (2002) and Pohler (1994)

Overall, opposed to the CO_2 and alkane systems, the accuracy of the binary systems decreases as the chain length increases and as the pressure increases for the CO_2 and alcohol systems.

Figure 5-17 illustrates the ANN results for binary systems containing CO_2 and carboxylic acids with experimental data as obtained from Byun and Kwak (2000) (for the CO_2 and pentanoic acid and hexanoic acid binary systems respectively) and Yau et al. (1992) (for the CO_2 and octanoic acid binary system) which resulted in $AAD\%$ values of 2.89%, 4.45% and 2.99% respectively. As observed from this figure, the predictions at lower pressures are more accurate compared to the predictions at high pressures.

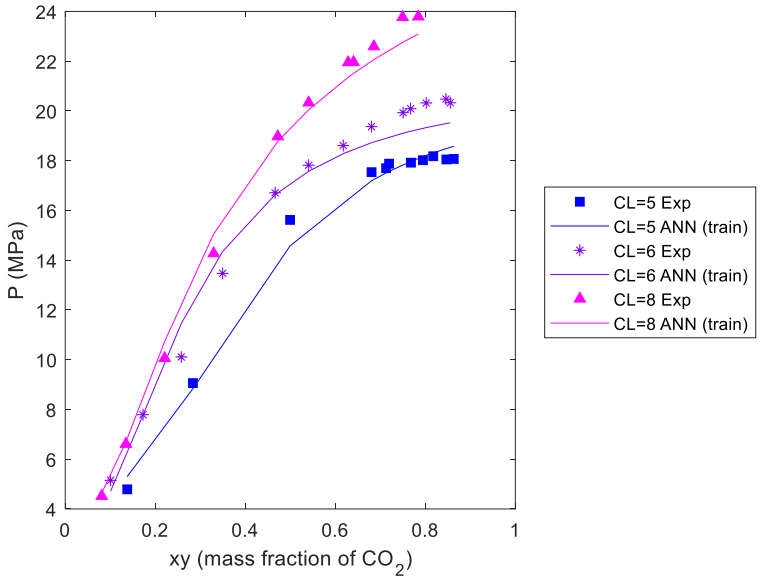

Figure 5-17: ANN results comparing the chain length, bubble point pressure and mass fraction for CO_2 of carboxylic acids at 373 K – data from Byun and Kwak (2000) and Yau et al. (1992)

Figure 5-18 illustrates the results of the ANN compared to with experimental results of CO_2 and decane at different temperatures (Reamer & Sage, 1963).

Table 5-4 compares the results of CO_2 and decane at various temperatures, as obtained by case studies 1 (as illustrated in Figure 4-15) and 2 (as illustrated in Figure 5-18). As seen in this table and Figures 4-15 and 5-18, the simpler neural network used in case study 1 resulted in more accurate results. As for case study 1, binary systems at higher temperatures for these binary systems resulted in more accurate predictions for case study 2.

Table 5-4: Comparing the AAD% values of case studies 1 and 2 for binary systems containing CO_2 and decane at different temperatures

CO_2 and decane at specific temperature	***AAD*% for case study 1**	***AAD*% for case study 2**
227 K	24.70%	35.60%
310 K	23.22%	41.48%
344 K	32.16%	74.25%
377 K	0.81%	1.62%

It should be noted that the binary system at 344 K is part of the testing data, therefore resulting in the poorest predictions with an *ADD*% of 74.25%. It should also be noted that overfitting of the neural network is possible, causing fluctuations at low pressures at a temperature of 310 K.

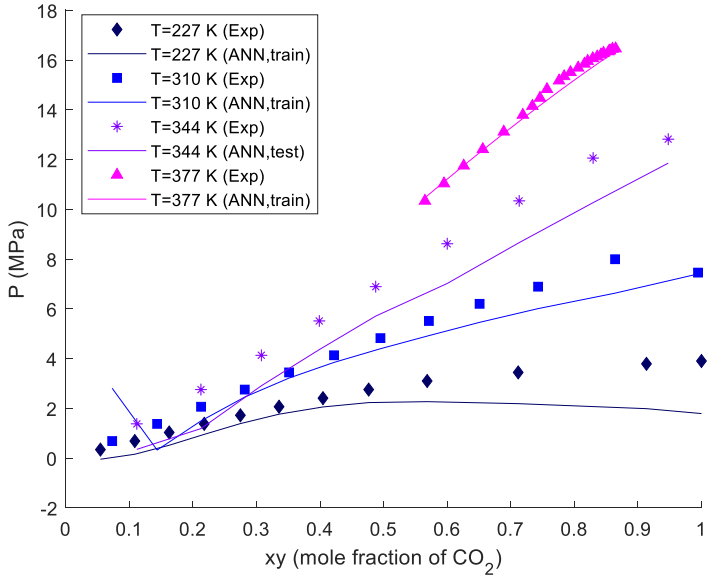

Figure 5-18: ANN predictions of the bubble point pressures compared to experimental results from (Reamer & Sage (1963) for case study 2

5.4. Relative importance of the input variables

The same approach that was used in case study 1 (as discussed in Section 4.4) was used to implement the weights. The weight and bias matrixes of the neural network, as determined in Sections 5.2 and 5.3 are listed in Tables D-4 to D-6 in Appendix D. As seen in these tables, the magnitude of the bias values is in the same order, indicated that the model is not overfitted, as discussed in Section 2.2.1. Further observed in these tables, as for case study 1, some of the connection weights have values close to zero, indicating that the connection weight plays a small role when determining the output of the neural network. These weight with a small impact to the neural network will be outlined, as discussed further in this section.

The relative importance of the input variables, as determined in Sections 5.2 and 5.3 were determined using Equations 2-23 and 2-24 listed in Section 2.2.7. Figure 5-19 depicts the relative importance of the two outputs of the neural network (bubble and dew point pressures) using the binary phase equilibrium data containing CO_2 and various hydrocarbons.

As seen in Figure 5-19, the relative importance of the inputs to the neural network are 9.3%, 1.1%, 2.4%, 30.7%, 18.4%, 1.9%, 11.6% 8.2% and 16.2% for the bubble point pressure output and 3.3%, 0.3%, 7.7%, 8.0%, 16.2%, 18.2%, 8.9%, 4.7% and 32.6% for the dew point pressure output for input variable FG_1, FG_2, w, T_c, T, MM, x/y, x and y, respectively.

As mentioned in Section 3.1, the vapour composition and dew point pressure were set to zero if values were assigned to the liquid composition and bubble point pressures and the liquid composition and bubble point pressure were set to zero if values were assigned to the vapour composition and dew point pressure. It is therefore interesting to note that y has a high relative importance when determining both output variables. When looking at x and y individually, x is relatively important when determining the bubble point pressure and y is relatively important when determining the dew point pressure.

Typically, at low concentrations of CO_2, bubble point pressures are observed where at high concentrations of CO_2, dew point pressures are observed. At an intermediate composition of CO_2, the mixture critical point is observed. Using x/y is therefore beneficial especially at the mixture critical point, since there isn't a large distinction between the composition of CO_2 in this region.

It is further interesting to note that the relative importance of the acentric factor and the molecular mass is high when determining the dew point pressures and low when determining the bubble point pressures.

As seen from this figure, the relative importance of the acentric factor is low relative to other input parameters. This finding confirms the results obtained in Section 4.5, concluding that the acentric factor is not so important when modelling high-pressure phase equilibrium using neural networks.

It is further evident that only one functional group variable (FG_1) is important where the other variable (FG_2) has an insignificant relative importance. Although FG_2 has a low relative importance, FG_1 and FG_2 are used in combination to define the functional group (as discussed using Table 2-7 in Section 2.2.6 and as mentioned in Section 5.2).

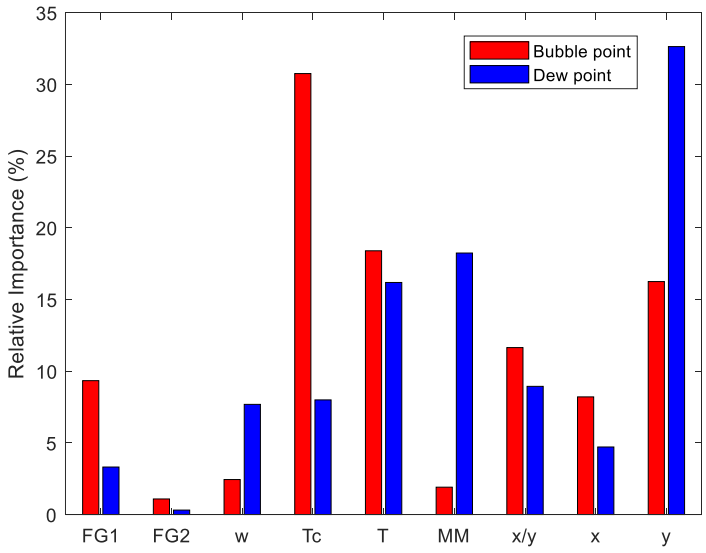

Figure 5-19: Relative importance of the input variables for the bubble point pressure as output variable to the neural network using CO_2 and various hydrocarbons as input and training data

As mentioned in Sections 2.1.4 and in 4.4, the parameters required for the RK Aspen EOS are $T_{c,m}$, $P_{c,m}$, $w_{c,m}$, η_m, $k^0_{a,mn}$, $k^1_{a,mn}$, $k^0_{b,mn}$ and $k^1_{b,mn}$. To determine η_m, additional vapour pressure data for the pure component are required where for the BIPs, additional phase equilibrium data are required. Table 5-5 compares the parameters used for the ANN and the RK-Aspen EOS. As seen in this table, the contrasting parameters are the vapour pressure data and the critical pressure used for the RK-Aspen EOS and the MM and functional group distinctions used in the ANN.

Table 5-5: Comparison between the parameters required for the ANN and the RK Aspen EOS

	Parameters required for RK Aspen EOS	**Parameters required for ANN**
Identical parameters for the models	Phase equilibrium data, w, T_c	Phase equilibrium data, w, T_c
Contrasting parameters for the models	Vapour pressure data, P_c	MM, FG_1 and FG_2

5.5. Neural networks relative to traditional modelling methods

In this section, a neural network using the optimised hyperparameters as determined in Sections 5.2 and 5.3 will be used to predict the bubble (P_b) and dew (P_d) point pressures of the test data where these results will be compared to experimental data and RK-Aspen models.

Figure 5-20 illustrates the regression plot of the testing data using the neural network with optimised hyperparameters with R^2 and $AAD\%$ values of 0.986 and 13.4%. As determined from this figure, the

maximum pressure deviation for the bubble and dew point pressures are 2.5 MPa and 5.8 MPa, respectively.

Figure 5-20 also depicts the regression plot of the optimised neural network (as determined in Sections 5.2 and 5.3) for the training and validation sets with combined R^2 and $AAD\%$ values of 0.942 and 19.0% and testing sets with R^2 and $AAD\%$ values of 0.986 and 13.4% for the bubble and dew point pressures. For the training data, bubble and dew point pressures are accurate within 25% (indicated by the dashed dot lines) for pressures above 26 MPa (for bubble and dew point pressures), where the maximum pressure deviations are within 17.4 MPa and 11.6 MPa, respectively, for the bubble and dew point pressures. For the testing data, bubble and dew point pressures are accurate within 10% (as indicated by the dashed lines) for the entire pressure range for bubble point pressures and accurate within 25% above 20 MPa for dew point pressures, where the maximum pressure deviations are within 2.1 MPa and 5.8 MPa, respectively. For the validation data, bubble and dew point pressures are accurate within 10% for pressures above 22 MPa and 9 MPa for bubble and dew point pressures, where the maximum pressure deviations are within 10.4 MPa and 6.1 MPa for bubble and dew point pressures.

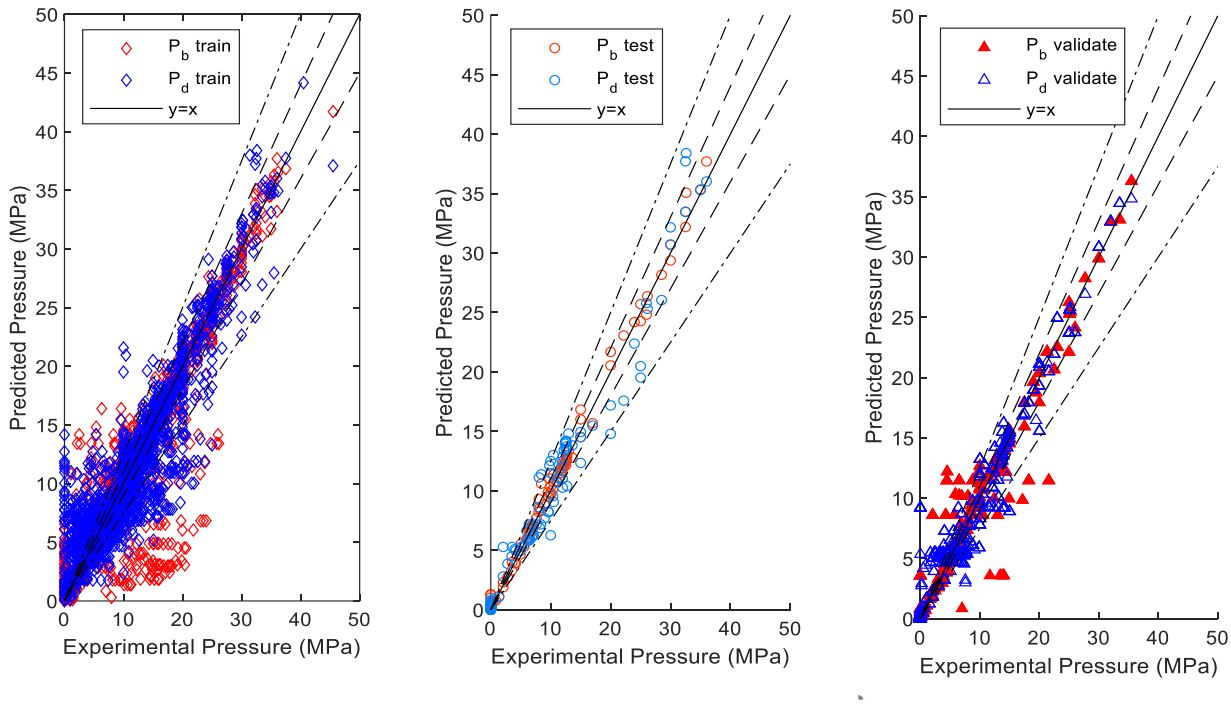

Figure 5-20: Predicted pressure vs experimental pressure using the training, testing and validation data

Figure 5-21 to Figure *5-27* illustrate the P-xy diagrams obtained using testing data of the binary systems containing CO_2 and pentane, decane and hexadecane for the alkane functional group, 1-butanol, 1-octanol and 1-dodecanol for the alcohol functional group and tetradecanoic acid for the carboxylic acid functional group. As seen in these figures, the dots illustrate the experimental data

obtained by Cheng, et al. (1989), Nagarajan & Robinson (1986) and D'souza, et al., (1988) for the alkanes, Elizalde-Solis, et al. (2003), Feng, et al. (2001) and Scheidgen (1997) for the alcohols and Pohler (1994) for the carboxylic acids. The solid lines represent the RK-Aspen correlations and the dotted lines the neural network predictions.

The Antoine parameters to determine the vapour pressure for pure components are listed in Table D-1 where the VLE data to regress the binary interaction parameters are listed in Tables A-1 to A-3. The polar factors and binary interaction parameters, as determined using Aspen Plus, are listed in Table D-2. The RK-Aspen models (as illustrated in the figures below) fail at high pressures due to unstable behaviour (oscillations in correlated pressures) in these regions.

As concluded from Section 4.6, it is unlikely for a third phase to form, for the binary systems containing pentane and CO_2, decane and CO_2 and hexadecane and CO_2, as depicted in Figure 5-21 to Figure 5-23.

As seen in Figure 5-21 for a binary system containing CO_2 and pentane at 311 K, the RK-Aspen model makes accurate correlations for low pressures, and starts to oscillate and become unstable above 4.3 MPa (oscillations are not indicated on this figure). The neural network predictions are accurate at low pressures predicting bubble point pressures and high pressures predicting the dew point pressures. Predictions for bubble point pressures have an error deviation of approximately 0.3 MPa where for dew point pressures, predictions are under predicted by approximately 2.1 MPa.

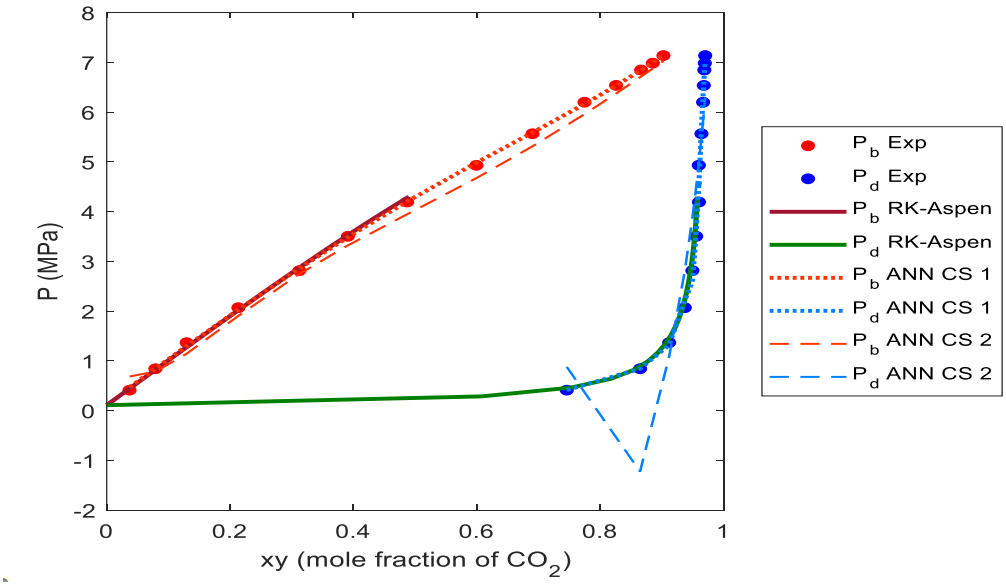

Figure 5-21: Bubble and dew point pressures of a binary system with CO_2 and pentane at 311 K obtained from experimental data (Cheng et al., *1989), an RK-Aspen model (with η_m, $k^0_{a,mn}$ and $k^0_{b,mn}$ values of 0.1024, 0.1344 and -0.00476) and the attained ANN using CO_2 and various hydrocarbons as testing data*

As mentioned earlier, since the methodology of this study minimized the geometric distance between R^2 and $AAD\%$ and since data points were duplicated, it is possible that the model is overfitted. When looking at the results as illustrated in Figure 5-21, the discontinuities occurs at low pressures, opposed to EOS failing at high pressures. The two models can therefore complement each other if used in hybrid systems.

For the binary system containing CO_2 and decane at 344 K, the RK-Aspen model was accurate (with errors within 0.2 MPa) for pressures up to 11.4 MPa, but was unable to make any correlations above this point. The neural network made accurate predictions for bubble point pressures with errors within 0.3 MPa where dew point pressures where accurate up to 12.0 MPa. For dew point pressures above this point, the error range was 2.3 MPa, which is still good, compared to the RK-Aspen model that could not make any correlations.

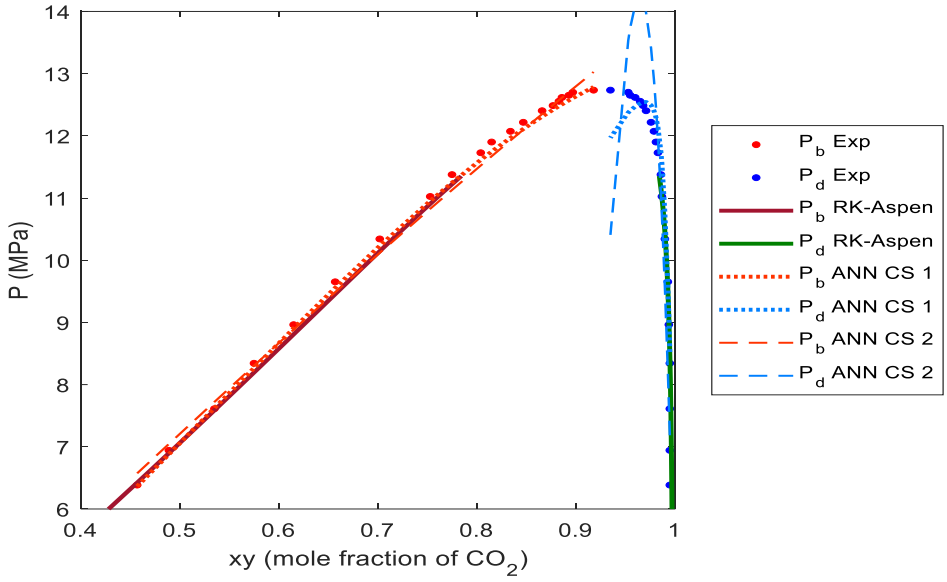

Figure 5-22: Bubble and dew point pressures of a binary system with CO_2 and decane at 344 K obtained from experimental data (Nagarajan & Robinson, 1986), an RK-Aspen model (with η_m, $k^0_{a,mn}$ and $k^0_{b,mn}$ values of 0.0497, 0.1015 and -0.02771) and the attained ANN using CO_2 and various hydrocarbons as training data

In Figure 5-23, the results obtained by the optimised neural network, an RK-Aspen model, and experimental results as obtained by D'souza, et al., (1988) for a binary system containing CO_2 and hexadecane at 314 K, as used for case study 1, are compared. As for the comparison done in case study 1, the maximum correlation pressure for the RK-Aspen model is 8.6 MPa. As discussed earlier, correlations in the vicinity of the critical region fail due to simulation errors and similar densities of the vapour and liquid phases. The neural network, however, was able to make predictions in the

critical region, resulting in maximum bubble and dew point pressure deviations of 2.2 MPa and 3.1 MPa.

Latsky et al., (2020) modelled binary systems containing CO_2 and hexadecane at temperatures of 328 K, 338 K, 348 K and 358 K respectively, therefore excluding the binary system at a temperature of 314 K. Comparing the RK-Aspen results as illustrated in Figure 5-23 (at a lower temperature) with the results as obtained by Latsky et al., (2020), more accurate correlations at higher pressures were obtained. This could be because of BIPs overestimating the interactions at low temperatures since high interactions occur at low temperatures.

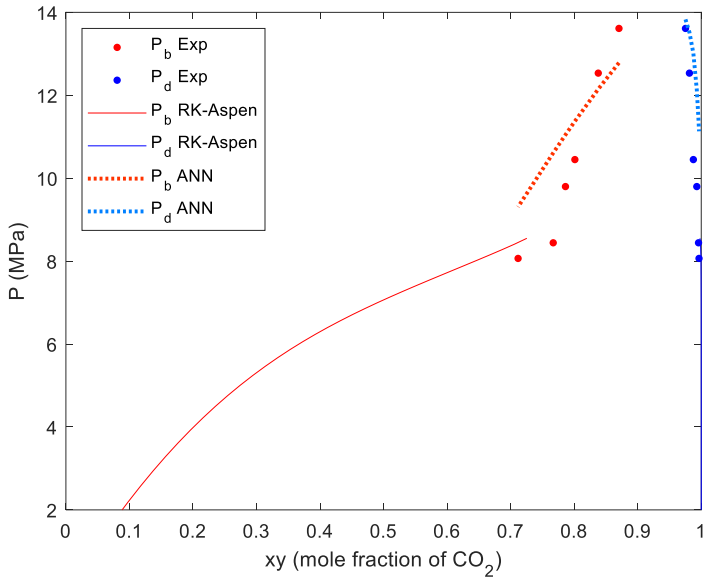

Figure 5-23: Bubble and dew point pressures of a binary system with CO_2 and hexadecane at 314 K obtained from experimental data (D'souza, et al., 1988), an RK-Aspen model (with η_m, $k^0_{a,mn}$ and $k^0_{b,mn}$ values of 0.0233, 0.085 and -0.07291) and the attained ANN using CO_2 and various hydrocarbons as testing data

When comparing Figure 4-20 to Figure 4-22 as illustrated in Section 4.6 with Figure 5-21 to Figure 5-23, it was expected that the more complex ANN (case study 2) would result in less accurate results than the simpler ANN used for case study 1. Although the results obtained in case study 2 are less accurate than the results obtained by the simpler neural network, the ANN predictions are still better than RK-Aspen correlations at high pressures.

Figure 5-24 compares different results of a binary system containing CO_2 and 1-butanol at 354 K. As mentioned in Section 2.1.3, binary systems containing CO_2 and 1-butanol are expected to behave like type II systems. At 354 K, the system is at supercritical conditions, therefore making it unlikely for a third phase to form. As seen in this figure, the RK-Aspen model resulted in accurate correlations, but can only correlate pressures up to 11.1 MPa accurate within 2.1 MPa for dew point pressures and 0.2

MPa for bubble point pressures where the neural network has a maximum pressure deviation of 3.2 MPa for dew point pressures and 0.5 MPa for bubble point pressures. Although the RK-Aspen model makes more accurate correlations, the neural network can make predictions for the whole pressure range. The two models therefore complement each other and can both be used when predicting binary phase behaviour for CO_2 and 1-butanol at 354 K.

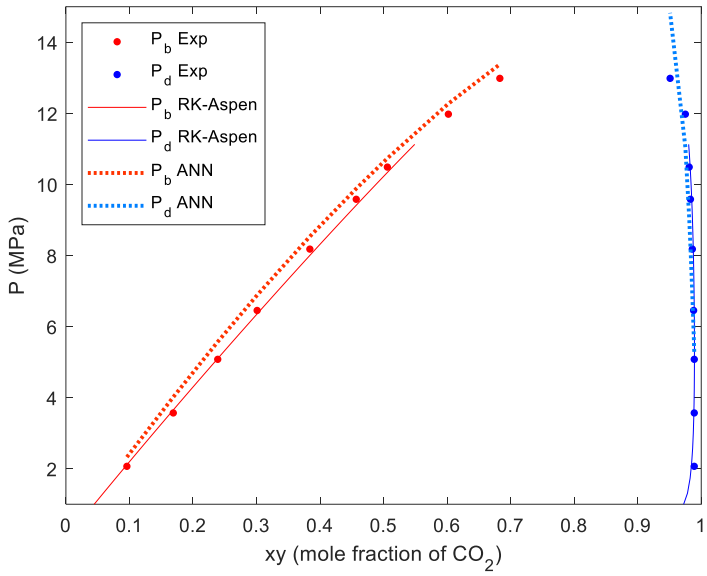

Figure 5-24: Bubble and dew point pressures of a binary system with CO_2 and 1-butanol at 354 K obtained from experimental data (Elizalde-Soliz, et al., 2003)), an RK-Aspen model (with η_m, $k^0_{a,mn}$ and $k^0_{b,mn}$ values of -0.2572, 0.0692 and -0.0281) and the attained ANN using CO_2 and various hydrocarbons as testing data

In Figure 5-25 the experimental results are compared with two models (RK-Aspen and the optimised neural network) of a binary system containing CO_2 and 1-octanol at 328 K. Binary systems containing CO2 and alcohol CLs longer than 5 are expected to have type III behaviour. Since this system is at supercritical temperatures with a T_{c,CO_2} value of 1.08, it is unlikely for the liquid phase to split. The RK-Aspen model can only make correlations up to 10.5 MPa accurate within 0.6 MPa for bubble point correlations and 4.2 MPa for dew point correlations where the neural network predictions are relatively accurate with a pressure deviation of 1.3 MPa for bubble point pressures and 3.7 MPa for dew point pressures. The RK-Aspen model over predicts at low pressures and under predicts at medium pressures for bubble point predictions.

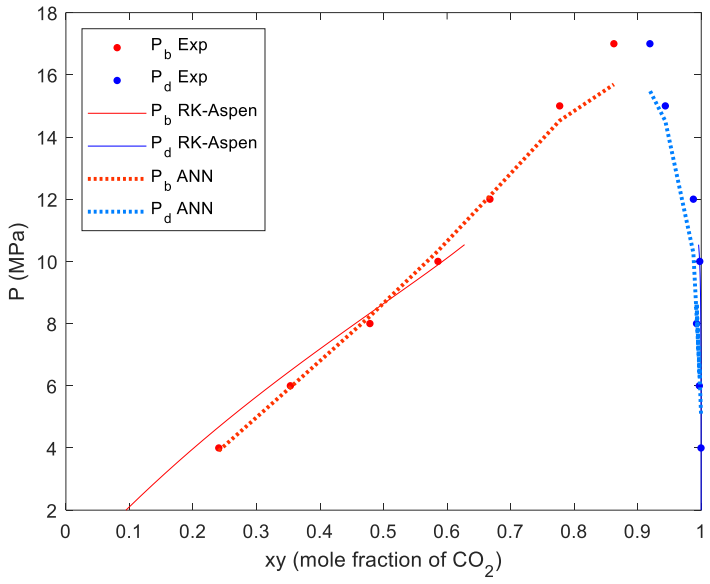

Figure 5-25: Bubble and dew point pressures of a binary system with CO_2 and 1-octanol at 328 K obtained from experimental data (Feng, et al., 2001), an RK-Aspen model (with η_m, $k^0_{a,mn}$ and $k^0_{b,mn}$ values of -0.443, 0.0763 and -0.05099) and the attained ANN using CO_2 and various hydrocarbons as testing data

In Figure 5-26, the P-xy plots of binary systems containing CO_2 and 1-dodecanol at 393 K are depicted. As mentioned above using Figure 5-25, binary systems containing CO_2 and alcohols with CLs longer than 5 are expected to have type III behaviour. Since this binary system is also at supercritical temperatures ($T_{r,CO_2} = 1.3$), it is unlikely for a third phase to form. As seen in this figure, the neural network predictions (accurate within 1.3 MPa for bubble point pressures and 3.7 MPa for dew point pressures) are more accurate than the RK-Aspen correlations (accurate within 6.8 MPa for bubble point pressures and 8.0 MPa for dew point pressures). Temperature inversions have been observed for a binary system containing CO_2 and dodecanol at 343 K (Bonthuys, Schwarz, Burger, & Knoetze, 2011). The binary system as illustrated in Figure 5-26 is also at a low temperature with high interaction between the molecules. It is therefore possible that the poor RK-Aspen correlations could be because of a temperature inversion or overestimation of the BIPs. Although the EOS struggles to predict this system possibly due to a temperature inversion, the ANN has no problem with this occurrence.

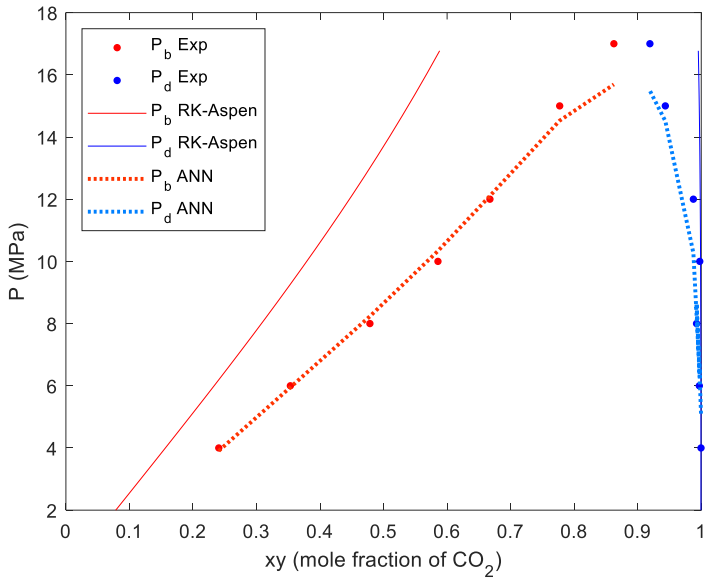

Figure 5-26: Bubble and dew point pressures of a binary system with CO_2 and 1-dodecanol at 393 K obtained from experimental data (Scheidgen, 1997), an RK-Aspen model (with η_m, $k^0_{a,mn}$ and $k^0_{b,mn}$ values of -0.1744, -1.3589 and -2.8313) and the attained ANN using CO_2 and various hydrocarbons as testing data

The binary system for CO_2 and tetradecanoic acid at 393 K is depicted in Figure 5-27. As mentioned for the previous figures in this subsection, it is unlikely for a third phase to form for this binary system, since it is at supercritical temperatures ($T_{r,CO_2} = 1.3$).

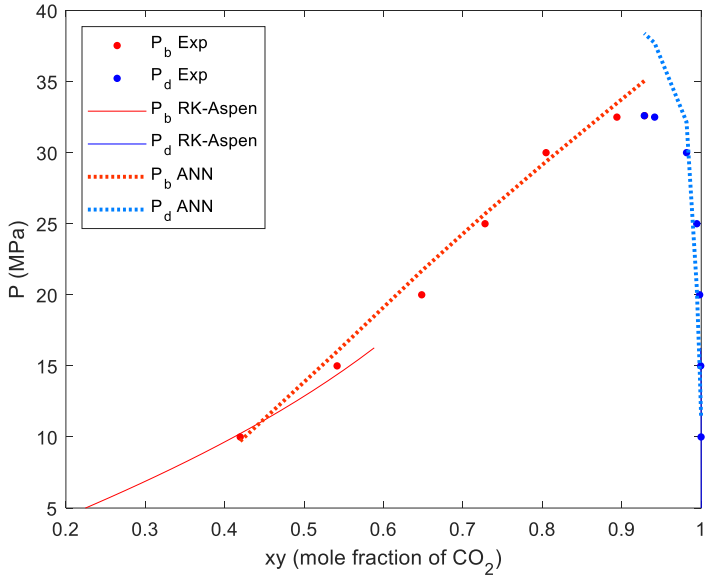

Figure 5-27: Bubble and dew point pressures of a binary system with CO_2 and tetradecanoic acid at 393 K obtained from experimental data (Pohler, 1994), *an RK-Aspen model (with η_m, $k^0_{a,mn}$ and $k^0_{b,mn}$ values of -0.2088, 0.0645 and -0.01511) and the attained ANN using CO_2 and various hydrocarbons as testing data*

As observed in this figure, the maximum pressure that the RK-Aspen model can correlate is 16.3 MPa (accurate within 0.6 MPa for bubble point pressures and 2.5 MPa for dew point pressures) where the neural network is able to predict pressures for the whole pressure range, accurate within 2.5 MPa for bubble point pressures and 5.8 MPa for dew point pressures.

6. Results and discussion of case study 3: Evaluation of published results

As discussed in Sections 2.3 and 3.1, there are two methods to consider when dividing the training, testing and validation data for modelling high-pressure phase equilibrium using neural networks. The first option is to randomly select data points from each binary system for the validation and testing data sets, therefore, interpolating between trained data points (for validation during the training of the neural network and testing the neural network after training), as used in previous studies. The second option is to select complete binary systems as validation and testing data sets. It was further concluded from case studies 1 and 2 (Chapters 4 and 5) that it is more beneficial to use two hidden layers instead of a single hidden layer.

In this chapter, two articles, published by Lashkarbolooki & Vaferi, et al., (2013) and Vaferi, et al., (2018) will be used to investigate the two methods to divide the training, testing and validation sets and to evaluate whether two hidden layers will be more benificial than a single hidden layer, using the same data as used in these studies. As discussed in Section 3.1, the first method to divide the data (selecting random data points from each binary system) result in very accurate results, as obtained by previous studies, since neural networks interpolate data very well. The second method to divide data (where complete binary systems are selected as testing and validation data) will be more beneficial since it is more likely for a whole data system to be unavailable in practice and no single data points to be interpolated. For the second methodology, data points were duplicated for the training data until all binary systems had the same number of data points.

These case studies used the critical pressure, reduced temperature (a function of temperature) and acentric factors of the heavier compound to distinguish between the different compounds and systems and the CO_2 composition of the liquid and vapour phases to distinguish between the data points.

It should be noted that the $AARD\%$ (as opposed to $AAD\%$ used for case studies 1 and 2) will be used in case study 3 to determine the optimum neural network, since $AARD\%$ was used by Lashkarbolooki & Vaferi, et al., (2013) and Vaferi, *et al.*, (2018). It should also be noted that for the first article (as discussed in Section 6.1), the author specified the specific data splits, but for the second article (as discussed in Section 6.2), only the ratios were used.

6.1. A case study published by Lashkarbolooki et al. (2013)

In the case study published by Lashkarbolooki & Vaferi, et al., (2013), the binary systems containing CO_2 and a cyclic compound, as listed in Table 6-1 were used, specifying the cyclic compound, temperature, pressure range, mole fraction range of the liquid and vapour phase (x, y) and the number of data points available. Further, a cascade feedforward backpropagation neural network with a size of $5 \times 15 \times 2$ using the log-sigmoid transfer function was used.

Table 6-1: Binary systems as used by Lashkarbolooki & Vaferi, et al., (2013)

Cyclic compound	T (K)	P (MPa)	xy (mole fraction)	N_b	Reference
Bisephenol A	403	2, 4-8,9	0,052-0,150	4	Margon, et al., (2005)
	407	2,5-9,1	0,052-0,150	4	Margon, et al., (2005)
	411	2,5-9,2	0,052-0,150	4	Margon, et al., (2005)
	415	2,6-9,3	0,052-0,150	4	Margon, et al., (2005)
	419	2,7-9,4	0,052-0,150	4	Margon, et al., (2005)
	423	2,7-9,5	0,052-0,150	4	Margon, et al., (2005)
	427	2,7-9,5	0,052-0,150	4	Margon, et al., (2005)
	431	2,7-9,5	0,052-0,150	4	Margon, et al., (2005)
Dephenyl carbonate	353	2,3-6,7	0,149-0,360	5	Margon, et al., (2005)
	363	2,6-7,4	0,149-0,360	5	Margon, et al., (2005)
	373	2,8-8,1	0,149-0,360	5	Margon, et al., (2005)
	383	3,0-8,7	0,149-0,360	5	Margon, et al., (2005)
	304	3,5-10,0	0,149-0,360	5	Margon, et al., (2005)
	413	3,7-10,6	0,149-0,360	5	Margon, et al., (2005)
	423	3,9-11,2	0,149-0,360	5	Margon, et al., (2005)
	433	4,1-11,7	0,149-0,360	5	Margon, et al., (2005)
	443	6,1-12,2	0,149-0,360	5	Margon, et al., (2005)
	453	4,4-9,9	0,149-0,298	4	Margon, et al., (2005)
Quinoline	308	3,5-7,9	0,246-0,990	16	Shan-Chun, et al., (2012)
	313	3,6-8,8	0,246-0,990	16	Shan-Chun, et al., (2012)
	318	7,6-9,8	0,443-0,990	16	Shan-Chun, et al., (2012)
	328	4,0-26,9	0,246-0,990	16	Shan-Chun, et al., (2012)
	333	4,4-27,7	0,246-0,990	16	Shan-Chun, et al., (2012)
Nicotene	313	6,0-8,2	0,652-0,994	9	Ruiz-Rodrigues, et al., (2009)
Benzene	298	0,9-5,8	0,106-0,996	16	Danesh (1998)
	313	1,5-6,1	0,149-0,986	19	Danesh (1998)
Tetra-hydropuran	313	6,5-7,7	0,017-0,972	30	Li, et al., (2007)
	323	7,8-8,4	0,025-0,938	15	Li, et al., (2007)
	333	9,1-9,0	0,052-0,885	16	Li, et al., (2007)

Using the same hyperparameters as used by Lashkarbolooki & Vaferi, *et al*., (2013) and the binary systems as listed in Table 6-1, a neural network was trained where the predicted pressure and the experimental pressure are illustrated in Figure 6-1 for the training and testing data. It is expected that the results obtained by this study and the results obtained by Lashkarbolooki & Vaferi, *et al*., (2013) will not be exactly the same since random initial weights and bias values are selected when training neural networks. Approximately the same results were obtained for this study, as those obtained by Lashkarbolooki & Vaferi, *et al*., (2013). The R^2 values for the training and testing data obtained here were 0.9995 and 0.9974 respectively, which is slightly higher than the training and testing data obtained by Lashkarbolooki & Vaferi, *et al*., (2013) with an R^2 value of 0.9989 for both the training and testing data. The $AARD\%$ value of 1.47 for the training data was the same as obtained by Lashkarbolooki & Vaferi, *et al*., (2013), whereas the $AARD\%$ value of the testing data was higher with 2.11%. It should be noted that the validation data are not displayed on this figure since Lashkarbolooki & Vaferi, *et al*., (2013) only displayed the training and testing regression data in the published article.

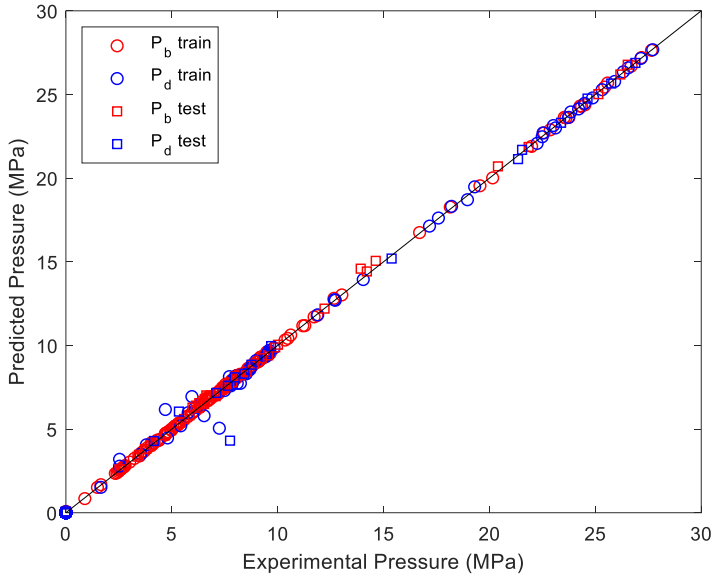

Figure 6-1: Predicted pressure versus experimental pressure using MATLAB

Since extremely similar results were obtained here, compared to those obtained by Lashkarbolooki & Vaferi, et al., (2013), using a neural network with a single hidden layer will be compared to a neural network with two hidden layers where data were divided by selecting data points randomly (the first option as discussed above), as illustrated in Figure 6-2 and Figure 6-3. Using Figure 6-5 and Figure 6-6, the second option to divide the training, testing and validation will be compared using one and two hidden layers respectively.

Figure 6-2 illustrates the R^2 and $AARD\%$ values of the training and testing data using a cascade feedforward backpropagation neural network and a log-sigmoid transfer funcion (as used by Lashkarbolooki & Vaferi, et al., (2013)) with *one* hidden layer where the training, testing and validation data were divided using the first option as discussed earlier in this section. As observed in Figure 6-2 and Table B-11, following the same approach as used in case studies 1 and 2, R^2 was maximised and $AARD\%$ and the geometric distance were minimised. Twenty-four nodes per hidden layer resulted in the optimal results with R^2 values of 0.998 and 0.999 for the training and testing data and $AARD\%$ values of 4.14% and 3.21% for the training and testing data.

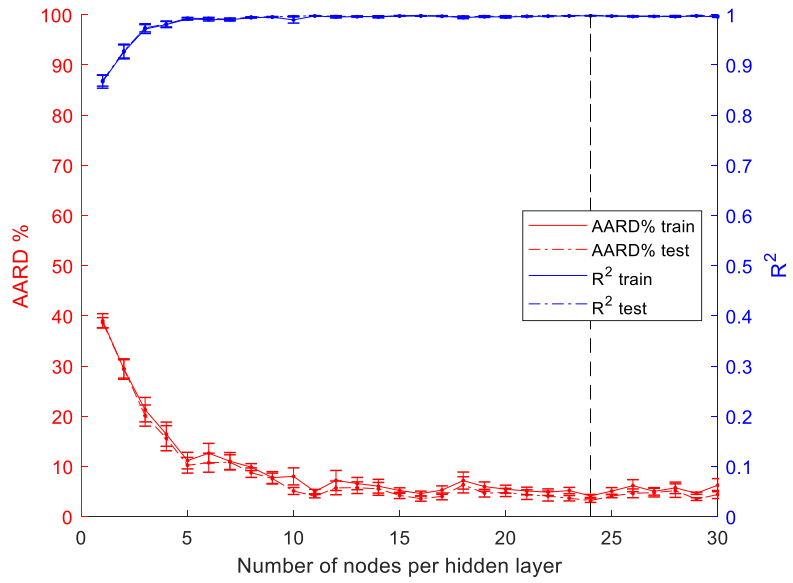

Figure 6-2: The AARD% and R^2 values for the training and testing data of neural networks using one hidden layer and the first option to divide the training, testing and validation data

Figure 6-3 depicts the R^2 and $AARD\%$ values of the training and testing data using a cascade feedforward backpropagation neural network and a log-sigmoid transfer funcion (as used by Lashkarbolooki & Vaferi, et al., (2013)) with *two* hidden layers where the training, testing and validation data were divided using the first option as discussed above.

As seen in Figure 6-3 and Table B-12, the optimal R^2 (0.999 for both the training and testing data) and $AARD\%$ (4.22% and 3.29% for the training and testing data) values were at 16 nodes per hidden layer with relatively low geometric distance values for the entrie range.

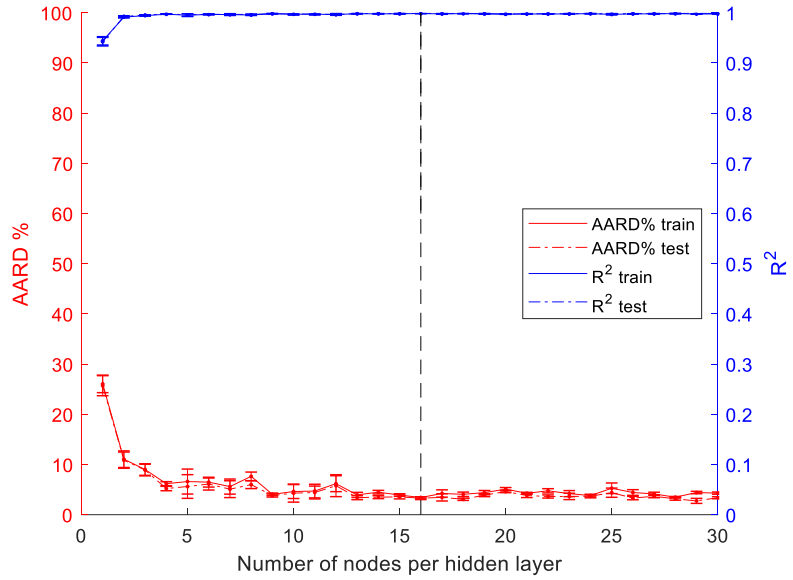

Figure 6-3: The AARD% and R^2 values for the training and testing data of neural networks using two hidden layers and the first option to divide the training, testing and validation data

Comparing the results as obtained by the neural networks with one (a neural network with a size of $5 \times 24 \times 2$ as obtained by Figure 6-2) and two (a neural network with a size of $5 \times 26 \times 16 \times 2$ as obtained by Figure 6-3) hidden layers respectively, where validation and testing data points were selected randomly (the first option to divide the training testing and validation data), the neural network with two hidden layers resulted in better R^2 values where the neural network with one hidden layer resulted in better $AARD\%$ values.

Since the results were inconclusive when comparing one and two hidden layers (using the first option to divide the training, testing and validation data), the P-xy results (as observed in Figure 6-4) of these two neural networks will be compared using a binary system containing CO_2 and quinoline at 333 K.

As seen in Figure 6-4, both neural networks perform well when predicting the bubble and dew point pressures, but the neural network with two hidden layers performs slightly better, especially at high pressures for bubble point predicitons.

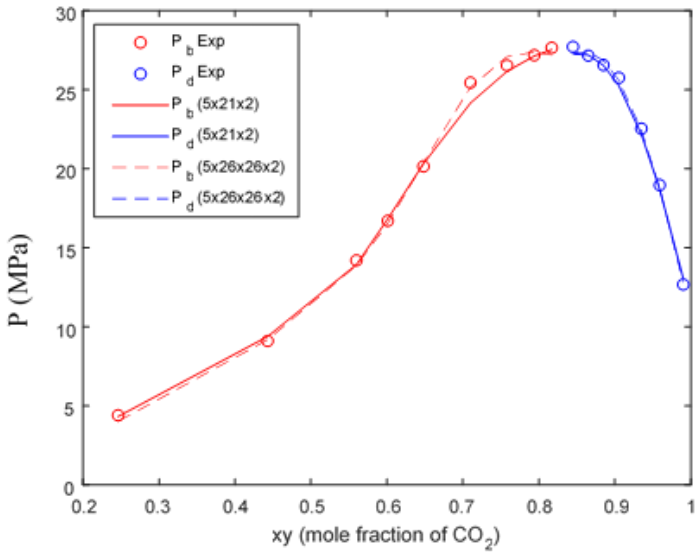

Figure 6-4: Bubble and dew point pressures of a binary system with CO_2 and quinoline at 333 K comparing neural networks with one and two hidden layers where training, testing and validation data were divided using option 1 for case study 3 using data obtained from Lashkarbolooki & Vaferi, et al., (2013)

In conclusion, when using the first option to divide the training, testing and validation data, using two hidden layers instead of a single hidden layer is more benificial when predicting phase equilibrium at high pressures.

Figure 6-5 and Figure 6-6 illustrate the R^2 and $AARD\%$ values of the training and testing data, using the same hyperparameters as used in Figure 6-2 and Figure 6-3, however, the training, testing and validation data were divided using the second option (where complete binary systems were selected as validation and testing data).

As seen in Figure 6-5 and Table B-13 (using a neural network with one hidden layer and the second option to divide the training, testing and validation data), at 26 nodes per hidden layer, $AARD\%$ is minimized (19.0% for the training data and 22.0% for the testing data) where the R^2 values (0.901 and 0.869 for the training and testing data) are relatively high and the geometric distances are relatively low.

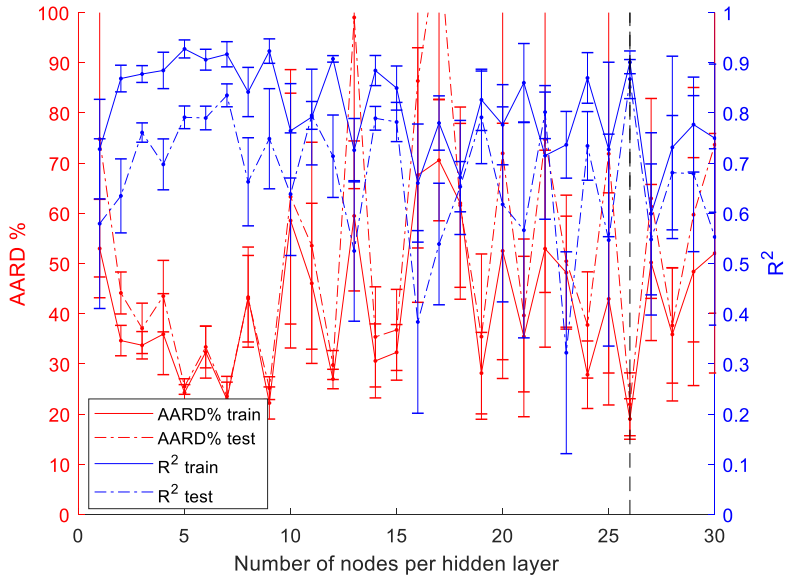

Figure 6-5: The AARD% and R^2 values for the training and testing data of neural networks using one hidden layer and the second option to divide the training, testing and validation data

The optimal nodes per hidden layer is 25 using a neural network with two hidden layers and the second option to divide the training, testing and validation data, as seen using Figure 6-6 and Table B-14 with R^2 values of 0.950 and 0.864 and $AARD\%$ values of 12.0% and 16.0% for the training and testing data, respectively.

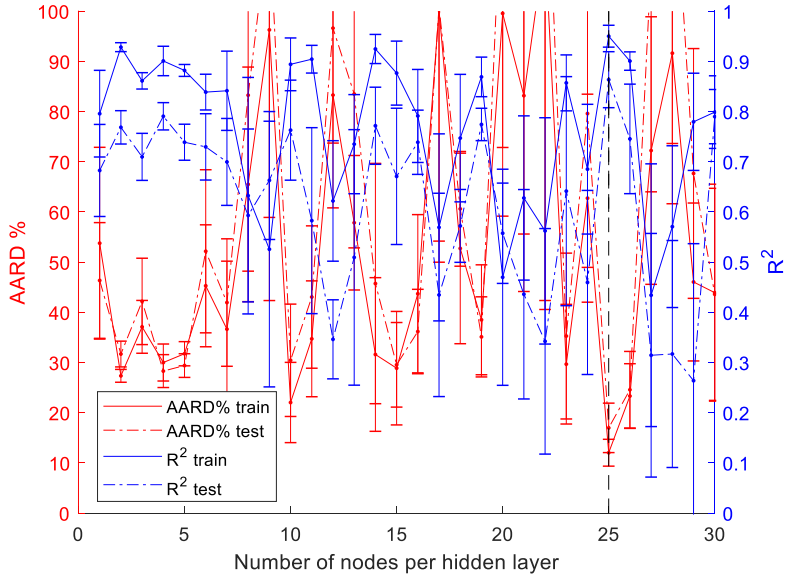

Figure 6-6: The AARD% and R^2 values for the training and testing data of neural networks using two hidden layers and the second option to divide the training, testing and validation data

Figure 6-7 illustrates the P-xy results of CO_2 and quinoline at 333 K, a binary system from the testing data using the neural network with one and two hidden layers as obtained using Figure 6-5 (which resulted in neural network with an optimal size of $5 \times 26 \times 2$) and Figure 6-6 (which resulted in

neural network with an optimal size of $5 \times 25 \times 25 \times 2$). As seen from this figure, the neural network with two hidden layers performs better than the neural network with one hidden layer, especially at high pressures.

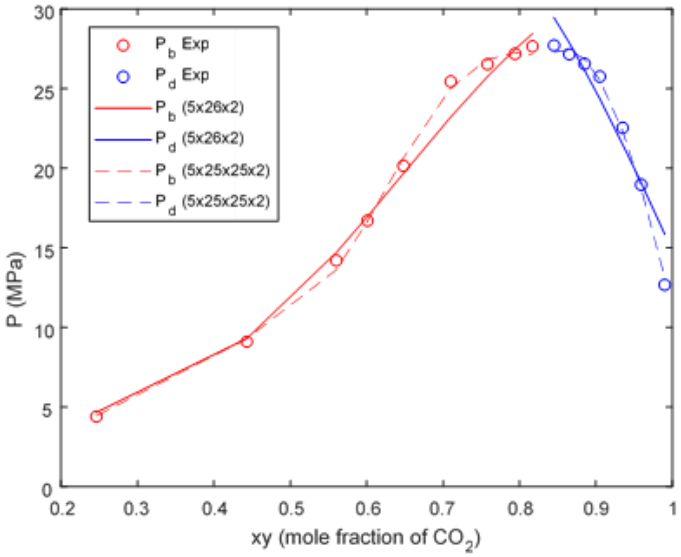

Figure 6-7: Bubble and dew point pressures of a binary system with CO_2 and quinoline at 333 K comparing neural networks with one and two hidden layers where training, testing and validation data were divided using option 2 for case study 3 using data obtained from Lashkarbolooki & Vaferi, et al., (2013)

Table 6-2 lists the optimal R^2 and $AARD\%$ values as presented in Figure 6-2, Figure 6-3, Figure 6-5 and Figure *6-6* and the results as obtained in the published article. As seen in this table, the neural networks using option 1 for dividing the training, testing and validation data and the neural network as obtained in the published article resulted in better R^2 and $AARD\%$ values. This was expected, since complete binary systems were used (for option 2) as testing and validation data opposed to interpolated data points, as used for option 1. Furthermore, the neural networks with two hidden layers performed better than the neural networks with a single hidden layer. This was expected since the same conclusion was made in case studies 1 and 2.

Table 6-2: R^2 and AAD% values comparing different options to divide the training, testing and validation data and comparing one and two hidden layers using data as obtained by Lashkarbolooki & Vaferi, et al., (2013)

Option for dividing the training, testing and validation data		Training	Testing	Neural network structure ($N_{HL} \times N_{nodes}$)
Published article	R^2	0.999	0.999	$5 \times 15 \times 2$
	$AARD$ %	1.47	2.11	
Option 1	R^2	0.998	0.999	$5 \times 24 \times 2$
	$AARD$ %	4.14	3.21	
Option 1	R^2	0.999	0.999	$5 \times 16 \times 16 \times 2$
	$AARD$ %	4.2	3.3	
Option 2	R^2	0.901	0.867	$5 \times 26 \times 2$
	$AARD$ %	19.0	22.0	
Option 2	R^2	0.950	0.864	$5 \times 25 \times 25 \times 2$
	$AARD$ %	12.0	17.0	

6.2. A case study published by Vaferi et al. (2018)

In the case study as published by Vaferi et al. (2018), the binary systems containing CO_2 and refrigerants are listed in Table 6-3. A multilayer perception neural network with one hidden layer containing 14 nodes using the sigmoid transfer function was used. The input data for each independent and dependent variable were normalised between 0.01 and 0.99.

Table 6-3: Binary systems as used by Vaferi, et al., (2018)

Refrigerants	T (K)	P (MPa)	xy (mole fraction)	N_b	Reference
R30 (dichloro-methane)	312	4,1-7,9	0,350-0,951	7	Gonzalez, et al., (2002)
	327	4,5-9,1	0,350-0,903	7	Gonzalez, et al., (2002)
R32 (difluoro-methane)	283	1,1-4,5	0,043-0,893	16	Madani, et al., (2012)
	293	1,5-5,7	0,063-0,951	16	Madani, et al., (2012)
	303	2,3-7,2	0,087-0,940	13	Madani, et al., (2012)
	305	2,0-6,9	0,072-0,153	13	Madani, et al., (2012)
	313	2,5-7,3	0,025-0,822	15	Madani, et al., (2012)
	323	3,1-7,5	0,025-0,656	16	Madani, et al., (2012)
	333	4,0-7,1	0,031-0,465	12	Madani, et al., (2012)
	343	4,9-6,6	0,069-0,228	12	Madani, et al., (2012)

Table 6-3 continued

Refrigerants	T (K)	P (MPa)	xy (mole fraction)	N_b	Reference
HFC-134a (1,1,1,2-tetrafluoro-ethane)	323	1,7-5,0	0,115-0,740	12	Lim, et al., (2008)
	328	2,0-7,1	0,092-0,759	16	Lim, et al., (2008)
	333	2,4-6,8	0,102-0,712	15	Lim, et al., (2008)
	338	2,2-6,8	0,062-0,660	16	Lim, et al., (2008)
	343	2,5-6,3	0,074-0,599	14	Lim, et al., (2008)
R227ea (1,1,1,2,3,3,3,-heptafluoro propane)	276	0,4-3,4	0,093-0,987	20	Valtz, et al., (2008)
	293	0,4-5,7	0,042-0,951	26	Valtz, et al., (2008)
	303	0,5-7,1	0,031-961	30	Valtz, et al., (2008)
	313	1,0-7,1	0,060-0,794	30	Valtz, et al., (2008)
	333	1,2-6,7	0,120-0,764	25	Valtz, et al., (2008)
	353	1,9-5,0	0,034-0,503	22	Valtz, et al., (2008)
	376	2,5-3,8	0,025-0,215	16	Valtz, et al., (2008)
R610 (decafluoro-butane)	263	0,2-2,4	0,030-0,983	24	Valtz, et al., (2011)
	283	0,5-4,0	0,064-0,976	22	Valtz, et al., (2011)
	303	0,7-6,6	0,059-0,960	26	Valtz, et al., (2011)
	308	0,5-6,9	0,022-0,940	20	Valtz, et al., (2011)
	323	1,0-6,7	0,057-0,832	24	Valtz, et al., (2011)
	338	1,4-6,2	0,071-0,732	23	Valtz, et al., (2011)
	352	1,7-5,1	0,064-0,601	21	Valtz, et al., (2011)

Using the same approach as Vaferi, et al. (2018) and the data listed in Table 6-3, a neural network was set up to evaluate the results. Data points (513) were collected from the listed references in the article, which is more than the number of data points (503) used by Vaferi, et al. (2018). Using all of the collected data points, lower R^2 and higher AARD% values (0.989 and 5.6% respectively) were obtained compared to those in the article. If, however, some of the high-pressure data points of the dew point pressures were eliminated, the same number of data points and approximately the same R^2 and higner AARD% values were obtained.

Figure 6-8 (using 503 data points) shows the predicted pressure versus the experimental pressure as obtained in this work with overall AARD% and R^2 values of 3.4% and 0.996 respectively, which is in line with the results as published by Vaferi, et al. (2018) with AARD% and R^2 values of 2.08% and 0.999 respectively. As mentioned in Section 6.1, it is expected that the results will not be exactly the same, since random initial weight and bias matrixes are assigned when training neural networks.

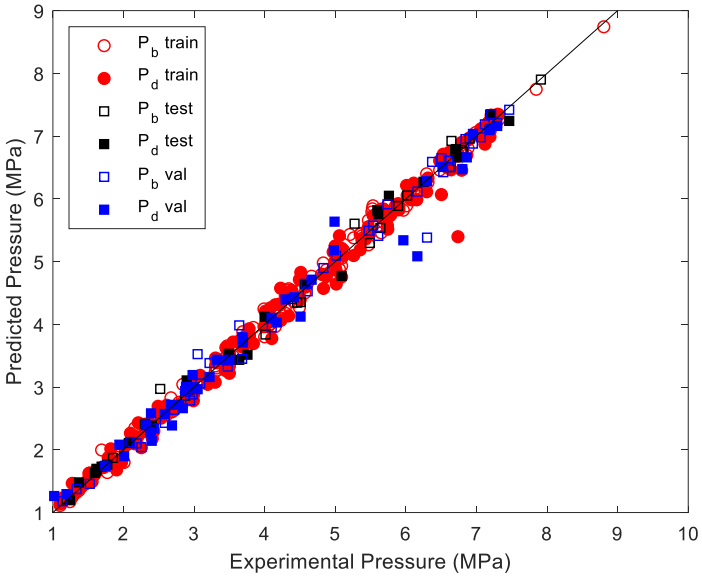

Figure 6-8: Predicted pressure versus experimental pressure as obtained using MATLAB

Since approximately the same results were obtained as obtained by Vaferi, et al. (2018), using a neural network with one and two hidden layers will be compared and presented in Figure 6-9 and Figure 6-10 where two different methods dividing the training, testing and validation data will be compared and presented in Figure 6-12 and Figure 6-13.

Figure 6-9 illustrates the R^2 and $AARD\%$ values of the training and testing data using a feedforward neural network and a log-sigmoid transfer funcion (as used by Vaferi, et al. (2018)) with *one* hidden layer where the training, testing and validation data were divided using the first option (selecting random data points from each binary system). As seen in Figure 6-9 and Table B-15, following the same approach as used in case studies 1 and 2 and Section 6.1, R^2 was maximised and $AARD\%$ and the geometric distance were minimised. Twenty-one nodes per hidden layer resulted in the optimal results with R^2 values of 0.997 and 0.998 for the training and testing data and $AARD\%$ values of 2.8% and 2.5% for the training and testing data.

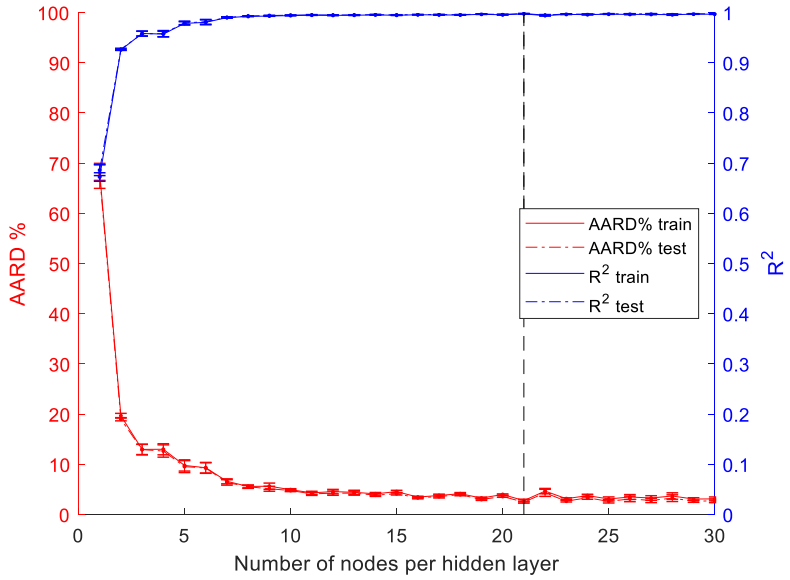

Figure 6-9: The AARD% and R^2 values for the training and testing data of neural networks using one hidden layer and the first option to divide the training, testing and validation data

Figure 6-10 illustrates the R^2 and $AARD\%$ values of the training and testing data using a neural network with two hidden layers. As seen in this figure and Table B-16, the optimal number of nodes per hidden layer is 27, resulting in R^2 values of 0.998 and 0.999 and AARD% values of 1.5% and 1.0% respectively.

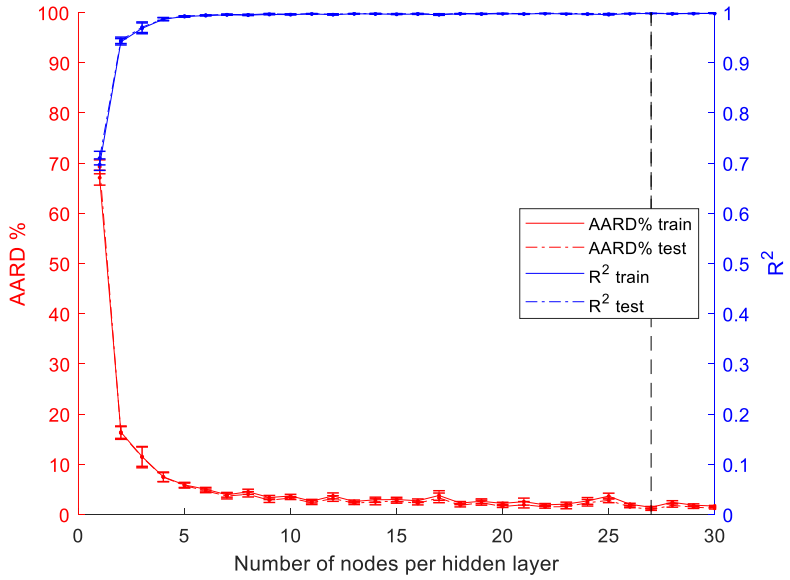

Figure 6-10: The AARD% and R^2 values for the training and testing data of neural networks using two hidden layers and the first option to divide the training, testing and validation data

Figure 6-11 illustrates the P-xy results of R32 and CO_2 at 303 K using the optimal neural networks as presented in Figure 6-9 (a neural network with a size of $5 \times 21 \times 2$) and Figure 6-10 (a neural network with a size of $5 \times 26 \times 26 \times 2$) where the training, testing and validation data were divided

using the first option. As seen in this figure, the neural network with a size of $5 \times 26 \times 26 \times 2$ makes accurate predictions through the whole range where the neural network with a size of $5 \times 21 \times 2$ is slightly less accurate at low and high pressures for dew point predictions and high pressures for bubble point predictions. The neural network with two hidden layers predicts both the bubble and dew point pressures better compared to the neural network using only one hidden layer.

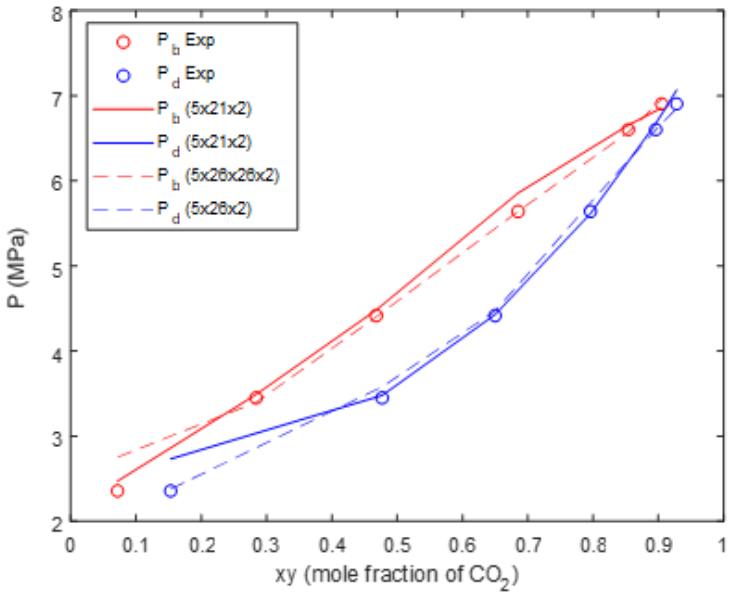

Figure 6-11: Bubble and dew point pressures of a binary system with CO_2 and R32 at 303 K comparing neural networks with one and two hidden layers where training, testing and validation data were divided using option 1 for case study 3 using data obtained from Vaferi, et al., (2018)

Figure 6-12 and Figure 6-13 illustrate the R^2 and $AARD\%$ values of the training and testing data using a neural network with one and two hidden layers respectively, where training, testing and validation data were divided using option 2.

As seen in Figure 6-12 and Table B-17, the optimal nodes per hidden layer were 25, resulting in R^2 values of 0.991 and 0.994 and $AARD\%$ values of 6.0% and 5.5% for the training and testing data.

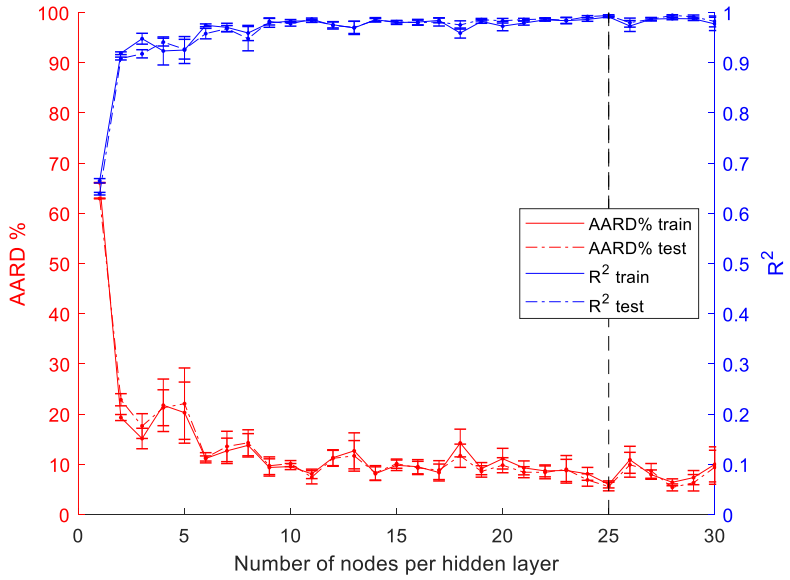

Figure 6-12: The AARD% and R^2 values for the training and testing data of neural networks using one hidden layer and the second option to divide the training, testing and validation data

The optimal nodes per hidden layer for a neural network with two hidden layers were 21, as seen in Figure 6-13 with R^2 values of 0.993 and 0.997 and $AARD\%$ values of 4.3% and 3.5% for the training and testing data respectively.

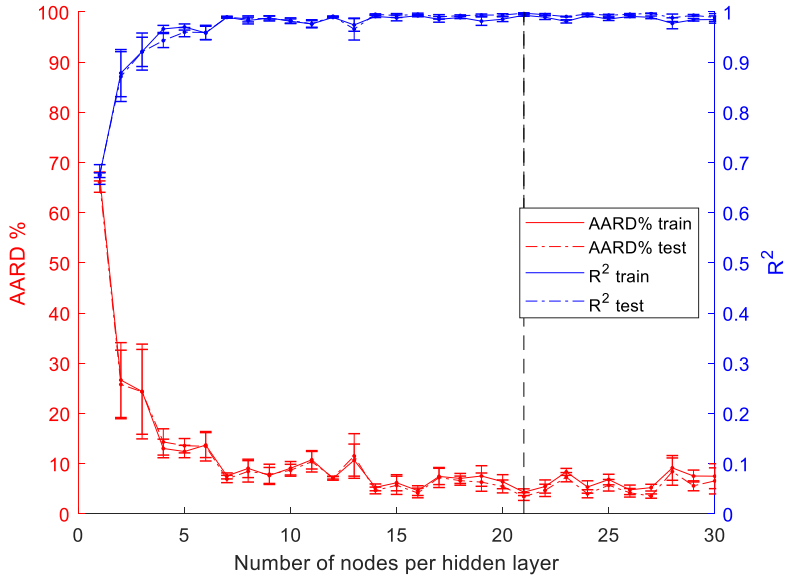

Figure 6-13: The AARD% and R^2 values for the training and testing data of neural networks using two hidden layers and the second option to divide the training, testing and validation data

Figure 6-14 illustrates the bubble and dew point pressures of the results as presented in Figure 6-12 (which resulted in a neural network with a size of $5 \times 25 \times 2$) and Figure 6-13 (which resulted in a neural network with a size of $5 \times 21 \times 21 \times 2$). As seen in this figure, the neural network with a size of $5 \times 25 \times 2$ resulted in slightly better results compared to the neural network with a size of

$5 \times 21 \times 21 \times 2$ where the neural network with a size of $5 \times 21 \times 21 \times 2$ resulted in better results predicting the bubble point pressures. Overall, as for the previous neural networks in this section, the network with two hidden layers resulted in better predictions.

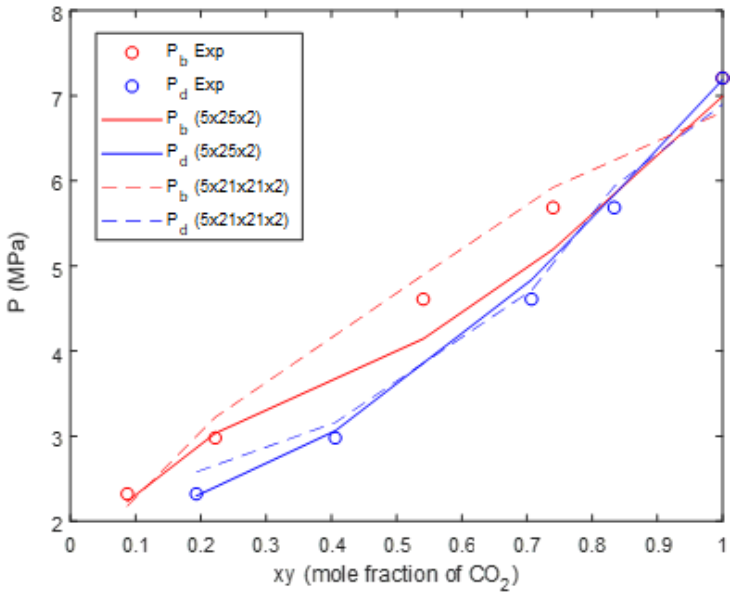

Figure 6-14: Bubble and dew point pressures of a binary system with CO_2 and R32 at 303 K comparing neural networks with one and two hidden layers where training, testing and validation data were divided using option 2 for case study 3 using data obtained from Vaferi, et al., (2018)

Table 6-4 lists the optimal R^2 and $AARD\%$ values as obtained using Figure 6-9, Figure 6-10, Figure 6-12 and Figure 6-13 and the results obtained in the published article. As for the results obtained in Section 6.1, the neural networks using option 1 and the neural network as obtained by the published article resulted in better R^2 and $AARD\%$ values. Furthermore (with the same conclusion as found in Section 6.1), the neural networks with two hidden layers performed better than the neural networks with a single hidden layer.

Table 6-4: R^2 and AAD% values comparing different options to divide the training, testing and validation data and comparing one and two hidden layers using data as obtained by Vaferi, et al., (2018)

Option for dividing the training, testing and validation data		**Training**	**Testing**	**Neural network structure ($N_{HL} \times N_{nodes}$)**
Published article	R^2	0.999	0.999	$5 \times 14 \times 2$
	$AARD\ \%$	2.08	2.08	
Option 1	R^2	0.997	0.998	$5 \times 21 \times 2$
	$AARD\ \%$	2.8	2.5	
Option 1	R^2	0.998	0.999	$5 \times 27 \times 27 \times 2$
	$AARD\ \%$	1.5	1.0	
Option 2	R^2	0.991	0.994	$5 \times 25 \times 2$
	$AARD\ \%$	6.0	5.6	
Option 2	R^2	0.993	0.997	$5 \times 21 \times 21 \times 2$
	$AARD\ \%$	4.3	3.5	

As concluded from Sections 6.1 and 6.2, a neural network with two hidden layers performs better compared to a neural network with a single hidden layer. It was also expected that neural networks would perform worse if data were divided by selecting complete binary systems as testing and validation data sets, which was the case for these case studies. However, using the second method is more beneficial in practice, since prediction of phase equilibrium is more than interpolation between data points. Comparing the input parameters of case study 2 with the input parameters with case study 3, there are no distinction between the functional groups, chemical compounds or branches. It is therefore recommended to add additional inputs to the neural network used in case study 3 to distinguish between these parameters.

7. Conclusions

7.1. Investigation of the structure of the neural network

For case study 1, considering the acentric factor, critical temperature and pressure of the alkane, system temperature, CL and MM of the alkane and the liquid and vapour composition of CO_2 as initial inputs to the neural network and randomising the inputs to determine the significant inputs, the CL and the critical pressure were eliminated as inputs.

For case study 2, the acentric factor, functional group, critical temperature and critical pressure of the hydrocarbon, system temperature, CL and MM of the hydrocarbon and liquid and vapour composition of CO_2 were considered as initial inputs to the neural network, where, as for case study 1, the CL and the critical pressure were eliminated as inputs.

Case study 3 was not applicable to this objective.

7.2. Determination of the optimal hyperparameters

For both case studies 1 and 2, a feedforward neural network with two hidden layers using the log-sigmoid transfer function was selected. For case study 1, the optimal neural network size was $7 \times 26 \times 26 \times 2$ where the optimal neural network size for case study 2 was $9 \times 30 \times 30 \times 2$.

For case study 3, it was concluded that two hidden layers performs better than a single hidden layer. It was further concluded that neural networks where data were divided by selecting complete binary systems as testing and validation data sets resulted in less accurate results, compared to when data are divided by selecting random data points as testing and validation data. Although less accurate results were obtained when selecting complete binary systems as testing and validation data, the results were still acceptable with R^2 differences of 0.005 and 0.002 and $ADD\%$ differences of 2.8% and 2.5% respectively for the training and testing data if neural networks with two hidden layers were considered. Dividing the data selecting complete binary systems is a better method to use in practice, compared to selecting random data points from each binary system, since it is more likely that predictions of complete binary systems will be required, compared to interpolating data points.

It should be noted that the adjustable parameters are a lot compared to the number of data points, but smaller neural networks were considered in the sections where the hyperparameters were determined. The larger neural networks resulted in better results. The trade-off was between larger neural networks possibly being slightly overfitted.

7.3. Comparison of the results with traditional modelling methods

For case study 1, the bubble point pressure data were accurate within a 4.4 MPa and 0.6 MPa region, for the training and testing data respectively, where for the dew point pressure error region, 6.3MPa and 3.2 MPa.

For case study 2, the maximum pressure deviation for the bubble and dew point test data were 2.5 MPa and 5.8 MPa, respectively.

For both case studies 1 and 2, the neural networks were able to predict pressures through the whole pressure range, where the RK-Aspen models failed at high pressures. The neural network predictions achieved relatively the same, or more accurate results relative to the RK-Aspen models.

Case study 3, this objective was not applicable.

As concluded by answering the objectives above, it is possible to model phase behaviour of binary systems containing supercritical CO_2 and hydrocarbons using ANNs.

8. Recommendations

One of the advantages of using neural networks is that available data can be used to make interpolated predictions, as mentioned in Section 2.2.1. The performance of neural networks is, however, highly dependent on the quality and quantity of the data (Aldrich & Slater, 2001). It is therefore recommended to avoid the collection of inconsistent data (as discussed in Section 2.1.1) and to ensure that sufficient data were collected.

Using the weights and bias matrixes as determined by this study, and as listed in Appendix D, the outputs using any inputs within the scope of this study can be determined using Equation 2-14, as listed in Section 2.2.1.

The addition of binary systems with different functional groups resulted in larger pressure deviations. It is therefore recommended to use larger training data sets if additional dimensions are to be added to the network.

The selected initial inputs to the neural network can be performed in different ways. Using deep RNNs or deep CNNs, SMILES strings or images of the molecule (as discussed in Section 2.2) can be used as inputs to the neural network to describe the molecular structure, as mentioned in Section 2.2.

Since the ANNs and the RK-Aspen model complement each other in some cases, it is recommended to use a hybrid scheme, as mentioned in Section 2.3.

9. References

Abdi, H., Valentin, D., & Edelman, B. (2011). *Neural Networks.* Thousand Oaks: SAGE Publications, Inc. .

Adams, W. R., Zollweg, J. A., & Streett, W. B. (1988). New Apparatus for Measurement of Supercritical Fluid-Liquid Phase Equilibria. *AIChE Journal, 34*, 1387-1391.

Aggarwal, C. C. (2018). *Neural Networks and Deep Learning.* Yorktown Heights, NY, USA: Springer.

Aldrich, C., & Slater, M. J. (2001). Simulation of liquid-liquid extraction data with artificial neural networks. *Application of neural networks and other learning technologies in process engineering*, 3-22.

Ambrose, D., & Ghiassee, N. B. (1987). Vapor PRessures and Critial Temperatues and Critical Pressures of Some Alkanoic Acids. *The Journal of Chemical Thermodynamics, 19*, 505.

Ambrose, D., & Sparke, C. H. (1970). Thermodynamic properties of organic oxygen compounds XXV, Vapour pressures and normal boiling temperatures of aliphatic alcohols. *The Journal of Chemical Thermodynamics, 2*, 5.

Ambrose, D., Ellender, J. H., & Sparke, C. H. (1974). Thermodynamic properties of organic oxygen compounds XXXV. Vapour pressures of aliphatic alcohols. *The Journal of Chemical Thermodynamics, 6*, 909-914.

Beier, A., Kuranov, J., Stephan, K., & Hasse, H. (2003). High-Pressure Phase Equilibria of Carbon Dioxide + 1-Hexanol at 303.15 and 313.15 K. *Journal of Chemical & Engineering Data, 48*, 1365-1367.

Bharath, R., Yamane, S., Inomata, H., Adschiri, T., & Arai, K. (1993). Phase Equilibria of Supercritical CO2 - Fatty oil Component. *Fluid Phase Equilibria, 83*, 183-192.

Bishop, C. M. (1995). *Neural Networks for Pattern Recognition.* Oxford: Clarendon Press.

Bishop, C. M. (2006). *Pattern recognition and machine learining.* California: Springer.

Bonthuys, G. J., Schwarz, C. E., Burger, A. J., & Knoetze, J. H. (2011). Separation of alkanes and alcohols with supercritical fluids. Part I: Phase equilibria and viability study. *The Journal of Supercritical Fluids, 57*, 101-111.

Boston, J. F., & Mathias, P. M. (1980). Phase Equilibria in a Third- Generation Process Simulator. *2nd International Conference on Phase Equilibria and Fluid Properties in the Chemical Process*, (pp. 823-849).

Bravo-Sa´nchez, U. I., Rico-Martınez, R., & Iglesias-Silva, G. A. (2002). Improvement of the Empiricism in the BACK Equation of State via. *Industrial & Engineering Chemistry, 41*, 3705-3713.

Brown, T. S., Kidnay, A. J., & Sloan, E. D. (1988). Vapor-Liquid Equilibria in the Carbon Dioxide-Ethane System. *Fluid Phase Equilibria*, 169-184.

Byun, H., & Kwak, C. (2002). High pressure phase behavior for carbon dioxide-1-butanol and carbon dioxide-1-octanol systems. *Korean Journal of Chemical Engineering, 19*, 1007-1013.

Byun, H., Kim, K., & McHuge, M. A. (2000). Phase Behavior and Modeling of Supercritical Carbon Dioxide−Organic Acid Mixtures. *Industrial & Engineering Chemistry Research, 39*, 4580-4587.

Camacho-Camacho, L. E., Galicia-Luna, L. A., Elizalde-Solis, O., & Mart´ınez-Ram´ırez, Z. (2007). New isothermal vapor–liquid equilibria for the. *Fluid Phase Equilibria, 259*, 45-50.

Camin, D. L., Forziat, A. F., & Rossini, F. D. (1954). Physical Properties of n-Hexadecane, n-Decylcyclopentane, n-Decylcyclohexane, 1-Hexadecene and n-Decylbenzene. *Journal of Physical Chemistry, 58*, 440-442.

Cheng, H., Fernandez, M. E., Zollweg, J. A., & Streett, W. B. (1989). Vapor-Liquid Equilibrium in the System Carbon Dioxide + n-Pentane from 252 to 458 K at Pressures to 10 MPa. *Journal of chemical and engineering data, 34*, 319-323.

Chester, T. L., & Haynes, B. S. (1997). stimation of pressure-temperature critical loci of CO2 binary mixtures with methyl-tert-butyl ether, ethyl acetate, methyl-ethyl ketone, dioxane and decane. *The Journal of Supercritical Fluids*, 15-20.

Chieming, C., Kou-Long, C., & Chang-Yih, D. (1998). A new apparatus for the determination of Pxy diagrams and Henry's constants in high pressure alcohols with critical carbon dioxide. *Journal of Supercritical Fluids, 12*, 223-237.

Chiu, H., Jung, R., Lee, M., & Lin, H. (2008). Vapor–liquid phase equilibrium behavior of mixtures containing supercritical carbon dioxide near critical region. *The Journal of Supercritical Fluids, 44*, 273-278.

Chrisochoou, A. A., Schaber, K., & Stephan, K. (1997). Phase Equilibria with Supercritical Carbon Dioxide for the Enzymatic Production of an Enantiopure Pyrethroid Component. Part 1. Binary Systems. *Journal of Chemical Engineering Data, 42*, 551-557.

Dahm, K. &. (2015). *Chemical Engineering Thermodynamics.* US: Timothy Anderson.

Danesh, A. (1998). PVT and phase behaviour of petroleum reservoir fluids. *Elsevier Science*.

Demuth, H., & Beale, M. (2004). *Neural network toolbox.* The MathWorks.

Dohrn, R., Peper, S., & Fonseca, J. J. (2010). High-pressure fluid-phase equilibria: Experimental methods and systems investigated (2000-2004). *Fluid phase equilibria, 288*, 1-54.

Don, W., Green, D. W., & Perry, R. H. (2007). *Perry's Chemical Engineers' Handbook.* Oklahama: McGrawl-Hill Professional.

D'Souza, R., & Teja, A. S. (1987). THe prediction of the vapor pressures of carboxylic acids. *Chemical Engineering Communication, 61*, 13.

D'Souza, R., Patrick, J. R., & Teja, A. S. (1988). High pressure phase equilibria in the carbon dioxide - n-Hexadecane and carbon dioxide — water systems. *The Canadian Journal of Chemical Engineering, 66*, 319-323.

Eikens, B., Karim, M. N., & Simon, L. (2001). Combining neuraln networks and first principle models for bioprocess modeling. *Application of Neural Networks and Other Learning Technologies in Process Engineering*, 121-148.

Elizalde-Solis, O., Galicia-Luna, L. A., & Camacho-Camacho, L. E. (2007). High-pressure vapor–liquid equilibria for CO2 + alkanol systems and densities of n-dodecane and n-tridecane. *Fluid Phase Equilibria, 259*, 23-32.

Elizalde-Solis, O., Galicia-Luna, L. A., Sandler, S. I., & Sampayo-Hernandez, J. G. (2003). Vapor–liquid equilibria and critical points of the CO2 + 1-hexanol and CO2 + 1-heptanol systems. *Fluid phase equilibria, 210*, 215-227.

Eze, P. C., & Masuku, C. M. (2018). Vapour–liquid equilibrium prediction for synthesis gas conversion usingartificial neural networks. *South African Journal of Chemical Engineering, 26*, 80-85.

Feng, L., Cheng, K., Tang, M., & Chen, Y. (2001). Vapor–liquid equilibria of carbon dioxide with ethyl benzoate, diethyl succinate and isoamyl acetate binary mixtures at elevated pressures. *The Journal of Supercritical Fluids, 21*, 111-121.

Feng, L., Zheng, D., Chen, J., Dai, X., & Shi, L. (2017). Exploration and Analysis of CO2 + Hydrocarbons Mixtures as Working Fluids for Trans-critical ORC. *Energy Procedia, 129*, 145-151.

Ferreira, M. (2018). *Phase equilibria & thermodynamic modelling of the ternary system CO2 + 1-decanol + n-tetradecane.* Stellenbosch: Faculty of Engineering at Stellenbosch University.

Fourie, F. C., Knoetze, J. H., & Schwarz, C. E. (2018). *The high pressure phase behaviour of detergent range alcohols and alkanes.* Stellenbosch: Stellenbosch University.

Fu, Y., & Aldrich, C. (2018). Froth image analysis by use of transfer learning and convolutional neural networks. *Minerals engineering*, 68-78.

Gao, L., & Loney, N. W. (2002). New Hybrid Neural Network Model for Prediction of Phase. *Industrial & Engineering Chemistry, 41*, 112-119.

Gardeler, H., Fischer, K., & Gmehling, J. (2002). Experimental Determination of Vapor−Liquid Equilibrium Data for Asymmetric Systems. *Industrial & Engineering Chemistry Research, 41*, 1051-1056.

Geiseler, G., Fruwert, J., & Huttig, R. (1966). Dampfdruck- und Schwingungsverhalten der stellungsisomeren n-Octanole und hydroxydeuterierten n-Octanole. *Chemische Berichte, 99*, 1594-1601.

Ghanadzadeh, H., & Ahmadifar, H. (2008). Estimation of (vapour + liquid) equilibrium of binary systems (tert-butanol + 2-ethyl-1-hexanol) and (n-butanol + 2-ethyl-1-hexanol) using an artificial neural network. *The Journal of Chemical Thermodynamics, 40*, 1152-1156.

Glorot, X., Bordes, A., & Yoshua, B. (2010). *Deep Sparse Rectifier Neural Networks.* USA: Now publishers.

Goh, G. B., Siegel, C., Hodas, N., & Vishnu, A. (2018). *An Interpretable General-Purpose Deep Neural Network for Predicting Chemical Properties.* New York: Cornell University.

Goh, G. B., Siegel, C., Vishnu, A., Hodas, N. O., & Baker, N. (2017). *Chemception: A Deep Neural Network with Minimal Chemistry Knowledge Matches the Performance of Expert-developed QSAR/QSPR Models.* New York: Cornell University.

Gonzalez, A. V., Tufeu, R., & Subra, P. (2002). High-Pressure Vapor−Liquid Equilibrium for the Binary Systems Carbon Dioxide + Dimethyl Sulfoxide and Carbon Dioxide + Dichloromethane. *Journal of Chemical Engineering Data, 47*, 492-495.

Greaves, M. A., Mujtaba, I. M., & Hussain, M. A. (2001). Neural networks in hybrid scheme for optimisation of dynamic processes. *Application of Neural Networks and Other Learning Technologies in Process Engineering*, 149-171.

Gupta, R. B., & Shim, J. (2007). *Solubility in Supercritical Carbon Dioxide.* Boca Raton: Taylor & Francis Group, LLC.

Hammer, E., & Lydersen, A. L. (1957). The Vapour Pressure of di-n-Butylphthalate, di-n-Butylsebacate, Lauric Acid and Myristic Acid. *Chemical Engineering Science, 7*, 66-72.

Heaton, J. (2005). *Introduction to neural networks with Java.* St. Louis: Heaton Research.

Heo, J., Shin, H. Y., Park, J., Joung, S. N., Kim, S. Y., & Yoo, K. (2001). Vapor-Liquid Equilibria for Binary Mixtures of CO2 with. *Journal of Chemical Engineering Data, 46*, 355-358.

Hoffmann, L. (2019, June). Reaching new heights with artificial neural networks. *Communications of the ACM, 62*, p. 96.

Holsher, I. F. (1988). *Fluidphasengleichgewichte binarer und ternarer alkohol mischsysteme mit uberkritischem kohlendioxid bei drucken bis 33 MPa.* Bochum: Fakultat fur Chemie der Ruhr-Universitat Bochum.

Horn, Z. C., Auret, L., McCoy, J. T., Aldrich, C., & Herbst, B. M. (2017). Performance of Convolutional Neural Networks for Feature Extraction in Froth Flotation Sensing. *IFAC-PapersOnLine*, 13-18.

Hoskins, J. C., Kaliyur, K. M., & Himmelblau, D. M. (1991). Fault diagnosis in complex chemical plants using artificial neural networks. *AlChe Journal*.

Hosseini, A., & Pazuki, G. (2014). A study on the predictive capability of the SAFT-VR equation of state for solubility of solids in supercritical CO2. *Journal of Supercritical Fluids, 90*, 73-83.

Huang, S. H., Lin, H., & Chao, K. (1988). Solubility of Carbon Dioxide, Methane, and Ethane in n-Octacosane. *Journal of Chemical & Engineering Data, 33*, 143-145.

Hussain, B., & Ahsan, M. (2018). A Numerical Comparison of Soave Redlich Kwong and Peng-Robinson Equations of State for Predicting Hydrocarbons' Thermodynamic Properties. *Engineering, Technology & Applied Science Research, 8*, 2422-2426.

Hwu, W., Cheng, J., Cheng, K., & Chen, Y. (2004). Vapor–liquid equilibrium of carbon dioxide with ethyl caproate, ethyl caprylate and ethyl caprate at elevated pressures. *The Journal of Supercritical Fluids, 28*, 1-9.

Inomata, H., Kondo, A., & Kakehashi, H. (2005). Vapor–liquid equilibria for CO2–fermentation alcohol mixtures: Application of a new group contribution equation of state to isomeric compounds. *Fluid PHase Equilibria, 228-229*, 335-343.

Ioniţă, S., Feroiu, V., & Geană, D. (2013). Phase Equilibria of the Carbon Dioxide + 1-Decanol System at High Pressures. *Journal of Chemical & Engineering Data, 58*, 3069-3077.

Iwai, Y., Hosotani, N., Morotomi, T., Koga, Y., & Arai, Y. (1994). High-Pressure Vapor-Liquid Equilibria for Carbon Dioxide + Linalool. *Journal of Chemical Engineering Data, 39*, 900-902.

Jabbar, H. K., & Khan, R. Z. (2015). *Methods to avoid over-fitting and under-fitting in supervised machine learning.* Iraq: Computer Science, Communication & Instrumentation Devices.

Jan, D., Mai, C., & Tsai, F. (1994). Solubility of Carbon Dioxide in 1-Tetradecanol, 1-Hexadecanol, and 1-Octadecanol. *Journal of Chemical Engineering Data, 39*, 384-387.

Jennings, D. W., & Schucker, R. C. (1996). Comparison of High-Pressure Vapor-Liquid Equilibria of Mixtures. *Journal of Chemical Engineering Data, 41*, 831-838.

Jime´nez-Gallegos, R., Galicia-Luna, L. A., & Elizalde-Solis, O. (2006). Experimental Vapor-Liquid Equilibria for the Carbon Dioxide + Octane and. *Journal of Chemical Engineering Data, 51*, 1624-1628.

Jothilakshmi, S., & Gudivada, V. N. (2016). *Handbook of Statistics.* Elsevier.

Kahlbaum, G. W. (1894). Studien uber Dampfspannkraftsmessungen. *Zeitschrift für Physikalische Chemie, 13*, 14-55.

Kalra, H., Kubota, H., Robinson, D. B., & Ng, H. (1978). Equilibrium Phase Properties of the. *Journal of Chemical and Engineering Data, 23*, 317-321.

Kamali, M. J., & Mousavi, M. (2008). Analytic, neural network, and hybrid modeling of. *The Journal of Supercritical Fluids, 47*, 168-173.

Kemme, H. R., & Kreps, S. I. (1969). Vapor pressure of primary n-alkyl chlorides and alcohols. *Journal of Chemical Engineering Data, 14*, 98-102.

Kian, K., & Scurto, A. M. (2018). Viscosity of compressed CO2-saturated n-alkanes: CO2/n-hexane,CO2/n-decane, and CO2/n-tetradecane. *The Journal of Supercritical Fluids, 133*, 411-420.

Kiran, E., Debenedetti, P. G., & Peters, C. J. (1998). *Supercritical fluids: Fundamentals and applications* (Vol. 366). Turkey: Springer-Science+Business Media.

Kordikowski, A. (1992). *Fluidphasengleichgewichte trenarer und quaternarer mischungen schwerfluchtiger organischer substanzen mit uberkritischen kohlendioxid bei temperaturen zwischen 298 K und 393 K und drucken zwishen 10 MPa und 100 Mpa.* Buchum.

Kordikowski, A., & Schneider, G. M. (1993). Fluid phase equilibria of binary and ternary mixtures of supercritical carbon dioxide with low-volatility organic substances up to 100 MPa and 393 K: cosolvency effects and miscibility windows. *Fluid Phase Equilibria, 90*, 149-162.

Kremme, H. R., & Kreps, S. I. (1969). Vapor pressure of primary n-alkyl chlorides and alcohols. *Journal of Chemical Engineering Data, 1*, 98-102.

Kubat, M. (2017). *An Introduction to Machine Learning.* Switzerland: Springer International Publishing.

Lashkarbolooki, M., Shafipour, Z. S., Hezave, A. Z., & Fermani, H. (2013). Use of artificial neural networks for prediction of phase equilibria in the binary. *The Journal of Supercritical Fluids, 75*, 144-151.

Lashkarbolooki, M., Vaferi, B., & Rahimpour, M. R. (2011). Comparison the capability of artificial neural network (ANN) and EOS for. *Fluid Phase Equilibria, 308*, 35-43.

Lashkarbolooki, M., Vaferi, B., Shariati, A., & Hezave, A. Z. (2013). Investigating vapor–liquid equilibria of binary mixtures containing supercritical. *Fluid phase equilibria, 343*, 24-29.

Latsky, C. (2019). *High pressure phase equilibria of the system CO2 + N-Dodecane + 3,7-dimethyl-1-octanol + 1-decanol.* Stellenbosch: The Faculty of Engineering at Stellenbosch University.

Latsky, C., Cordeiro, B., & Schwarz, C. E. (2020). High pressure bubble- and dew-point data for systems containing CO2 with 1-decanol and n-hexadecane. *Fluid Phase Equilibria, 512*, 112702.

Lawrence, J. (1988). *Introduction to Neural Networks.* United States of America: California Scientific Software.

Lee, M. J., & Chen, J. T. (1994). Vapor-liquid equilibrium for carbon dioxide/alcohol systems. *Fluid Phase Equilibria, 15*, 215-231.

Li, J., Rodrigues, M., Paiva, A., Matos, H. A., & de Azevedo, E. G. (2007). Vapor-liquid equilibria and volume expantion of the tetrahydrofuran/CO2 system: application to a SAS-atomization process. *Journal of Supercritical Fluids, 41*, 343-351.

Li, Y., Dillard, K. H., & Robinson, R. L. (1981). Vapor-Liquid Phase Equilibrium for Carbon Dioxide-n-Hexane at 40,. *Journal of Chemical Engineering Data, 26*, 53-55.

Lim, J. S., Jin, J. M., & Yoo, K. P. (2008). VLW measurements for binary systems containing CO2 + 1,1,1,2-tetrafluoroethane (HFC-134a) at high pressures. *Journal of Supercritical Fluids, 44*, 279-283.

Lindberg, V. (2000). *Uncertainties and Error Propagation.* Spiff.

Lombard, J. E. (2015). *Thermodynamic modelling of hydrocarbon chains and light weight supercritical solvents.* Stellenboshc: Stellenbosch University.

Madani, H., Coquelet, C., & Richon, D. (2012). Vapor-liquid Equilibrium Data Concerning Refrigerant Systems (R116 + R143a). *Energy Procedia, 18*, 21-34.

Margon, V., Agarwal, U. S., Peters, C. J., de Wit, G., Bailly, C., van Kasteren, J. M., & Lemstra, P. J. (2005). Phase equilibria of binary, ternary and quaternary systems for polymerization/depolymerization of polycarbonate. *Journal of Supercritical Fluids, 34*, 309-321.

Mathias, P. M. (1983). A versatile phase equilibrium equation of state. *Industrial & Engineering Chemistry Process Design and Development, 22*, 358-391.

McHuge, M. A., & Krukonis, V. J. (1994). *Supercritical Fluid Extraction.* USA: Butterworth-Heinemann.

Meleiro, L., Filho, R., Campello, R., & Amaral, W. (2001). Hierarchical neural fuzzy models as a tool for process identification: a bioprocess application. *Application of Neural Networks and Other Learning Technologies in Process Engineering*, 173-198.

Nagarajan, N., & Robinson, R. L. (1986). Equilibrium phase compositions, phase densities, and interfacial tensions for carbon dioxide + hydrocarbon systems. 2. Carbon dioxide + n-decane. *Journal of Chemical Engineering Data, 31*, 168-171.

Nielsen, M. (2019). *Neural Networks and Deep Learning.* Creative Commons Attribution.

Olden, J. D., & Jackson, D. A. (2002). Illuminating the ‘‘black box’’: a randomization approach for understanding variable contributions in artificial neural networks. *Ecological Modelling, 154*, 135–150.

Olden, J. D., Joy, M. K., & Death, R. G. (2004). An accurate comparison of methods for quantifying variable importance in artificial neural networks using simulated data. *Ecological Modelling, 178*, 389–397.

Oliveira, M. B., Queimada, A. J., Kontogeorgis, G. M., & Coutinho, J. A. (2011). Evaluation of the CO2 behavior in binary mixtures with alkanes, alcohols, acids and esters using the Cubic-Plus-Association Equation of State. *The Journal of Supercritical Fluids, 55*, 876-892.

Osborn, A. G., & Douslin, D. R. (1974). Vapor-pressure relations for 15 hydrocarbons. *Journal of Chemical Engineering Data, 19*, 114-117.

Parinet, J., Julien, M., Nun, P., Robins, R. J., Remaud, G., & Hohener, P. (2015). Predicting equilibrium vapour pressure isotope effects by using artificial. *Chemosphere, 134*, 521-527.

Peng, D., & Robinson, D. B. (1976). A New Two-Constant Equation of State. *Industrial & Engineering Chemistry Fundamentals, 15*, 59-64.

Peters, C. J., & Gauter, K. (1999). Occurrence of Holes in Ternary Fluid Multiphase Systems of Near-Critical Carbon Dioxide and Certain Solutes. *Chemical Reviews, 99*, 419-432.

Peters, C. J., Florusse, L. J., Hahre, S., & de Swaan Arons, J. (1995). Fluid multiphase equilibrla and critical phenomena in binary and ternary mixtures. *Fluid Phase Equilibria, 110*, 157-179.

Pfohl, O., Pagel, A., & Brunner, G. (1999). Phase equilibria in systems containing o-cresol, p-cresol, carbon dioxide, and ethanol at 323.15–473.15 K and 10–35 MPa. *Fluid Phase Equilibria, 157*, 53-79.

Phillips, L., Goh, G., & Hodas, N. (2018). *Explanatory masks for neural network intepretability.* Pacific Northwest: ICLR.

Picton, P. (1994). *Introduction to Neural Networks.* Great Britain: Antony Rowe Ltd.

Pohler, H. (1994). *Fluidphasengleichgewichte binarer und ternarer kohlendioxidmischungen mit schwerfluchtigen organischen substanzen bei temperaturen von 303 K bis 393 K und drucken von 10 MPa bis 100 MPa.* Fakultat fur Chemie der Ruht-Universitat Bochum: Bochum.

Raeissi, S., Florusse, L., & Peters, C. J. (2010). Scott–van Konynenburg phase diagram of carbon dioxide + alkylimidazolium-based ionic liquids. *The Journal of Supercritical Fluids, 55*, 825-832.

Reamer, H. H., & Sage, B. H. (1963). Phase Equilibria in Hydrocarbon Systems. Volumetric and Phase Behavior of the n-Decane-CO“ System. *Journal of chemical and engineering data, 8*, 508-513.

Redlich, O., & Kwong, J. (1979). On the Thermodynamics of Solutions V. An Equation-of-state. *Chemical Reviews, 44*, 223-244.

Rosenthal, D. J., & Teja, A. S. (1989). Critical pressuers and temperatures of isomeric alkohols. *Industrial & Engineering Chemistry Research, 28*, 1693.

Ruiz-Rodriguez, A., Najdanovic-Visak, V., Visak, Z. P., Bronze, M., Antunes, C., & Nunes da Ponte, M. (2009). High-pressure phase equilibria of binary (CO2 + nicotene) and ternary (CO2 + nicotene + solanesol) mixtures. *Fluid Phase Equilibria, 282*, 58-64.

Sandler, S. I. (2006). *Chemical, biochemical, and engineering thermodynamics.* Hoboken: John Wiley & Sons, Inc.

Scheidgen, A. (1997). *Fluidphasengleichgewichte binare und ternarer Kohlendioxidmischungen mit schwerfluchtigen organischen Substanzen bis 100 MPa.* Bochum.

Schiemann, H., Weidner, E., & Peter, S. (1993). Interfacial tension in binary systems containing a dense gas. *The Journal of Supercritical Fluids, 6*, 181-189.

Schmelzer, J., Creutziger, V., Lieberwirth, I., & Pfestorf, R. (1983). Vapour-liquid equilibria and heats of mixing in n-alkane-1-alcohol systems. III. Vapour-liquid equilibria in n-alkane-1-dodecanol systems. *Fluid Phase Equilibria, 15*, 107-119.

Secuianu, C., Feroiu, V., & Geana, D. (2008). High-pressure vapor–liquid and vapor–liquid–liquid equilibria in the carbon dioxide + 1-heptanol system. *Fluid Phase Equilibria, 25*, 109-115.

Secuianu, C., Froiu, V., & Geana, D. (2010). High-pressure phase equilibria in the (carbon dioxide + 1-hexanol) system. *The Journal of Chemical Thermodynamics, 42*, 1286-1291.

Secuianu, C., Ionita, S., Feroiu, V., & Geana, D. (2016). High pressures phase equilibria of (carbon dioxide + 1-undecanol) system and their potential role in carbon capture and storage. *The Journal of Chemical Thermodynamics, 93*, 360-373.

Shan-Chun, C., Tien-Hao, H., Yu-Heng, C., Ho-mu, L., & Ming-Jer, L. (2012). Micronization of aztreonam with supercritical anti-solvent process. *Journal of the Taiwan Institute of Chemical Engineers, 43*, 790-797.

Smith, J. M. (2005). *Introduction to Chemical Engineering Thermodynamics.* New York: McGraw-Hill.

Smith, M. (1993). *Neural networks for statistical modeling.* United States of America: International Thomson Publishing.

Soave, G. (1972). Equilibrium constants from a modified Redkh-Kwong. *Chemical Engineering Science, 27*, 1197-1203.

Spee, M. (1990). *Fluidphasengleichgewichte der quaternaren systeme CO2 + 1-dodecanol + hexadecan + 1,8-octandiol und CO2 + 1,dodecanol + hexadecan + dotriacontan sowie einiger binarer und ternarer teilsysteme zwischen 293 K und 413 K bei drucken bis 100 MPa.* Bochum: der Fakultat fur Chemie der Ruhr-Universitat Bochum.

Spee, M., & Schneider, G. M. (1991). Fluid phase equilibrium studies on binary and ternary mixtures of carbon dioxide with hexadecane, 1-dodecanol, 1,8-octanediol and dotriacontane at 393.2 K and at pressures up to 100 MPa. *Fluid Phase Equilibria*, *65*, 263-274.

Ting, P. D., Joyce, P. C., Jog, P. K., Chapman, W. G., & Thies, M. C. (2003). Phase equilibrium modeling of mixtures of long-chain and. *Fluid Phase Equilibria, 206*, 267-286.

Tsai, F. N., & Yau, J. S. (1990). Solubility of carbon dioxide in n-tetracosane and in n-dotriacontane. *Journal of Chemical & Engineering Data*, *35*, 43-45.

Vaferi, B., Lashkarbolooki, M., Esmaeili, H., & Shariati, A. (2018). Toward artificial intelligence-based modeling of vapor liquid. *Journal of Serbian Chemical Society, 83*, 199-211.

Vaferi, B., Rahnama, Y., Darvishi, P., Toorani, P., & Lashkarbolooki, M. (2013). Phase equilibria modeling of binary systems containing ethanol using. *The Journal of Supercritical Fluids, 84*, 80-88.

Valderrama, J. O. (2003). The State of the Cubic Equations of State. *Industrial & Engineering Chemistry Research, 42*, 1603-1618.

Valtz, A., Coquelet, C., Baba-Ahmed, A., & Richon, D. (2008). Vapor–liquid equilibrium data for the CO2+ 1, 1, 1, 2, 3, 3, 3,-heptafluoropropane (R227ea) system at temperatures from 276.01 to 367.30 K and pressures up to 7.4 MPa. *Fluid Phase Equilibria, 207*, 53-67.

Valtz, A., Courtial, X., Johansson, E., Coquelet, C., & Rabiuoemath, D. (2011). Thermodynamic study of binary systems containing sulpher dioxide: Measurements and molecular modelling. *Fluid Phase Equilibria, 304*, 21-34.

van der Waals, J. D. (1873). *Over de constinuiteit van den gas- en vloeistoftoestand.* PhD Thesis, University of Leiden.

van Konynenburg, P. H., & Scott, R. L. (1980). Critical lines and phase equilibria in binary van der Waals mixtures. *Philisophical Transactions of the Royal Society*, 495-540.

Vincent, J. (2019, March 27). 'Godfathers of AI' honored with Turing Award, the Nobel Prize of computing. *The Verge*.

Vitu, S., Privat, R., Jaubert, J., & Mutelet, F. (2008). Predicting the phase equilibria of CO2 + hydrocarbon systems with the PPR78 model (PR EOS and kij calculated through a group contribution method). *Journal of Supercritical Fluids, 45*, 1-26.

Weber, L. A. (1989). Simple Apparatus for Vapor-Liquid Equilibrium Measurements with Data for the Binary Systems of Carbon Dioxide with n-Butane and Isobutane. *J. Chem. Eng. Data*, 34, 171.

Weng, W. L., & Lee, M. J. (1992). Vapor-liquid equilibrium of the octane/carbon dioxide, octane/ethane, and octane/ethylene systems. *Journal of Chemical & Engineering Data, 37*, 213-215.

Weng, W., Chen, J., & Lee, M. (1994). High-Pressure Vapor-Liquid Equilibria for Mixtures Containing a Supercritical Fluid. *Industrial & Engineering Chemistry Research, 33*, 1955-1961.

Williamham, C. B., Taylor, W. J., Pignocco, W. J., & Rossini, F. D. (1945). Vapor Pressures and Boiling Points of Some Paraffin, Alkylcyclopentane, Alkylcyclohexane, and Alkylbenzene Hydrocarbons. *Journal of Research of the National Bureau of Standards, 35*, 219-244.

Yau, J., Chiang, Y., Shy, D., & Tsai, F. (1992). Solubilities of Carbon Dioxide in Carboxylic Acids under High Pressures. *Journal of Chemical Engineering of Japan, 25*, 544-548.

Yu, J., Wang, S., & Tian, Y. (2006). Experimental determination and calculation of thermodynamic properties of CO2 + octane to high temperatures and high pressures. *Fluid Phase Equilibria, 246*, 6-14.

Zamudio, M. (2014). *The Separation of Detergent Range Alkanes and Alcohol Isomers with Supercritical Carbon Dioxide*. Stellenbosch: Stellenbosch University.

Zamudio, M., Schwarz, C. E., & Knoetze, J. H. (2013). Experimental measurement and modelling with Aspen Plus (R) of the phase behaviour of supercritical CO2 + (n-dodecane + 1-decanol + 3,7-dimethyl-1-octanol). *Journal of Supercritical Fluids, 84*, 132-145.

Appendix A: Neural network input data

Table A-1: Bubble and dew point pressures at specific compositions and temperatures for alkanes.

Name	MM	CL	T (K)	x (mol/mol)	y (mol/mol)	P (MPa)	Reference
Pentane	72.15	5	311.6	0.037	0.746	0.41	Cheng, *et al.*, (1989)
Pentane	72.15	5	311.6	0.079	0.865	0.84	Cheng, *et al.*, (1989)
Pentane	72.15	5	311.6	0.130	0.912	1.37	Cheng, *et al.*, (1989)
Pentane	72.15	5	311.6	0.214	0.937	2.07	Cheng, *et al.*, (1989)
Pentane	72.15	5	311.6	0.312	0.950	2.81	Cheng, *et al.*, (1989)
Pentane	72.15	5	311.6	0.391	0.956	3.50	Cheng, *et al.*, (1989)
Pentane	72.15	5	311.6	0.487	0.960	4.19	Cheng, *et al.*, (1989)
Pentane	72.15	5	311.6	0.599	0.960	4.93	Cheng, *et al.*, (1989)
Pentane	72.15	5	311.6	0.690	0.964	5.56	Cheng, *et al.*, (1989)
Pentane	72.15	5	311.6	0.775	0.967	6.20	Cheng, *et al.*, (1989)
Pentane	72.15	5	311.6	0.826	0.968	6.54	Cheng, *et al.*, (1989)
Pentane	72.15	5	311.6	0.866	0.969	6.85	Cheng, *et al.*, (1989)
Pentane	72.15	5	311.6	0.885	0.970	6.98	Cheng, *et al.*, (1989)
Pentane	72.15	5	311.6	0.903	0.970	7.14	Cheng, *et al.*, (1989)
Pentane	72.15	5	344.3	0.014	0.343	0.47	Cheng, *et al.*, (1989)
Pentane	72.15	5	344.3	0.032	0.541	0.66	Cheng, *et al.*, (1989)
Pentane	72.15	5	344.3	0.053	0.661	0.90	Cheng, *et al.*, (1989)
Pentane	72.15	5	344.3	0.103	0.785	1.53	Cheng, *et al.*, (1989)
Pentane	72.15	5	344.3	0.169	0.845	2.28	Cheng, *et al.*, (1989)
Pentane	72.15	5	344.3	0.227	0.876	2.97	Cheng, *et al.*, (1989)
Pentane	72.15	5	344.3	0.307	0.896	3.94	Cheng, *et al.*, (1989)
Pentane	72.15	5	344.3	0.396	0.908	5.01	Cheng, *et al.*, (1989)
Pentane	72.15	5	344.3	0.460	0.912	5.72	Cheng, *et al.*, (1989)
Pentane	72.15	5	344.3	0.579	0.914	7.07	Cheng, *et al.*, (1989)
Pentane	72.15	5	344.3	0.638	0.911	7.74	Cheng, *et al.*, (1989)
Pentane	72.15	5	344.3	0.704	0.904	8.44	Cheng, *et al.*, (1989)
Pentane	72.15	5	344.3	0.746	0.896	8.86	Cheng, *et al.*, (1989)
Pentane	72.15	5	344.3	0.777	0.886	9.10	Cheng, *et al.*, (1989)
Pentane	72.15	5	377.7	0.010	0.167	0.79	Cheng, *et al.*, (1989)
Pentane	72.15	5	377.7	0.049	0.483	1.32	Cheng, *et al.*, (1989)
Pentane	72.15	5	377.7	0.108	0.661	2.20	Cheng, *et al.*, (1989)
Pentane	72.15	5	377.7	0.156	0.727	2.90	Cheng, *et al.*, (1989)
Pentane	72.15	5	377.7	0.207	0.766	3.61	Cheng, *et al.*, (1989)
Pentane	72.15	5	377.7	0.263	0.793	4.43	Cheng, *et al.*, (1989)
Pentane	72.15	5	377.7	0.316	0.809	5.21	Cheng, *et al.*, (1989)
Pentane	72.15	5	377.7	0.369	0.818	5.96	Cheng, *et al.*, (1989)
Pentane	72.15	5	377.7	0.423	0.823	6.75	Cheng, *et al.*, (1989)
Pentane	72.15	5	377.7	0.511	0.817	8.04	Cheng, *et al.*, (1989)
Pentane	72.15	5	377.7	0.548	0.815	8.54	Cheng, *et al.*, (1989)

Table A-1 continued

Pentane	72.15	5	377.7	0.594	0.807	9.07	Cheng, *et al.*, (1989)
Pentane	72.15	5	377.7	0.649	0.786	9.62	Cheng, *et al.*, (1989)
Pentane	72.15	5	394.3	0.006	0.076	0.99	Cheng, *et al.*, (1989)
Pentane	72.15	5	394.3	0.000	0.347	1.46	Cheng, *et al.*, (1989)
Pentane	72.15	5	394.3	0.056	0.435	1.74	Cheng, *et al.*, (1989)
Pentane	72.15	5	394.3	0.078	0.515	2.13	Cheng, *et al.*, (1989)
Pentane	72.15	5	394.3	0.145	0.643	3.14	Cheng, *et al.*, (1989)
Pentane	72.15	5	394.3	0.222	0.711	4.32	Cheng, *et al.*, (1989)
Pentane	72.15	5	394.3	0.262	0.731	5.07	Cheng, *et al.*, (1989)
Pentane	72.15	5	394.3	0.345	0.753	6.27	Cheng, *et al.*, (1989)
Pentane	72.15	5	394.3	0.396	0.758	7.05	Cheng, *et al.*, (1989)
Pentane	72.15	5	394.3	0.444	0.756	7.76	Cheng, *et al.*, (1989)
Pentane	72.15	5	394.3	0.514	0.739	8.63	Cheng, *et al.*, (1989)
Pentane	72.15	5	394.3	0.562	0.719	9.14	Cheng, *et al.*, (1989)
Hexane	86.18	6	353.2	0.052	0.815	0.86	Li, *et al.*, (1981)
Hexane	86.18	6	353.2	0.110	0.894	1.63	Li, *et al.*, (1981)
Hexane	86.18	6	353.2	0.167	0.923	2.45	Li, *et al.*, (1981)
Hexane	86.18	6	353.2	0.207	0.934	3.06	Li, *et al.*, (1981)
Hexane	86.18	6	353.2	0.287	0.943	4.09	Li, *et al.*, (1981)
Hexane	86.18	6	353.2	0.353	0.948	4.96	Li, *et al.*, (1981)
Hexane	86.18	6	353.2	0.422	0.947	5.89	Li, *et al.*, (1981)
Hexane	86.18	6	353.2	0.486	0.947	6.71	Li, *et al.*, (1981)
Hexane	86.18	6	353.2	0.541	0.949	7.47	Li, *et al.*, (1981)
Hexane	86.18	6	353.2	0.599	0.945	8.29	Li, *et al.*, (1981)
Hexane	86.18	6	353.2	0.683	0.930	9.15	Li, *et al.*, (1981)
Hexane	86.18	6	353.2	0.752	0.918	10.05	Li, *et al.*, (1981)
Hexane	86.18	6	353.2	0.805	0.906	10.47	Li, *et al.*, (1981)
Hexane	86.18	6	353.2	0.821	0.886	10.66	Li, *et al.*, (1981)
Hexane	86.18	6	393.2	0.028	0.507	0.90	Li, *et al.*, (1981)
Hexane	86.18	6	393.2	0.080	0.715	1.73	Li, *et al.*, (1981)
Hexane	86.18	6	393.2	0.135	0.808	2.64	Li, *et al.*, (1981)
Hexane	86.18	6	393.2	0.180	0.843	3.52	Li, *et al.*, (1981)
Hexane	86.18	6	393.2	0.243	0.853	4.44	Li, *et al.*, (1981)
Hexane	86.18	6	393.2	0.289	0.862	5.30	Li, *et al.*, (1981)
Hexane	86.18	6	393.2	0.339	0.873	6.10	Li, *et al.*, (1981)
Hexane	86.18	6	393.2	0.380	0.875	6.95	Li, *et al.*, (1981)
Hexane	86.18	6	393.2	0.433	0.877	7.76	Li, *et al.*, (1981)
Hexane	86.18	6	393.2	0.486	0.874	8.68	Li, *et al.*, (1981)
Hexane	86.18	6	393.2	0.538	0.866	9.51	Li, *et al.*, (1981)
Hexane	86.18	6	393.2	0.570	0.853	10.09	Li, *et al.*, (1981)
Hexane	86.18	6	393.2	0.632	0.828	10.98	Li, *et al.*, (1981)
Hexane	86.18	6	393.2	0.676	0.801	11.45	Li, *et al.*, (1981)
Hexane	86.18	6	393.2	0.693	0.793	11.60	Li, *et al.*, (1981)
Heptane	100.21	7	352.6	0.031	0.860	0.42	Li, *et al.*, (1981)

Table A-1 continued

Heptane	100.21	7	352.6	0.126	0.956	1.59	Li, *et al.*, (1981)
Heptane	100.21	7	352.6	0.127	0.957	1.61	Li, *et al.*, (1981)
Heptane	100.21	7	352.6	0.240	0.966	3.14	Li, *et al.*, (1981)
Heptane	100.21	7	352.6	0.256	0.968	3.34	Li, *et al.*, (1981)
Heptane	100.21	7	352.6	0.263	0.968	3.43	Li, *et al.*, (1981)
Heptane	100.21	7	352.6	0.379	0.974	5.01	Li, *et al.*, (1981)
Heptane	100.21	7	352.6	0.381	0.972	5.06	Li, *et al.*, (1981)
Heptane	100.21	7	352.6	0.490	0.972	6.59	Li, *et al.*, (1981)
Heptane	100.21	7	352.6	0.498	0.974	6.62	Li, *et al.*, (1981)
Heptane	100.21	7	352.6	0.624	0.972	8.54	Li, *et al.*, (1981)
Heptane	100.21	7	352.6	0.625	0.971	8.58	Li, *et al.*, (1981)
Heptane	100.21	7	352.6	0.715	0.963	9.83	Li, *et al.*, (1981)
Heptane	100.21	7	352.6	0.719	0.963	9.85	Li, *et al.*, (1981)
Heptane	100.21	7	352.6	0.769	0.954	10.60	Li, *et al.*, (1981)
Heptane	100.21	7	352.6	0.775	0.952	10.65	Li, *et al.*, (1981)
Heptane	100.21	7	352.6	0.847	0.905	11.61	Li, *et al.*, (1981)
Heptane	100.21	7	394.3	0.073	0.819	1.13	Li, *et al.*, (1981)
Heptane	100.21	7	394.3	0.074	0.819	1.13	Li, *et al.*, (1981)
Heptane	100.21	7	394.3	0.193	0.921	3.10	Li, *et al.*, (1981)
Heptane	100.21	7	394.3	0.195	0.915	3.13	Li, *et al.*, (1981)
Heptane	100.21	7	394.3	0.296	0.936	4.83	Li, *et al.*, (1981)
Heptane	100.21	7	394.3	0.296	0.936	4.86	Li, *et al.*, (1981)
Heptane	100.21	7	394.3	0.345	0.939	5.77	Li, *et al.*, (1981)
Heptane	100.21	7	394.3	0.376	0.942	6.25	Li, *et al.*, (1981)
Heptane	100.21	7	394.3	0.378	0.942	6.32	Li, *et al.*, (1981)
Heptane	100.21	7	394.3	0.384	0.941	6.45	Li, *et al.*, (1981)
Heptane	100.21	7	394.3	0.500	0.939	8.62	Li, *et al.*, (1981)
Heptane	100.21	7	394.3	0.503	0.939	8.69	Li, *et al.*, (1981)
Heptane	100.21	7	394.3	0.589	0.934	10.38	Li, *et al.*, (1981)
Heptane	100.21	7	394.3	0.594	0.934	10.44	Li, *et al.*, (1981)
Heptane	100.21	7	394.3	0.686	0.914	12.04	Li, *et al.*, (1981)
Heptane	100.21	7	394.3	0.761	0.878	13.24	Li, *et al.*, (1981)
Heptane	100.21	7	394.3	0.768	0.882	13.31	Li, *et al.*, (1981)
Octane	114.23	8	313.2	0.143	0.995	1.50	Weng & Lee (1992)
Octane	114.23	8	313.2	0.291	0.996	3.00	Weng & Lee (1992)
Octane	114.23	8	313.2	0.455	0.996	4.50	Weng & Lee (1992)
Octane	114.23	8	313.2	0.616	0.995	5.89	Weng & Lee (1992)
Octane	114.23	8	313.2	0.711	0.995	6.50	Weng & Lee (1992)
Octane	114.23	8	313.2	0.890	0.992	7.55	Weng & Lee (1992)
Octane	114.23	8	328.2	0.174	0.993	2.00	Weng & Lee (1992)
Octane	114.23	8	328.2	0.332	0.994	4.00	Weng & Lee (1992)
Octane	114.23	8	328.2	0.462	0.994	5.50	Weng & Lee (1992)
Octane	114.23	8	328.2	0.551	0.994	6.50	Weng & Lee (1992)
Octane	114.23	8	328.2	0.709	0.990	8.00	Weng & Lee (1992)

Table A-1 continued

Octane	114.23	8	328.2	0.882	0.974	9.50	Weng & Lee (1992)
Octane	114.23	8	348.2	0.145	0.986	2.00	Weng & Lee (1992)
Octane	114.23	8	348.2	0.275	0.989	4.00	Weng & Lee (1992)
Octane	114.23	8	348.2	0.360	0.990	5.26	Weng & Lee (1992)
Octane	114.23	8	348.2	0.486	0.987	7.10	Weng & Lee (1992)
Octane	114.23	8	348.2	0.631	0.982	8.10	Weng & Lee (1992)
Octane	114.23	8	348.2	0.677	0.979	9.70	Weng & Lee (1992)
Octane	114.23	8	348.2	0.754	0.962	10.80	Weng & Lee (1992)
Octane	114.23	8	348.2	0.813	0.958	11.35	Weng & Lee (1992)
Octane	114.23	8	313.2	0.110	0.986	1.15	Yu, *et al.*, (2006)
Octane	114.23	8	313.2	0.213	0.994	2.08	Yu, *et al.*, (2006)
Octane	114.23	8	313.2	0.338	0.993	3.15	Yu, *et al.*, (2006)
Octane	114.23	8	313.2	0.434	0.992	4.15	Yu, *et al.*, (2006)
Octane	114.23	8	313.2	0.553	0.990	5.14	Yu, *et al.*, (2006)
Octane	114.23	8	313.2	0.675	0.990	6.14	Yu, *et al.*, (2006)
Octane	114.23	8	313.2	0.752	0.993	6.64	Yu, *et al.*, (2006)
Octane	114.23	8	313.2	0.858	0.992	7.35	Yu, *et al.*, (2006)
Octane	114.23	8	313.2	0.945	0.945	7.85	Yu, *et al.*, (2006)
Octane	114.23	8	333.2	0.157	0.977	1.70	Yu, *et al.*, (2006)
Octane	114.23	8	333.2	0.206	0.988	2.17	Yu, *et al.*, (2006)
Octane	114.23	8	333.2	0.289	0.993	3.25	Yu, *et al.*, (2006)
Octane	114.23	8	333.2	0.359	0.994	4.15	Yu, *et al.*, (2006)
Octane	114.23	8	333.2	0.430	0.992	5.14	Yu, *et al.*, (2006)
Octane	114.23	8	333.2	0.496	0.989	6.14	Yu, *et al.*, (2006)
Octane	114.23	8	333.2	0.592	0.989	7.14	Yu, *et al.*, (2006)
Octane	114.23	8	333.2	0.741	0.985	9.17	Yu, *et al.*, (2006)
Octane	114.23	8	333.2	0.856	0.982	9.97	Yu, *et al.*, (2006)
Octane	114.23	8	333.2	0.938	0.936	10.48	Yu, *et al.*, (2006)
Octane	114.23	8	353.2	0.145	0.991	1.70	Yu, *et al.*, (2006)
Octane	114.23	8	353.2	0.245	0.989	2.78	Yu, *et al.*, (2006)
Octane	114.23	8	353.2	0.360	0.988	4.01	Yu, *et al.*, (2006)
Octane	114.23	8	353.2	0.437	0.987	5.33	Yu, *et al.*, (2006)
Octane	114.23	8	353.2	0.495	0.987	6.49	Yu, *et al.*, (2006)
Octane	114.23	8	353.2	0.578	0.983	7.96	Yu, *et al.*, (2006)
Octane	114.23	8	353.2	0.624	0.983	8.97	Yu, *et al.*, (2006)
Octane	114.23	8	353.2	0.776	0.979	11.02	Yu, *et al.*, (2006)
Octane	114.23	8	353.2	0.826	0.979	11.99	Yu, *et al.*, (2006)
Octane	114.23	8	353.2	0.915	0.915	12.33	Yu, *et al.*, (2006)
Octane	114.23	8	373.2	0.217	0.979	1.85	Yu, *et al.*, (2006)
Octane	114.23	8	373.2	0.369	0.988	3.73	Yu, *et al.*, (2006)
Octane	114.23	8	373.2	0.513	0.988	6.02	Yu, *et al.*, (2006)
Octane	114.23	8	373.2	0.571	0.980	7.80	Yu, *et al.*, (2006)
Octane	114.23	8	373.2	0.654	0.976	9.40	Yu, *et al.*, (2006)
Octane	114.23	8	373.2	0.784	0.959	12.19	Yu, *et al.*, (2006)

Table A-1 continued

Octane	114.23	8	373.2	0.852	0.934	13.28	Yu, et al., (2006)
Octane	114.23	8	373.2	0.902	0.902	13.85	Yu, et al., (2006)
Octane	114.23	8	393.2	0.156	0.921	1.11	Yu, et al., (2006)
Octane	114.23	8	393.2	0.269	0.959	2.76	Yu, et al., (2006)
Octane	114.23	8	393.2	0.393	0.967	3.98	Yu, et al., (2006)
Octane	114.23	8	393.2	0.458	0.962	5.26	Yu, et al., (2006)
Octane	114.23	8	393.2	0.522	0.974	6.79	Yu, et al., (2006)
Octane	114.23	8	393.2	0.592	0.970	8.31	Yu, et al., (2006)
Octane	114.23	8	393.2	0.674	0.967	10.00	Yu, et al., (2006)
Octane	114.23	8	393.2	0.746	0.965	11.44	Yu, et al., (2006)
Octane	114.23	8	393.2	0.815	0.964	12.97	Yu, et al., (2006)
Octane	114.23	8	393.2	0.873	0.873	14.44	Yu, et al., (2006)
Octane	114.23	8	322.4	0.178	0.995	2.01	Jime´nez-Gallegos, et al., (2006)
Octane	114.23	8	322.4	0.355	0.995	3.91	Jime´nez-Gallegos, et al., (2006)
Octane	114.23	8	322.4	0.562	0.995	5.73	Jime´nez-Gallegos, et al., (2006)
Octane	114.23	8	322.4	0.657	0.994	6.61	Jime´nez-Gallegos, et al., (2006)
Octane	114.23	8	322.4	0.742	0.992	7.45	Jime´nez-Gallegos, et al., (2006)
Octane	114.23	8	322.4	0.838	0.989	8.17	Jime´nez-Gallegos, et al., (2006)
Octane	114.23	8	322.4	0.889	0.986	8.53	Jime´nez-Gallegos, et al., (2006)
Octane	114.23	8	348.3	0.142	0.985	2.08	Jime´nez-Gallegos, et al., (2006)
Octane	114.23	8	348.3	0.285	0.987	4.07	Jime´nez-Gallegos, et al., (2006)
Octane	114.23	8	348.3	0.367	0.988	5.31	Jime´nez-Gallegos, et al., (2006)
Octane	114.23	8	348.3	0.474	0.986	6.99	Jime´nez-Gallegos, et al., (2006)
Octane	114.23	8	348.3	0.614	0.982	9.10	Jime´nez-Gallegos, et al., (2006)
Octane	114.23	8	348.3	0.683	0.978	9.94	Jime´nez-Gallegos, et al., (2006)
Octane	114.23	8	348.3	0.742	0.973	10.70	Jime´nez-Gallegos, et al., (2006)
Octane	114.23	8	348.3	0.779	0.967	10.98	Jime´nez-Gallegos, et al., (2006)
Octane	114.23	8	348.3	0.815	0.958	11.46	Jime´nez-Gallegos, et al., (2006)
Octane	114.23	8	372.5	0.255	0.975	4.26	Jime´nez-Gallegos, et al., (2006)
Octane	114.23	8	372.5	0.312	0.977	5.29	Jime´nez-Gallegos, et al., (2006)
Octane	114.23	8	372.5	0.356	0.977	6.06	Jime´nez-Gallegos, et al., (2006)
Octane	114.23	8	372.5	0.405	0.977	7.03	Jime´nez-Gallegos, et al., (2006)
Octane	114.23	8	372.5	0.475	0.977	8.39	Jime´nez-Gallegos, et al., (2006)
Octane	114.23	8	372.5	0.518	0.973	9.42	Jime´nez-Gallegos, et al., (2006)
Octane	114.23	8	372.5	0.567	0.970	10.47	Jime´nez-Gallegos, et al., (2006)
Octane	114.23	8	372.5	0.623	0.967	11.60	Jime´nez-Gallegos, et al., (2006)
Octane	114.23	8	372.5	0.687	0.962	12.80	Jime´nez-Gallegos, et al., (2006)
Octane	114.23	8	372.5	0.749	0.949	13.28	Jime´nez-Gallegos, et al., (2006)
Octane	114.23	8	372.5	0.829	0.939	13.77	Jime´nez-Gallegos, et al., (2006)
Nonane	128.26	9	343.3	0.296	0.996	3.73	Jennings & Schucker (1996)
Nonane	128.26	9	343.3	0.416	0.996	5.45	Jennings & Schucker (1996)
Nonane	128.26	9	343.3	0.517	0.995	6.96	Jennings & Schucker (1996)
Nonane	128.26	9	343.3	0.627	0.993	8.56	Jennings & Schucker (1996)
Nonane	128.26	9	343.3	0.778	0.986	10.63	Jennings & Schucker (1996)

Table A-1 continued

Nonane	128.26	9	343.3	0.883	0.967	11.80	Jennings & Schucker (1996)
Nonane	128.26	9	344.5	0.178	0.995	2.11	Camacho-Camacho, *et al.*, (2007)
Nonane	128.26	9	344.5	0.299	0.996	3.75	Camacho-Camacho, *et al.*, (2007)
Nonane	128.26	9	344.5	0.415	0.996	5.46	Camacho-Camacho, *et al.*, (2007)
Nonane	128.26	9	344.5	0.513	0.995	6.94	Camacho-Camacho, *et al.*, (2007)
Nonane	128.26	9	344.5	0.630	0.993	8.65	Camacho-Camacho, *et al.*, (2007)
Nonane	128.26	9	344.5	0.718	0.988	10.06	Camacho-Camacho, *et al.*, (2007)
Nonane	128.26	9	344.5	0.835	0.978	11.24	Camacho-Camacho, *et al.*, (2007)
Nonane	128.26	9	344.5	0.905	0.964	11.99	Camacho-Camacho, *et al.*, (2007)
Nonane	128.26	9	315.1	0.221	0.999	2.03	Camacho-Camacho, *et al.*, (2007)
Nonane	128.26	9	315.1	0.325	0.999	3.10	Camacho-Camacho, *et al.*, (2007)
Nonane	128.26	9	315.1	0.460	0.999	4.31	Camacho-Camacho, *et al.*, (2007)
Nonane	128.26	9	315.1	0.570	0.998	5.45	Camacho-Camacho, *et al.*, (2007)
Nonane	128.26	9	315.1	0.709	0.998	6.67	Camacho-Camacho, *et al.*, (2007)
Nonane	128.26	9	315.1	0.798	0.997	7.20	Camacho-Camacho, *et al.*, (2007)
Nonane	128.26	9	315.1	0.899	0.996	7.80	Camacho-Camacho, *et al.*, (2007)
Nonane	128.26	9	315.1	0.934	0.996	8.03	Camacho-Camacho, *et al.*, (2007)
Nonane	128.26	9	373.3	0.147	0.987	2.06	Camacho-Camacho, *et al.*, (2007)
Nonane	128.26	9	373.3	0.238	0.989	3.51	Camacho-Camacho, *et al.*, (2007)
Nonane	128.26	9	373.3	0.321	0.989	4.98	Camacho-Camacho, *et al.*, (2007)
Nonane	128.26	9	373.3	0.406	0.990	6.48	Camacho-Camacho, *et al.*, (2007)
Nonane	128.26	9	373.3	0.475	0.989	7.94	Camacho-Camacho, *et al.*, (2007)
Nonane	128.26	9	373.3	0.577	0.986	9.59	Camacho-Camacho, *et al.*, (2007)
Nonane	128.26	9	373.3	0.647	0.983	11.03	Camacho-Camacho, *et al.*, (2007)
Nonane	128.26	9	373.3	0.731	0.976	12.58	Camacho-Camacho, *et al.*, (2007)
Nonane	128.26	9	373.3	0.788	0.968	13.55	Camacho-Camacho, *et al.*, (2007)
Nonane	128.26	9	373.3	0.868	0.934	14.84	Camacho-Camacho, *et al.*, (2007)
Nonane	128.26	9	373.3	0.897	0.919	14.97	Camacho-Camacho, *et al.*, (2007)
Decane	142.28	10	313.2	0.147	0.000	1.43	Adams, *et al.*, (1988)
Decane	142.28	10	313.2	0.345	0.000	3.44	Adams, *et al.*, (1988)
Decane	142.28	10	313.2	0.496	0.000	4.81	Adams, *et al.*, (1988)
Decane	142.28	10	313.2	0.651	0.000	6.18	Adams, *et al.*, (1988)
Decane	142.28	10	313.2	0.826	0.000	7.41	Adams, *et al.*, (1988)
Decane	142.28	10	313.2	0.000	0.999	5.672	Adams, *et al.*, (1988)
Decane	142.28	10	313.2	0.000	0.999	6.346	Adams, *et al.*, (1988)
Decane	142.28	10	313.2	0.000	0.999	6.969	Adams, *et al.*, (1988)
Decane	142.28	10	313.2	0.000	0.998	7.510	Adams, *et al.*, (1988)
Decane	142.28	10	313.2	0.000	0.997	7.835	Adams, *et al.*, (1988)
Decane	142.28	10	344.3	0.457	0.995	6.38	Nagarajan & Robinson (1986)
Decane	142.28	10	344.3	0.489	0.995	6.94	Nagarajan & Robinson (1986)
Decane	142.28	10	344.3	0.535	0.995	7.61	Nagarajan & Robinson (1986)
Decane	142.28	10	344.3	0.575	0.995	8.34	Nagarajan & Robinson (1986)
Decane	142.28	10	344.3	0.615	0.994	8.96	Nagarajan & Robinson (1986)
Decane	142.28	10	344.3	0.657	0.993	9.65	Nagarajan & Robinson (1986)

Table A-1 continued

Decane	142.28	10	344.3	0.702	0.990	10.34	Nagarajan & Robinson (1986)
Decane	142.28	10	344.3	0.753	0.987	11.02	Nagarajan & Robinson (1986)
Decane	142.28	10	344.3	0.775	0.986	11.38	Nagarajan & Robinson (1986)
Decane	142.28	10	344.3	0.804	0.983	11.73	Nagarajan & Robinson (1986)
Decane	142.28	10	344.3	0.815	0.981	11.90	Nagarajan & Robinson (1986)
Decane	142.28	10	344.3	0.834	0.979	12.07	Nagarajan & Robinson (1986)
Decane	142.28	10	344.3	0.847	0.976	12.22	Nagarajan & Robinson (1986)
Decane	142.28	10	344.3	0.866	0.971	12.40	Nagarajan & Robinson (1986)
Decane	142.28	10	344.3	0.877	0.968	12.49	Nagarajan & Robinson (1986)
Decane	142.28	10	344.3	0.883	0.965	12.56	Nagarajan & Robinson (1986)
Decane	142.28	10	344.3	0.886	0.960	12.62	Nagarajan & Robinson (1986)
Decane	142.28	10	344.3	0.893	0.955	12.65	Nagarajan & Robinson (1986)
Decane	142.28	10	344.3	0.897	0.953	12.70	Nagarajan & Robinson (1986)
Decane	142.28	10	344.3	0.918	0.935	12.73	Nagarajan & Robinson (1986)
Decane	142.28	10	377.6	0.565	0.987	10.34	Nagarajan & Robinson (1986)
Decane	142.28	10	377.6	0.595	0.985	11.04	Nagarajan & Robinson (1986)
Decane	142.28	10	377.6	0.626	0.984	11.76	Nagarajan & Robinson (1986)
Decane	142.28	10	377.6	0.656	0.981	12.42	Nagarajan & Robinson (1986)
Decane	142.28	10	377.6	0.689	0.978	13.12	Nagarajan & Robinson (1986)
Decane	142.28	10	377.6	0.719	0.975	13.80	Nagarajan & Robinson (1986)
Decane	142.28	10	377.6	0.734	0.973	14.16	Nagarajan & Robinson (1986)
Decane	142.28	10	377.6	0.746	0.970	14.48	Nagarajan & Robinson (1986)
Decane	142.28	10	377.6	0.757	0.968	14.83	Nagarajan & Robinson (1986)
Decane	142.28	10	377.6	0.776	0.964	15.18	Nagarajan & Robinson (1986)
Decane	142.28	10	377.6	0.784	0.962	15.35	Nagarajan & Robinson (1986)
Decane	142.28	10	377.6	0.794	0.959	15.51	Nagarajan & Robinson (1986)
Decane	142.28	10	377.6	0.806	0.957	15.69	Nagarajan & Robinson (1986)
Decane	142.28	10	377.6	0.816	0.953	15.85	Nagarajan & Robinson (1986)
Decane	142.28	10	377.6	0.821	0.950	15.96	Nagarajan & Robinson (1986)
Decane	142.28	10	377.6	0.829	0.946	16.07	Nagarajan & Robinson (1986)
Decane	142.28	10	377.6	0.836	0.944	16.14	Nagarajan & Robinson (1986)
Decane	142.28	10	377.6	0.842	0.940	16.22	Nagarajan & Robinson (1986)
Decane	142.28	10	377.6	0.846	0.937	16.29	Nagarajan & Robinson (1986)
Decane	142.28	10	377.6	0.854	0.933	16.35	Nagarajan & Robinson (1986)
Decane	142.28	10	377.6	0.856	0.930	16.38	Nagarajan & Robinson (1986)
Decane	142.28	10	377.6	0.860	0.926	16.45	Nagarajan & Robinson (1986)
Decane	142.28	10	377.6	0.865	0.922	16.46	Nagarajan & Robinson (1986)
Decane	142.28	10	344.3	0.338	0.998	4.33	Jennings & Schucker (1996)
Decane	142.28	10	344.3	0.446	0.998	5.96	Jennings & Schucker (1996)
Decane	142.28	10	344.2	0.507	0.997	6.96	Jennings & Schucker (1996)
Decane	142.28	10	344.2	0.631	0.996	8.98	Jennings & Schucker (1996)
Decane	142.28	10	344.3	0.722	0.992	10.45	Jennings & Schucker (1996)
Decane	142.28	10	344.3	0.821	0.984	11.85	Jennings & Schucker (1996)
Decane	142.28	10	311.0	0.446	0.999	4.55	Iwai, *et al.*, (1994)

Table A-1 continued

Decane	142.28	10	311.0	0.747	0.999	6.86	Iwai, *et al.*, (1994)
Decane	142.28	10	344.3	0.383	0.998	5.51	Iwai, *et al.*, (1994)
Decane	142.28	10	344.3	0.594	0.997	8.55	Iwai, *et al.*, (1994)
Decane	142.28	10	344.3	0.806	0.988	11.85	Iwai, *et al.*, (1994)
Decane	142.28	10	277.6	0.055	1.000	0.34	Reamer, *et al.*, (1963)
Decane	142.28	10	277.6	0.109	1.000	0.69	Reamer, *et al.*, (1963)
Decane	142.28	10	277.6	0.163	1.000	1.03	Reamer, *et al.*, (1963)
Decane	142.28	10	277.6	0.218	1.000	1.38	Reamer, *et al.*, (1963)
Decane	142.28	10	277.6	0.275	1.000	1.72	Reamer, *et al.*, (1963)
Decane	142.28	10	277.6	0.336	1.000	2.07	Reamer, *et al.*, (1963)
Decane	142.28	10	277.6	0.405	1.000	2.41	Reamer, *et al.*, (1963)
Decane	142.28	10	277.6	0.477	1.000	2.76	Reamer, *et al.*, (1963)
Decane	142.28	10	277.6	0.569	1.000	3.10	Reamer, *et al.*, (1963)
Decane	142.28	10	277.6	0.712	1.000	3.45	Reamer, *et al.*, (1963)
Decane	142.28	10	277.6	0.914	1.000	3.79	Reamer, *et al.*, (1963)
Decane	142.28	10	277.6	1.000	1.000	3.91	Reamer, *et al.*, (1963)
Decane	142.28	10	310.9	0.073	0.999	0.69	Reamer, *et al.*, (1963)
Decane	142.28	10	310.9	0.144	0.999	1.38	Reamer, *et al.*, (1963)
Decane	142.28	10	310.9	0.213	0.999	2.07	Reamer, *et al.*, (1963)
Decane	142.28	10	310.9	0.282	0.999	2.76	Reamer, *et al.*, (1963)
Decane	142.28	10	310.9	0.351	0.999	3.45	Reamer, *et al.*, (1963)
Decane	142.28	10	310.9	0.422	0.999	4.14	Reamer, *et al.*, (1963)
Decane	142.28	10	310.9	0.495	0.999	4.83	Reamer, *et al.*, (1963)
Decane	142.28	10	310.9	0.571	0.999	5.52	Reamer, *et al.*, (1963)
Decane	142.28	10	310.9	0.651	0.999	6.21	Reamer, *et al.*, (1963)
Decane	142.28	10	310.9	0.743	0.999	6.89	Reamer, *et al.*, (1963)
Decane	142.28	10	310.9	0.864	0.999	8.00	Reamer, *et al.*, (1963)
Decane	142.28	10	310.9	0.995	0.995	7.46	Reamer, *et al.*, (1963)
Decane	142.28	10	344.3	0.112	0.996	1.38	Reamer, *et al.*, (1963)
Decane	142.28	10	344.3	0.213	0.997	2.76	Reamer, *et al.*, (1963)
Decane	142.28	10	344.3	0.308	0.998	4.14	Reamer, *et al.*, (1963)
Decane	142.28	10	344.3	0.399	0.998	5.52	Reamer, *et al.*, (1963)
Decane	142.28	10	344.3	0.488	0.998	6.89	Reamer, *et al.*, (1963)
Decane	142.28	10	344.3	0.600	0.997	8.62	Reamer, *et al.*, (1963)
Decane	142.28	10	344.3	0.713	0.994	10.34	Reamer, *et al.*, (1963)
Decane	142.28	10	344.3	0.830	0.982	12.07	Reamer, *et al.*, (1963)
Decane	142.28	10	344.3	0.948	0.948	12.82	Reamer, *et al.*, (1963)
Decane	142.28	10	377.6	0.093	0.989	1.38	Reamer, *et al.*, (1963)
Decane	142.28	10	377.6	0.177	0.993	2.76	Reamer, *et al.*, (1963)
Decane	142.28	10	377.6	0.255	0.993	4.14	Reamer, *et al.*, (1963)
Decane	142.28	10	377.6	0.327	0.994	5.52	Reamer, *et al.*, (1963)
Decane	142.28	10	377.6	0.396	0.994	6.89	Reamer, *et al.*, (1963)
Decane	142.28	10	377.6	0.480	0.993	8.62	Reamer, *et al.*, (1963)
Decane	142.28	10	377.6	0.560	0.991	10.34	Reamer, *et al.*, (1963)

Table A-1 continued

Decane	142.28	10	377.6	0.639	0.988	12.07	Reamer, *et al.*, (1963)
Decane	142.28	10	377.6	0.717	0.979	13.79	Reamer, *et al.*, (1963)
Decane	142.28	10	377.6	0.797	0.964	15.51	Reamer, *et al.*, (1963)
Decane	142.28	10	377.6	0.905	0.905	16.49	Reamer, *et al.*, (1963)
Decane	142.28	10	319.1	0.340	0.999	3.49	Jime´nez-Gallegos, *et al.*, (2006)
Decane	142.28	10	319.1	0.424	0.999	4.58	Jime´nez-Gallegos, *et al.*, (2006)
Decane	142.28	10	319.1	0.526	0.999	5.68	Jime´nez-Gallegos, *et al.*, (2006)
Decane	142.28	10	319.1	0.633	0.998	6.87	Jime´nez-Gallegos, *et al.*, (2006)
Decane	142.28	10	319.1	0.734	0.996	7.88	Jime´nez-Gallegos, *et al.*, (2006)
Decane	142.28	10	319.1	0.885	0.993	8.51	Jime´nez-Gallegos, *et al.*, (2006)
Decane	142.28	10	319.1	0.924	0.989	8.68	Jime´nez-Gallegos, *et al.*, (2006)
Decane	142.28	10	319.1	0.973	0.987	8.90	Jime´nez-Gallegos, *et al.*, (2006)
Decane	142.28	10	344.7	0.342	0.998	4.59	Jime´nez-Gallegos, *et al.*, (2006)
Decane	142.28	10	344.7	0.399	0.997	5.52	Jime´nez-Gallegos, *et al.*, (2006)
Decane	142.28	10	344.7	0.493	0.997	6.89	Jime´nez-Gallegos, *et al.*, (2006)
Decane	142.28	10	344.7	0.582	0.996	8.18	Jime´nez-Gallegos, *et al.*, (2006)
Decane	142.28	10	344.7	0.647	0.994	9.45	Jime´nez-Gallegos, *et al.*, (2006)
Decane	142.28	10	344.7	0.737	0.988	10.09	Jime´nez-Gallegos, *et al.*, (2006)
Decane	142.28	10	344.7	0.838	0.973	12.13	Jime´nez-Gallegos, *et al.*, (2006)
Decane	142.28	10	344.7	0.896	0.968	12.65	Jime´nez-Gallegos, *et al.*, (2006)
Decane	142.28	10	372.9	0.215	0.994	3.24	Jime´nez-Gallegos, *et al.*, (2006)
Decane	142.28	10	372.9	0.277	0.994	4.40	Jime´nez-Gallegos, *et al.*, (2006)
Decane	142.28	10	372.9	0.335	0.993	5.48	Jime´nez-Gallegos, *et al.*, (2006)
Decane	142.28	10	372.9	0.380	0.993	6.41	Jime´nez-Gallegos, *et al.*, (2006)
Decane	142.28	10	372.9	0.445	0.993	7.70	Jime´nez-Gallegos, *et al.*, (2006)
Decane	142.28	10	372.9	0.486	0.992	8.70	Jime´nez-Gallegos, *et al.*, (2006)
Decane	142.28	10	372.9	0.513	0.990	9.42	Jime´nez-Gallegos, *et al.*, (2006)
Decane	142.28	10	372.9	0.575	0.988	10.40	Jime´nez-Gallegos, *et al.*, (2006)
Decane	142.28	10	372.9	0.632	0.983	11.89	Jime´nez-Gallegos, *et al.*, (2006)
Decane	142.28	10	372.9	0.697	0.978	13.21	Jime´nez-Gallegos, *et al.*, (2006)
Decane	142.28	10	372.9	0.745	0.971	14.24	Jime´nez-Gallegos, *et al.*, (2006)
Decane	142.28	10	372.9	0.791	0.964	15.30	Jime´nez-Gallegos, *et al.*, (2006)
Decane	142.28	10	372.9	0.856	0.927	16.06	Jime´nez-Gallegos, *et al.*, (2006)
Undecane	156.31	11	315.0	0.243	0.999	2.37	Camacho-Camacho, *et al.*, (2007)
Undecane	156.31	11	315.0	0.309	0.999	3.16	Camacho-Camacho, *et al.*, (2007)
Undecane	156.31	11	315.0	0.380	1.000	4.01	Camacho-Camacho, *et al.*, (2007)
Undecane	156.31	11	315.0	0.454	0.999	4.92	Camacho-Camacho, *et al.*, (2007)
Undecane	156.31	11	315.0	0.526	0.999	5.70	Camacho-Camacho, *et al.*, (2007)
Undecane	156.31	11	315.0	0.583	0.999	6.29	Camacho-Camacho, *et al.*, (2007)
Undecane	156.31	11	315.0	0.637	0.999	6.88	Camacho-Camacho, *et al.*, (2007)
Undecane	156.31	11	315.0	0.737	0.998	7.64	Camacho-Camacho, *et al.*, (2007)
Undecane	156.31	11	315.0	0.913	0.993	8.29	Camacho-Camacho, *et al.*, (2007)
Undecane	156.31	11	373.1	0.225	0.996	3.47	Camacho-Camacho, *et al.*, (2007)
Undecane	156.31	11	373.1	0.328	0.997	5.52	Camacho-Camacho, *et al.*, (2007)

Table A-1 continued

Undecane	156.31	11	373.1	0.399	0.996	7.01	Camacho-Camacho, *et al.*, (2007)
Undecane	156.31	11	373.1	0.464	0.995	8.53	Camacho-Camacho, *et al.*, (2007)
Undecane	156.31	11	373.1	0.519	0.993	9.96	Camacho-Camacho, *et al.*, (2007)
Undecane	156.31	11	373.1	0.584	0.992	11.61	Camacho-Camacho, *et al.*, (2007)
Undecane	156.31	11	373.1	0.641	0.989	13.15	Camacho-Camacho, *et al.*, (2007)
Undecane	156.31	11	373.1	0.715	0.981	14.84	Camacho-Camacho, *et al.*, (2007)
Undecane	156.31	11	373.1	0.762	0.960	16.00	Camacho-Camacho, *et al.*, (2007)
Undecane	156.31	11	373.1	0.871	0.932	17.11	Camacho-Camacho, *et al.*, (2007)
Dodecane	170.34	12	318.2	0.114	1.000	0.95	Gardeler, *et al.*, (2002)
Dodecane	170.34	12	318.2	0.190	1.000	1.77	Gardeler, *et al.*, (2002)
Dodecane	170.34	12	318.2	0.257	1.000	2.47	Gardeler, *et al.*, (2002)
Dodecane	170.34	12	318.2	0.341	1.000	3.47	Gardeler, *et al.*, (2002)
Dodecane	170.34	12	318.2	0.421	1.000	4.53	Gardeler, *et al.*, (2002)
Dodecane	170.34	12	318.2	0.505	1.000	5.46	Gardeler, *et al.*, (2002)
Dodecane	170.34	12	318.2	0.583	0.999	6.42	Gardeler, *et al.*, (2002)
Dodecane	170.34	12	318.2	0.645	0.997	7.31	Gardeler, *et al.*, (2002)
Dodecane	170.34	12	318.2	0.732	0.995	8.16	Gardeler, *et al.*, (2002)
Dodecane	170.34	12	318.2	0.805	0.985	8.94	Gardeler, *et al.*, (2002)
Pentadecane	212.46	15	292.0	0.620	1.000	4.57	Scheidgen (1997)
Pentadecane	212.46	15	292.0	0.662	0.999	5.20	Scheidgen (1997)
Pentadecane	212.46	15	292.0	0.989	0.772	5.89	Scheidgen (1997)
Pentadecane	212.46	15	292.0	0.983	0.814	6.52	Scheidgen (1997)
Pentadecane	212.46	15	292.0	0.980	0.823	6.93	Scheidgen (1997)
Pentadecane	212.46	15	292.0	0.980	0.826	8.00	Scheidgen (1997)
Pentadecane	212.46	15	292.0	0.977	0.836	9.93	Scheidgen (1997)
Pentadecane	212.46	15	292.0	0.967	0.847	12.40	Scheidgen (1997)
Pentadecane	212.46	15	292.0	0.967	0.873	14.92	Scheidgen (1997)
Pentadecane	212.46	15	292.0	0.960	0.885	17.17	Scheidgen (1997)
Pentadecane	212.46	15	292.0	0.000	0.935	19.45	Scheidgen (1997)
Pentadecane	212.46	15	316.0	0.642	0.999	7.29	Scheidgen (1997)
Pentadecane	212.46	15	316.0	0.701	0.999	8.08	Scheidgen (1997)
Pentadecane	212.46	15	316.0	0.768	1.000	8.56	Scheidgen (1997)
Pentadecane	212.46	15	316.0	0.787	0.999	9.01	Scheidgen (1997)
Pentadecane	212.46	15	316.0	0.812	0.999	9.50	Scheidgen (1997)
Pentadecane	212.46	15	316.0	0.827	0.996	9.98	Scheidgen (1997)
Pentadecane	212.46	15	316.0	0.836	0.990	10.01	Scheidgen (1997)
Pentadecane	212.46	15	316.0	0.855	0.990	12.10	Scheidgen (1997)
Pentadecane	212.46	15	316.0	0.882	0.959	12.93	Scheidgen (1997)
Pentadecane	212.46	15	316.0	0.000	0.928	13.18	Scheidgen (1997)
Hexadecane	226.44	16	323.2	0.703	0.999	10.00	Pohler (1994)
Hexadecane	226.44	16	323.2	0.834	0.999	12.50	Pohler (1994)
Hexadecane	226.44	16	323.2	0.880	0.990	15.00	Pohler (1994)
Hexadecane	226.44	16	323.2	0.931	0.983	16.00	Pohler (1994)
Hexadecane	226.44	16	323.2	0.954	0.954	16.40	Pohler (1994)

Table A-1 continued

Hexadecane	226.44	16	353.2	0.604	0.999	10.00	Kordikowski & Schneider (1993)
Hexadecane	226.44	16	353.2	0.684	0.999	12.50	Kordikowski & Schneider (1993)
Hexadecane	226.44	16	353.2	0.765	0.996	15.00	Kordikowski & Schneider (1993)
Hexadecane	226.44	16	353.2	0.822	0.988	17.50	Kordikowski & Schneider (1993)
Hexadecane	226.44	16	353.2	0.834	0.981	18.50	Kordikowski & Schneider (1993)
Hexadecane	226.44	16	353.2	0.868	0.967	19.60	Kordikowski & Schneider (1993)
Hexadecane	226.44	16	353.2	0.936	0.936	20.00	Kordikowski & Schneider (1993)
Hexadecane	226.44	16	393.2	0.497	0.998	10.10	Spee & Schneider (1991)
Hexadecane	226.44	16	393.2	0.591	0.997	13.10	Spee & Schneider (1991)
Hexadecane	226.44	16	393.2	0.635	0.997	15.10	Spee & Schneider (1991)
Hexadecane	226.44	16	393.2	0.695	0.994	17.40	Spee & Schneider (1991)
Hexadecane	226.44	16	393.2	0.747	0.991	20.00	Spee & Schneider (1991)
Hexadecane	226.44	16	393.2	0.789	0.987	21.50	Spee & Schneider (1991)
Hexadecane	226.44	16	393.2	0.800	0.986	22.50	Spee & Schneider (1991)
Hexadecane	226.44	16	393.2	0.837	0.978	23.80	Spee & Schneider (1991)
Hexadecane	226.44	16	393.2	0.847	0.974	24.10	Spee & Schneider (1991)
Hexadecane	226.44	16	393.2	0.841	0.975	24.00	Spee & Schneider (1991)
Hexadecane	226.44	16	393.2	0.875	0.963	25.10	Spee & Schneider (1991)
Hexadecane	226.44	16	393.2	0.873	0.961	25.00	Spee & Schneider (1991)
Hexadecane	226.44	16	393.2	0.875	0.967	25.00	Spee & Schneider (1991)
Hexadecane	226.44	16	393.2	0.927	0.930	25.60	Spee & Schneider (1991)
Hexadecane	226.44	16	393.2	0.917	0.920	25.60	Spee & Schneider (1991)
Hexadecane	226.44	16	314.2	0.871	0.975	13.61	D'Souza, *et al.*, (1988)
Hexadecane	226.44	16	314.2	0.838	0.981	12.53	D'Souza, *et al.*, (1988)
Hexadecane	226.44	16	314.2	0.801	0.988	10.45	D'Souza, *et al.*, (1988)
Hexadecane	226.44	16	314.2	0.786	0.993	9.80	D'Souza, *et al.*, (1988)
Hexadecane	226.44	16	314.2	0.767	0.996	8.44	D'Souza, *et al.*, (1988)
Hexadecane	226.44	16	314.2	0.712	0.997	8.07	D'Souza, *et al.*, (1988)
Hexadecane	226.44	16	333.2	0.823	0.989	14.87	D'Souza, *et al.*, (1988)
Hexadecane	226.44	16	333.2	0.785	0.991	13.02	D'Souza, *et al.*, (1988)
Hexadecane	226.44	16	333.2	0.707	0.995	11.07	D'Souza, *et al.*, (1988)
Hexadecane	226.44	16	333.2	0.647	0.997	9.74	D'Souza, *et al.*, (1988)
Hexadecane	226.44	16	333.2	0.607	0.998	8.76	D'Souza, *et al.*, (1988)
Hexadecane	226.44	16	333.2	0.537	0.998	7.69	D'Souza, *et al.*, (1988)
Hexadecane	226.44	16	353.2	0.809	0.989	16.12	D'Souza, *et al.*, (1988)
Hexadecane	226.44	16	353.2	0.758	0.991	14.52	D'Souza, *et al.*, (1988)
Hexadecane	226.44	16	353.2	0.739	0.995	13.36	D'Souza, *et al.*, (1988)
Hexadecane	226.44	16	353.2	0.677	0.996	12.20	D'Souza, *et al.*, (1988)
Hexadecane	226.44	16	353.2	0.646	0.998	11.21	D'Souza, *et al.*, (1988)
Hexadecane	226.44	16	353.0	0.678	0.999	10.00	Kordikowski & Schneider (1993)
Hexadecane	226.44	16	353.0	0.684	0.999	12.50	Kordikowski & Schneider (1993)
Hexadecane	226.44	16	353.0	0.765	0.996	15.00	Kordikowski & Schneider (1993)
Hexadecane	226.44	16	353.0	0.822	0.988	17.50	Kordikowski & Schneider (1993)
Hexadecane	226.44	16	353.0	0.834	0.981	18.50	Kordikowski & Schneider (1993)

Table A-1 continued

Hexadecane	226.44	16	353.0	0.868	0.967	19.60	Kordikowski & Schneider (1993)
Hexadecane	226.44	16	353.0	0.936	0.936	20.00	Kordikowski & Schneider (1993)
Heptadecane	240.47	17	323.2	0.612	1.000	10.00	Pohler (1994)
Heptadecane	240.47	17	323.2	0.700	0.998	15.00	Pohler (1994)
Heptadecane	240.47	17	323.2	0.785	1.000	17.50	Pohler (1994)
Heptadecane	240.47	17	323.2	0.854	0.999	20.00	Pohler (1994)
Heptadecane	240.47	17	323.2	0.877	0.980	21.50	Pohler (1994)
Heptadecane	240.47	17	323.2	0.931	0.931	22.20	Pohler (1994)
Heptadecane	240.47	17	333.2	0.639	0.999	10.00	Pohler (1994)
Heptadecane	240.47	17	333.2	0.752	0.996	15.00	Pohler (1994)
Heptadecane	240.47	17	333.2	0.809	0.990	17.50	Pohler (1994)
Heptadecane	240.47	17	333.2	0.853	0.982	19.00	Pohler (1994)
Heptadecane	240.47	17	333.2	0.876	0.975	20.00	Pohler (1994)
Heptadecane	240.47	17	333.2	0.930	0.930	21.30	Pohler (1994)
Heptadecane	240.47	17	373.2	0.560	0.999	10.00	Pohler (1994)
Heptadecane	240.47	17	373.2	0.650	0.998	15.00	Pohler (1994)
Heptadecane	240.47	17	373.2	0.714	0.996	17.50	Pohler (1994)
Heptadecane	240.47	17	373.2	0.789	0.991	20.00	Pohler (1994)
Heptadecane	240.47	17	373.2	0.826	0.988	22.50	Pohler (1994)
Heptadecane	240.47	17	373.2	0.861	0.981	24.00	Pohler (1994)
Heptadecane	240.47	17	373.2	0.929	0.929	25.30	Pohler (1994)
Heptadecane	240.47	17	393.2	0.545	0.999	10.00	Pohler (1994)
Heptadecane	240.47	17	393.2	0.623	0.998	15.00	Pohler (1994)
Heptadecane	240.47	17	393.2	0.699	0.997	17.50	Pohler (1994)
Heptadecane	240.47	17	393.2	0.725	0.996	20.00	Pohler (1994)
Heptadecane	240.47	17	393.2	0.792	0.992	22.50	Pohler (1994)
Heptadecane	240.47	17	393.2	0.845	0.986	25.00	Pohler (1994)
Heptadecane	240.47	17	393.2	0.866	0.981	26.00	Pohler (1994)
Heptadecane	240.47	17	393.2	0.923	0.923	27.30	Pohler (1994)
Octadecane	254.51	18	323.2	0.759	0.969	10.00	Pohler (1994)
Octadecane	254.51	18	323.2	0.791	0.982	15.00	Pohler (1994)
Octadecane	254.51	18	323.2	0.847	0.991	17.50	Pohler (1994)
Octadecane	254.51	18	323.2	0.876	0.996	20.00	Pohler (1994)
Octadecane	254.51	18	323.2	0.913	0.999	23.00	Pohler (1994)
Octadecane	254.51	18	323.2	0.977	0.999	25.00	Pohler (1994)
Octadecane	254.51	18	333.2	0.649	0.999	10.00	Pohler (1994)
Octadecane	254.51	18	333.2	0.720	0.996	15.00	Pohler (1994)
Octadecane	254.51	18	333.2	0.791	0.992	17.50	Pohler (1994)
Octadecane	254.51	18	333.2	0.852	0.986	20.00	Pohler (1994)
Octadecane	254.51	18	333.2	0.888	0.975	22.50	Pohler (1994)
Octadecane	254.51	18	333.2	0.941	0.941	24.00	Pohler (1994)
Octadecane	254.51	18	353.2	0.635	1.000	10.00	Pohler (1994)
Octadecane	254.51	18	353.2	0.680	0.998	15.00	Pohler (1994)
Octadecane	254.51	18	353.2	0.760	0.996	17.50	Pohler (1994)

Table A-1 continued

Octadecane	254.51	18	353.2	0.845	0.992	20.00	Pohler (1994)
Octadecane	254.51	18	353.2	0.870	0.985	22.50	Pohler (1994)
Octadecane	254.51	18	353.2	0.940	0.940	25.00	Pohler (1994)
Octadecane	254.51	18	373.2	0.574	1.000	10.00	Pohler (1994)
Octadecane	254.51	18	373.2	0.657	0.999	15.00	Pohler (1994)
Octadecane	254.51	18	373.2	0.714	0.997	17.50	Pohler (1994)
Octadecane	254.51	18	373.2	0.759	0.996	20.00	Pohler (1994)
Octadecane	254.51	18	373.2	0.824	0.992	22.50	Pohler (1994)
Octadecane	254.51	18	373.2	0.858	0.983	25.00	Pohler (1994)
Octadecane	254.51	18	373.2	0.936	0.936	26.60	Pohler (1994)
Octadecane	254.51	18	393.2	0.540	1.000	10.00	Pohler (1994)
Octadecane	254.51	18	393.2	0.609	1.000	15.00	Pohler (1994)
Octadecane	254.51	18	393.2	0.693	0.999	17.50	Pohler (1994)
Octadecane	254.51	18	393.2	0.762	0.996	20.00	Pohler (1994)
Octadecane	254.51	18	393.2	0.800	0.994	22.50	Pohler (1994)
Octadecane	254.51	18	393.2	0.824	0.990	25.00	Pohler (1994)
Octadecane	254.51	18	393.2	0.879	0.979	27.50	Pohler (1994)
Octadecane	254.51	18	393.2	0.929	0.929	28.70	Pohler (1994)
Nonadecane	268.52	19	318.2	0.639	1.000	10.00	Pohler (1994)
Nonadecane	268.52	19	318.2	0.691	0.989	20.00	Pohler (1994)
Nonadecane	268.52	19	318.2	0.821	0.984	30.00	Pohler (1994)
Nonadecane	268.52	19	318.2	0.874	0.961	35.50	Pohler (1994)
Nonadecane	268.52	19	318.2	0.922	0.922	45.50	Pohler (1994)
Nonadecane	268.52	19	323.2	0.683	0.993	10.00	Pohler (1994)
Nonadecane	268.52	19	323.2	0.730	0.990	20.00	Pohler (1994)
Nonadecane	268.52	19	323.2	0.802	0.986	25.00	Pohler (1994)
Nonadecane	268.52	19	323.2	0.918	0.918	33.50	Pohler (1994)
Nonadecane	268.52	19	333.2	0.626	1.000	10.00	Pohler (1994)
Nonadecane	268.52	19	333.2	0.677	0.996	15.00	Pohler (1994)
Nonadecane	268.52	19	333.2	0.768	0.988	20.00	Pohler (1994)
Nonadecane	268.52	19	333.2	0.931	0.931	28.60	Pohler (1994)
Nonadecane	268.52	19	343.2	0.573	1.000	10.00	Pohler (1994)
Nonadecane	268.52	19	343.2	0.616	0.998	12.50	Pohler (1994)
Nonadecane	268.52	19	343.2	0.646	0.997	15.00	Pohler (1994)
Nonadecane	268.52	19	343.2	0.675	0.996	17.50	Pohler (1994)
Nonadecane	268.52	19	343.2	0.716	0.990	20.00	Pohler (1994)
Nonadecane	268.52	19	343.2	0.771	0.987	22.50	Pohler (1994)
Nonadecane	268.52	19	343.2	0.800	0.971	25.00	Pohler (1994)
Nonadecane	268.52	19	343.2	0.842	0.971	26.00	Pohler (1994)
Nonadecane	268.52	19	343.2	0.934	0.934	27.70	Pohler (1994)
Nonadecane	268.52	19	348.2	0.571	1.000	10.00	Pohler (1994)
Nonadecane	268.52	19	348.2	0.694	0.999	15.00	Pohler (1994)
Nonadecane	268.52	19	348.2	0.733	0.994	20.00	Pohler (1994)
Nonadecane	268.52	19	348.2	0.798	0.988	22.50	Pohler (1994)

Table A-1 continued

Nonadecane	268.52	19	348.2	0.845	0.979	25.00	Pohler (1994)
Nonadecane	268.52	19	348.2	0.884	0.970	26.50	Pohler (1994)
Nonadecane	268.52	19	348.2	0.937	0.937	27.50	Pohler (1994)
Nonadecane	268.52	19	353.2	0.536	1.000	10.00	Kordikowski (1992)
Nonadecane	268.52	19	353.2	0.547	0.999	15.00	Kordikowski (1992)
Nonadecane	268.52	19	353.2	0.643	0.996	20.00	Kordikowski (1992)
Nonadecane	268.52	19	353.2	0.919	0.919	27.50	Kordikowski (1992)
Nonadecane	268.52	19	393.2	0.468	1.000	10.00	Kordikowski (1992)
Nonadecane	268.52	19	393.2	0.547	0.999	15.00	Kordikowski (1992)
Nonadecane	268.52	19	393.2	0.663	0.998	20.00	Kordikowski (1992)
Nonadecane	268.52	19	393.2	0.775	0.992	25.00	Kordikowski (1992)
Nonadecane	268.52	19	393.2	0.808	0.985	27.50	Kordikowski (1992)
Nonadecane	268.52	19	393.2	0.860	0.957	30.00	Kordikowski (1992)
Nonadecane	268.52	19	393.2	0.929	0.931	30.30	Kordikowski (1992)
Eicosane	282.55	20	323.3	0.114	0.000	0.99	Huang, *et al.*, (1988)
Eicosane	282.55	20	323.3	0.217	0.000	2.02	Huang, *et al.*, (1988)
Eicosane	282.55	20	323.3	0.305	0.000	3.06	Huang, *et al.*, (1988)
Eicosane	282.55	20	323.3	0.379	0.000	4.05	Huang, *et al.*, (1988)
Eicosane	282.55	20	323.3	0.446	0.000	5.01	Huang, *et al.*, (1988)
Eicosane	282.55	20	373.5	0.084	0.000	1.02	Huang, *et al.*, (1988)
Eicosane	282.55	20	373.5	0.157	0.000	2.01	Huang, *et al.*, (1988)
Eicosane	282.55	20	373.5	0.228	0.000	3.04	Huang, *et al.*, (1988)
Eicosane	282.55	20	373.5	0.286	0.000	4.02	Huang, *et al.*, (1988)
Eicosane	282.55	20	373.5	0.342	0.000	5.06	Huang, *et al.*, (1988)
Eicosane	282.55	20	353.2	0.517	1.000	10.00	Kordikowski & Schneider (1993)
Eicosane	282.55	20	353.2	0.599	0.999	15.00	Kordikowski & Schneider (1993)
Eicosane	282.55	20	353.2	0.709	0.995	20.00	Kordikowski & Schneider (1993)
Eicosane	282.55	20	353.2	0.785	0.980	25.00	Kordikowski & Schneider (1993)
Eicosane	282.55	20	353.2	0.838	0.974	27.50	Kordikowski & Schneider (1993)
Eicosane	282.55	20	353.2	0.887	0.923	30.00	Kordikowski & Schneider (1993)
Eicosane	282.55	20	353.2	0.916	0.916	30.20	Kordikowski & Schneider (1993)
Eicosane	282.55	20	393.2	0.464	1.000	10.00	Kordikowski & Schneider (1993)
Eicosane	282.55	20	393.2	0.525	1.000	15.00	Kordikowski & Schneider (1993)
Eicosane	282.55	20	393.2	0.616	0.997	20.00	Kordikowski & Schneider (1993)
Eicosane	282.55	20	393.2	0.706	0.994	25.00	Kordikowski & Schneider (1993)
Eicosane	282.55	20	393.2	0.806	0.991	27.50	Kordikowski & Schneider (1993)
Eicosane	282.55	20	393.2	0.821	0.982	30.00	Kordikowski & Schneider (1993)
Eicosane	282.55	20	393.2	0.865	0.975	31.00	Kordikowski & Schneider (1993)
Eicosane	282.55	20	393.2	0.935	0.934	32.00	Kordikowski & Schneider (1993)
Eicosane	282.55	20	353.0	0.517	1.000	10.00	Kordikowski (1992)
Eicosane	282.55	20	353.0	0.599	0.999	15.00	Kordikowski (1992)
Eicosane	282.55	20	353.0	0.709	0.995	20.00	Kordikowski (1992)
Eicosane	282.55	20	353.0	0.785	0.980	25.00	Kordikowski (1992)
Eicosane	282.55	20	353.0	0.838	0.974	27.50	Kordikowski (1992)

Table A-1 continued

Eicosane	282.55	20	353.0	0.887	0.923	30.00	Kordikowski (1992)
Eicosane	282.55	20	353.0	0.916	0.916	30.20	Kordikowski (1992)
Eicosane	282.55	20	393.0	0.464	1.000	10.00	Kordikowski (1992)
Eicosane	282.55	20	393.0	0.525	1.000	15.00	Kordikowski (1992)
Eicosane	282.55	20	393.0	0.616	0.997	20.00	Kordikowski (1992)
Eicosane	282.55	20	393.0	0.706	0.994	25.00	Kordikowski (1992)
Eicosane	282.55	20	393.0	0.806	0.991	27.50	Kordikowski (1992)
Eicosane	282.55	20	393.0	0.821	0.982	30.00	Kordikowski (1992)
Eicosane	282.55	20	393.0	0.865	0.975	31.00	Kordikowski (1992)
Eicosane	282.55	20	393.0	0.935	0.934	32.00	Kordikowski (1992)

Table A-2: Bubble and dew point pressures at specific compositions and temperatures for alcohols.

Name	MM	CL	T (K)	x (mol/mol)	y (mol/mol)	P (MPa)	Reference
Propanol	60.10	3	344.8	0.600	0.944	11.46	Elizalde-Solis, *et al.*, (2007)
Propanol	60.10	3	344.8	0.695	0.907	12.02	Elizalde-Solis, *et al.*, (2007)
Propanol	60.10	3	344.8	0.753	0.894	12.23	Elizalde-Solis, *et al.*, (2007)
Propanol	60.10	3	344.8	0.802	0.889	12.32	Elizalde-Solis, *et al.*, (2007)
Propanol	60.10	3	373.2	0.493	0.938	12.06	Elizalde-Solis, *et al.*, (2007)
Propanol	60.10	3	373.2	0.597	0.917	13.74	Elizalde-Solis, *et al.*, (2007)
Propanol	60.10	3	373.2	0.690	0.869	14.56	Elizalde-Solis, *et al.*, (2007)
Propanol	60.10	3	373.2	0.729	0.852	14.77	Elizalde-Solis, *et al.*, (2007)
Propanol	60.10	3	373.2	0.744	0.842	14.86	Elizalde-Solis, *et al.*, (2007)
Propanol	60.10	3	373.2	0.756	0.831	14.88	Elizalde-Solis, *et al.*, (2007)
Propanol	60.10	3	373.2	0.769	0.821	14.98	Elizalde-Solis, *et al.*, (2007)
Propanol	60.10	3	397.5	0.417	0.877	12.35	Elizalde-Solis, *et al.*, (2007)
Propanol	60.10	3	397.5	0.486	0.858	14.05	Elizalde-Solis, *et al.*, (2007)
Propanol	60.10	3	397.5	0.620	0.822	15.44	Elizalde-Solis, *et al.*, (2007)
Propanol	60.10	3	397.5	0.689	0.785	15.76	Elizalde-Solis, *et al.*, (2007)
Propanol	60.10	3	397.5	0.705	0.781	15.77	Elizalde-Solis, *et al.*, (2007)
Butanol	74.12	4	313.2	0.290	0.000	4.38	Byun, *et al.*, (2002)
Butanol	74.12	4	313.2	0.460	0.000	6.48	Byun, *et al.*, (2002)
Butanol	74.12	4	313.2	0.510	0.000	6.93	Byun, *et al.*, (2002)
Butanol	74.12	4	313.2	0.565	0.000	7.55	Byun, *et al.*, (2002)
Butanol	74.12	4	313.2	0.614	0.000	7.76	Byun, *et al.*, (2002)
Butanol	74.12	4	313.2	0.680	0.000	7.97	Byun, *et al.*, (2002)
Butanol	74.12	4	313.2	0.760	0.000	8.07	Byun, *et al.*, (2002)
Butanol	74.12	4	313.2	0.780	0.000	8.15	Byun, *et al.*, (2002)
Butanol	74.12	4	313.2	0.793	0.000	8.20	Byun, *et al.*, (2002)
Butanol	74.12	4	313.2	0.860	0.000	8.25	Byun, *et al.*, (2002)
Butanol	74.12	4	313.2	0.905	0.000	8.28	Byun, *et al.*, (2002)
Butanol	74.12	4	313.2	0.906	0.000	8.27	Byun, *et al.*, (2002)
Butanol	74.12	4	313.2	0.914	0.000	8.29	Byun, *et al.*, (2002)
Butanol	74.12	4	313.2	0.915	0.000	8.30	Byun, *et al.*, (2002)
Butanol	74.12	4	313.2	0.937	0.000	8.29	Byun, *et al.*, (2002)
Butanol	74.12	4	313.2	0.953	0.000	8.29	Byun, *et al.*, (2002)
Butanol	74.12	4	313.2	0.980	0.000	8.31	Byun, *et al.*, (2002)
Butanol	74.12	4	313.2	0.987	0.000	8.38	Byun, *et al.*, (2002)
Butanol	74.12	4	313.2	0.290	0.000	8.31	Byun, *et al.*, (2002)
Butanol	74.12	4	333.2	0.460	0.000	8.24	Byun, *et al.*, (2002)
Butanol	74.12	4	333.2	0.510	0.000	8.97	Byun, *et al.*, (2002)
Butanol	74.12	4	333.2	0.565	0.000	9.52	Byun, *et al.*, (2002)
Butanol	74.12	4	333.2	0.614	0.000	10.17	Byun, *et al.*, (2002)
Butanol	74.12	4	333.2	0.680	0.000	10.79	Byun, *et al.*, (2002)
Butanol	74.12	4	333.2	0.760	0.000	11.23	Byun, *et al.*, (2002)
Butanol	74.12	4	333.2	0.780	0.000	11.35	Byun, *et al.*, (2002)
Butanol	74.12	4	333.2	0.793	0.000	11.43	Byun, *et al.*, (2002)

Table A-2 continued

Butanol	74.12	4	333.2	0.860	0.000	11.50	Byun, *et al.*, (2002)
Butanol	74.12	4	333.2	0.905	0.000	11.55	Byun, *et al.*, (2002)
Butanol	74.12	4	333.2	0.906	0.000	11.57	Byun, *et al.*, (2002)
Butanol	74.12	4	333.2	0.914	0.000	11.58	Byun, *et al.*, (2002)
Butanol	74.12	4	333.2	0.915	0.000	11.51	Byun, *et al.*, (2002)
Butanol	74.12	4	333.2	0.937	0.000	11.48	Byun, *et al.*, (2002)
Butanol	74.12	4	353.2	0.290	0.000	6.38	Byun, *et al.*, (2002)
Butanol	74.12	4	353.2	0.460	0.000	9.69	Byun, *et al.*, (2002)
Butanol	74.12	4	353.2	0.510	0.000	10.60	Byun, *et al.*, (2002)
Butanol	74.12	4	353.2	0.565	0.000	11.62	Byun, *et al.*, (2002)
Butanol	74.12	4	353.2	0.614	0.000	12.41	Byun, *et al.*, (2002)
Butanol	74.12	4	353.2	0.680	0.000	13.14	Byun, *et al.*, (2002)
Butanol	74.12	4	353.2	0.760	0.000	13.86	Byun, *et al.*, (2002)
Butanol	74.12	4	353.2	0.780	0.000	14.03	Byun, *et al.*, (2002)
Butanol	74.12	4	353.2	0.793	0.000	14.14	Byun, *et al.*, (2002)
Butanol	74.12	4	353.2	0.860	0.000	14.15	Byun, *et al.*, (2002)
Butanol	74.12	4	353.2	0.905	0.000	14.16	Byun, *et al.*, (2002)
Butanol	74.12	4	353.2	0.906	0.000	14.17	Byun, *et al.*, (2002)
Butanol	74.12	4	353.2	0.000	0.914	14.03	Byun, *et al.*, (2002)
Butanol	74.12	4	353.2	0.000	0.915	13.97	Byun, *et al.*, (2002)
Butanol	74.12	4	353.2	0.000	0.937	13.76	Byun, *et al.*, (2002)
Butanol	74.12	4	353.2	0.000	0.953	13.41	Byun, *et al.*, (2002)
Butanol	74.12	4	353.2	0.000	0.980	11.69	Byun, *et al.*, (2002)
Butanol	74.12	4	373.2	0.290	0.000	6.93	Byun, *et al.*, (2002)
Butanol	74.12	4	373.2	0.460	0.000	10.79	Byun, *et al.*, (2002)
Butanol	74.12	4	373.2	0.510	0.000	11.83	Byun, *et al.*, (2002)
Butanol	74.12	4	373.2	0.565	0.000	13.21	Byun, *et al.*, (2002)
Butanol	74.12	4	373.2	0.614	0.000	14.07	Byun, *et al.*, (2002)
Butanol	74.12	4	373.2	0.680	0.000	15.14	Byun, *et al.*, (2002)
Butanol	74.12	4	373.2	0.760	0.000	15.76	Byun, *et al.*, (2002)
Butanol	74.12	4	373.2	0.780	0.000	16.03	Byun, *et al.*, (2002)
Butanol	74.12	4	373.2	0.793	0.000	16.13	Byun, *et al.*, (2002)
Butanol	74.12	4	373.2	0.860	0.000	16.19	Byun, *et al.*, (2002)
Butanol	74.12	4	373.2	0.000	0.905	15.96	Byun, *et al.*, (2002)
Butanol	74.12	4	373.2	0.000	0.906	15.93	Byun, *et al.*, (2002)
Butanol	74.12	4	373.2	0.000	0.914	15.71	Byun, *et al.*, (2002)
Butanol	74.12	4	373.2	0.000	0.915	15.68	Byun, *et al.*, (2002)
Butanol	74.12	4	373.2	0.000	0.937	15.07	Byun, *et al.*, (2002)
Butanol	74.12	4	373.2	0.000	0.953	14.31	Byun, *et al.*, (2002)
Butanol	74.12	4	373.2	0.000	0.980	10.90	Byun, *et al.*, (2002)
Butanol	74.12	4	393.2	0.290	0.000	7.62	Byun, *et al.*, (2002)
Butanol	74.12	4	393.2	0.460	0.000	11.52	Byun, *et al.*, (2002)
Butanol	74.12	4	393.2	0.510	0.000	12.93	Byun, *et al.*, (2002)
Butanol	74.12	4	393.2	0.565	0.000	14.52	Byun, *et al.*, (2002)

Table A-2 continued

Butanol	74.12	4	393.2	0.614	0.000	15.35	Byun, *et al.*, (2002)
Butanol	74.12	4	393.2	0.680	0.000	16.83	Byun, *et al.*, (2002)
Butanol	74.12	4	393.2	0.760	0.000	17.27	Byun, *et al.*, (2002)
Butanol	74.12	4	393.2	0.780	0.000	17.33	Byun, *et al.*, (2002)
Butanol	74.12	4	393.2	0.793	0.000	17.30	Byun, *et al.*, (2002)
Butanol	74.12	4	393.2	0.000	0.860	17.07	Byun, *et al.*, (2002)
Butanol	74.12	4	393.2	0.000	0.905	16.30	Byun, *et al.*, (2002)
Butanol	74.12	4	393.2	0.000	0.906	16.28	Byun, *et al.*, (2002)
Butanol	74.12	4	393.2	0.000	0.914	15.90	Byun, *et al.*, (2002)
Butanol	74.12	4	393.2	0.000	0.915	15.90	Byun, *et al.*, (2002)
Butanol	74.12	4	393.2	0.000	0.937	15.10	Byun, *et al.*, (2002)
Butanol	74.12	4	354.1	0.096	0.989	2.07	Elizalde-Solis, *et al.*, (2007)
Butanol	74.12	4	354.1	0.169	0.989	3.57	Elizalde-Solis, *et al.*, (2007)
Butanol	74.12	4	354.1	0.239	0.989	5.08	Elizalde-Solis, *et al.*, (2007)
Butanol	74.12	4	354.1	0.301	0.988	6.45	Elizalde-Solis, *et al.*, (2007)
Butanol	74.12	4	354.1	0.384	0.986	8.18	Elizalde-Solis, *et al.*, (2007)
Butanol	74.12	4	354.1	0.457	0.983	9.58	Elizalde-Solis, *et al.*, (2007)
Butanol	74.12	4	354.1	0.506	0.981	10.49	Elizalde-Solis, *et al.*, (2007)
Butanol	74.12	4	354.1	0.602	0.975	11.98	Elizalde-Solis, *et al.*, (2007)
Butanol	74.12	4	354.1	0.683	0.951	12.98	Elizalde-Solis, *et al.*, (2007)
Butanol	74.12	4	399.0	0.080	0.942	2.13	Elizalde-Solis, *et al.*, (2007)
Butanol	74.12	4	399.0	0.134	0.949	3.54	Elizalde-Solis, *et al.*, (2007)
Butanol	74.12	4	399.0	0.188	0.955	5.01	Elizalde-Solis, *et al.*, (2007)
Butanol	74.12	4	399.0	0.241	0.956	6.57	Elizalde-Solis, *et al.*, (2007)
Butanol	74.12	4	399.0	0.307	0.955	8.23	Elizalde-Solis, *et al.*, (2007)
Butanol	74.12	4	399.0	0.358	0.953	9.66	Elizalde-Solis, *et al.*, (2007)
Butanol	74.12	4	399.0	0.416	0.950	11.02	Elizalde-Solis, *et al.*, (2007)
Butanol	74.12	4	399.0	0.479	0.944	12.53	Elizalde-Solis, *et al.*, (2007)
Butanol	74.12	4	399.0	0.545	0.934	14.01	Elizalde-Solis, *et al.*, (2007)
Butanol	74.12	4	399.0	0.622	0.909	15.53	Elizalde-Solis, *et al.*, (2007)
Hexanol	102.18	6	303.2	0.051	0.000	0.77	Beier, *et al.*, (2003)
Hexanol	102.18	6	303.2	0.101	0.000	1.35	Beier, *et al.*, (2003)
Hexanol	102.18	6	303.2	0.142	0.000	2.11	Beier, *et al.*, (2003)
Hexanol	102.18	6	303.2	0.195	0.000	2.58	Beier, *et al.*, (2003)
Hexanol	102.18	6	303.2	0.241	0.000	3.03	Beier, *et al.*, (2003)
Hexanol	102.18	6	303.2	0.339	0.000	4.22	Beier, *et al.*, (2003)
Hexanol	102.18	6	303.2	0.396	0.000	5.02	Beier, *et al.*, (2003)
Hexanol	102.18	6	303.2	0.517	0.000	6.03	Beier, *et al.*, (2003)
Hexanol	102.18	6	303.2	0.579	0.000	6.52	Beier, *et al.*, (2003)
Hexanol	102.18	6	303.2	0.594	0.000	6.55	Beier, *et al.*, (2003)
Hexanol	102.18	6	303.2	0.720	0.000	7.13	Beier, *et al.*, (2003)
Hexanol	102.18	6	303.2	0.719	0.000	7.14	Beier, *et al.*, (2003)
Hexanol	102.18	6	303.2	0.723	0.000	7.14	Beier, *et al.*, (2003)
Hexanol	102.18	6	303.2	0.745	0.000	7.59	Beier, *et al.*, (2003)

Table A-2 continued

Hexanol	102.18	6	303.2	0.753	0.000	7.74	Beier, *et al.*, (2003)
Hexanol	102.18	6	303.2	0.970	0.000	7.13	Beier, *et al.*, (2003)
Hexanol	102.18	6	303.2	0.915	0.000	7.52	Beier, *et al.*, (2003)
Hexanol	102.18	6	303.2	0.885	0.000	7.70	Beier, *et al.*, (2003)
Hexanol	102.18	6	303.2	0.000	0.984	0.58	Beier, *et al.*, (2003)
Hexanol	102.18	6	303.2	0.000	0.994	0.99	Beier, *et al.*, (2003)
Hexanol	102.18	6	303.2	0.000	0.995	1.54	Beier, *et al.*, (2003)
Hexanol	102.18	6	303.2	0.000	0.820	7.96	Beier, *et al.*, (2003)
Hexanol	102.18	6	313.2	0.028	0.000	0.53	Beier, *et al.*, (2003)
Hexanol	102.18	6	313.2	0.065	0.000	1.00	Beier, *et al.*, (2003)
Hexanol	102.18	6	313.2	0.142	0.000	2.22	Beier, *et al.*, (2003)
Hexanol	102.18	6	313.2	0.188	0.000	3.01	Beier, *et al.*, (2003)
Hexanol	102.18	6	313.2	0.276	0.000	4.25	Beier, *et al.*, (2003)
Hexanol	102.18	6	313.2	0.335	0.000	4.98	Beier, *et al.*, (2003)
Hexanol	102.18	6	313.2	0.419	0.000	5.98	Beier, *et al.*, (2003)
Hexanol	102.18	6	313.2	0.446	0.000	6.42	Beier, *et al.*, (2003)
Hexanol	102.18	6	313.2	0.474	0.000	6.90	Beier, *et al.*, (2003)
Hexanol	102.18	6	313.2	0.546	0.000	7.60	Beier, *et al.*, (2003)
Hexanol	102.18	6	313.2	0.607	0.000	8.16	Beier, *et al.*, (2003)
Hexanol	102.18	6	313.2	0.661	0.000	8.59	Beier, *et al.*, (2003)
Hexanol	102.18	6	313.2	0.719	0.000	9.27	Beier, *et al.*, (2003)
Hexanol	102.18	6	313.2	0.765	0.000	9.72	Beier, *et al.*, (2003)
Hexanol	102.18	6	313.2	0.000	0.986	0.54	Beier, *et al.*, (2003)
Hexanol	102.18	6	313.2	0.000	0.995	1.01	Beier, *et al.*, (2003)
Hexanol	102.18	6	313.2	0.000	0.989	8.14	Beier, *et al.*, (2003)
Hexanol	102.18	6	313.2	0.000	0.985	8.59	Beier, *et al.*, (2003)
Hexanol	102.18	6	313.2	0.000	0.946	9.25	Beier, *et al.*, (2003)
Hexanol	102.18	6	313.2	0.000	0.872	9.82	Beier, *et al.*, (2003)
Hexanol	102.18	6	324.6	0.548	0.997	8.02	Elizalde-Solis, *et al.*, (2003)
Hexanol	102.18	6	324.6	0.634	0.992	9.19	Elizalde-Solis, *et al.*, (2003)
Hexanol	102.18	6	324.6	0.715	0.000	10.04	Elizalde-Solis, *et al.*, (2003)
Hexanol	102.18	6	353.9	0.604	0.000	11.51	Elizalde-Solis, *et al.*, (2003)
Hexanol	102.18	6	353.9	0.705	0.920	13.82	Elizalde-Solis, *et al.*, (2003)
Hexanol	102.18	6	353.9	0.761	0.935	14.71	Elizalde-Solis, *et al.*, (2003)
Hexanol	102.18	6	353.9	0.807	0.952	15.57	Elizalde-Solis, *et al.*, (2003)
Hexanol	102.18	6	353.9	0.860	0.934	16.01	Elizalde-Solis, *et al.*, (2003)
Hexanol	102.18	6	353.9	0.901	0.929	16.05	Elizalde-Solis, *et al.*, (2003)
Hexanol	102.18	6	353.9	0.919	0.000	16.08	Elizalde-Solis, *et al.*, (2003)
Hexanol	102.18	6	397.8	0.305	0.987	7.06	Elizalde-Solis, *et al.*, (2003)
Hexanol	102.18	6	397.8	0.365	0.986	8.62	Elizalde-Solis, *et al.*, (2003)
Hexanol	102.18	6	397.8	0.409	0.984	10.09	Elizalde-Solis, *et al.*, (2003)
Hexanol	102.18	6	397.8	0.452	0.985	11.15	Elizalde-Solis, *et al.*, (2003)
Hexanol	102.18	6	397.8	0.500	0.981	12.45	Elizalde-Solis, *et al.*, (2003)
Hexanol	102.18	6	397.8	0.501	0.979	12.47	Elizalde-Solis, *et al.*, (2003)

Table A-2 continued

Hexanol	102.18	6	397.8	0.575	0.978	14.34	Elizalde-Solis, *et al.*, (2003)
Hexanol	102.18	6	397.8	0.660	0.970	16.36	Elizalde-Solis, *et al.*, (2003)
Hexanol	102.18	6	397.8	0.742	0.957	18.18	Elizalde-Solis, *et al.*, (2003)
Hexanol	102.18	6	397.8	0.797	0.925	19.18	Elizalde-Solis, *et al.*, (2003)
Hexanol	102.18	6	397.8	0.841	0.906	19.57	Elizalde-Solis, *et al.*, (2003)
Hexanol	102.18	6	397.8	0.856	0.887	19.62	Elizalde-Solis, *et al.*, (2003)
Hexanol	102.18	6	397.8	0.872	0.000	19.63	Elizalde-Solis, *et al.*, (2003)
Heptanol	116.20	7	316.0	0.364	0.999	7.09	Scheidgen (1997)
Heptanol	116.20	7	316.0	0.433	1.000	7.98	Scheidgen (1997)
Heptanol	116.20	7	316.0	0.510	0.999	8.46	Scheidgen (1997)
Heptanol	116.20	7	316.0	0.550	0.999	8.93	Scheidgen (1997)
Heptanol	116.20	7	316.0	0.625	0.996	9.50	Scheidgen (1997)
Heptanol	116.20	7	316.0	0.675	0.995	10.02	Scheidgen (1997)
Heptanol	116.20	7	316.0	0.752	0.981	10.99	Scheidgen (1997)
Heptanol	116.20	7	316.0	0.802	0.950	12.02	Scheidgen (1997)
Heptanol	116.20	7	316.0	0.000	0.909	12.51	Scheidgen (1997)
Heptanol	116.20	7	393.0	0.421	0.998	10.10	Scheidgen (1997)
Heptanol	116.20	7	393.0	0.483	0.996	12.59	Scheidgen (1997)
Heptanol	116.20	7	393.0	0.557	0.995	15.12	Scheidgen (1997)
Heptanol	116.20	7	393.0	0.677	0.993	17.52	Scheidgen (1997)
Heptanol	116.20	7	393.0	0.766	0.985	19.72	Scheidgen (1997)
Heptanol	116.20	7	393.0	0.000	0.937	20.17	Scheidgen (1997)
Heptanol	116.20	7	374.6	0.217	0.998	4.04	Elizalde-Solis, *et al.*, (2003)
Heptanol	116.20	7	374.6	0.283	0.998	5.55	Elizalde-Solis, *et al.*, (2003)
Heptanol	116.20	7	374.6	0.348	0.996	6.94	Elizalde-Solis, *et al.*, (2003)
Heptanol	116.20	7	374.6	0.410	0.997	8.54	Elizalde-Solis, *et al.*, (2003)
Heptanol	116.20	7	374.6	0.462	0.996	10.03	Elizalde-Solis, *et al.*, (2003)
Heptanol	116.20	7	374.6	0.513	0.995	11.48	Elizalde-Solis, *et al.*, (2003)
Heptanol	116.20	7	374.6	0.574	0.993	13.15	Elizalde-Solis, *et al.*, (2003)
Heptanol	116.20	7	374.6	0.625	0.990	14.57	Elizalde-Solis, *et al.*, (2003)
Heptanol	116.20	7	303.2	0.046	0.994	0.58	Secuianu, *et al.*, (2008)
Heptanol	116.20	7	303.2	0.117	0.995	1.42	Secuianu, *et al.*, (2008)
Heptanol	116.20	7	303.2	0.206	0.997	2.60	Secuianu, *et al.*, (2008)
Heptanol	116.20	7	303.2	0.309	0.998	3.88	Secuianu, *et al.*, (2008)
Heptanol	116.20	7	303.2	0.390	0.999	4.38	Secuianu, *et al.*, (2008)
Heptanol	116.20	7	303.2	0.466	0.998	5.48	Secuianu, *et al.*, (2008)
Heptanol	116.20	7	303.2	0.521	0.997	6.01	Secuianu, *et al.*, (2008)
Heptanol	116.20	7	303.2	0.595	0.995	6.51	Secuianu, *et al.*, (2008)
Heptanol	116.20	7	313.2	0.136	0.994	1.68	Secuianu, *et al.*, (2008)
Heptanol	116.20	7	313.2	0.223	0.997	2.75	Secuianu, *et al.*, (2008)
Heptanol	116.20	7	313.2	0.310	0.997	3.99	Secuianu, *et al.*, (2008)
Heptanol	116.20	7	313.2	0.385	0.997	4.79	Secuianu, *et al.*, (2008)
Heptanol	116.20	7	313.2	0.450	0.995	5.83	Secuianu, *et al.*, (2008)
Heptanol	116.20	7	313.2	0.480	0.995	6.37	Secuianu, *et al.*, (2008)

Table A-2 continued

Heptanol	116.20	7	313.2	0.525	0.994	6.93	Secuianu, *et al.*, (2008)
Heptanol	116.20	7	313.2	0.602	0.992	7.82	Secuianu, *et al.*, (2008)
Heptanol	116.20	7	313.2	0.657	0.990	8.63	Secuianu, *et al.*, (2008)
Heptanol	116.20	7	313.2	0.666	0.990	8.75	Secuianu, *et al.*, (2008)
Heptanol	116.20	7	313.2	0.706	0.976	10.05	Secuianu, *et al.*, (2008)
Heptanol	116.20	7	313.2	0.738	0.951	10.99	Secuianu, *et al.*, (2008)
Heptanol	116.20	7	313.2	0.744	0.932	11.19	Secuianu, *et al.*, (2008)
Heptanol	116.20	7	313.2	0.766	0.903	11.55	Secuianu, *et al.*, (2008)
Heptanol	116.20	7	333.2	0.072	0.997	1.14	Secuianu, *et al.*, (2008)
Heptanol	116.20	7	333.2	0.139	0.997	2.00	Secuianu, *et al.*, (2008)
Heptanol	116.20	7	333.2	0.199	0.998	3.02	Secuianu, *et al.*, (2008)
Heptanol	116.20	7	333.2	0.261	0.998	4.26	Secuianu, *et al.*, (2008)
Heptanol	116.20	7	333.2	0.318	0.998	5.18	Secuianu, *et al.*, (2008)
Heptanol	116.20	7	333.2	0.336	0.998	5.72	Secuianu, *et al.*, (2008)
Heptanol	116.20	7	333.2	0.415	0.998	6.86	Secuianu, *et al.*, (2008)
Heptanol	116.20	7	333.2	0.474	0.997	8.15	Secuianu, *et al.*, (2008)
Heptanol	116.20	7	333.2	0.492	0.997	8.56	Secuianu, *et al.*, (2008)
Heptanol	116.20	7	333.2	0.528	0.996	9.34	Secuianu, *et al.*, (2008)
Heptanol	116.20	7	333.2	0.740	0.968	12.92	Secuianu, *et al.*, (2008)
Heptanol	116.20	7	333.2	0.780	0.952	14.02	Secuianu, *et al.*, (2008)
Heptanol	116.20	7	353.2	0.087	0.994	1.54	Secuianu, *et al.*, (2008)
Heptanol	116.20	7	353.2	0.161	0.996	2.57	Secuianu, *et al.*, (2008)
Heptanol	116.20	7	353.2	0.225	0.997	3.57	Secuianu, *et al.*, (2008)
Heptanol	116.20	7	353.2	0.252	0.997	4.55	Secuianu, *et al.*, (2008)
Heptanol	116.20	7	353.2	0.304	0.997	5.73	Secuianu, *et al.*, (2008)
Heptanol	116.20	7	353.2	0.362	0.997	7.23	Secuianu, *et al.*, (2008)
Heptanol	116.20	7	353.2	0.406	0.997	7.80	Secuianu, *et al.*, (2008)
Heptanol	116.20	7	353.2	0.425	0.997	8.71	Secuianu, *et al.*, (2008)
Heptanol	116.20	7	353.2	0.449	0.997	9.08	Secuianu, *et al.*, (2008)
Heptanol	116.20	7	353.2	0.489	0.997	10.16	Secuianu, *et al.*, (2008)
Octanol	130.23	8	328.3	0.182	1.000	3.00	Hwu, *et al.*, (2004)
Octanol	130.23	8	328.3	0.293	1.000	5.00	Hwu, *et al.*, (2004)
Octanol	130.23	8	328.3	0.414	1.000	7.00	Hwu, *et al.*, (2004)
Octanol	130.23	8	328.3	0.593	0.998	10.10	Hwu, *et al.*, (2004)
Octanol	130.23	8	328.3	0.661	0.991	11.90	Hwu, *et al.*, (2004)
Octanol	130.23	8	328.3	0.724	0.976	13.30	Hwu, *et al.*, (2004)
Octanol	130.23	8	348.2	0.048	0.999	1.00	Lee & Chen (1994)
Octanol	130.23	8	348.2	0.101	0.999	2.00	Lee & Chen (1994)
Octanol	130.23	8	348.2	0.152	0.999	3.00	Lee & Chen (1994)
Octanol	130.23	8	348.2	0.203	0.999	4.00	Lee & Chen (1994)
Octanol	130.23	8	348.2	0.255	0.999	5.00	Lee & Chen (1994)
Octanol	130.23	8	313.2	0.270	0.000	4.00	Lee & Chen (1994)
Octanol	130.23	8	313.2	0.364	0.000	5.30	Lee & Chen (1994)
Octanol	130.23	8	313.2	0.492	1.000	7.00	Lee & Chen (1994)

Table A-2 continued

Octanol	130.23	8	313.2	0.617	0.997	8.50	Lee & Chen (1994)
Octanol	130.23	8	313.2	0.669	0.975	10.00	Lee & Chen (1994)
Octanol	130.23	8	313.2	0.702	0.963	11.50	Lee & Chen (1994)
Octanol	130.23	8	313.2	0.750	0.941	13.50	Lee & Chen (1994)
Octanol	130.23	8	313.2	0.814	0.920	15.50	Lee & Chen (1994)
Octanol	130.23	8	328.2	0.241	1.000	4.00	Lee & Chen (1994)
Octanol	130.23	8	328.2	0.353	0.997	6.00	Lee & Chen (1994)
Octanol	130.23	8	328.2	0.479	0.993	8.00	Lee & Chen (1994)
Octanol	130.23	8	328.2	0.586	0.998	10.00	Lee & Chen (1994)
Octanol	130.23	8	328.2	0.667	0.988	12.00	Lee & Chen (1994)
Octanol	130.23	8	328.2	0.777	0.943	15.00	Lee & Chen (1994)
Octanol	130.23	8	328.2	0.863	0.919	17.00	Lee & Chen (1994)
Octanol	130.23	8	348.2	0.205	0.999	4.00	Lee & Chen (1994)
Octanol	130.23	8	348.2	0.302	0.993	6.00	Lee & Chen (1994)
Octanol	130.23	8	348.2	0.415	0.999	8.50	Lee & Chen (1994)
Octanol	130.23	8	348.2	0.529	0.997	11.00	Lee & Chen (1994)
Octanol	130.23	8	348.2	0.626	0.991	13.50	Lee & Chen (1994)
Octanol	130.23	8	348.2	0.725	0.968	16.00	Lee & Chen (1994)
Octanol	130.23	8	348.2	0.869	0.933	19.00	Lee & Chen (1994)
Octanol	130.23	8	313.2	0.216	0.000	3.25	Chiu, *et al.*, (2008)
Octanol	130.23	8	313.2	0.325	0.000	4.73	Chiu, *et al.*, (2008)
Octanol	130.23	8	313.2	0.468	0.000	6.82	Chiu, *et al.*, (2008)
Octanol	130.23	8	313.2	0.539	0.000	7.74	Chiu, *et al.*, (2008)
Octanol	130.23	8	313.2	0.637	0.000	8.58	Chiu, *et al.*, (2008)
Octanol	130.23	8	313.2	0.651	0.000	9.33	Chiu, *et al.*, (2008)
Octanol	130.23	8	313.2	0.744	0.000	12.86	Chiu, *et al.*, (2008)
Octanol	130.23	8	313.2	0.816	0.000	15.54	Chiu, *et al.*, (2008)
Octanol	130.23	8	313.2	0.841	0.000	15.74	Chiu, *et al.*, (2008)
Octanol	130.23	8	313.2	0.856	0.000	15.95	Chiu, *et al.*, (2008)
Octanol	130.23	8	313.2	0.870	0.000	16.12	Chiu, *et al.*, (2008)
Octanol	130.23	8	313.2	0.000	0.887	16.03	Chiu, *et al.*, (2008)
Octanol	130.23	8	313.2	0.000	0.907	15.83	Chiu, *et al.*, (2008)
Octanol	130.23	8	313.2	0.000	0.921	15.22	Chiu, *et al.*, (2008)
Octanol	130.23	8	313.2	0.000	0.943	14.45	Chiu, *et al.*, (2008)
Octanol	130.23	8	313.2	0.000	0.958	12.88	Chiu, *et al.*, (2008)
Octanol	130.23	8	313.2	0.000	0.984	9.56	Chiu, *et al.*, (2008)
Octanol	130.23	8	328.2	0.229	0.000	3.92	Chiu, *et al.*, (2008)
Octanol	130.23	8	328.2	0.354	0.000	5.62	Chiu, *et al.*, (2008)
Octanol	130.23	8	328.2	0.468	0.000	7.62	Chiu, *et al.*, (2008)
Octanol	130.23	8	328.2	0.539	0.000	9.22	Chiu, *et al.*, (2008)
Octanol	130.23	8	328.2	0.637	0.000	11.27	Chiu, *et al.*, (2008)
Octanol	130.23	8	328.2	0.744	0.000	14.42	Chiu, *et al.*, (2008)
Octanol	130.23	8	328.2	0.816	0.000	15.62	Chiu, *et al.*, (2008)
Octanol	130.23	8	328.2	0.841	0.000	15.99	Chiu, *et al.*, (2008)

Table A-2 continued

Octanol	130.23	8	328.2	0.856	0.000	16.07	Chiu, *et al.*, (2008)
Octanol	130.23	8	328.2	0.870	0.000	16.25	Chiu, *et al.*, (2008)
Octanol	130.23	8	328.2	0.000	0.887	16.23	Chiu, *et al.*, (2008)
Octanol	130.23	8	328.2	0.000	0.907	16.14	Chiu, *et al.*, (2008)
Octanol	130.23	8	328.2	0.000	0.921	15.83	Chiu, *et al.*, (2008)
Octanol	130.23	8	328.2	0.000	0.943	15.28	Chiu, *et al.*, (2008)
Octanol	130.23	8	328.2	0.000	0.958	14.45	Chiu, *et al.*, (2008)
Octanol	130.23	8	328.2	0.000	0.984	12.21	Chiu, *et al.*, (2008)
Octanol	130.23	8	348.2	0.229	0.000	4.86	Chiu, *et al.*, (2008)
Octanol	130.23	8	348.2	0.354	0.000	7.03	Chiu, *et al.*, (2008)
Octanol	130.23	8	348.2	0.468	0.000	9.45	Chiu, *et al.*, (2008)
Octanol	130.23	8	348.2	0.539	0.000	11.15	Chiu, *et al.*, (2008)
Octanol	130.23	8	348.2	0.637	0.000	13.52	Chiu, *et al.*, (2008)
Octanol	130.23	8	348.2	0.744	0.000	16.58	Chiu, *et al.*, (2008)
Octanol	130.23	8	348.2	0.816	0.000	17.57	Chiu, *et al.*, (2008)
Octanol	130.23	8	348.2	0.841	0.000	17.95	Chiu, *et al.*, (2008)
Octanol	130.23	8	348.2	0.856	0.000	18.05	Chiu, *et al.*, (2008)
Octanol	130.23	8	348.2	0.870	0.000	18.21	Chiu, *et al.*, (2008)
Octanol	130.23	8	348.2	0.887	0.000	18.29	Chiu, *et al.*, (2008)
Octanol	130.23	8	348.2	0.000	0.907	18.23	Chiu, *et al.*, (2008)
Octanol	130.23	8	348.2	0.000	0.921	17.95	Chiu, *et al.*, (2008)
Octanol	130.23	8	348.2	0.000	0.943	17.55	Chiu, *et al.*, (2008)
Octanol	130.23	8	348.2	0.000	0.958	16.78	Chiu, *et al.*, (2008)
Octanol	130.23	8	348.2	0.000	0.984	14.79	Chiu, *et al.*, (2008)
Octanol	130.23	8	328.2	0.169	0.999	3.00	Feng, *et al.*, (2001)
Octanol	130.23	8	328.2	0.308	0.999	5.45	Feng, *et al.*, (2001)
Octanol	130.23	8	328.2	0.427	0.999	7.38	Feng, *et al.*, (2001)
Octanol	130.23	8	328.2	0.573	0.998	9.89	Feng, *et al.*, (2001)
Octanol	130.23	8	328.2	0.665	0.985	12.14	Feng, *et al.*, (2001)
Octanol	130.23	8	328.2	0.710	0.973	13.38	Feng, *et al.*, (2001)
Octanol	130.23	8	308.2		1.000	1.51	Chieming, *et al.*, (1998)
Octanol	130.23	8	308.2	0.159	1.000	2.18	Chieming, *et al.*, (1998)
Octanol	130.23	8	308.2	0.209	1.000	2.85	Chieming, *et al.*, (1998)
Octanol	130.23	8	308.2	0.261	1.000	3.61	Chieming, *et al.*, (1998)
Octanol	130.23	8	308.2	0.314	1.000	4.25	Chieming, *et al.*, (1998)
Octanol	130.23	8	308.2	0.367	1.000	4.97	Chieming, *et al.*, (1998)
Octanol	130.23	8	308.2	0.421	0.990	5.65	Chieming, *et al.*, (1998)
Octanol	130.23	8	308.2	0.480	0.990	6.34	Chieming, *et al.*, (1998)
Octanol	130.23	8	308.2	0.511	0.998	6.69	Chieming, *et al.*, (1998)
Octanol	130.23	8	308.2	0.543	0.996	7.04	Chieming, *et al.*, (1998)
Octanol	130.23	8	308.2	0.573	0.995	7.39	Chieming, *et al.*, (1998)
Octanol	130.23	8	308.2	0.601	0.993	7.74	Chieming, *et al.*, (1998)
Octanol	130.23	8	318.2	0.134	1.000	2.17	Chieming, *et al.*, (1998)
Octanol	130.23	8	318.2	0.227	1.000	3.57	Chieming, *et al.*, (1998)

Table A-2 continued

Octanol	130.23	8	318.2	0.324	1.000	4.98	Chieming, *et al.*, (1998)
Octanol	130.23	8	318.2	0.424	1.000	6.31	Chieming, *et al.*, (1998)
Octanol	130.23	8	318.2	0.482	0.999	7.04	Chieming, *et al.*, (1998)
Octanol	130.23	8	318.2	0.533	0.998	7.74	Chieming, *et al.*, (1998)
Octanol	130.23	8	318.2	0.575	0.997	8.44	Chieming, *et al.*, (1998)
Octanol	130.23	8	318.2	0.600	0.996	9.14	Chieming, *et al.*, (1998)
Octanol	130.23	8	318.2	0.632	0.993	9.78	Chieming, *et al.*, (1998)
Octanol	130.23	8	328.2	0.176	1.000	2.89	Chieming, *et al.*, (1998)
Octanol	130.23	8	328.2	0.264	1.000	4.42	Chieming, *et al.*, (1998)
Octanol	130.23	8	328.2	0.332	1.000	5.63	Chieming, *et al.*, (1998)
Octanol	130.23	8	328.2	0.416	1.000	7.00	Chieming, *et al.*, (1998)
Octanol	130.23	8	328.2	0.458	0.999	7.67	Chieming, *et al.*, (1998)
Octanol	130.23	8	328.2	0.497	0.999	8.31	Chieming, *et al.*, (1998)
Octanol	130.23	8	328.2	0.539	0.999	9.07	Chieming, *et al.*, (1998)
Octanol	130.23	8	328.2	0.574	0.999	9.75	Chieming, *et al.*, (1998)
Octanol	130.23	8	328.2	0.604	0.996	10.41	Chieming, *et al.*, (1998)
Octanol	130.23	8	328.2	0.630	0.994	11.03	Chieming, *et al.*, (1998)
Octanol	130.23	8	328.2	0.659	0.990	11.76	Chieming, *et al.*, (1998)
Octanol	130.23	8	328.2	0.682	0.983	12.40	Chieming, *et al.*, (1998)
Octanol	130.23	8	328.2	0.707	0.974	13.10	Chieming, *et al.*, (1998)
Octanol	130.23	8	328.2	0.733	0.962	13.82	Chieming, *et al.*, (1998)
Octanol	130.23	8	328.2	0.756	0.952	14.44	Chieming, *et al.*, (1998)
Octanol	130.23	8	328.2	0.782	0.942	15.11	Chieming, *et al.*, (1998)
Octanol	130.23	8	313.2	0.046	0.000	0.50	Chrisochoou, *et al.*, (1997)
Octanol	130.23	8	313.2	0.069	0.000	0.75	Chrisochoou, *et al.*, (1997)
Octanol	130.23	8	313.2	0.094	0.000	1.00	Chrisochoou, *et al.*, (1997)
Octanol	130.23	8	313.2	0.146	0.000	1.60	Chrisochoou, *et al.*, (1997)
Octanol	130.23	8	313.2	0.179	0.000	2.00	Chrisochoou, *et al.*, (1997)
Octanol	130.23	8	313.2	0.229	0.000	2.50	Chrisochoou, *et al.*, (1997)
Octanol	130.23	8	313.2	0.262	0.000	3.40	Chrisochoou, *et al.*, (1997)
Octanol	130.23	8	313.2	0.333	0.000	4.20	Chrisochoou, *et al.*, (1997)
Octanol	130.23	8	313.2	0.447	1.000	5.90	Chrisochoou, *et al.*, (1997)
Octanol	130.23	8	313.2	0.547	0.999	7.70	Chrisochoou, *et al.*, (1997)
Octanol	130.23	8	313.2	0.650	0.999	8.30	Chrisochoou, *et al.*, (1997)
Octanol	130.23	8	313.2	0.715	0.988	9.20	Chrisochoou, *et al.*, (1997)
Octanol	130.23	8	313.2	0.706	0.980	10.10	Chrisochoou, *et al.*, (1997)
Octanol	130.23	8	313.2	0.729	0.967	11.50	Chrisochoou, *et al.*, (1997)
Octanol	130.23	8	313.2	0.754	0.949	12.60	Chrisochoou, *et al.*, (1997)
Octanol	130.23	8	313.2	0.785	0.943	13.20	Chrisochoou, *et al.*, (1997)
Octanol	130.23	8	313.2	0.791	0.924	15.20	Chrisochoou, *et al.*, (1997)
Octanol	130.23	8	313.2	0.220	0.000	2.93	Byun & Kwak (2002)
Octanol	130.23	8	313.2	0.327	0.000	4.66	Byun & Kwak (2002)
Octanol	130.23	8	313.2	0.491	0.000	6.93	Byun & Kwak (2002)
Octanol	130.23	8	313.2	0.544	0.000	7.66	Byun & Kwak (2002)

Table A-2 continued

Octanol	130.23	8	313.2	0.665	0.000	9.69	Byun & Kwak (2002)
Octanol	130.23	8	313.2	0.749	0.000	12.45	Byun & Kwak (2002)
Octanol	130.23	8	313.2	0.819	0.000	13.97	Byun & Kwak (2002)
Octanol	130.23	8	313.2	0.881	0.000	16.10	Byun & Kwak (2002)
Octanol	130.23	8	313.2	0.905	0.000	16.03	Byun & Kwak (2002)
Octanol	130.23	8	313.2	0.923	0.000	15.48	Byun & Kwak (2002)
Octanol	130.23	8	313.2	0.965	0.000	12.38	Byun & Kwak (2002)
Octanol	130.23	8	333.2	0.220	0.000	3.62	Byun & Kwak (2002)
Octanol	130.23	8	333.2	0.327	0.000	5.41	Byun & Kwak (2002)
Octanol	130.23	8	333.2	0.491	0.000	8.62	Byun & Kwak (2002)
Octanol	130.23	8	333.2	0.544	0.000	9.83	Byun & Kwak (2002)
Octanol	130.23	8	333.2	0.665	0.000	12.10	Byun & Kwak (2002)
Octanol	130.23	8	333.2	0.749	0.000	14.03	Byun & Kwak (2002)
Octanol	130.23	8	333.2	0.819	0.000	16.07	Byun & Kwak (2002)
Octanol	130.23	8	333.2	0.881	0.000	16.76	Byun & Kwak (2002)
Octanol	130.23	8	333.2	0.905	0.000	16.72	Byun & Kwak (2002)
Octanol	130.23	8	333.2	0.923	0.000	16.52	Byun & Kwak (2002)
Octanol	130.23	8	333.2	0.965	0.000	14.93	Byun & Kwak (2002)
Octanol	130.23	8	353.2	0.220	0.000	4.17	Byun & Kwak (2002)
Octanol	130.23	8	353.2	0.327	0.000	6.24	Byun & Kwak (2002)
Octanol	130.23	8	353.2	0.491	0.000	10.31	Byun & Kwak (2002)
Octanol	130.23	8	353.2	0.544	0.000	11.22	Byun & Kwak (2002)
Octanol	130.23	8	353.2	0.665	0.000	14.35	Byun & Kwak (2002)
Octanol	130.23	8	353.2	0.749	0.000	16.66	Byun & Kwak (2002)
Octanol	130.23	8	353.2	0.819	0.000	18.24	Byun & Kwak (2002)
Octanol	130.23	8	353.2	0.881	0.000	18.86	Byun & Kwak (2002)
Octanol	130.23	8	353.2	0.905	0.000	18.79	Byun & Kwak (2002)
Octanol	130.23	8	353.2	0.923	0.000	18.72	Byun & Kwak (2002)
Octanol	130.23	8	353.2	0.000	0.965	17.45	Byun & Kwak (2002)
Octanol	130.23	8	373.2	0.220	0.000	4.41	Byun & Kwak (2002)
Octanol	130.23	8	373.2	0.327	0.000	6.83	Byun & Kwak (2002)
Octanol	130.23	8	373.2	0.491	0.000	11.62	Byun & Kwak (2002)
Octanol	130.23	8	373.2	0.544	0.000	12.72	Byun & Kwak (2002)
Octanol	130.23	8	373.2	0.665	0.000	16.21	Byun & Kwak (2002)
Octanol	130.23	8	373.2	0.749	0.000	18.17	Byun & Kwak (2002)
Octanol	130.23	8	373.2	0.819	0.000	20.14	Byun & Kwak (2002)
Octanol	130.23	8	373.2	0.881	0.000	20.72	Byun & Kwak (2002)
Octanol	130.23	8	373.2	0.905	0.000	20.93	Byun & Kwak (2002)
Octanol	130.23	8	373.2	0.000	0.923	20.38	Byun & Kwak (2002)
Octanol	130.23	8	373.2	0.000	0.965	19.14	Byun & Kwak (2002)
Octanol	130.23	8	393.2	0.220	0.000	4.66	Byun & Kwak (2002)
Octanol	130.23	8	393.2	0.327	0.000	7.52	Byun & Kwak (2002)
Octanol	130.23	8	393.2	0.491	0.000	12.59	Byun & Kwak (2002)
Octanol	130.23	8	393.2	0.544	0.000	13.97	Byun & Kwak (2002)

Table A-2 continued

Octanol	130.23	8	393.2	0.665	0.000	17.52	Byun & Kwak (2002)
Octanol	130.23	8	393.2	0.749	0.000	19.69	Byun & Kwak (2002)
Octanol	130.23	8	393.2	0.819	0.000	21.55	Byun & Kwak (2002)
Octanol	130.23	8	393.2	0.881	0.000	21.97	Byun & Kwak (2002)
Octanol	130.23	8	393.2	0.905	0.000	21.97	Byun & Kwak (2002)
Octanol	130.23	8	393.2	0.000	0.923	21.83	Byun & Kwak (2002)
Octanol	130.23	8	393.2	0.000	0.965	19.97	Byun & Kwak (2002)
Nonanol	144.26	9	308.1	0.162	1.000	2.23	Chieming, *et al.*, (1998)
Nonanol	144.26	9	308.1	0.211	1.000	2.88	Chieming, *et al.*, (1998)
Nonanol	144.26	9	308.1	0.263	1.000	3.63	Chieming, *et al.*, (1998)
Nonanol	144.26	9	308.1	0.324	1.000	4.38	Chieming, *et al.*, (1998)
Nonanol	144.26	9	308.1	0.372	1.000	5.04	Chieming, *et al.*, (1998)
Nonanol	144.26	9	308.1	0.441	0.999	5.89	Chieming, *et al.*, (1998)
Nonanol	144.26	9	308.1	0.499	0.997	6.55	Chieming, *et al.*, (1998)
Nonanol	144.26	9	308.1	0.555	0.996	7.18	Chieming, *et al.*, (1998)
Nonanol	144.26	9	308.1	0.611	0.991	7.91	Chieming, *et al.*, (1998)
Nonanol	144.26	9	318.1	0.165	1.000	2.52	Chieming, *et al.*, (1998)
Nonanol	144.26	9	318.1	0.225	1.000	3.38	Chieming, *et al.*, (1998)
Nonanol	144.26	9	318.1	0.286	1.000	4.25	Chieming, *et al.*, (1998)
Nonanol	144.26	9	318.1	0.354	0.999	5.21	Chieming, *et al.*, (1998)
Nonanol	144.26	9	318.1	0.429	0.999	6.27	Chieming, *et al.*, (1998)
Nonanol	144.26	9	318.1	0.489	0.998	7.05	Chieming, *et al.*, (1998)
Nonanol	144.26	9	318.1	0.540	0.995	7.90	Chieming, *et al.*, (1998)
Nonanol	144.26	9	318.1	0.591	0.991	8.83	Chieming, *et al.*, (1998)
Nonanol	144.26	9	318.1	0.630	0.989	9.61	Chieming, *et al.*, (1998)
Nonanol	144.26	9	318.1	0.652	0.985	10.44	Chieming, *et al.*, (1998)
Nonanol	144.26	9	328.2	0.179	1.000	2.86	Chieming, *et al.*, (1998)
Nonanol	144.26	9	328.2	0.220	1.000	3.58	Chieming, *et al.*, (1998)
Nonanol	144.26	9	328.2	0.267	1.000	4.34	Chieming, *et al.*, (1998)
Nonanol	144.26	9	328.2	0.310	0.999	5.08	Chieming, *et al.*, (1998)
Nonanol	144.26	9	328.2	0.349	0.999	5.78	Chieming, *et al.*, (1998)
Nonanol	144.26	9	328.2	0.400	0.999	6.60	Chieming, *et al.*, (1998)
Nonanol	144.26	9	328.2	0.449	0.999	7.40	Chieming, *et al.*, (1998)
Nonanol	144.26	9	328.2	0.504	0.996	8.43	Chieming, *et al.*, (1998)
Nonanol	144.26	9	328.2	0.558	0.994	9.51	Chieming, *et al.*, (1998)
Nonanol	144.26	9	328.2	0.600	0.992	10.51	Chieming, *et al.*, (1998)
Nonanol	144.26	9	328.2	0.635	0.988	11.42	Chieming, *et al.*, (1998)
Nonanol	144.26	9	328.2	0.670	0.984	12.55	Chieming, *et al.*, (1998)
Nonanol	144.26	9	328.2	0.698	0.980	13.51	Chieming, *et al.*, (1998)
Nonanol	144.26	9	328.2	0.730	0.978	14.56	Chieming, *et al.*, (1998)
Nonanol	144.26	9	328.2	0.758	0.974	15.60	Chieming, *et al.*, (1998)
Nonanol	144.26	9	303.2	0.652	0.980	11.30	Pfohl, *et al.*, (1999)
Nonanol	144.26	9	303.2	0.682	0.972	15.00	Pfohl, *et al.*, (1999)
Nonanol	144.26	9	303.2	0.702	0.969	16.80	Pfohl, *et al.*, (1999)

Table A-2 continued

Nonanol	144.26	9	303.2	0.740	0.955	23.60	Pfohl, *et al.*, (1999)
Nonanol	144.26	9	303.2	0.792	0.934	29.70	Pfohl, *et al.*, (1999)
Nonanol	144.26	9	303.2	0.814	0.922	31.90	Pfohl, *et al.*, (1999)
Nonanol	144.26	9	303.2	0.841	0.896	34.00	Pfohl, *et al.*, (1999)
Nonanol	144.26	9	308.2	0.142	0.999	1.76	Secuicano, *et al.*, (2010)
Nonanol	144.26	9	308.2	0.216	0.999	2.76	Secuicano, *et al.*, (2010)
Nonanol	144.26	9	308.2	0.300	1.000	3.85	Secuicano, *et al.*, (2010)
Nonanol	144.26	9	308.2	0.384	1.000	4.84	Secuicano, *et al.*, (2010)
Nonanol	144.26	9	308.2	0.451	0.999	5.92	Secuicano, *et al.*, (2010)
Nonanol	144.26	9	308.2	0.520	0.998	6.95	Secuicano, *et al.*, (2010)
Nonanol	144.26	9	308.2	0.536	0.998	7.02	Secuicano, *et al.*, (2010)
Nonanol	144.26	9	313.2	0.090	1.000	1.15	Secuicano, *et al.*, (2010)
Nonanol	144.26	9	313.2	0.150	1.000	1.98	Secuicano, *et al.*, (2010)
Nonanol	144.26	9	313.2	0.236	1.000	3.14	Secuicano, *et al.*, (2010)
Nonanol	144.26	9	313.2	0.338	1.000	4.56	Secuicano, *et al.*, (2010)
Nonanol	144.26	9	313.2	0.423	0.999	5.83	Secuicano, *et al.*, (2010)
Nonanol	144.26	9	313.2	0.523	0.998	7.44	Secuicano, *et al.*, (2010)
Nonanol	144.26	9	333.2	0.008	1.000	1.15	Secuicano, *et al.*, (2010)
Nonanol	144.26	9	333.2	0.129	1.000	2.08	Secuicano, *et al.*, (2010)
Nonanol	144.26	9	333.2	0.191	1.000	3.10	Secuicano, *et al.*, (2010)
Nonanol	144.26	9	333.2	0.260	1.000	4.33	Secuicano, *et al.*, (2010)
Nonanol	144.26	9	333.2	0.310	1.000	5.27	Secuicano, *et al.*, (2010)
Nonanol	144.26	9	333.2	0.372	0.999	6.41	Secuicano, *et al.*, (2010)
Nonanol	144.26	9	333.2	0.398	0.999	6.80	Secuicano, *et al.*, (2010)
Nonanol	144.26	9	333.2	0.420	0.999	7.31	Secuicano, *et al.*, (2010)
Nonanol	144.26	9	333.2	0.466	0.998	8.25	Secuicano, *et al.*, (2010)
Nonanol	144.26	9	333.2	0.489	0.997	8.94	Secuicano, *et al.*, (2010)
Nonanol	144.26	9	353.2	0.068	1.000	1.15	Secuicano, *et al.*, (2010)
Nonanol	144.26	9	353.2	0.124	1.000	2.25	Secuicano, *et al.*, (2010)
Nonanol	144.26	9	353.2	0.171	1.000	3.16	Secuicano, *et al.*, (2010)
Nonanol	144.26	9	353.2	0.243	1.000	4.56	Secuicano, *et al.*, (2010)
Nonanol	144.26	9	353.2	0.297	1.000	5.73	Secuicano, *et al.*, (2010)
Nonanol	144.26	9	353.2	0.359	0.999	7.10	Secuicano, *et al.*, (2010)
Nonanol	144.26	9	353.2	0.406	0.999	8.31	Secuicano, *et al.*, (2010)
Nonanol	144.26	9	353.2	0.472	0.998	9.88	Secuicano, *et al.*, (2010)
Nonanol	144.26	9	353.2	0.484	0.997	10.15	Secuicano, *et al.*, (2010)
Nonanol	144.26	9	353.2	0.491	0.997	10.33	Secuicano, *et al.*, (2010)
Decanol	158.28	10	313.2	0.600	0.994	12.10	Pohler (1994)
Decanol	158.28	10	313.2	0.683	0.990	15.20	Pohler (1994)
Decanol	158.28	10	313.2	0.731	0.986	16.80	Pohler (1994)
Decanol	158.28	10	313.2	0.748	0.973	20.00	Pohler (1994)
Decanol	158.28	10	313.2	0.782	0.960	22.90	Pohler (1994)
Decanol	158.28	10	313.2	0.800	0.949	25.00	Pohler (1994)
Decanol	158.28	10	313.2	0.886	0.887	32.30	Pohler (1994)

Table A-2 continued

Decanol	158.28	10	323.2	0.536	0.994	12.40	Pohler (1994)
Decanol	158.28	10	323.2	0.625	0.990	15.20	Pohler (1994)
Decanol	158.28	10	323.2	0.675	0.981	17.40	Pohler (1994)
Decanol	158.28	10	323.2	0.687	0.970	20.00	Pohler (1994)
Decanol	158.28	10	323.2	0.739	0.953	22.50	Pohler (1994)
Decanol	158.28	10	323.2	0.766	0.935	24.00	Pohler (1994)
Decanol	158.28	10	323.2	0.896	0.895	24.40	Pohler (1994)
Decanol	158.28	10	333.2	0.603	0.999	10.00	Pohler (1994)
Decanol	158.28	10	333.2	0.672	0.997	12.40	Pohler (1994)
Decanol	158.28	10	333.2	0.728	0.995	14.70	Pohler (1994)
Decanol	158.28	10	333.2	0.778	0.984	17.40	Pohler (1994)
Decanol	158.28	10	333.2	0.803	0.975	18.70	Pohler (1994)
Decanol	158.28	10	333.2	0.902	0.902	21.60	Pohler (1994)
Decanol	158.28	10	353.2	0.562	0.999	10.00	Pohler (1994)
Decanol	158.28	10	353.2	0.602	0.997	12.20	Pohler (1994)
Decanol	158.28	10	353.2	0.681	0.995	14.80	Pohler (1994)
Decanol	158.28	10	353.2	0.742	0.989	17.50	Pohler (1994)
Decanol	158.28	10	353.2	0.790	0.975	19.90	Pohler (1994)
Decanol	158.28	10	353.2	0.897	0.897	21.90	Pohler (1994)
Decanol	158.28	10	373.2	0.469	0.998	10.30	Pohler (1994)
Decanol	158.28	10	373.2	0.594	0.996	15.00	Pohler (1994)
Decanol	158.28	10	373.2	0.662	0.994	17.40	Pohler (1994)
Decanol	158.28	10	373.2	0.724	0.983	20.00	Pohler (1994)
Decanol	158.28	10	373.2	0.773	0.964	22.60	Pohler (1994)
Decanol	158.28	10	373.2	0.898	0.899	23.50	Pohler (1994)
Decanol	158.28	10	393.2	0.446	0.998	10.00	Pohler (1994)
Decanol	158.28	10	393.2	0.561	0.996	15.00	Pohler (1994)
Decanol	158.28	10	393.2	0.631	0.990	17.50	Pohler (1994)
Decanol	158.28	10	393.2	0.693	0.986	20.00	Pohler (1994)
Decanol	158.28	10	393.2	0.757	0.973	22.50	Pohler (1994)
Decanol	158.28	10	393.2	0.812	0.959	24.00	Pohler (1994)
Decanol	158.28	10	393.2	0.898	0.898	24.80	Pohler (1994)
Decanol	158.28	10	303.2	0.201	0.000	1.85	Ioniţă, *et al.*, (2013)
Decanol	158.28	10	303.2	0.199	0.000	2.01	Ioniţă, *et al.*, (2013)
Decanol	158.28	10	303.2	0.245	0.000	2.75	Ioniţă, *et al.*, (2013)
Decanol	158.28	10	303.2	0.277	0.000	2.83	Ioniţă, *et al.*, (2013)
Decanol	158.28	10	303.2	0.355	0.000	4.01	Ioniţă, *et al.*, (2013)
Decanol	158.28	10	303.2	0.499	0.000	5.66	Ioniţă, *et al.*, (2013)
Decanol	158.28	10	303.2	0.539	0.000	6.19	Ioniţă, *et al.*, (2013)
Decanol	158.28	10	303.2	0.557	0.000	6.45	Ioniţă, *et al.*, (2013)
Decanol	158.28	10	303.2	0.557	0.000	6.45	Ioniţă, *et al.*, (2013)
Decanol	158.28	10	303.2	0.592	0.000	7.65	Ioniţă, *et al.*, (2013)
Decanol	158.28	10	303.2	0.608	0.000	10.03	Ioniţă, *et al.*, (2013)
Decanol	158.28	10	303.2	0.626	0.000	12.63	Ioniţă, *et al.*, (2013)

Table A-2 continued

Decanol	158.28	10	303.2	0.630	0.000	15.08	Ioniţă, *et al.*, (2013)
Decanol	158.28	10	323.2	0.164	0.000	2.36	Ioniţă, *et al.*, (2013)
Decanol	158.28	10	308.2	0.115	0.000	1.68	Ioniţă, *et al.*, (2013)
Decanol	158.28	10	308.2	0.186	0.000	2.56	Ioniţă, *et al.*, (2013)
Decanol	158.28	10	308.2	0.234	0.000	3.16	Ioniţă, *et al.*, (2013)
Decanol	158.28	10	308.2	0.238	0.000	3.22	Ioniţă, *et al.*, (2013)
Decanol	158.28	10	308.2	0.242	0.000	3.30	Ioniţă, *et al.*, (2013)
Decanol	158.28	10	308.2	0.266	0.000	3.66	Ioniţă, *et al.*, (2013)
Decanol	158.28	10	308.2	0.287	0.000	3.84	Ioniţă, *et al.*, (2013)
Decanol	158.28	10	308.2	0.320	0.000	4.40	Ioniţă, *et al.*, (2013)
Decanol	158.28	10	308.2	0.325	0.000	4.41	Ioniţă, *et al.*, (2013)
Decanol	158.28	10	308.2	0.343	0.000	4.64	Ioniţă, *et al.*, (2013)
Decanol	158.28	10	308.2	0.405	0.000	5.56	Ioniţă, *et al.*, (2013)
Decanol	158.28	10	323.2	0.225	0.000	3.30	Ioniţă, *et al.*, (2013)
Decanol	158.28	10	323.2	0.287	0.000	4.07	Ioniţă, *et al.*, (2013)
Decanol	158.28	10	323.2	0.332	0.000	4.91	Ioniţă, *et al.*, (2013)
Decanol	158.28	10	323.2	0.412	0.000	6.18	Ioniţă, *et al.*, (2013)
Decanol	158.28	10	323.2	0.475	0.000	7.36	Ioniţă, *et al.*, (2013)
Decanol	158.28	10	323.2	0.509	0.000	8.12	Ioniţă, *et al.*, (2013)
Decanol	158.28	10	323.2	0.558	0.000	9.03	Ioniţă, *et al.*, (2013)
Decanol	158.28	10	323.2	0.608	0.000	10.15	Ioniţă, *et al.*, (2013)
Decanol	158.28	10	323.2	0.645	0.000	11.24	Ioniţă, *et al.*, (2013)
Decanol	158.28	10	323.2	0.660	0.000	12.08	Ioniţă, *et al.*, (2013)
Decanol	158.28	10	333.2	0.142	0.000	2.30	Ioniţă, *et al.*, (2013)
Decanol	158.28	10	333.2	0.188	0.000	2.99	Ioniţă, *et al.*, (2013)
Decanol	158.28	10	333.2	0.229	0.000	3.89	Ioniţă, *et al.*, (2013)
Decanol	158.28	10	333.2	0.283	0.000	4.80	Ioniţă, *et al.*, (2013)
Decanol	158.28	10	333.2	0.311	0.000	5.15	Ioniţă, *et al.*, (2013)
Decanol	158.28	10	333.2	0.388	0.000	6.32	Ioniţă, *et al.*, (2013)
Decanol	158.28	10	333.2	0.428	0.000	7.38	Ioniţă, *et al.*, (2013)
Decanol	158.28	10	333.2	0.492	0.000	8.38	Ioniţă, *et al.*, (2013)
Decanol	158.28	10	333.2	0.514	0.000	9.40	Ioniţă, *et al.*, (2013)
Decanol	158.28	10	333.2	0.536	0.000	9.86	Ioniţă, *et al.*, (2013)
Decanol	158.28	10	333.2	0.552	0.000	10.21	Ioniţă, *et al.*, (2013)
Decanol	158.28	10	333.2	0.582	0.000	11.18	Ioniţă, *et al.*, (2013)
Decanol	158.28	10	333.2	0.635	0.000	12.83	Ioniţă, *et al.*, (2013)
Decanol	158.28	10	333.2	0.650	0.000	13.26	Ioniţă, *et al.*, (2013)
Decanol	158.28	10	343.2	0.125	0.000	1.92	Ioniţă, *et al.*, (2013)
Decanol	158.28	10	343.2	0.184	0.000	2.95	Ioniţă, *et al.*, (2013)
Decanol	158.28	10	343.2	0.237	0.000	3.96	Ioniţă, *et al.*, (2013)
Decanol	158.28	10	343.2	0.295	0.000	5.13	Ioniţă, *et al.*, (2013)
Decanol	158.28	10	343.2	0.345	0.000	6.03	Ioniţă, *et al.*, (2013)
Decanol	158.28	10	343.2	0.389	0.000	7.14	Ioniţă, *et al.*, (2013)
Decanol	158.28	10	343.2	0.433	0.000	7.97	Ioniţă, *et al.*, (2013)

Table A-2 continued

Decanol	158.28	10	343.2	0.497	0.000	9.35	Ioniță, *et al.*, (2013)
Decanol	158.28	10	343.2	0.543	0.000	10.39	Ioniță, *et al.*, (2013)
Decanol	158.28	10	343.2	0.571	0.000	11.49	Ioniță, *et al.*, (2013)
Decanol	158.28	10	343.2	0.607	0.000	12.63	Ioniță, *et al.*, (2013)
Decanol	158.28	10	348.2	0.050	0.000	1.00	Lee & Chen (1994)
Decanol	158.28	10	348.2	0.107	0.000	2.00	Lee & Chen (1994)
Decanol	158.28	10	348.2	0.164	0.000	3.00	Lee & Chen (1994)
Decanol	158.28	10	348.2	0.218	0.000	4.00	Lee & Chen (1994)
Decanol	158.28	10	348.2	0.270	0.000	5.00	Lee & Chen (1994)
Decanol	158.28	10	348.2	0.000	1.000	1.00	Lee & Chen (1994)
Decanol	158.28	10	348.2	0.000	1.000	2.00	Lee & Chen (1994)
Decanol	158.28	10	348.2	0.000	1.000	3.00	Lee & Chen (1994)
Decanol	158.28	10	348.2	0.000	1.000	4.00	Lee & Chen (1994)
Decanol	158.28	10	348.2	0.000	1.000	5.00	Lee & Chen (1994)
Decanol	158.28	10	308.1	0.162	1.000	2.23	Chieming, *et al.*, (1998)
Decanol	158.28	10	308.1	0.211	1.000	2.88	Chieming, *et al.*, (1998)
Decanol	158.28	10	308.1	0.263	1.000	3.63	Chieming, *et al.*, (1998)
Decanol	158.28	10	308.1	0.324	1.000	4.38	Chieming, *et al.*, (1998)
Decanol	158.28	10	308.1	0.372	1.000	5.04	Chieming, *et al.*, (1998)
Decanol	158.28	10	308.1	0.424	1.000	5.76	Chieming, *et al.*, (1998)
Decanol	158.28	10	308.1	0.476	0.999	6.41	Chieming, *et al.*, (1998)
Decanol	158.28	10	308.1	0.524	0.999	7.05	Chieming, *et al.*, (1998)
Decanol	158.28	10	308.1	0.581	0.997	7.75	Chieming, *et al.*, (1998)
Decanol	158.28	10	318.1	0.152	1.000	2.18	Chieming, *et al.*, (1998)
Decanol	158.28	10	318.1	0.223	1.000	3.20	Chieming, *et al.*, (1998)
Decanol	158.28	10	318.1	0.304	1.000	4.30	Chieming, *et al.*, (1998)
Decanol	158.28	10	318.1	0.372	1.000	5.27	Chieming, *et al.*, (1998)
Decanol	158.28	10	318.1	0.448	0.999	6.43	Chieming, *et al.*, (1998)
Decanol	158.28	10	318.1	0.513	0.999	7.34	Chieming, *et al.*, (1998)
Decanol	158.28	10	318.1	0.558	0.997	8.38	Chieming, *et al.*, (1998)
Decanol	158.28	10	318.1	0.626	0.994	9.41	Chieming, *et al.*, (1998)
Decanol	158.28	10	318.1	0.648	0.992	10.47	Chieming, *et al.*, (1998)
Decanol	158.28	10	328.2	0.181	1.000	2.89	Chieming, *et al.*, (1998)
Decanol	158.28	10	328.2	0.243	1.000	3.87	Chieming, *et al.*, (1998)
Decanol	158.28	10	328.2	0.315	1.000	5.00	Chieming, *et al.*, (1998)
Decanol	158.28	10	328.2	0.375	1.000	6.07	Chieming, *et al.*, (1998)
Decanol	158.28	10	328.2	0.437	1.000	7.03	Chieming, *et al.*, (1998)
Decanol	158.28	10	328.2	0.495	0.999	8.24	Chieming, *et al.*, (1998)
Decanol	158.28	10	328.2	0.538	0.999	9.09	Chieming, *et al.*, (1998)
Decanol	158.28	10	328.2	0.574	0.999	10.07	Chieming, *et al.*, (1998)
Decanol	158.28	10	328.2	0.612	0.997	11.03	Chieming, *et al.*, (1998)
Decanol	158.28	10	328.2	0.642	0.994	12.06	Chieming, *et al.*, (1998)
Decanol	158.28	10	328.2	0.666	0.990	13.20	Chieming, *et al.*, (1998)
Decanol	158.28	10	328.2	0.689	0.984	14.07	Chieming, *et al.*, (1998)

Table A-2 continued

Decanol	158.28	10	328.2	0.710	0.978	15.17	Chieming, *et al.*, (1998)
Decanol	158.28	10	348.2	0.367	1.000	7.00	Weng, *et al.*, (1994)
Decanol	158.28	10	348.2	0.437	1.000	8.50	Weng, *et al.*, (1994)
Decanol	158.28	10	348.2	0.501	0.999	10.00	Weng, *et al.*, (1994)
Decanol	158.28	10	348.2	0.572	0.998	11.50	Weng, *et al.*, (1994)
Decanol	158.28	10	348.2	0.640	0.997	13.00	Weng, *et al.*, (1994)
Decanol	158.28	10	348.2	0.690	0.995	14.50	Weng, *et al.*, (1994)
Decanol	158.28	10	348.2	0.736	0.985	17.00	Weng, *et al.*, (1994)
Decanol	158.28	10	348.2	0.795	0.970	19.00	Weng, *et al.*, (1994)
Dodecanol	186.34	12	313.2	0.092	0.995	1.09	Secuianu, *et al.*, (2016)
Dodecanol	186.34	12	313.2	0.184	0.996	2.05	Secuianu, *et al.*, (2016)
Dodecanol	186.34	12	313.2	0.249	0.997	3.01	Secuianu, *et al.*, (2016)
Dodecanol	186.34	12	313.2	0.317	0.997	4.02	Secuianu, *et al.*, (2016)
Dodecanol	186.34	12	313.2	0.405	0.997	5.11	Secuianu, *et al.*, (2016)
Dodecanol	186.34	12	313.2	0.456	0.998	6.02	Secuianu, *et al.*, (2016)
Dodecanol	186.34	12	313.2	0.492	0.997	6.79	Secuianu, *et al.*, (2016)
Dodecanol	186.34	12	313.2	0.495	0.997	6.82	Secuianu, *et al.*, (2016)
Dodecanol	186.34	12	333.2	0.098	0.996	1.00	Secuianu, *et al.*, (2016)
Dodecanol	186.34	12	333.2	0.150	0.997	2.04	Secuianu, *et al.*, (2016)
Dodecanol	186.34	12	333.2	0.217	0.997	3.08	Secuianu, *et al.*, (2016)
Dodecanol	186.34	12	333.2	0.286	0.997	4.14	Secuianu, *et al.*, (2016)
Dodecanol	186.34	12	333.2	0.330	0.998	5.02	Secuianu, *et al.*, (2016)
Dodecanol	186.34	12	333.2	0.381	0.998	5.98	Secuianu, *et al.*, (2016)
Dodecanol	186.34	12	333.2	0.424	0.998	7.01	Secuianu, *et al.*, (2016)
Dodecanol	186.34	12	333.2	0.450	0.998	7.49	Secuianu, *et al.*, (2016)
Dodecanol	186.34	12	333.2	0.479	0.998	8.29	Secuianu, *et al.*, (2016)
Dodecanol	186.34	12	353.2	0.071	0.996	1.04	Secuianu, *et al.*, (2016)
Dodecanol	186.34	12	353.2	0.138	0.998	2.02	Secuianu, *et al.*, (2016)
Dodecanol	186.34	12	353.2	0.190	0.998	3.06	Secuianu, *et al.*, (2016)
Dodecanol	186.34	12	353.2	0.241	0.999	4.05	Secuianu, *et al.*, (2016)
Dodecanol	186.34	12	353.2	0.282	0.999	4.96	Secuianu, *et al.*, (2016)
Dodecanol	186.34	12	353.2	0.338	0.999	6.04	Secuianu, *et al.*, (2016)
Dodecanol	186.34	12	353.2	0.379	0.999	6.95	Secuianu, *et al.*, (2016)
Dodecanol	186.34	12	353.2	0.423	0.999	8.06	Secuianu, *et al.*, (2016)
Dodecanol	186.34	12	353.2	0.446	0.999	9.36	Secuianu, *et al.*, (2016)
Dodecanol	186.34	12	353.2	0.463	0.998	10.00	Kordikowski & Schneider (1993)
Dodecanol	186.34	12	353.2	0.624	0.997	15.00	Kordikowski & Schneider (1993)
Dodecanol	186.34	12	353.2	0.727	0.983	20.00	Kordikowski & Schneider (1993)
Dodecanol	186.34	12	353.2	0.774	0.965	23.00	Kordikowski & Schneider (1993)
Dodecanol	186.34	12	353.2	0.853	0.946	25.10	Kordikowski & Schneider (1993)
Dodecanol	186.34	12	353.2	0.904	0.904	25.20	Kordikowski & Schneider (1993)
Dodecanol	186.34	12	393.2	0.422	0.995	10.00	Spee & Schneider (1991)
Dodecanol	186.34	12	393.2	0.513	0.993	12.90	Spee & Schneider (1991)
Dodecanol	186.34	12	393.2	0.554	0.994	15.00	Spee & Schneider (1991)

Table A-2 continued

Dodecanol	186.34	12	393.2	0.608	0.992	17.30	Spee & Schneider (1991)
Dodecanol	186.34	12	393.2	0.665	0.985	20.00	Spee & Schneider (1991)
Dodecanol	186.34	12	393.2	0.727	0.984	22.50	Spee & Schneider (1991)
Dodecanol	186.34	12	393.2	0.784	0.970	25.00	Spee & Schneider (1991)
Dodecanol	186.34	12	393.2	0.840	0.950	27.00	Spee & Schneider (1991)
Dodecanol	186.34	12	393.2	0.888	0.886	27.50	Spee & Schneider (1991)
Dodecanol	186.34	12	374.9	0.827	0.983	23.97	Scheidgen (1997)
Dodecanol	186.34	12	374.9	0.859	0.967	25.98	Scheidgen (1997)
Dodecanol	186.34	12	374.9	0.000	0.940	26.14	Scheidgen (1997)
Dodecanol	186.34	12	333.2	0.567	1.000	10.00	Holsher (1988)
Dodecanol	186.34	12	333.2	0.650	0.990	15.00	Holsher (1988)
Dodecanol	186.34	12	333.2	0.703	0.985	17.40	Holsher (1988)
Dodecanol	186.34	12	333.2	0.714	0.975	19.70	Holsher (1988)
Dodecanol	186.34	12	333.2	0.738	0.968	22.70	Holsher (1988)
Dodecanol	186.34	12	333.2	0.770	0.963	24.80	Holsher (1988)
Dodecanol	186.34	12	333.2	0.763	0.957	25.10	Holsher (1988)
Dodecanol	186.34	12	333.2	0.767	0.961	25.10	Holsher (1988)
Dodecanol	186.34	12	333.2	0.805	0.950	27.30	Holsher (1988)
Dodecanol	186.34	12	333.2	0.820	0.934	28.70	Holsher (1988)
Dodecanol	186.34	12	393.2	0.437	0.998	10.30	Holsher (1988)
Dodecanol	186.34	12	393.2	0.502	0.996	13.30	Holsher (1988)
Dodecanol	186.34	12	393.2	0.554	0.995	16.10	Holsher (1988)
Dodecanol	186.34	12	393.2	0.592	0.991	17.90	Holsher (1988)
Dodecanol	186.34	12	393.2	0.644	0.993	19.30	Holsher (1988)
Dodecanol	186.34	12	393.2	0.703	0.985	22.20	Holsher (1988)
Dodecanol	186.34	12	393.2	0.753	0.978	23.90	Holsher (1988)
Dodecanol	186.34	12	393.2	0.790	0.967	25.60	Holsher (1988)
Dodecanol	186.34	12	393.2	0.818	0.961	26.30	Holsher (1988)
Dodecanol	186.34	12	393.2	0.867	0.920	27.30	Holsher (1988)
Dodecanol	186.34	12	393.2	0.422	0.995	10.00	Spee (1990)
Dodecanol	186.34	12	393.2	0.513	0.993	12.90	Spee (1990)
Dodecanol	186.34	12	393.2	0.554	0.994	15.00	Spee (1990)
Dodecanol	186.34	12	393.2	0.608	0.992	17.30	Spee (1990)
Dodecanol	186.34	12	393.2	0.665	0.985	20.00	Spee (1990)
Dodecanol	186.34	12	393.2	0.727	0.984	22.50	Spee (1990)
Dodecanol	186.34	12	393.2	0.784	0.970	25.00	Spee (1990)
Dodecanol	186.34	12	393.2	0.840	0.950	27.00	Spee (1990)
Dodecanol	186.34	12	393.2	0.888	0.886	27.50	Spee (1990)
Tetradecanol	214.39	14	373.2	0.995	0.062	1.01	Jan, *et al.*, (1994)
Tetradecanol	214.39	14	373.2	0.996	0.119	2.03	Jan, *et al.*, (1994)
Tetradecanol	214.39	14	373.2	0.997	0.172	3.04	Jan, *et al.*, (1994)
Tetradecanol	214.39	14	373.2	0.998	0.226	4.05	Jan, *et al.*, (1994)
Tetradecanol	214.39	14	373.2	0.998	0.270	5.07	Jan, *et al.*, (1994)
Hexadecanol	242.44	16	373.2	0.064	0.994	1.01	Jan, *et al.*, (1994)

Table A-2 continued

Hexadecanol	242.44	16	373.2	0.125	0.995	2.03	Jan, *et al.*, (1994)
Hexadecanol	242.44	16	373.2	0.191	0.996	3.04	Jan, *et al.*, (1994)
Hexadecanol	242.44	16	373.2	0.249	0.997	4.05	Jan, *et al.*, (1994)
Hexadecanol	242.44	16	373.2	0.304	0.998	5.07	Jan, *et al.*, (1994)
Hexadecanol	242.44	16	393.2	0.452	0.999	10.40	Holsher (1988)
Hexadecanol	242.44	16	393.2	0.544	0.997	14.00	Holsher (1988)
Hexadecanol	242.44	16	393.2	0.645	0.996	18.70	Holsher (1988)
Hexadecanol	242.44	16	393.2	0.665	0.994	19.30	Holsher (1988)
Hexadecanol	242.44	16	393.2	0.720	0.991	23.50	Holsher (1988)
Hexadecanol	242.44	16	393.2	0.726	0.989	24.50	Holsher (1988)
Hexadecanol	242.44	16	393.2	0.769	0.982	26.70	Holsher (1988)
Hexadecanol	242.44	16	393.2	0.803	0.974	28.70	Holsher (1988)
Hexadecanol	242.44	16	393.2	0.850	0.957	31.40	Holsher (1988)
Hexadecanol	242.44	16	393.2	0.880	0.939	32.30	Holsher (1988)
Octadecanol	270.51	18	373.2	0.072	0.998	1.01	Jan, *et al.*, (1994)
Octadecanol	270.51	18	373.2	0.139	0.998	2.03	Jan, *et al.*, (1994)
Octadecanol	270.51	18	373.2	0.197	0.999	3.04	Jan, *et al.*, (1994)
Octadecanol	270.51	18	373.2	0.245	1.000	4.05	Jan, *et al.*, (1994)
Octadecanol	270.51	18	373.2	0.292	1.000	5.07	Jan, *et al.*, (1994)

Table A-3: Bubble and dew point pressures at specific compositions and temperatures for carboxylic acid.

Acid Name	MM	CL	T (K)	x (mol/mol)	y (mol/mol)	P (MPa)	Reference
Butyric	88.11	4	313.2	0.000	0.250	3.03	Byun, *et al.*, (2000)
Butyric	88.11	4	313.2	0.000	0.520	5.62	Byun, *et al.*, (2000)
Butyric	88.11	4	313.2	0.000	0.678	6.85	Byun, *et al.*, (2000)
Butyric	88.11	4	313.2	0.000	0.799	7.58	Byun, *et al.*, (2000)
Butyric	88.11	4	313.2	0.000	0.831	7.68	Byun, *et al.*, (2000)
Butyric	88.11	4	313.2	0.000	0.846	7.86	Byun, *et al.*, (2000)
Butyric	88.11	4	313.2	0.000	0.863	8.1	Byun, *et al.*, (2000)
Butyric	88.11	4	313.2	0.000	0.902	8.22	Byun, *et al.*, (2000)
Butyric	88.11	4	313.2	0.000	0.923	8.3	Byun, *et al.*, (2000)
Butyric	88.11	4	313.2	0.000	0.942	8.44	Byun, *et al.*, (2000)
Butyric	88.11	4	313.2	0.000	0.960	8.65	Byun, *et al.*, (2000)
Butyric	88.11	4	313.2	0.000	0.979	8.72	Byun, *et al.*, (2000)
Butyric	88.11	4	313.2	0.000	0.983	8.82	Byun, *et al.*, (2000)
Butyric	88.11	4	313.2	0.000	0.991	8.84	Byun, *et al.*, (2000)
Butyric	88.11	4	313.2	0.000	0.997	8.84	Byun, *et al.*, (2000)
Butyric	88.11	4	313.2	0.000	0.999	8.74	Byun, *et al.*, (2000)
Butyric	88.11	4	333.2	0.000	0.250	3.72	Byun, *et al.*, (2000)
Butyric	88.11	4	333.2	0.000	0.520	7.68	Byun, *et al.*, (2000)
Butyric	88.11	4	333.2	0.000	0.678	9.47	Byun, *et al.*, (2000)
Butyric	88.11	4	333.2	0.000	0.799	10.42	Byun, *et al.*, (2000)
Butyric	88.11	4	333.2	0.000	0.831	10.65	Byun, *et al.*, (2000)
Butyric	88.11	4	333.2	0.000	0.846	10.79	Byun, *et al.*, (2000)
Butyric	88.11	4	333.2	0.000	0.863	10.93	Byun, *et al.*, (2000)
Butyric	88.11	4	333.2	0.000	0.902	11.03	Byun, *et al.*, (2000)
Butyric	88.11	4	333.2	0.000	0.923	11.13	Byun, *et al.*, (2000)
Butyric	88.11	4	333.2	0.000	0.942	11.27	Byun, *et al.*, (2000)
Butyric	88.11	4	333.2	0.000	0.960	11.34	Byun, *et al.*, (2000)
Butyric	88.11	4	333.2	0.000	0.979	11.34	Byun, *et al.*, (2000)
Butyric	88.11	4	333.2	0.000	0.983	11.232	Byun, *et al.*, (2000)
Butyric	88.11	4	333.2	0.000	0.991	11.00	Byun, *et al.*, (2000)
Butyric	88.11	4	353.2	0.000	0.250	4.51	Byun, *et al.*, (2000)
Butyric	88.11	4	353.2	0.000	0.520	9.82	Byun, *et al.*, (2000)
Butyric	88.11	4	353.2	0.000	0.678	12.27	Byun, *et al.*, (2000)
Butyric	88.11	4	353.2	0.000	0.799	13.47	Byun, *et al.*, (2000)
Butyric	88.11	4	353.2	0.000	0.831	13.68	Byun, *et al.*, (2000)
Butyric	88.11	4	353.2	0.000	0.846	13.72	Byun, *et al.*, (2000)
Butyric	88.11	4	353.2	0.000	0.863	13.89	Byun, *et al.*, (2000)
Butyric	88.11	4	353.2	0.000	0.902	14.22	Byun, *et al.*, (2000)
Butyric	88.11	4	353.2	0.000	0.923	14.31	Byun, *et al.*, (2000)
Butyric	88.11	4	353.2	0.000	0.942	14.39	Byun, *et al.*, (2000)
Butyric	88.11	4	353.2	0.000	0.960	13.96	Byun, *et al.*, (2000)
Butyric	88.11	4	353.2	0.000	0.979	13.09	Byun, *et al.*, (2000)
Butyric	88.11	4	353.2	0.000	0.983	12.16	Byun, *et al.*, (2000)

Table A-3 continued

Butyric	88.11	4	373.2	0.000	0.250	5.37	Byun, *et al.*, (2000)
Butyric	88.11	4	373.2	0.000	0.520	11.68	Byun, *et al.*, (2000)
Butyric	88.11	4	373.2	0.000	0.678	14.82	Byun, *et al.*, (2000)
Butyric	88.11	4	373.2	0.000	0.799	16.08	Byun, *et al.*, (2000)
Butyric	88.11	4	373.2	0.000	0.831	16.23	Byun, *et al.*, (2000)
Butyric	88.11	4	373.2	0.000	0.846	16.37	Byun, *et al.*, (2000)
Butyric	88.11	4	373.2	0.000	0.863	16.47	Byun, *et al.*, (2000)
Butyric	88.11	4	373.2	0.000	0.902	16.69	Byun, *et al.*, (2000)
Butyric	88.11	4	373.2	0.000	0.923	16.82	Byun, *et al.*, (2000)
Butyric	88.11	4	373.2	0.000	0.942	16.77	Byun, *et al.*, (2000)
Butyric	88.11	4	373.2	0.000	0.960	16.47	Byun, *et al.*, (2000)
Butyric	88.11	4	373.2	0.000	0.979	14.54	Byun, *et al.*, (2000)
Butyric	88.11	4	373.2	0.000	0.983	11.34	Byun, *et al.*, (2000)
Butyric	88.11	4	393.2	0.000	0.250	6.31	Byun, *et al.*, (2000)
Butyric	88.11	4	393.2	0.000	0.520	13.75	Byun, *et al.*, (2000)
Butyric	88.11	4	393.2	0.000	0.678	17.2	Byun, *et al.*, (2000)
Butyric	88.11	4	393.2	0.000	0.799	18.55	Byun, *et al.*, (2000)
Butyric	88.11	4	393.2	0.000	0.831	18.76	Byun, *et al.*, (2000)
Butyric	88.11	4	393.2	0.000	0.846	18.82	Byun, *et al.*, (2000)
Butyric	88.11	4	393.2	0.000	0.863	18.96	Byun, *et al.*, (2000)
Butyric	88.11	4	393.2	0.000	0.902	18.95	Byun, *et al.*, (2000)
Butyric	88.11	4	393.2	0.000	0.923	18.82	Byun, *et al.*, (2000)
Butyric	88.11	4	393.2	0.000	0.942	18.71	Byun, *et al.*, (2000)
Butyric	88.11	4	393.2	0.000	0.960	18.23	Byun, *et al.*, (2000)
Butyric	88.11	4	393.2	0.000	0.979	9.61	Byun, *et al.*, (2000)
Pentanoic	102.13	5	333.2	0.212	0.000	3.27	Byun, *et al.*, (2000)
Pentanoic	102.13	5	333.2	0.400	0.000	6.1	Byun, *et al.*, (2000)
Pentanoic	102.13	5	333.2	0.627	0.000	9.51	Byun, *et al.*, (2000)
Pentanoic	102.13	5	333.2	0.782	0.000	10.99	Byun, *et al.*, (2000)
Pentanoic	102.13	5	333.2	0.807	0.000	11.13	Byun, *et al.*, (2000)
Pentanoic	102.13	5	333.2	0.812	0.000	11.21	Byun, *et al.*, (2000)
Pentanoic	102.13	5	333.2	0.848	0.000	11.33	Byun, *et al.*, (2000)
Pentanoic	102.13	5	333.2	0.867	0.000	11.44	Byun, *et al.*, (2000)
Pentanoic	102.13	5	333.2	0.883	0.000	11.68	Byun, *et al.*, (2000)
Pentanoic	102.13	5	333.2	0.903	0.000	11.79	Byun, *et al.*, (2000)
Pentanoic	102.13	5	333.2	0.914	0.000	11.83	Byun, *et al.*, (2000)
Pentanoic	102.13	5	333.2	0.932	0.000	11.82	Byun, *et al.*, (2000)
Pentanoic	102.13	5	333.2	0.948	0.000	11.94	Byun, *et al.*, (2000)
Pentanoic	102.13	5	333.2	0.979	0.000	12.06	Byun, *et al.*, (2000)
Pentanoic	102.13	5	333.2	0.982	0.000	12.01	Byun, *et al.*, (2000)
Pentanoic	102.13	5	333.2	0.000	0.982	12.01	Byun, *et al.*, (2000)
Pentanoic	102.13	5	353.2	0.212	0.000	3.96	Byun, *et al.*, (2000)
Pentanoic	102.13	5	353.2	0.400	0.000	7.55	Byun, *et al.*, (2000)
Pentanoic	102.13	5	353.2	0.627	0.000	12.76	Byun, *et al.*, (2000)

Table A-3 continued

Pentanoic	102.13	5	353.2	0.782	0.000	14.61	Byun, *et al.*, (2000)
Pentanoic	102.13	5	353.2	0.807	0.000	14.85	Byun, *et al.*, (2000)
Pentanoic	102.13	5	353.2	0.812	0.000	14.92	Byun, *et al.*, (2000)
Pentanoic	102.13	5	353.2	0.848	0.000	14.92	Byun, *et al.*, (2000)
Pentanoic	102.13	5	353.2	0.867	0.000	15.13	Byun, *et al.*, (2000)
Pentanoic	102.13	5	353.2	0.883	0.000	15.29	Byun, *et al.*, (2000)
Pentanoic	102.13	5	353.2	0.903	0.000	15.4	Byun, *et al.*, (2000)
Pentanoic	102.13	5	353.2	0.914	0.000	15.4	Byun, *et al.*, (2000)
Pentanoic	102.13	5	353.2	0.932	0.000	15.47	Byun, *et al.*, (2000)
Pentanoic	102.13	5	353.2	0.948	0.000	15.34	Byun, *et al.*, (2000)
Pentanoic	102.13	5	353.2	0.000	0.948	15.34	Byun, *et al.*, (2000)
Pentanoic	102.13	5	353.2	0.000	0.979	14.72	Byun, *et al.*, (2000)
Pentanoic	102.13	5	353.2	0.000	0.982	14.53	Byun, *et al.*, (2000)
Pentanoic	102.13	5	373.2	0.212	0.000	4.79	Byun, *et al.*, (2000)
Pentanoic	102.13	5	373.2	0.400	0.000	9.06	Byun, *et al.*, (2000)
Pentanoic	102.13	5	373.2	0.627	0.000	15.62	Byun, *et al.*, (2000)
Pentanoic	102.13	5	373.2	0.782	0.000	17.54	Byun, *et al.*, (2000)
Pentanoic	102.13	5	373.2	0.807	0.000	17.7	Byun, *et al.*, (2000)
Pentanoic	102.13	5	373.2	0.812	0.000	17.88	Byun, *et al.*, (2000)
Pentanoic	102.13	5	373.2	0.848	0.000	17.921	Byun, *et al.*, (2000)
Pentanoic	102.13	5	373.2	0.867	0.000	18.02	Byun, *et al.*, (2000)
Pentanoic	102.13	5	373.2	0.883	0.000	18.18	Byun, *et al.*, (2000)
Pentanoic	102.13	5	373.2	0.903	0.000	18.05	Byun, *et al.*, (2000)
Pentanoic	102.13	5	373.2	0.914	0.000	18.07	Byun, *et al.*, (2000)
Pentanoic	102.13	5	373.2	0.000	0.914	18.07	Byun, *et al.*, (2000)
Pentanoic	102.13	5	373.2	0.000	0.932	17.82	Byun, *et al.*, (2000)
Pentanoic	102.13	5	373.2	0.000	0.948	17.1	Byun, *et al.*, (2000)
Pentanoic	102.13	5	393.2	0.212	0.000	5.34	Byun, *et al.*, (2000)
Pentanoic	102.13	5	393.2	0.400	0.000	10.44	Byun, *et al.*, (2000)
Pentanoic	102.13	5	393.2	0.627	0.000	17.96	Byun, *et al.*, (2000)
Pentanoic	102.13	5	393.2	0.782	0.000	20.09	Byun, *et al.*, (2000)
Pentanoic	102.13	5	393.2	0.807	0.000	20.34	Byun, *et al.*, (2000)
Pentanoic	102.13	5	393.2	0.812	0.000	20.44	Byun, *et al.*, (2000)
Pentanoic	102.13	5	393.2	0.848	0.000	20.5	Byun, *et al.*, (2000)
Pentanoic	102.13	5	393.2	0.867	0.000	20.6	Byun, *et al.*, (2000)
Pentanoic	102.13	5	393.2	0.883	0.000	20.79	Byun, *et al.*, (2000)
Pentanoic	102.13	5	393.2	0.000	0.903	20.61	Byun, *et al.*, (2000)
Pentanoic	102.13	5	393.2	0.000	0.914	20.28	Byun, *et al.*, (2000)
Pentanoic	102.13	5	393.2	0.000	0.932	19.23	Byun, *et al.*, (2000)
Hexanoic	116.16	6	313.2	0.319	0.000	2.76	Bharath, *et al.*, (1993)
Hexanoic	116.16	6	313.2	0.535	0.999	5.29	Bharath, *et al.*, (1993)
Hexanoic	116.16	6	313.2	0.732	0.999	7.4	Bharath, *et al.*, (1993)
Hexanoic	116.16	6	313.2	0.911	0.999	8.46	Bharath, *et al.*, (1993)
Hexanoic	116.16	6	353.2	0.171	0.000	2.72	Bharath, *et al.*, (1993)

Table A-3 continued

Hexanoic	116.16	6	353.2	0.332	0.999	5.43	Bharath, *et al.*, (1993)
Hexanoic	116.16	6	353.2	0.430	0.999	7.55	Bharath, *et al.*, (1993)
Hexanoic	116.16	6	353.2	0.517	0.999	9.4	Bharath, *et al.*, (1993)
Hexanoic	116.16	6	353.2	0.704	0.989	13.68	Bharath, *et al.*, (1993)
Hexanoic	116.16	6	353.2	0.866	0.964	15.88	Bharath, *et al.*, (1993)
Hexanoic	116.16	6	308.2	0.751	0.000	2.53	Byun, *et al.*, (2000)
Hexanoic	116.16	6	308.2	0.618	0.000	3.72	Byun, *et al.*, (2000)
Hexanoic	116.16	6	308.2	0.493	0.000	4.75	Byun, *et al.*, (2000)
Hexanoic	116.16	6	308.2	0.386	0.000	5.89	Byun, *et al.*, (2000)
Hexanoic	116.16	6	308.2	0.279	0.000	6.62	Byun, *et al.*, (2000)
Hexanoic	116.16	6	308.2	0.223	0.000	6.91	Byun, *et al.*, (2000)
Hexanoic	116.16	6	308.2	0.173	0.000	7.12	Byun, *et al.*, (2000)
Hexanoic	116.16	6	308.2	0.137	0.000	7.37	Byun, *et al.*, (2000)
Hexanoic	116.16	6	308.2	0.101	0.000	7.38	Byun, *et al.*, (2000)
Hexanoic	116.16	6	308.2	0.093	0.000	7.42	Byun, *et al.*, (2000)
Hexanoic	116.16	6	308.2	0.077	0.000	7.49	Byun, *et al.*, (2000)
Hexanoic	116.16	6	308.2	0.076	0.000	7.51	Byun, *et al.*, (2000)
Hexanoic	116.16	6	308.2	0.058	0.000	7.51	Byun, *et al.*, (2000)
Hexanoic	116.16	6	308.2	0.055	0.000	7.58	Byun, *et al.*, (2000)
Hexanoic	116.16	6	308.2	0.054	0.000	7.63	Byun, *et al.*, (2000)
Hexanoic	116.16	6	308.2	0.039	0.000	7.53	Byun, *et al.*, (2000)
Hexanoic	116.16	6	308.2	0.023	0.000	7.8	Byun, *et al.*, (2000)
Hexanoic	116.16	6	308.2	0.012	0.000	7.91	Byun, *et al.*, (2000)
Hexanoic	116.16	6	308.2	0.006	0.994	7.81	Byun, *et al.*, (2000)
Hexanoic	116.16	6	308.2	0.000	0.997	7	Byun, *et al.*, (2000)
Hexanoic	116.16	6	328.2	0.249	0.000	3.27	Byun, *et al.*, (2000)
Hexanoic	116.16	6	328.2	0.382	0.000	4.82	Byun, *et al.*, (2000)
Hexanoic	116.16	6	328.2	0.507	0.000	6.89	Byun, *et al.*, (2000)
Hexanoic	116.16	6	328.2	0.614	0.000	8.03	Byun, *et al.*, (2000)
Hexanoic	116.16	6	328.2	0.721	0.000	9.63	Byun, *et al.*, (2000)
Hexanoic	116.16	6	328.2	0.777	0.000	10.03	Byun, *et al.*, (2000)
Hexanoic	116.16	6	328.2	0.827	0.000	10.58	Byun, *et al.*, (2000)
Hexanoic	116.16	6	328.2	0.863	0.000	10.99	Byun, *et al.*, (2000)
Hexanoic	116.16	6	328.2	0.899	0.000	11.28	Byun, *et al.*, (2000)
Hexanoic	116.16	6	328.2	0.907	0.000	11.25	Byun, *et al.*, (2000)
Hexanoic	116.16	6	328.2	0.923	0.000	11.34	Byun, *et al.*, (2000)
Hexanoic	116.16	6	328.2	0.924	0.000	11.37	Byun, *et al.*, (2000)
Hexanoic	116.16	6	328.2	0.942	0.000	11.39	Byun, *et al.*, (2000)
Hexanoic	116.16	6	328.2	0.945	0.000	11.31	Byun, *et al.*, (2000)
Hexanoic	116.16	6	328.2	0.946	0.000	11.41	Byun, *et al.*, (2000)
Hexanoic	116.16	6	328.2	0.961	0.000	11.49	Byun, *et al.*, (2000)
Hexanoic	116.16	6	328.2	0.000	0.977	11.3	Byun, *et al.*, (2000)
Hexanoic	116.16	6	328.2	0.000	0.988	11.11	Byun, *et al.*, (2000)
Hexanoic	116.16	6	328.2	0.000	0.994	10.68	Byun, *et al.*, (2000)

Table A-3 continued

Hexanoic	116.16	6	328.2	0.000	0.997	10.1	Byun, *et al.*, (2000)
Hexanoic	116.16	6	348.2	0.249	0.000	4.05	Byun, *et al.*, (2000)
Hexanoic	116.16	6	348.2	0.382	0.000	6.12	Byun, *et al.*, (2000)
Hexanoic	116.16	6	348.2	0.507	0.000	8.05	Byun, *et al.*, (2000)
Hexanoic	116.16	6	348.2	0.614	0.000	10.47	Byun, *et al.*, (2000)
Hexanoic	116.16	6	348.2	0.721	0.000	12.91	Byun, *et al.*, (2000)
Hexanoic	116.16	6	348.2	0.777	0.000	13.58	Byun, *et al.*, (2000)
Hexanoic	116.16	6	348.2	0.827	0.000	14.51	Byun, *et al.*, (2000)
Hexanoic	116.16	6	348.2	0.863	0.000	15.02	Byun, *et al.*, (2000)
Hexanoic	116.16	6	348.2	0.899	0.000	15.2	Byun, *et al.*, (2000)
Hexanoic	116.16	6	348.2	0.907	0.000	15.23	Byun, *et al.*, (2000)
Hexanoic	116.16	6	348.2	0.923	0.000	15.4	Byun, *et al.*, (2000)
Hexanoic	116.16	6	348.2	0.924	0.000	15.44	Byun, *et al.*, (2000)
Hexanoic	116.16	6	348.2	0.942	0.000	15.87	Byun, *et al.*, (2000)
Hexanoic	116.16	6	348.2	0.946	0.000	15.7	Byun, *et al.*, (2000)
Hexanoic	116.16	6	348.2	0.000	0.961	15.86	Byun, *et al.*, (2000)
Hexanoic	116.16	6	348.2	0.000	0.977	14.89	Byun, *et al.*, (2000)
Hexanoic	116.16	6	348.2	0.000	0.988	13.82	Byun, *et al.*, (2000)
Hexanoic	116.16	6	348.2	0.000	0.994	12.25	Byun, *et al.*, (2000)
Hexanoic	116.16	6	373.2	0.249	0.000	5.15	Byun, *et al.*, (2000)
Hexanoic	116.16	6	373.2	0.382	0.000	7.79	Byun, *et al.*, (2000)
Hexanoic	116.16	6	373.2	0.507	0.000	10.11	Byun, *et al.*, (2000)
Hexanoic	116.16	6	373.2	0.614	0.000	13.47	Byun, *et al.*, (2000)
Hexanoic	116.16	6	373.2	0.721	0.000	16.71	Byun, *et al.*, (2000)
Hexanoic	116.16	6	373.2	0.777	0.000	17.82	Byun, *et al.*, (2000)
Hexanoic	116.16	6	373.2	0.827	0.000	18.61	Byun, *et al.*, (2000)
Hexanoic	116.16	6	373.2	0.863	0.000	19.37	Byun, *et al.*, (2000)
Hexanoic	116.16	6	373.2	0.899	0.000	19.93	Byun, *et al.*, (2000)
Hexanoic	116.16	6	373.2	0.907	0.000	20.09	Byun, *et al.*, (2000)
Hexanoic	116.16	6	373.2	0.923	0.000	20.32	Byun, *et al.*, (2000)
Hexanoic	116.16	6	373.2	0.942	0.000	20.48	Byun, *et al.*, (2000)
Hexanoic	116.16	6	373.2	0.946	0.000	20.33	Byun, *et al.*, (2000)
Hexanoic	116.16	6	373.2	0.000	0.946	20.33	Byun, *et al.*, (2000)
Hexanoic	116.16	6	373.2	0.000	0.961	19.86	Byun, *et al.*, (2000)
Hexanoic	116.16	6	373.2	0.000	0.977	18.85	Byun, *et al.*, (2000)
Hexanoic	116.16	6	373.2	0.000	0.988	15.01	Byun, *et al.*, (2000)
Hexanoic	116.16	6	373.2	0.000	0.994	10.68	Byun, *et al.*, (2000)
Hexanoic	116.16	6	373.2	0.000	0.997	10.1	Byun, *et al.*, (2000)
Octanoic	144.21	8	313.2	0.000	0.908	10.4	Heo, *et al.*, (2001)
Octanoic	144.21	8	313.2	0.000	0.847	9.99	Heo, *et al.*, (2001)
Octanoic	144.21	8	313.2	0.000	0.798	9.2	Heo, *et al.*, (2001)
Octanoic	144.21	8	313.2	0.000	0.704	8.13	Heo, *et al.*, (2001)
Octanoic	144.21	8	313.2	0.000	0.655	7.48	Heo, *et al.*, (2001)
Octanoic	144.21	8	313.2	0.000	0.602	6.89	Heo, *et al.*, (2001)

Table A-3 continued

Octanoic	144.21	8	313.2	0.000	0.546	5.89	Heo, *et al.*, (2001)
Octanoic	144.21	8	323.2	0.000	0.908	13.23	Heo, *et al.*, (2001)
Octanoic	144.21	8	323.2	0.000	0.847	12.71	Heo, *et al.*, (2001)
Octanoic	144.21	8	323.2	0.000	0.798	11.09	Heo, *et al.*, (2001)
Octanoic	144.21	8	323.2	0.000	0.704	9.06	Heo, *et al.*, (2001)
Octanoic	144.21	8	323.2	0.000	0.655	8.42	Heo, *et al.*, (2001)
Octanoic	144.21	8	323.2	0.000	0.602	7.88	Heo, *et al.*, (2001)
Octanoic	144.21	8	323.2	0.000	0.546	6.83	Heo, *et al.*, (2001)
Octanoic	144.21	8	333.2	0.000	0.908	15.87	Heo, *et al.*, (2001)
Octanoic	144.21	8	333.2	0.000	0.847	15.28	Heo, *et al.*, (2001)
Octanoic	144.21	8	333.2	0.000	0.798	13.49	Heo, *et al.*, (2001)
Octanoic	144.21	8	333.2	0.000	0.704	10.46	Heo, *et al.*, (2001)
Octanoic	144.21	8	333.2	0.000	0.655	9.44	Heo, *et al.*, (2001)
Octanoic	144.21	8	333.2	0.000	0.602	8.45	Heo, *et al.*, (2001)
Octanoic	144.21	8	333.2	0.000	0.546	7.47	Heo, *et al.*, (2001)
Octanoic	144.21	8	343.2	0.000	0.908	18.41	Heo, *et al.*, (2001)
Octanoic	144.21	8	343.2	0.000	0.847	17.92	Heo, *et al.*, (2001)
Octanoic	144.21	8	343.2	0.000	0.798	16.08	Heo, *et al.*, (2001)
Octanoic	144.21	8	343.2	0.000	0.704	12.29	Heo, *et al.*, (2001)
Octanoic	144.21	8	343.2	0.000	0.655	10.66	Heo, *et al.*, (2001)
Octanoic	144.21	8	343.2	0.000	0.602	9.73	Heo, *et al.*, (2001)
Octanoic	144.21	8	343.2	0.000	0.546	8.49	Heo, *et al.*, (2001)
Octanoic	144.21	8	353.2	0.000	0.908	20.59	Heo, *et al.*, (2001)
Octanoic	144.21	8	353.2	0.000	0.847	20.15	Heo, *et al.*, (2001)
Octanoic	144.21	8	353.2	0.000	0.798	18.3	Heo, *et al.*, (2001)
Octanoic	144.21	8	353.2	0.000	0.704	14.51	Heo, *et al.*, (2001)
Octanoic	144.21	8	353.2	0.000	0.655	12.49	Heo, *et al.*, (2001)
Octanoic	144.21	8	353.2	0.000	0.602	11.05	Heo, *et al.*, (2001)
Octanoic	144.21	8	353.2	0.000	0.546	9.52	Heo, *et al.*, (2001)
Octanoic	144.21	8	308.2	0.241	0.000	2.33	Byun, *et al.*, (2000)
Octanoic	144.21	8	308.2	0.359	0.000	3.41	Byun, *et al.*, (2000)
Octanoic	144.21	8	308.2	0.505	0.000	4.72	Byun, *et al.*, (2000)
Octanoic	144.21	8	308.2	0.639	0.000	6.22	Byun, *et al.*, (2000)
Octanoic	144.21	8	308.2	0.763	0.000	7.3	Byun, *et al.*, (2000)
Octanoic	144.21	8	308.2	0.809	0.000	7.55	Byun, *et al.*, (2000)
Octanoic	144.21	8	308.2	0.859	0.000	7.58	Byun, *et al.*, (2000)
Octanoic	144.21	8	308.2	0.865	0.000	7.68	Byun, *et al.*, (2000)
Octanoic	144.21	8	308.2	0.887	0.000	7.78	Byun, *et al.*, (2000)
Octanoic	144.21	8	308.2	0.915	0.000	7.75	Byun, *et al.*, (2000)
Octanoic	144.21	8	308.2	0.929	0.000	7.8	Byun, *et al.*, (2000)
Octanoic	144.21	8	308.2	0.942	0.000	7.8	Byun, *et al.*, (2000)
Octanoic	144.21	8	308.2	0.959	0.000	7.8	Byun, *et al.*, (2000)
Octanoic	144.21	8	308.2	0.965	0.000	7.89	Byun, *et al.*, (2000)
Octanoic	144.21	8	308.2	0.971	0.000	7.77	Byun, *et al.*, (2000)

Table A-3 continued

Octanoic	144.21	8	308.2	0.975	0.000	7.84	Byun, *et al.*, (2000)
Octanoic	144.21	8	308.2	0.980	0.000	7.84	Byun, *et al.*, (2000)
Octanoic	144.21	8	308.2	0.986	0.000	7.84	Byun, *et al.*, (2000)
Octanoic	144.21	8	308.2	0.994	0.000	7.94	Byun, *et al.*, (2000)
Octanoic	144.21	8	308.2	0.000	0.994	7.94	Byun, *et al.*, (2000)
Octanoic	144.21	8	308.2	0.000	0.998	7.72	Byun, *et al.*, (2000)
Octanoic	144.21	8	308.2	0.000	0.999	7.62	Byun, *et al.*, (2000)
Octanoic	144.21	8	328.2	0.241	0.000	2.95	Byun, *et al.*, (2000)
Octanoic	144.21	8	328.2	0.359	0.000	4.36	Byun, *et al.*, (2000)
Octanoic	144.21	8	328.2	0.505	0.000	6.37	Byun, *et al.*, (2000)
Octanoic	144.21	8	328.2	0.639	0.000	8.6	Byun, *et al.*, (2000)
Octanoic	144.21	8	328.2	0.763	0.000	10.79	Byun, *et al.*, (2000)
Octanoic	144.21	8	328.2	0.809	0.000	11.59	Byun, *et al.*, (2000)
Octanoic	144.21	8	328.2	0.859	0.000	12.51	Byun, *et al.*, (2000)
Octanoic	144.21	8	328.2	0.865	0.000	12.56	Byun, *et al.*, (2000)
Octanoic	144.21	8	328.2	0.887	0.000	12.87	Byun, *et al.*, (2000)
Octanoic	144.21	8	328.2	0.915	0.000	13.47	Byun, *et al.*, (2000)
Octanoic	144.21	8	328.2	0.929	0.000	13.59	Byun, *et al.*, (2000)
Octanoic	144.21	8	328.2	0.942	0.000	13.68	Byun, *et al.*, (2000)
Octanoic	144.21	8	328.2	0.959	0.000	13.67	Byun, *et al.*, (2000)
Octanoic	144.21	8	328.2	0.000	0.959	13.67	Byun, *et al.*, (2000)
Octanoic	144.21	8	328.2	0.000	0.965	13.36	Byun, *et al.*, (2000)
Octanoic	144.21	8	328.2	0.000	0.971	13.2	Byun, *et al.*, (2000)
Octanoic	144.21	8	328.2	0.000	0.980	12.97	Byun, *et al.*, (2000)
Octanoic	144.21	8	328.2	0.000	0.986	12.65	Byun, *et al.*, (2000)
Octanoic	144.21	8	328.2	0.000	0.994	11.84	Byun, *et al.*, (2000)
Octanoic	144.21	8	328.2	0.000	0.998	10.85	Byun, *et al.*, (2000)
Octanoic	144.21	8	348.2	0.241	0.000	3.74	Byun, *et al.*, (2000)
Octanoic	144.21	8	348.2	0.359	0.000	5.44	Byun, *et al.*, (2000)
Octanoic	144.21	8	348.2	0.505	0.000	8.01	Byun, *et al.*, (2000)
Octanoic	144.21	8	348.2	0.639	0.000	11.2	Byun, *et al.*, (2000)
Octanoic	144.21	8	348.2	0.763	0.000	14.73	Byun, *et al.*, (2000)
Octanoic	144.21	8	348.2	0.809	0.000	15.82	Byun, *et al.*, (2000)
Octanoic	144.21	8	348.2	0.859	0.000	17.19	Byun, *et al.*, (2000)
Octanoic	144.21	8	348.2	0.865	0.000	17.32	Byun, *et al.*, (2000)
Octanoic	144.21	8	348.2	0.887	0.000	17.57	Byun, *et al.*, (2000)
Octanoic	144.21	8	348.2	0.915	0.000	17.92	Byun, *et al.*, (2000)
Octanoic	144.21	8	348.2	0.929	0.000	18.29	Byun, *et al.*, (2000)
Octanoic	144.21	8	348.2	0.942	0.000	18.54	Byun, *et al.*, (2000)
Octanoic	144.21	8	348.2	0.000	0.942	18.54	Byun, *et al.*, (2000)
Octanoic	144.21	8	348.2	0.000	0.959	18.18	Byun, *et al.*, (2000)
Octanoic	144.21	8	348.2	0.000	0.965	18.07	Byun, *et al.*, (2000)
Octanoic	144.21	8	348.2	0.000	0.971	17.59	Byun, *et al.*, (2000)
Octanoic	144.21	8	348.2	0.000	0.986	16.76	Byun, *et al.*, (2000)

Table A-3 continued

Octanoic	144.21	8	348.2	0.000	0.994	15.09	Byun, *et al.*, (2000)
Octanoic	144.21	8	348.2	0.000	0.998	12.23	Byun, *et al.*, (2000)
Octanoic	144.21	8	373.2	0.241	0.000	4.52	Byun, *et al.*, (2000)
Octanoic	144.21	8	373.2	0.359	0.000	6.61	Byun, *et al.*, (2000)
Octanoic	144.21	8	373.2	0.505	0.000	10.06	Byun, *et al.*, (2000)
Octanoic	144.21	8	373.2	0.639	0.000	14.27	Byun, *et al.*, (2000)
Octanoic	144.21	8	373.2	0.763	0.000	18.97	Byun, *et al.*, (2000)
Octanoic	144.21	8	373.2	0.809	0.000	20.33	Byun, *et al.*, (2000)
Octanoic	144.21	8	373.2	0.859	0.000	21.95	Byun, *et al.*, (2000)
Octanoic	144.21	8	373.2	0.865	0.000	21.96	Byun, *et al.*, (2000)
Octanoic	144.21	8	373.2	0.887	0.000	22.59	Byun, *et al.*, (2000)
Octanoic	144.21	8	373.2	0.915	0.000	23.77	Byun, *et al.*, (2000)
Octanoic	144.21	8	373.2	0.929	0.000	23.79	Byun, *et al.*, (2000)
Octanoic	144.21	8	373.2	0.000	0.942	24.01	Byun, *et al.*, (2000)
Octanoic	144.21	8	373.2	0.000	0.965	23.54	Byun, *et al.*, (2000)
Octanoic	144.21	8	373.2	0.000	0.971	23.05	Byun, *et al.*, (2000)
Octanoic	144.21	8	373.2	0.000	0.986	19.75	Byun, *et al.*, (2000)
Octanoic	144.21	8	373.2	0.000	0.994	16.66	Byun, *et al.*, (2000)
Nonanoic	158.24	9	313.0	0.000	0.214	1.9	Schieman, *et al.*, (1993)
Nonanoic	158.24	9	313.0	0.000	0.394	4	Schieman, *et al.*, (1993)
Nonanoic	158.24	9	313.0	0.000	0.548	6	Schieman, *et al.*, (1993)
Nonanoic	158.24	9	313.0	0.000	0.586	6.6	Schieman, *et al.*, (1993)
Nonanoic	158.24	9	313.0	0.000	0.632	7.3	Schieman, *et al.*, (1993)
Nonanoic	158.24	9	313.0	0.000	0.682	8.1	Schieman, *et al.*, (1993)
Nonanoic	158.24	9	313.0	0.000	0.746	9	Schieman, *et al.*, (1993)
Nonanoic	158.24	9	313.0	0.000	0.816	10	Schieman, *et al.*, (1993)
Nonanoic	158.24	9	313.0	0.000	0.839	10.5	Schieman, *et al.*, (1993)
Nonanoic	158.24	9	333.0	0.000	0.181	2.05	Schieman, *et al.*, (1993)
Nonanoic	158.24	9	333.0	0.000	0.333	4.25	Schieman, *et al.*, (1993)
Nonanoic	158.24	9	333.0	0.000	0.417	5.75	Schieman, *et al.*, (1993)
Nonanoic	158.24	9	333.0	0.000	0.573	8.8	Schieman, *et al.*, (1993)
Nonanoic	158.24	9	333.0	0.000	0.658	10.5	Schieman, *et al.*, (1993)
Nonanoic	158.24	9	333.0	0.000	0.745	13	Schieman, *et al.*, (1993)
Nonanoic	158.24	9	353.0	0.000	0.156	2	Schieman, *et al.*, (1993)
Nonanoic	158.24	9	353.0	0.000	0.274	4.1	Schieman, *et al.*, (1993)
Nonanoic	158.24	9	353.0	0.000	0.381	6.25	Schieman, *et al.*, (1993)
Nonanoic	158.24	9	353.0	0.000	0.459	8.1	Schieman, *et al.*, (1993)
Nonanoic	158.24	9	353.0	0.000	0.552	10.5	Schieman, *et al.*, (1993)
Nonanoic	158.24	9	353.0	0.000	0.601	12	Schieman, *et al.*, (1993)
Nonanoic	158.24	9	353.0	0.000	0.625	12.8	Schieman, *et al.*, (1993)
Nonanoic	158.24	9	353.0	0.000	0.670	14.3	Schieman, *et al.*, (1993)
Nonanoic	158.24	9	373.0	0.000	0.072	1.1	Schieman, *et al.*, (1993)
Nonanoic	158.24	9	373.0	0.000	0.124	2	Schieman, *et al.*, (1993)
Nonanoic	158.24	9	373.0	0.000	0.238	4.4	Schieman, *et al.*, (1993)

Table A-3 continued

Nonanoic	158.24	9	373.0	0.000	0.352	6.9	Schieman, *et al.*, (1993)
Nonanoic	158.24	9	373.0	0.000	0.464	10.1	Schieman, *et al.*, (1993)
Nonanoic	158.24	9	373.0	0.000	0.536	12.35	Schieman, *et al.*, (1993)
Nonanoic	158.24	9	373.0	0.000	0.658	16.7	Schieman, *et al.*, (1993)
Nonanoic	158.24	9	373.0	0.000	0.731	19.95	Schieman, *et al.*, (1993)
Nonanoic	158.24	9	373.0	0.000	0.790	23	Schieman, *et al.*, (1993)
Nonanoic	158.24	9	393.0	0.000	0.000	20	Schieman, *et al.*, (1993)
Nonanoic	158.24	9	393.0	0.000	0.000	40.5	Schieman, *et al.*, (1993)
Nonanoic	158.24	9	393.0	0.000	0.000	60.5	Schieman, *et al.*, (1993)
Nonanoic	158.24	9	393.0	0.000	0.000	82	Schieman, *et al.*, (1993)
Nonanoic	158.24	9	393.0	0.000	0.000	110	Schieman, *et al.*, (1993)
Nonanoic	158.24	9	393.0	0.000	0.000	131	Schieman, *et al.*, (1993)
Nonanoic	158.24	9	393.0	0.000	0.000	143.5	Schieman, *et al.*, (1993)
Nonanoic	158.24	9	393.0	0.000	0.000	169	Schieman, *et al.*, (1993)
Nonanoic	158.24	9	393.0	0.000	0.000	201	Schieman, *et al.*, (1993)
Nonanoic	158.24	9	393.0	0.000	0.100	20	Schieman, *et al.*, (1993)
Nonanoic	158.24	9	393.0	0.000	0.213	40.5	Schieman, *et al.*, (1993)
Nonanoic	158.24	9	393.0	0.000	0.286	60.5	Schieman, *et al.*, (1993)
Nonanoic	158.24	9	393.0	0.000	0.369	82	Schieman, *et al.*, (1993)
Nonanoic	158.24	9	393.0	0.000	0.424	110	Schieman, *et al.*, (1993)
Nonanoic	158.24	9	393.0	0.000	0.504	131	Schieman, *et al.*, (1993)
Nonanoic	158.24	9	393.0	0.000	0.545	143.5	Schieman, *et al.*, (1993)
Nonanoic	158.24	9	393.0	0.000	0.606	169	Schieman, *et al.*, (1993)
Nonanoic	158.24	9	393.0	0.000	0.679	201	Schieman, *et al.*, (1993)
Decanoic	172.27	10	313.2	0.000	0.898	13.79	Heo, *et al.*, (2001)
Decanoic	172.27	10	313.2	0.000	0.822	10.3	Heo, *et al.*, (2001)
Decanoic	172.27	10	313.2	0.000	0.694	7.54	Heo, *et al.*, (2001)
Decanoic	172.27	10	313.2	0.000	0.602	5.14	Heo, *et al.*, (2001)
Decanoic	172.27	10	313.2	0.000	0.498	3.97	Heo, *et al.*, (2001)
Decanoic	172.27	10	313.2	0.000	0.393	2.2	Heo, *et al.*, (2001)
Decanoic	172.27	10	323.2	0.000	0.898	16.76	Heo, *et al.*, (2001)
Decanoic	172.27	10	323.2	0.000	0.822	13.16	Heo, *et al.*, (2001)
Decanoic	172.27	10	323.2	0.000	0.694	8.48	Heo, *et al.*, (2001)
Decanoic	172.27	10	323.2	0.000	0.602	6.61	Heo, *et al.*, (2001)
Decanoic	172.27	10	323.2	0.000	0.498	4.69	Heo, *et al.*, (2001)
Decanoic	172.27	10	323.2	0.000	0.393	2.85	Heo, *et al.*, (2001)
Decanoic	172.27	10	333.2	0.000	0.898	19.39	Heo, *et al.*, (2001)
Decanoic	172.27	10	333.2	0.000	0.822	15.8	Heo, *et al.*, (2001)
Decanoic	172.27	10	333.2	0.000	0.694	9.32	Heo, *et al.*, (2001)
Decanoic	172.27	10	333.2	0.000	0.602	7.77	Heo, *et al.*, (2001)
Decanoic	172.27	10	333.2	0.000	0.498	5.71	Heo, *et al.*, (2001)
Decanoic	172.27	10	333.2	0.000	0.393	3.81	Heo, *et al.*, (2001)
Decanoic	172.27	10	343.2	0.000	0.898	21.59	Heo, *et al.*, (2001)
Decanoic	172.27	10	343.2	0.000	0.822	18.22	Heo, *et al.*, (2001)

Table A-3 continued

Decanoic	172.27	10	343.2	0.000	0.694	10.75	Heo, *et al.*, (2001)
Decanoic	172.27	10	343.2	0.000	0.602	8.77	Heo, *et al.*, (2001)
Decanoic	172.27	10	343.2	0.000	0.498	6.52	Heo, *et al.*, (2001)
Decanoic	172.27	10	343.2	0.000	0.393	4.45	Heo, *et al.*, (2001)
Decanoic	172.27	10	353.2	0.000	0.898	23.77	Heo, *et al.*, (2001)
Decanoic	172.27	10	353.2	0.000	0.822	20.43	Heo, *et al.*, (2001)
Decanoic	172.27	10	353.2	0.000	0.694	11.91	Heo, *et al.*, (2001)
Decanoic	172.27	10	353.2	0.000	0.602	10.09	Heo, *et al.*, (2001)
Decanoic	172.27	10	353.2	0.000	0.498	7.73	Heo, *et al.*, (2001)
Decanoic	172.27	10	353.2	0.000	0.393	5.07	Heo, *et al.*, (2001)
Decanoic	172.27	10	323.2	0.677	1.000	10	Pohler (1994)
Decanoic	172.27	10	323.2	0.767	0.998	12.5	Pohler (1994)
Decanoic	172.27	10	323.2	0.866	0.987	15	Pohler (1994)
Decanoic	172.27	10	323.2	0.923	0.980	16	Pohler (1994)
Decanoic	172.27	10	323.2	0.948	0.948	16.4	Pohler (1994)
Decanoic	172.27	10	353.2	0.612	1.000	10	Pohler (1994)
Decanoic	172.27	10	353.2	0.693	1.000	12.5	Pohler (1994)
Decanoic	172.27	10	353.2	0.747	0.999	15	Pohler (1994)
Decanoic	172.27	10	353.2	0.791	0.996	17.5	Pohler (1994)
Decanoic	172.27	10	353.2	0.852	0.990	20	Pohler (1994)
Decanoic	172.27	10	353.2	0.896	0.977	22.5	Pohler (1994)
Decanoic	172.27	10	353.2	0.943	0.943	22.9	Pohler (1994)
Decanoic	172.27	10	393.2	0.479	1.000	10	Pohler (1994)
Decanoic	172.27	10	393.2	0.568	1.000	15	Pohler (1994)
Decanoic	172.27	10	393.2	0.633	0.999	17.5	Pohler (1994)
Decanoic	172.27	10	393.2	0.679	0.996	20	Pohler (1994)
Decanoic	172.27	10	393.2	0.717	0.994	22.5	Pohler (1994)
Decanoic	172.27	10	393.2	0.771	0.989	25	Pohler (1994)
Decanoic	172.27	10	393.2	0.835	0.978	27.5	Pohler (1994)
Decanoic	172.27	10	393.2	0.928	0.928	28.7	Pohler (1994)
Dodecanoic	200.32	12	318.2	0.695	1.000	10	Pohler (1994)
Dodecanoic	200.32	12	318.2	0.781	0.998	15	Pohler (1994)
Dodecanoic	200.32	12	318.2	0.794	0.995	18	Pohler (1994)
Dodecanoic	200.32	12	318.2	0.808	0.992	20	Pohler (1994)
Dodecanoic	200.32	12	318.2	0.872	0.990	21	Pohler (1994)
Dodecanoic	200.32	12	318.2	0.891	0.984	22	Pohler (1994)
Dodecanoic	200.32	12	318.2	0.915	0.915	24.3	Pohler (1994)
Dodecanoic	200.32	12	323.2	0.584	1.000	10	Pohler (1994)
Dodecanoic	200.32	12	323.2	0.664	0.997	15	Pohler (1994)
Dodecanoic	200.32	12	323.2	0.761	0.993	17.5	Pohler (1994)
Dodecanoic	200.32	12	323.2	0.831	0.989	20	Pohler (1994)
Dodecanoic	200.32	12	323.2	0.917	0.917	23.6	Pohler (1994)
Dodecanoic	200.32	12	333.2	0.571	1.000	10	Pohler (1994)
Dodecanoic	200.32	12	333.2	0.648	0.998	15	Pohler (1994)

Table A-3 continued

Dodecanoic	200.32	12	333.2	0.745	0.996	17.5	Pohler (1994)
Dodecanoic	200.32	12	333.2	0.778	0.990	20	Pohler (1994)
Dodecanoic	200.32	12	333.2	0.842	0.978	22.5	Pohler (1994)
Dodecanoic	200.32	12	333.2	0.917	0.917	24.9	Pohler (1994)
Dodecanoic	200.32	12	343.2	0.461	1.000	10	Pohler (1994)
Dodecanoic	200.32	12	343.2	0.604	0.998	15	Pohler (1994)
Dodecanoic	200.32	12	343.2	0.654	0.996	17.5	Pohler (1994)
Dodecanoic	200.32	12	343.2	0.743	0.992	20	Pohler (1994)
Dodecanoic	200.32	12	343.2	0.764	0.984	22.5	Pohler (1994)
Dodecanoic	200.32	12	343.2	0.806	0.965	25	Pohler (1994)
Dodecanoic	200.32	12	343.2	0.916	0.916	26.5	Pohler (1994)
Dodecanoic	200.32	12	348.2	0.550	1.000	10	Pohler (1994)
Dodecanoic	200.32	12	348.2	0.584	1.000	15	Pohler (1994)
Dodecanoic	200.32	12	348.2	0.712	0.997	20	Pohler (1994)
Dodecanoic	200.32	12	348.2	0.774	0.995	22	Pohler (1994)
Dodecanoic	200.32	12	348.2	0.824	0.993	24	Pohler (1994)
Dodecanoic	200.32	12	348.2	0.867	0.987	26	Pohler (1994)
Dodecanoic	200.32	12	348.2	0.920	0.920	27.9	Pohler (1994)
Dodecanoic	200.32	12	353.2	0.523	1.000	10	Pohler (1994)
Dodecanoic	200.32	12	353.2	0.572	1.000	15	Pohler (1994)
Dodecanoic	200.32	12	353.2	0.675	0.997	17.5	Pohler (1994)
Dodecanoic	200.32	12	353.2	0.739	0.994	20	Pohler (1994)
Dodecanoic	200.32	12	353.2	0.790	0.993	23	Pohler (1994)
Dodecanoic	200.32	12	353.2	0.822	0.985	25	Pohler (1994)
Dodecanoic	200.32	12	353.2	0.860	0.960	27.5	Pohler (1994)
Dodecanoic	200.32	12	353.2	0.915	0.915	28.4	Pohler (1994)
Dodecanoic	200.32	12	373.2	0.488	1.000	10	Pohler (1994)
Dodecanoic	200.32	12	373.2	0.561	0.999	15	Pohler (1994)
Dodecanoic	200.32	12	373.2	0.638	0.997	20	Pohler (1994)
Dodecanoic	200.32	12	373.2	0.726	0.990	25	Pohler (1994)
Dodecanoic	200.32	12	373.2	0.778	0.981	27.5	Pohler (1994)
Dodecanoic	200.32	12	373.2	0.902	0.902	30.7	Pohler (1994)
Dodecanoic	200.32	12	333.1	0.247	0.000	2.57	Bharath, *et al.*, (1993)
Dodecanoic	200.32	12	333.1	0.433	0.000	5.34	Bharath, *et al.*, (1993)
Dodecanoic	200.32	12	333.1	0.482	0.000	6.41	Bharath, *et al.*, (1993)
Dodecanoic	200.32	12	333.1	0.597	0.000	8.92	Bharath, *et al.*, (1993)
Dodecanoic	200.32	12	333.1	0.667	0.000	11.58	Bharath, *et al.*, (1993)
Dodecanoic	200.32	12	333.1	0.720	0.000	13.27	Bharath, *et al.*, (1993)
Dodecanoic	200.32	12	333.1	0.777	0.000	16.81	Bharath, *et al.*, (1993)
Dodecanoic	200.32	12	333.1	0.825	0.000	20.39	Bharath, *et al.*, (1993)
Dodecanoic	200.32	12	333.1	0.853	0.000	22.69	Bharath, *et al.*, (1993)
Dodecanoic	200.32	12	333.1	0.883	0.000	24.64	Bharath, *et al.*, (1993)
Dodecanoic	200.32	12	333.1	0.000	0.000	2.57	Bharath, *et al.*, (1993)
Dodecanoic	200.32	12	333.1	0.000	0.000	5.34	Bharath, *et al.*, (1993)

Table A-3 continued

Dodecanoic	200.32	12	333.1	0.000	1.000	6.41	Bharath, *et al.*, (1993)
Dodecanoic	200.32	12	333.1	0.000	1.000	8.92	Bharath, *et al.*, (1993)
Dodecanoic	200.32	12	333.1	0.000	1.000	11.58	Bharath, *et al.*, (1993)
Dodecanoic	200.32	12	333.1	0.000	0.999	13.27	Bharath, *et al.*, (1993)
Dodecanoic	200.32	12	333.1	0.000	0.995	16.81	Bharath, *et al.*, (1993)
Dodecanoic	200.32	12	333.1	0.000	0.988	20.39	Bharath, *et al.*, (1993)
Dodecanoic	200.32	12	333.1	0.000	0.981	22.69	Bharath, *et al.*, (1993)
Dodecanoic	200.32	12	333.1	0.000	0.959	24.64	Bharath, *et al.*, (1993)
Dodecanoic	200.32	12	353.2	0.351	0.999	5.33	Bharath, *et al.*, (1993)
Dodecanoic	200.32	12	353.2	0.540	0.999	10.07	Bharath, *et al.*, (1993)
Dodecanoic	200.32	12	353.2	0.693	1.000	15.38	Bharath, *et al.*, (1993)
Dodecanoic	200.32	12	353.2	0.771	0.995	20.15	Bharath, *et al.*, (1993)
Dodecanoic	200.32	12	353.2	0.844	0.984	25.19	Bharath, *et al.*, (1993)
Dodecanoic	200.32	12	353.2	0.893	0.969	27.65	Bharath, *et al.*, (1993)
Dodecanoic	200.32	12	373.2	0.066	1.000	1.01	Yau, *et al.*, (1992)
Dodecanoic	200.32	12	373.2	0.134	1.000	2.03	Yau, *et al.*, (1992)
Dodecanoic	200.32	12	373.2	0.201	1.000	3.04	Yau, *et al.*, (1992)
Dodecanoic	200.32	12	373.2	0.269	1.000	4.05	Yau, *et al.*, (1992)
Dodecanoic	200.32	12	373.2	0.338	1.000	5.07	Yau, *et al.*, (1992)
Dodecanoic	200.32	12	393.0	0.419	1.000	10	Kordikowski (1992)
Dodecanoic	200.32	12	393.0	0.541	0.999	15	Kordikowski (1992)
Dodecanoic	200.32	12	393.0	0.648	0.998	20	Kordikowski (1992)
Dodecanoic	200.32	12	393.0	0.728	0.994	25	Kordikowski (1992)
Dodecanoic	200.32	12	393.0	0.805	0.982	30	Kordikowski (1992)
Dodecanoic	200.32	12	393.0	0.894	0.941	32.5	Kordikowski (1992)
Dodecanoic	200.32	12	393.0	0.929	0.928	32.6	Kordikowski (1992)
Tetradecanoic	228.38	14	328.2	0.696	0.999	10	Pohler (1994)
Tetradecanoic	228.38	14	328.2	0.736	0.996	15	Pohler (1994)
Tetradecanoic	228.38	14	328.2	0.790	0.994	20	Pohler (1994)
Tetradecanoic	228.38	14	328.2	0.833	0.989	25	Pohler (1994)
Tetradecanoic	228.38	14	328.2	0.874	0.978	30	Pohler (1994)
Tetradecanoic	228.38	14	328.2	0.885	0.976	32.5	Pohler (1994)
Tetradecanoic	228.38	14	328.2	0.913	0.963	35	Pohler (1994)
Tetradecanoic	228.38	14	328.2	0.931	0.931	36.2	Pohler (1994)
Tetradecanoic	228.38	14	333.2	0.718	0.999	10	Pohler (1994)
Tetradecanoic	228.38	14	333.2	0.795	0.997	20	Pohler (1994)
Tetradecanoic	228.38	14	333.2	0.848	0.991	25	Pohler (1994)
Tetradecanoic	228.38	14	333.2	0.881	0.982	30	Pohler (1994)
Tetradecanoic	228.38	14	333.2	0.909	0.977	32	Pohler (1994)
Tetradecanoic	228.38	14	333.2	0.911	0.969	33.5	Pohler (1994)
Tetradecanoic	228.38	14	333.2	0.941	0.941	35.5	Pohler (1994)
Tetradecanoic	228.38	14	343.2	0.617	0.999	10	Pohler (1994)
Tetradecanoic	228.38	14	343.2	0.728	0.998	15	Pohler (1994)
Tetradecanoic	228.38	14	343.2	0.801	0.998	20	Pohler (1994)

Table A-3 continued

Tetradecanoic	228.38	14	343.2	0.828	0.996	25	Pohler (1994)
Tetradecanoic	228.38	14	343.2	0.873	0.993	30	Pohler (1994)
Tetradecanoic	228.38	14	343.2	0.897	0.989	33.5	Pohler (1994)
Tetradecanoic	228.38	14	343.2	0.934	0.934	34.7	Pohler (1994)
Tetradecanoic	228.38	14	353.2	0.941	0.941	35	Pohler (1994)
Tetradecanoic	228.38	14	373.2	0.559	0.999	10	Pohler (1994)
Tetradecanoic	228.38	14	373.2	0.654	0.998	15	Pohler (1994)
Tetradecanoic	228.38	14	373.2	0.704	0.996	20	Pohler (1994)
Tetradecanoic	228.38	14	373.2	0.754	0.995	25	Pohler (1994)
Tetradecanoic	228.38	14	373.2	0.807	0.989	28.5	Pohler (1994)
Tetradecanoic	228.38	14	373.2	0.842	0.982	30	Pohler (1994)
Tetradecanoic	228.38	14	373.2	0.862	0.975	32.5	Pohler (1994)
Tetradecanoic	228.38	14	373.2	0.907	0.964	35	Pohler (1994)
Tetradecanoic	228.38	14	373.2	0.940	0.940	36	Pohler (1994)
Tetradecanoic	228.38	14	393.2	0.501	0.999	10	Pohler (1994)
Tetradecanoic	228.38	14	393.2	0.613	0.998	15	Pohler (1994)
Tetradecanoic	228.38	14	393.2	0.670	0.996	17.5	Pohler (1994)
Tetradecanoic	228.38	14	393.2	0.695	0.993	20	Pohler (1994)
Tetradecanoic	228.38	14	393.2	0.735	0.991	22.5	Pohler (1994)
Tetradecanoic	228.38	14	393.2	0.778	0.990	25	Pohler (1994)
Tetradecanoic	228.38	14	393.2	0.794	0.988	27.5	Pohler (1994)
Tetradecanoic	228.38	14	393.2	0.820	0.987	30	Pohler (1994)
Tetradecanoic	228.38	14	393.2	0.841	0.984	32.5	Pohler (1994)
Tetradecanoic	228.38	14	393.2	0.856	0.979	35	Pohler (1994)
Tetradecanoic	228.38	14	393.2	0.878	0.973	36	Pohler (1994)
Tetradecanoic	228.38	14	393.2	0.934	0.934	37.5	Pohler (1994)
Octadecanoic	284.48	18	353.0	0.000	0.199	2.15	Schiemann, *et al.*, (1993)
Octadecanoic	284.48	18	353.0	0.000	0.327	4.55	Schiemann, *et al.*, (1993)
Octadecanoic	284.48	18	353.0	0.000	0.504	8.45	Schiemann, *et al.*, (1993)
Octadecanoic	284.48	18	353.0	0.000	0.588	11.5	Schiemann, *et al.*, (1993)
Octadecanoic	284.48	18	353.0	0.000	0.641	14.2	Schiemann, *et al.*, (1993)
Octadecanoic	284.48	18	353.0	0.000	0.656	14.95	Schiemann, *et al.*, (1993)
Octadecanoic	284.48	18	353.0	0.000	0.699	18.15	Schiemann, *et al.*, (1993)
Octadecanoic	284.48	18	353.0	0.000	0.731	21.25	Schiemann, *et al.*, (1993)
Octadecanoic	284.48	18	353.0	0.000	0.778	25.8	Schiemann, *et al.*, (1993)
Octadecanoic	284.48	18	373.0	0.000	0.212	2.5	Schiemann, *et al.*, (1993)
Octadecanoic	284.48	18	373.0	0.000	0.334	5.4	Schiemann, *et al.*, (1993)
Octadecanoic	284.48	18	373.0	0.000	0.444	8.3	Schiemann, *et al.*, (1993)
Octadecanoic	284.48	18	373.0	0.000	0.529	11.1	Schiemann, *et al.*, (1993)
Octadecanoic	284.48	18	373.0	0.000	0.603	14.1	Schiemann, *et al.*, (1993)
Octadecanoic	284.48	18	373.0	0.000	0.660	17.55	Schiemann, *et al.*, (1993)
Octadecanoic	284.48	18	373.0	0.000	0.699	20.2	Schiemann, *et al.*, (1993)
Octadecanoic	284.48	18	373.0	0.000	0.723	22.7	Schiemann, *et al.*, (1993)
Octadecanoic	284.48	18	373.0	0.000	0.761	26	Schiemann, *et al.*, (1993)

Table A-3 continued

Octadecanoic	284.48	18	393.0	0.000	0.185	2.7	Schiemann, *et al.*, (1993)
Octadecanoic	284.48	18	393.0	0.000	0.321	5.75	Schiemann, *et al.*, (1993)
Octadecanoic	284.48	18	393.0	0.000	0.436	8.6	Schiemann, *et al.*, (1993)
Octadecanoic	284.48	18	393.0	0.000	0.464	9.85	Schiemann, *et al.*, (1993)
Octadecanoic	284.48	18	393.0	0.000	0.480	10.35	Schiemann, *et al.*, (1993)
Octadecanoic	284.48	18	393.0	0.000	0.548	13.1	Schiemann, *et al.*, (1993)
Octadecanoic	284.48	18	393.0	0.000	0.596	17.25	Schiemann, *et al.*, (1993)
Octadecanoic	284.48	18	393.0	0.000	0.720	24.75	Schiemann, *et al.*, (1993)
Octadecanoic	284.48	18	393.0	0.000	0.737	26.15	Schiemann, *et al.*, (1993)

Table A-4: Critical temperature, critical pressure and acentric factors of alkanes used to train neural networks

Component	T_c **(K)**	P_c **(Mpa)**	w	**Reference**
Pentane	469.7	3.36	0.251	Don, *et al.*, (2007)
Hexane	507.6	3.04	0.304	Don, *et al.*, (2007)
Heptane	540.2	2.72	0.346	Don, *et al.*, (2007)
Octane	568.7	2.47	0.396	Don, *et al.*, (2007)
Octane	568.7	2.47	0.396	Don, *et al.*, (2007)
Octane	568.7	2.47	0.396	Don, *et al.*, (2007)
Nonane	594.6	2.31	0.446	Don, *et al.*, (2007)
Nonane	594.6	2.31	0.446	Don, *et al.*, (2007)
Decane	617.7	2.09	0.488	Don, *et al.*, (2007)
Decane	617.7	2.09	0.488	Don, *et al.*, (2007)
Decane	617.7	2.09	0.488	Don, *et al.*, (2007)
Decane	617.7	2.09	0.488	Don, *et al.*, (2007)
Decane	617.7	2.09	0.488	Don, *et al.*, (2007)
Decane	617.7	2.09	0.488	Don, *et al.*, (2007)
Undecane	639	1.95	0.53	Don, *et al.*, (2007)
Dodecane	658.2	1.82	0.577	Don, *et al.*, (2007)
Pentadecane	708	1.47	0.685	Don, *et al.*, (2007)
Hexadecane	723	1.41	0.721	Don, *et al.*, (2007)
Hexadecane	723	1.41	0.721	Don, *et al.*, (2007)
Hexadecane	723	1.41	0.721	Don, *et al.*, (2007)
Hexadecane	723	1.41	0.721	Don, *et al.*, (2007)
Hexadecane	723	1.41	0.721	Don, *et al.*, (2007)
Heptadecane	736	1.34	0.771	Don, *et al.*, (2007)
Octadecane	747	1.26	0.806	Don, *et al.*, (2007)
Nonadecane	758	1.21	0.851	Don, *et al.*, (2007)
Nonadecane	758	1.21	0.851	Don, *et al.*, (2007)
Nonadecane	758	1.21	0.851	Don, *et al.*, (2007)
Eicosane	768	1.17	0.912	Don, *et al.*, (2007)
Eicosane	768	1.17	0.912	Don, *et al.*, (2007)
Eicosane	768	1.17	0.912	Don, *et al.*, (2007)

Table A-5: Critical temperature, critical pressure and acentric factors of alcohols used to train neural networks

Component	T_c (K)	P_c (Mpa)	w	Reference
1-propanol	536.78	5.12	0.670	Don, *et al.*, (2007)
1-butanol	563.05	4.34	0.585	Don, *et al.*, (2007)
1-butanol	563.05	4.34	0.585	Don, *et al.*, (2007)
1-hexanol	611.35	3.46	0.572	Don, *et al.*, (2007)
1-hexanol	611.35	3.46	0.572	Don, *et al.*, (2007)
1-heptanol	631.90	3.18	0.592	Don, *et al.*, (2007)
1-heptanol	631.90	3.18	0.592	Don, *et al.*, (2007)
1-heptanol	631.90	3.18	0.592	Don, *et al.*, (2007)
1-octanol	652.50	2.70	0.598	Ambrose & Sparke (1970)
1-octanol	652.50	2.70	0.598	Ambrose & Sparke (1970)
1-octanol	652.50	2.70	0.598	Ambrose & Sparke (1970)
1-octanol	652.50	2.70	0.598	Ambrose & Sparke (1970)
1-octanol	652.50	2.70	0.598	Ambrose & Sparke (1970)
1-octanol	652.50	2.70	0.598	Ambrose & Sparke (1970)
1-octanol	652.50	2.70	0.598	Ambrose & Sparke (1970)
1-octanol	652.50	2.70	0.598	Ambrose & Sparke (1970)
1-nonanol	672.00	2.55	0.591	Rosenthal & Teja (1989); Kremme & Kreps (1969)
1-nonanol	672.00	2.55	0.591	Rosenthal & Teja (1989); Kremme & Kreps (1969)
1-nonanol	672.00	2.55	0.591	Rosenthal & Teja (1989); Kremme & Kreps (1969)
1-decanol	690.00	2.32	0.603	Rosenthal & Teja (1989)
1-decanol	690.00	2.32	0.603	Rosenthal & Teja (1989)
1-decanol	690.00	2.32	0.603	Rosenthal & Teja (1989)
1-decanol	690.00	2.32	0.603	Rosenthal & Teja (1989)
1-decanol	690.00	2.32	0.603	Rosenthal & Teja (1989)
1-dodecanol	719.40	1.99	0.670	Ambrose & Sparke (1970)
1-dodecanol	719.40	1.99	0.670	Ambrose & Sparke (1970)
1-dodecanol	719.40	1.99	0.670	Ambrose & Sparke (1970)
1-dodecanol	719.40	1.99	0.670	Ambrose & Sparke (1970)
1-dodecanol	719.40	1.99	0.670	Ambrose & Sparke (1970)
1-dodecanol	719.40	1.99	0.670	Ambrose & Sparke (1970)
1-tetradecanol	769.95	1.64	0.518	Kremme & Kreps (1969)
1-hexadecanol	817.45	1.41	0.394	Kremme & Kreps (1969)
1-hexadecanol	817.45	1.41	0.394	Kremme & Kreps (1969)
1-octadecanol	536.78	5.12	0.670	Ambrose & Sparke (1970)

Table A-6: Critical temperature, critical pressure and acentric factors of carboxylic acids used to train neural networks

Component	T_c (K)	P_c (Mpa)	w	Reference
Butanoic Acid	627.90	4.06	0.604	Byun, *et al.*, (2000)
Pentanoic Acid	644.00	3.63	0.627	Byun, *et al.*, (2000)
Hexanoic Acid	663.00	3.20	0.670	Byun, *et al.*, (2000)
Hexanoic Acid	663.00	3.20	0.670	Byun, *et al.*, (2000)
Octanoic Acid	663.00	3.20	0.779	Byun, *et al.*, (2000)
Octanoic Acid	694.00	2.70	0.779	Byun, *et al.*, (2000)
Nonanoic Acid	712.00	2.35	0.764	Ambrose & Ghiassee (1987); Schiemann, *et al.,* (1993)
Decanoic Acid	726.00	2.10	0.775	Ambrose & Ghiassee (1987); Heo, *et al.*, (2001)
Decanoic Acid	726.00	2.10	0.775	Ambrose & Ghiassee (1987); Pohler (1994)
Dodecanoic Acid	743.43	1.87	0.785	D'Souza & Teja (1987); Pohler (1994)
Dodecanoic Acid	743.43	1.87	0.785	D'Souza & Teja (1987)
Dodecanoic Acid	743.43	1.87	0.785	D'Souza & Teja (1987)
Dodecanoic Acid	743.43	1.87	0.785	D'Souza & Teja (1987) ; Kordikowski (1992)
Tetradecanoic Acid	765.19	1.64	1.278	D'Souza & Teja (1987); Pohler (1994)
Octadecanoic Acid	805.09	1.3265	1.018	D'Souza & Teja (1987) ; Schiemann, *et al.,* (1993)

Appendix B: Neural network toolbox

In this section, the neural network toolbox as used in MATLAB will be discussed in terms of how it was used in this thesis.

After obtaining VLE data, data were divided by selecting complete binary systems for the validation and testing sets. The input (`inputs_nn_train` and `inputs_nn_validate`) and target (`target_nn_train` and `target_nn_validate`) data for the training and validation sets were fed into the neural network in the format as listed below. Note that the divide function should be set to `'divide block'` if data are split up selecting complete binary systems instead of selecting random data points.

```
% input and target vectors
inputs = [inputs_nn_train inputs_nn_validate];
target = [target_nn_train target_nn_validate];

net.divideFcn = 'divide block';
ratio_val =
length(inputs_nn_validate)/(length(inputs_nn_validate)+length(inputs_nn_train)
);
net.divideParam.trainRatio = 1-ratio_val;
net.divideParam.testRatio = 0;
net.divideParam.valRatio = ratio_val;
```

The training functions for the cascade feedforward backpropagation (`newcf`) and the feedforward backpropagation (`feedforwardnet`) functions had the following format for one and two hidden layers respectively:

```
% cascade-forward backpropagation training function for one hidden layer:
net = newcf(inputs,target, [N_nodes], {'logsig'});

% cascade-forward backpropagation training function for two hidden layers:
net = newcf(inputs,target, [N_nodes , N_nodes], {'logsig', 'logsig'});

% forward backpropagation training function for one hidden layer:
net = feedforwardnet([N_hl_1]);
net.layers{1}.transferFcn = 'logsig';

% forward backpropagation training function for two hidden layers:
net = feedforwardnet([N_hl_1, N_hl_1]);
net.layers{1}.transferFcn = 'logsig';
net.layers{2}.transferFcn = 'logsig';
```

Appendix C: Neural network optimisation

Table B-1: R^2, AAD% and geometric distance of the training and testing data for the preliminary neural network used in case study 1

Neural network size	R^2_{train}	R^2_{test}	GD_{R^2}	$AAD\%_{trai}$	$AAD\%_{test}$	$GD_{AAD\%}$
$9 \times 1 \times 2$	0,820	0,818	0,014	67,34	59,69	12,85
$9 \times 2 \times 2$	0,911	0,905	0,008	52,60	55,59	6,28
$9 \times 3 \times 2$	0,924	0,918	0,016	48,76	49,47	5,30
$9 \times 4 \times 2$	0,935	0,924	0,017	45,01	48,76	4,03
$9 \times 5 \times 2$	0,936	0,933	0,010	46,96	45,23	7,31
$9 \times 6 \times 2$	0,948	0,951	0,013	41,09	41,39	3,61
$9 \times 7 \times 2$	0,937	0,934	0,012	42,79	44,03	5,81
$9 \times 8 \times 2$	0,937	0,925	0,014	40,41	40,42	1,32
$9 \times 9 \times 2$	0,950	0,943	0,008	38,11	39,71	4,86
$9 \times 10 \times 2$	0,946	0,952	0,008	39,52	41,92	4,34
$9 \times 11 \times 2$	0,952	0,951	0,005	35,05	38,15	3,35
$9 \times 12 \times 2$	0,954	0,954	0,004	36,90	33,83	3,66
$9 \times 13 \times 2$	0,952	0,951	0,006	35,92	36,18	3,95
$9 \times 14 \times 2$	0,949	0,941	0,010	36,77	34,91	3,89
$9 \times 15 \times 2$	0,965	0,961	0,007	32,96	33,18	3,22
$9 \times 16 \times 2$	0,965	0,961	0,005	31,66	34,83	4,04
$9 \times 17 \times 2$	0,962	0,959	0,005	32,76	34,21	3,21
$9 \times 18 \times 2$	0,973	0,967	0,007	30,26	33,68	5,80
$9 \times 19 \times 2$	0,954	0,954	0,005	36,32	37,65	2,87
$9 \times 20 \times 2$	0,945	0,938	0,007	36,60	38,05	3,10
$9 \times 21 \times 2$	0,944	0,945	0,003	37,75	38,53	2,64
$9 \times 22 \times 2$	0,950	0,947	0,011	36,58	35,99	4,29
$9 \times 23 \times 2$	0,962	0,959	0,004	32,05	35,07	5,36
$9 \times 24 \times 2$	0,965	0,960	0,007	31,62	31,19	2,14
$9 \times 25 \times 2$	0,959	0,956	0,003	33,86	36,76	3,86
$9 \times 26 \times 2$	0,954	0,949	0,005	34,16	34,50	2,11
$9 \times 27 \times 2$	0,971	0,963	0,008	31,00	33,77	3,61
$9 \times 28 \times 2$	0,963	0,957	0,008	32,00	34,40	2,70
$9 \times 29 \times 2$	0,959	0,954	0,007	32,78	32,56	4,89
$9 \times 30 \times 2$	0,964	0,961	0,004	31,33	33,63	3,04

Table B-2: R^2, AAD% and geometric distance of the training and testing data for the feedforward neural network with one hidden layer used in case study 1

Neural network size	R^2_{train}	R^2_{test}	GD_{R^2}	$AAD\%_{train}$	$AAD\%_{test}$	$GD_{AAD\%}$
$7 \times 1 \times 2$	0.661	0.620	0.041	44.9	36.7	8.2
$7 \times 2 \times 2$	0.884	0.880	0.013	33.3	29.9	4.3
$7 \times 3 \times 2$	0.889	0.876	0.013	30.4	29.6	3.4
$7 \times 4 \times 2$	0.926	0.932	0.011	25.9	23.6	2.7
$7 \times 5 \times 2$	0.922	0.928	0.012	28.4	21.8	6.9
$7 \times 6 \times 2$	0.928	0.931	0.014	90.1	40.6	78.3
$7 \times 7 \times 2$	0.916	0.907	0.014	25.7	26.9	4.2
$7 \times 8 \times 2$	0.949	0.955	0.007	22.4	19.6	2.9
$7 \times 9 \times 2$	0.948	0.955	0.010	35.2	18.1	17.7
$7 \times 10 \times 2$	0.955	0.967	0.012	25.9	19.3	9.1
$7 \times 11 \times 2$	0.957	0.965	0.007	24.9	40.6	25.4
$7 \times 12 \times 2$	0.960	0.970	0.010	20.7	18.7	6.5
$7 \times 13 \times 2$	0.964	0.972	0.008	19.9	14.8	5.6
$7 \times 14 \times 2$	0.962	0.970	0.008	21.5	19.5	9.3
$7 \times 15 \times 2$	0.963	0.969	0.007	21.3	15.8	5.7
$7 \times 16 \times 2$	0.960	0.966	0.008	25.1	19.1	7.1
$7 \times 17 \times 2$	0.965	0.971	0.006	26.4	22.5	6.0
$7 \times 18 \times 2$	0.964	0.971	0.007	24.0	98.0	79.8
$7 \times 19 \times 2$	0.968	0.974	0.006	26.0	42.6	17.6
$7 \times 20 \times 2$	0.964	0.972	0.008	19.7	20.4	7.8
$7 \times 21 \times 2$	0.967	0.973	0.006	20.1	16.3	4.6
$7 \times 22 \times 2$	0.967	0.975	0.008	20.6	28.1	7.5
$7 \times 23 \times 2$	0.969	0.975	0.005	17.7	21.1	6.4
$7 \times 24 \times 2$	0.968	0.973	0.005	20.8	14.8	6.7
$7 \times 25 \times 2$	0.970	0.974	0.004	20.9	18.7	4.4
$7 \times 26 \times 2$	0.970	0.975	0.006	20.9	18.3	5.1
$7 \times 27 \times 2$	0.969	0.974	0.005	20.7	54.5	40.2
$7 \times 28 \times 2$	0.970	0.974	0.005	20.3	18.8	9.2
$7 \times 29 \times 2$	0.972	0.976	0.004	18.4	16.8	4.9
$7 \times 30 \times 2$	0.973	0.976	0.004	43.5	215.9	180.4

Table B-3: R^2, AAD% and geometric distance of the training and testing data for the feedforward neural network with two hidden layers used in case study 1

Neural network size	R^2_{train}	R^2_{test}	GD_{R^2}	$AAD\%_{train}$	$AAD\%_{test}$	$GD_{AAD\%}$
$7 \times 1 \times 1 \times 2$	0.636	0.615	0.031	46.3	37.3	9.0
$7 \times 2 \times 2 \times 2$	0.904	0.904	0.011	31.5	26.6	4.9
$7 \times 3 \times 3 \times 2$	0.932	0.928	0.017	26.6	34.1	9.4
$7 \times 4 \times 4 \times 2$	0.939	0.945	0.012	25.7	20.6	5.5
$7 \times 5 \times 5 \times 2$	0.952	0.956	0.006	22.7	19.3	3.7
$7 \times 6 \times 6 \times 2$	0.964	0.971	0.008	44.4	56.6	39.1
$7 \times 7 \times 7 \times 2$	0.956	0.959	0.010	21.6	21.8	5.3
$7 \times 8 \times 8 \times 2$	0.970	0.971	0.002	17.8	16.1	2.1
$7 \times 9 \times 9 \times 2$	0.965	0.966	0.002	20.0	16.6	3.4
$7 \times 10 \times 10 \times 2$	0.972	0.976	0.007	21.3	19.6	5.9
$7 \times 11 \times 11 \times 2$	0.975	0.976	0.006	17.9	12.6	5.3
$7 \times 12 \times 12 \times 2$	0.978	0.979	0.003	16.0	13.0	5.6
$7 \times 13 \times 13 \times 2$	0.975	0.976	0.003	16.2	14.7	2.4
$7 \times 14 \times 14 \times 2$	0.971	0.977	0.007	17.4	14.2	3.7
$7 \times 15 \times 15 \times 2$	0.977	0.980	0.004	16.8	14.3	4.7
$7 \times 16 \times 16 \times 2$	0.979	0.977	0.003	15.4	12.1	3.9
$7 \times 17 \times 17 \times 2$	0.973	0.975	0.003	16.4	16.5	2.5
$7 \times 18 \times 18 \times 2$	0.979	0.979	0.002	22.6	18.5	15.9
$7 \times 19 \times 19 \times 2$	0.978	0.978	0.002	22.1	10.7	11.4
$7 \times 20 \times 20 \times 2$	0.980	0.982	0.002	13.2	9.6	3.6
$7 \times 21 \times 21 \times 2$	0.984	0.983	0.003	15.2	7.9	7.3
$7 \times 22 \times 22 \times 2$	0.980	0.980	0.004	16.7	18.2	8.5
$7 \times 23 \times 23 \times 2$	0.985	0.984	0.003	17.0	48.7	35.2
$7 \times 24 \times 24 \times 2$	0.980	0.981	0.002	17.1	10.3	6.8
$7 \times 25 \times 25 \times 2$	0.980	0.980	0.002	16.5	27.5	18.5
$7 \times 26 \times 26 \times 2$	0.992	0.991	0.001	9.7	5.6	4.1
$7 \times 27 \times 27 \times 2$	0.981	0.982	0.002	14.7	10.2	4.5
$7 \times 28 \times 28 \times 2$	0.992	0.994	0.002	15.5	4.8	10.7
$7 \times 29 \times 29 \times 2$	0.984	0.985	0.003	12.8	13.0	5.0
$7 \times 30 \times 30 \times 2$	0.987	0.988	0.002	10.7	7.9	2.7

Table B-4: R^2, AAD% and geometric distance of the training and testing data for the cascade feedforward backpropagation neural network with one hidden layer used in case study 1

Neural network size	R^2_{train}	R^2_{test}	GD_{R^2}	$AAD\%_{train}$	$AAD\%_{test}$	$GD_{AAD\%}$
$7 \times 1 \times 2$	0.867	0.861	0.006	64.1	50.6	28.0
$7 \times 2 \times 2$	0.890	0.880	0.009	49.5	46.9	9.7
$7 \times 3 \times 2$	0.917	0.921	0.012	69.8	104.2	46.9
$7 \times 4 \times 2$	0.934	0.939	0.011	26.5	22.1	4.5
$7 \times 5 \times 2$	0.945	0.954	0.011	26.0	24.2	9.7
$7 \times 6 \times 2$	0.948	0.954	0.012	40.9	22.4	18.5
$7 \times 7 \times 2$	0.940	0.943	0.008	26.0	21.2	5.2
$7 \times 8 \times 2$	0.954	0.965	0.011	23.9	21.1	5.5
$7 \times 9 \times 2$	0.957	0.971	0.013	26.8	31.1	21.9
$7 \times 10 \times 2$	0.955	0.967	0.012	27.6	18.6	9.0
$7 \times 11 \times 2$	0.958	0.966	0.009	33.8	25.2	15.3
$7 \times 12 \times 2$	0.959	0.968	0.009	22.2	22.7	11.2
$7 \times 13 \times 2$	0.961	0.966	0.006	23.9	17.3	6.6
$7 \times 14 \times 2$	0.962	0.969	0.007	20.6	14.7	5.9
$7 \times 15 \times 2$	0.962	0.971	0.009	29.6	14.3	15.3
$7 \times 16 \times 2$	0.963	0.971	0.008	21.2	20.0	5.9
$7 \times 17 \times 2$	0.966	0.975	0.009	22.2	19.3	8.4
$7 \times 18 \times 2$	0.963	0.969	0.006	19.6	16.7	3.7
$7 \times 19 \times 2$	0.966	0.971	0.006	25.1	40.1	20.8
$7 \times 20 \times 2$	0.967	0.972	0.005	42.5	23.7	32.1
$7 \times 21 \times 2$	0.967	0.973	0.006	20.7	29.0	11.0
$7 \times 22 \times 2$	0.968	0.973	0.005	19.7	17.4	6.6
$7 \times 23 \times 2$	0.966	0.971	0.005	19.6	17.5	7.0
$7 \times 24 \times 2$	0.967	0.972	0.005	19.3	25.9	7.7
$7 \times 25 \times 2$	0.972	0.976	0.004	19.5	15.4	4.4
$7 \times 26 \times 2$	0.968	0.973	0.005	19.2	17.4	3.7
$7 \times 27 \times 2$	0.965	0.972	0.007	21.7	18.0	4.6
$7 \times 28 \times 2$	0.969	0.975	0.006	20.4	27.0	13.6
$7 \times 29 \times 2$	0.973	0.977	0.004	19.2	13.9	5.2
$7 \times 30 \times 2$	0.969	0.972	0.003	26.3	46.6	32.4

Table B-5: R^2, AAD% and geometric distance of the training and testing data for the cascade feedforward backpropagation neural network with two hidden layers used in case study 1

Neural network size	R^2_{train}	R^2_{test}	GD_{R^2}	$AAD\%_{train}$	$AAD\%_{test}$	$GD_{AAD\%}$
$7 \times 1 \times 1 \times 2$	0.883	0.867	0.016	34.0	38.7	4.8
$7 \times 2 \times 2 \times 2$	0.922	0.919	0.010	43.6	39.6	21.9
$7 \times 3 \times 3 \times 2$	0.948	0.949	0.008	60.2	20.3	40.1
$7 \times 4 \times 4 \times 2$	0.949	0.953	0.010	23.2	21.6	6.5
$7 \times 5 \times 5 \times 2$	0.958	0.972	0.014	24.9	16.3	8.6
$7 \times 6 \times 6 \times 2$	0.966	0.974	0.008	22.5	21.4	13.6
$7 \times 7 \times 7 \times 2$	0.970	0.974	0.005	30.6	143.2	118.1
$7 \times 8 \times 8 \times 2$	0.969	0.975	0.007	20.0	15.4	6.7
$7 \times 9 \times 9 \times 2$	0.972	0.974	0.003	18.0	19.8	9.7
$7 \times 10 \times 10 \times 2$	0.972	0.975	0.003	23.1	44.4	30.5
$7 \times 11 \times 11 \times 2$	0.976	0.974	0.004	16.0	15.3	2.9
$7 \times 12 \times 12 \times 2$	0.978	0.979	0.004	16.1	12.2	3.9
$7 \times 13 \times 13 \times 2$	0.979	0.979	0.003	51.2	12.8	38.4
$7 \times 14 \times 14 \times 2$	0.981	0.983	0.003	14.2	11.5	2.8
$7 \times 15 \times 15 \times 2$	0.981	0.980	0.002	14.9	12.1	2.8
$7 \times 16 \times 16 \times 2$	0.980	0.981	0.002	15.7	14.8	4.6
$7 \times 17 \times 17 \times 2$	0.981	0.980	0.002	17.9	10.5	7.3
$7 \times 18 \times 18 \times 2$	0.976	0.976	0.004	19.0	31.7	21.2
$7 \times 19 \times 19 \times 2$	0.981	0.981	0.004	16.4	13.4	8.1
$7 \times 20 \times 20 \times 2$	0.983	0.982	0.002	13.4	9.2	4.2
$7 \times 21 \times 21 \times 2$	0.983	0.984	0.001	14.3	19.5	12.5
$7 \times 22 \times 22 \times 2$	0.991	0.992	0.002	9.8	5.7	4.2
$7 \times 23 \times 23 \times 2$	0.985	0.985	0.002	16.9	22.6	11.8
$7 \times 24 \times 24 \times 2$	0.988	0.988	0.001	16.6	7.5	9.1
$7 \times 25 \times 25 \times 2$	0.984	0.985	0.002	13.9	11.1	5.0
$7 \times 26 \times 26 \times 2$	0.986	0.986	0.001	12.1	7.8	4.3
$7 \times 27 \times 27 \times 2$	0.983	0.985	0.002	12.5	12.8	4.8
$7 \times 28 \times 28 \times 2$	0.981	0.982	0.002	14.5	15.9	4.7
$7 \times 29 \times 29 \times 2$	0.987	0.987	0.002	11.3	7.6	3.7
$7 \times 30 \times 30 \times 2$	0.984	0.986	0.003	12.2	8.5	4.7

Table B-6: R^2, AAD% and geometric distance of the training and testing data for the preliminary neural network used in case study 2

Neural network size	R^2_{train}	R^2_{test}	GD_{R^2}	$AAD\%_{train}$	$AAD\%_{test}$	$GD_{AAD\%}$
$11 \times 1 \times 2$	0.699	0.875	0.176	36.7	33.6	8.1
$11 \times 2 \times 2$	0.716	0.885	0.169	34.6	31.8	3.9
$11 \times 3 \times 2$	0.723	0.902	0.179	37.8	32.1	6.6
$11 \times 4 \times 2$	0.745	0.905	0.161	34.0	29.6	5.9
$11 \times 5 \times 2$	0.759	0.916	0.157	36.8	31.5	6.5
$11 \times 6 \times 2$	0.731	0.891	0.159	38.7	28.9	9.8
$11 \times 7 \times 2$	0.769	0.906	0.137	33.6	48.3	25.3
$11 \times 8 \times 2$	0.787	0.947	0.160	42.0	54.4	48.8
$11 \times 9 \times 2$	0.795	0.950	0.155	37.0	23.3	13.7
$11 \times 10 \times 2$	0.770	0.921	0.150	34.3	34.2	11.4
$11 \times 11 \times 2$	0.799	0.943	0.145	38.5	22.5	16.1
$11 \times 12 \times 2$	0.786	0.948	0.162	35.1	30.6	11.5
$11 \times 13 \times 2$	0.800	0.947	0.146	37.0	46.1	29.4
$11 \times 14 \times 2$	0.806	0.955	0.148	32.8	24.1	8.8
$11 \times 15 \times 2$	0.814	0.940	0.126	38.1	23.8	14.2
$11 \times 16 \times 2$	0.814	0.948	0.134	47.2	30.9	18.0
$11 \times 17 \times 2$	0.836	0.949	0.113	58.0	33.0	32.2
$11 \times 18 \times 2$	0.817	0.954	0.137	37.9	22.4	15.5
$11 \times 19 \times 2$	0.820	0.949	0.128	31.6	21.6	10.0
$11 \times 20 \times 2$	0.821	0.949	0.128	32.8	34.4	14.0
$11 \times 21 \times 2$	0.809	0.932	0.123	44.9	23.2	21.7
$11 \times 22 \times 2$	0.812	0.933	0.121	42.5	24.5	18.0
$11 \times 23 \times 2$	0.830	0.956	0.126	34.9	19.8	15.1
$11 \times 24 \times 2$	0.824	0.958	0.134	36.0	24.7	12.9
$11 \times 25 \times 2$	0.828	0.960	0.132	39.0	18.1	20.8
$11 \times 26 \times 2$	0.840	0.958	0.118	33.7	21.5	12.2
$11 \times 27 \times 2$	0.834	0.964	0.130	48.9	24.7	30.7
$11 \times 28 \times 2$	0.828	0.960	0.132	39.0	18.1	20.8
$11 \times 29 \times 2$	0.840	0.958	0.118	33.7	21.5	12.2
$11 \times 30 \times 2$	0.834	0.964	0.130	48.9	24.7	30.7

Table B-7: R^2, AAD% and geometric distance of the training and testing data for the feedforward neural network with one hidden layer used in case study 2

Neural network size	R^2_{train}	R^2_{test}	GD_{R^2}	$AAD\%_{train}$	$AAD\%_{test}$	$GD_{AAD\%}$
$9 \times 1 \times 2$	0.477	0.607	0.130	48.8	43.7	5.1
$9 \times 2 \times 2$	0.648	0.845	0.198	39.9	33.4	6.6
$9 \times 3 \times 2$	0.671	0.834	0.163	41.9	32.9	9.0
$9 \times 4 \times 2$	0.695	0.873	0.178	47.1	32.3	14.9
$9 \times 5 \times 2$	0.714	0.898	0.184	36.5	30.5	6.1
$9 \times 6 \times 2$	0.729	0.893	0.164	41.6	54.3	17.5
$9 \times 7 \times 2$	0.745	0.918	0.173	55.8	27.5	28.9
$9 \times 8 \times 2$	0.741	0.901	0.160	110.3	34.4	77.2
$9 \times 9 \times 2$	0.739	0.904	0.165	43.1	39.7	15.7
$9 \times 10 \times 2$	0.781	0.931	0.150	36.6	51.7	30.4
$9 \times 11 \times 2$	0.781	0.935	0.154	38.6	23.6	15.0
$9 \times 12 \times 2$	0.779	0.941	0.162	44.5	25.0	19.4
$9 \times 13 \times 2$	0.782	0.940	0.157	39.2	24.4	14.8
$9 \times 14 \times 2$	0.797	0.941	0.144	35.3	22.4	12.9
$9 \times 15 \times 2$	0.831	0.943	0.112	33.1	21.7	11.5
$9 \times 16 \times 2$	0.793	0.942	0.149	41.0	25.5	15.5
$9 \times 17 \times 2$	0.813	0.956	0.142	63.1	27.3	35.8
$9 \times 18 \times 2$	0.797	0.949	0.151	31.7	31.0	9.4
$9 \times 19 \times 2$	0.797	0.942	0.145	38.7	22.8	16.0
$9 \times 20 \times 2$	0.817	0.950	0.133	43.1	33.5	15.0
$9 \times 21 \times 2$	0.818	0.953	0.135	35.6	35.6	18.5
$9 \times 22 \times 2$	0.801	0.956	0.155	44.1	23.6	20.5
$9 \times 23 \times 2$	0.814	0.958	0.144	35.2	20.8	14.4
$9 \times 24 \times 2$	0.812	0.964	0.152	35.6	21.8	15.0
$9 \times 25 \times 2$	0.805	0.953	0.148	52.7	24.8	28.2
$\times 26 \times 2$	0.822	0.958	0.135	43.0	22.7	21.8
$9 \times 27 \times 2$	0.811	0.952	0.141	42.9	26.9	19.8
$9 \times 28 \times 2$	0.815	0.947	0.133	150.5	23.8	129.0
$9 \times 29 \times 2$	0.833	0.958	0.125	34.1	24.8	9.3
$9 \times 30 \times 2$	0.826	0.954	0.128	175.4	1800.3	1648.2
$9 \times 31 \times 2$	0.825	0.960	0.135	33.1	18.1	15.1
$9 \times 32 \times 2$	0.823	0.949	0.126	32.0	21.8	11.2
$9 \times 33 \times 2$	0.854	0.964	0.110	35.2	34.2	25.3
$9 \times 34 \times 2$	0.827	0.963	0.135	33.3	64.4	44.8
$9 \times 35 \times 2$	0.815	0.950	0.135	34.5	22.2	12.2
$9 \times 36 \times 2$	0.842	0.961	0.119	34.0	17.0	16.9
$9 \times 37 \times 2$	0.834	0.954	0.120	36.9	61.2	49.6
$9 \times 38 \times 2$	0.843	0.964	0.121	32.2	20.4	11.8
$9 \times 39 \times 2$	0.846	0.959	0.113	44.2	18.4	25.8
$9 \times 40 \times 2$	0.850	0.957	0.107	35.8	18.7	17.1
$9 \times 41 \times 2$	0.837	0.961	0.124	33.4	19.1	14.3

Table B-7 continued

Neural network size	R^2_{train}	R^2_{test}	GD_{R^2}	$AAD\%_{trai}$	$AAD\%_{test}$	$GD_{AAD\%}$
$9 \times 42 \times 2$	0.835	0.958	0.123	79.9	21.4	58.5
$9 \times 43 \times 2$	0.829	0.960	0.131	36.6	31.7	20.9
$9 \times 44 \times 2$	0.850	0.957	0.107	37.5	23.2	17.6
$9 \times 45 \times 2$	0.838	0.961	0.122	35.4	21.1	14.3
$9 \times 46 \times 2$	0.850	0.960	0.110	36.6	19.4	17.2
$9 \times 47 \times 2$	0.836	0.960	0.124	33.0	22.9	12.2
$9 \times 48 \times 2$	0.833	0.962	0.129	37.8	18.7	19.2
$9 \times 49 \times 2$	0.845	0.957	0.112	29.1	20.6	9.7
$9 \times 50 \times 2$	0.842	0.961	0.119	30.8	17.8	13.0
$9 \times 51 \times 2$	0.837	0.962	0.124	30.8	32.1	15.4
$9 \times 52 \times 2$	0.839	0.959	0.120	42.8	20.4	22.4
$9 \times 53 \times 2$	0.844	0.958	0.114	30.2	20.9	10.0
$9 \times 54 \times 2$	0.833	0.964	0.131	28.9	20.8	9.9
$9 \times 55 \times 2$	0.853	0.961	0.108	28.9	28.0	14.2
$9 \times 56 \times 2$	0.850	0.963	0.113	31.9	21.7	10.2
$9 \times 57 \times 2$	0.843	0.964	0.121	51.4	18.0	33.3
$9 \times 58 \times 2$	0.850	0.961	0.111	38.5	17.3	21.2
$9 \times 59 \times 2$	0.839	0.959	0.120	38.6	41.8	27.2
$9 \times 60 \times 2$	0.862	0.964	0.102	32.5	17.1	15.4

Table B-8: R^2, AAD% and geometric distance of the training and testing data for the feedforward neural network with two hidden layers used in case study 2

Neural network size	R^2_{train}	R^2_{test}	GD_{R^2}	$AAD\%_{trai}$	$AAD\%_{test}$	$GD_{AAD\%}$
$9 \times 1 \times 1 \times 2$	0.495	0.615	0.120	47.9	43.3	4.6
$9 \times 2 \times 2 \times 2$	0.538	0.700	0.162	46.3	40.1	6.2
$9 \times 3 \times 3 \times 2$	0.717	0.884	0.167	38.0	28.5	9.5
$9 \times 4 \times 4 \times 2$	0.732	0.884	0.152	44.4	44.0	8.1
$9 \times 5 \times 5 \times 2$	0.675	0.847	0.172	39.4	34.2	6.6
$9 \times 6 \times 6 \times 2$	0.738	0.882	0.144	36.0	27.9	8.0
$9 \times 7 \times 7 \times 2$	0.734	0.879	0.145	41.5	32.0	9.5
$9 \times 8 \times 8 \times 2$	0.844	0.932	0.088	33.0	27.0	7.3
$9 \times 9 \times 9 \times 2$	0.828	0.929	0.101	28.9	22.5	6.5
$9 \times 10 \times 10 \times 2$	0.802	0.920	0.119	116.7	35.0	94.9
$9 \times 11 \times 11 \times 2$	0.841	0.937	0.097	31.5	21.3	10.2
$9 \times 12 \times 12 \times 2$	0.866	0.937	0.070	26.0	21.6	4.4
$9 \times 13 \times 13 \times 2$	0.836	0.950	0.115	46.8	22.0	24.8
$9 \times 14 \times 14 \times 2$	0.795	0.898	0.103	33.1	25.0	8.0
$9 \times 15 \times 15 \times 2$	0.872	0.947	0.076	242.3	70.2	261.5
$9 \times 16 \times 16 \times 2$	0.794	0.913	0.119	32.7	38.4	17.4

Table B-8 continued

Neural network size	R^2_{train}	R^2_{test}	GD_{R^2}	$AAD\%_{trai}$	$AAD\%_{test}$	$GD_{AAD\%}$
$9 \times 17 \times 17 \times 2$	0.862	0.947	0.085	28.8	23.2	6.5
$9 \times 18 \times 18 \times 2$	0.834	0.955	0.121	37.2	24.1	14.5
$9 \times 19 \times 19 \times 2$	0.921	0.975	0.054	22.2	18.5	5.5
$9 \times 20 \times 20 \times 2$	0.929	0.987	0.058	23.0	42.3	36.7
$9 \times 21 \times 21 \times 2$	0.821	0.946	0.124	30.1	21.8	8.3
$9 \times 22 \times 22 \times 2$	0.885	0.971	0.086	25.7	16.4	9.4
$9 \times 23 \times 23 \times 2$	0.887	0.969	0.081	23.2	15.1	8.1
$9 \times 24 \times 24 \times 2$	0.869	0.959	0.090	27.8	17.5	10.3
$9 \times 25 \times 25 \times 2$	0.866	0.962	0.095	25.4	33.7	17.6
$9 \times 26 \times 26 \times 2$	0.908	0.977	0.069	23.9	22.7	14.4
$9 \times 27 \times 27 \times 2$	0.900	0.975	0.075	20.6	13.6	6.9
$9 \times 28 \times 28 \times 2$	0.912	0.977	0.065	50.1	13.0	37.1
$9 \times 29 \times 29 \times 2$	0.908	0.982	0.074	19.4	10.9	8.5
$9 \times 30 \times 30 \times 2$	0.949	0.995	0.046	16.4	7.1	9.3
$9 \times 31 \times 31 \times 2$	0.947	0.992	0.045	16.0	9.2	6.9
$9 \times 32 \times 32 \times 2$	0.931	0.988	0.057	37.8	8.3	29.5
$9 \times 33 \times 33 \times 2$	0.889	0.974	0.085	23.6	17.0	10.8
$9 \times 34 \times 34 \times 2$	0.908	0.974	0.066	55.3	16.3	39.1
$9 \times 35 \times 35 \times 2$	0.898	0.973	0.074	23.7	15.6	8.1
$9 \times 36 \times 36 \times 2$	0.904	0.978	0.074	22.3	12.7	9.6
$9 \times 37 \times 37 \times 2$	0.895	0.976	0.081	21.4	11.0	10.4
$9 \times 38 \times 38 \times 2$	0.922	0.985	0.064	20.1	9.2	10.9
$9 \times 39 \times 39 \times 2$	0.931	0.986	0.056	19.5	10.3	9.2
$9 \times 40 \times 40 \times 2$	0.930	0.989	0.058	17.7	8.0	9.7
$9 \times 41 \times 41 \times 2$	0.903	0.980	0.077	20.2	14.2	6.1
$9 \times 42 \times 42 \times 2$	0.931	0.989	0.058	15.9	7.9	8.0
$9 \times 43 \times 43 \times 2$	0.873	0.942	0.069	26.6	17.3	9.8
$9 \times 44 \times 44 \times 2$	0.891	0.971	0.079	30.6	26.6	5.0
$9 \times 45 \times 45 \times 2$	0.905	0.979	0.074	22.1	12.8	9.3
$9 \times 46 \times 46 \times 2$	0.907	0.980	0.074	20.2	14.7	7.8
$9 \times 47 \times 47 \times 2$	0.890	0.973	0.083	22.9	11.8	11.1
$9 \times 48 \times 48 \times 2$	0.876	0.971	0.095	23.5	15.8	8.5
$9 \times 49 \times 49 \times 2$	0.902	0.979	0.077	19.1	10.4	8.6
$9 \times 50 \times 50 \times 2$	0.883	0.975	0.092	24.2	11.8	12.4

Table B-9: R^2, AAD% and geometric distance of the training and testing data for the cascade feedforward backpropagation neural network with one hidden layer used in case study 2

Neural network size	R^2_{train}	R^2_{test}	GD_{R^2}	$AAD\%_{train}$	$AAD\%_{test}$	$GD_{AAD\%}$
$9 \times 1 \times 2$	0.652	0.834	0.182	55.2	51.2	9.2
$9 \times 2 \times 2$	0.675	0.848	0.172	57.1	58.8	10.3
$9 \times 3 \times 2$	0.684	0.850	0.165	51.8	63.3	13.2
$9 \times 4 \times 2$	0.739	0.916	0.177	52.4	38.7	26.6
$9 \times 5 \times 2$	0.722	0.893	0.171	43.1	35.3	9.5
$9 \times 6 \times 2$	0.726	0.885	0.158	75.4	88.5	20.2
$9 \times 7 \times 2$	0.746	0.910	0.164	43.4	37.3	10.0
$9 \times 8 \times 2$	0.770	0.935	0.165	41.7	25.6	16.0
$9 \times 9 \times 2$	0.773	0.938	0.165	45.7	142.8	116.1
$9 \times 10 \times 2$	0.763	0.922	0.158	42.6	26.7	15.9
$9 \times 11 \times 2$	0.784	0.943	0.158	38.7	24.2	14.5
$9 \times 12 \times 2$	0.803	0.953	0.150	40.3	20.9	19.4
$9 \times 13 \times 2$	0.801	0.959	0.158	40.6	26.9	13.7
$9 \times 14 \times 2$	0.807	0.949	0.142	37.9	38.6	15.9
$9 \times 15 \times 2$	0.807	0.942	0.135	37.1	39.2	17.1
$9 \times 16 \times 2$	0.813	0.944	0.131	39.6	26.3	13.4
$9 \times 17 \times 2$	0.803	0.950	0.147	41.1	22.7	18.5
$9 \times 18 \times 2$	0.828	0.956	0.128	32.3	21.7	10.6
$9 \times 19 \times 2$	0.806	0.952	0.147	42.1	22.4	19.7
$9 \times 20 \times 2$	0.813	0.952	0.139	43.3	30.3	25.9
$9 \times 21 \times 2$	0.817	0.956	0.139	34.7	26.9	10.1
$9 \times 22 \times 2$	0.803	0.942	0.139	45.0	36.4	17.4
$9 \times 23 \times 2$	0.833	0.955	0.122	31.3	27.0	8.8
$9 \times 24 \times 2$	0.826	0.955	0.129	37.2	66.3	43.4
$9 \times 25 \times 2$	0.821	0.957	0.136	48.0	25.9	26.6
$9 \times 26 \times 2$	0.826	0.955	0.129	38.6	24.8	19.9
$9 \times 27 \times 2$	0.821	0.950	0.129	37.2	20.4	16.7
$9 \times 28 \times 2$	0.838	0.950	0.111	52.8	65.1	54.4
$9 \times 29 \times 2$	0.823	0.963	0.139	35.2	115.1	93.3
$9 \times 30 \times 2$	0.838	0.955	0.118	33.7	18.7	15.0
$9 \times 31 \times 2$	0.833	0.957	0.125	35.6	30.9	21.2
$9 \times 32 \times 2$	0.830	0.959	0.128	44.7	20.1	24.6
$9 \times 33 \times 2$	0.827	0.954	0.127	38.1	18.4	19.7
$9 \times 34 \times 2$	0.844	0.964	0.120	32.9	20.4	12.5
$9 \times 35 \times 2$	0.828	0.954	0.126	32.8	26.3	10.4
$9 \times 36 \times 2$	0.821	0.959	0.138	32.3	22.9	10.7
$9 \times 37 \times 2$	0.831	0.962	0.131	33.1	27.1	11.5
$9 \times 38 \times 2$	0.832	0.956	0.124	37.9	19.1	18.8
$9 \times 39 \times 2$	0.838	0.958	0.120	63.4	18.2	45.1
$9 \times 40 \times 2$	0.829	0.960	0.131	42.4	32.2	20.4
$9 \times 41 \times 2$	0.834	0.959	0.125	38.4	20.1	18.3

Table B-9 continued

Neural network size	R^2_{train}	R^2_{test}	GD_{R^2}	$AAD\%_{trai}$	$AAD\%_{test}$	$GD_{AAD\%}$
$9 \times 43 \times 2$	0.839	0.961	0.122	35.5	24.6	10.9
$9 \times 44 \times 2$	0.838	0.961	0.122	37.8	20.2	17.6
$9 \times 45 \times 2$	0.838	0.963	0.125	32.2	25.2	7.7
$9 \times 46 \times 2$	0.847	0.960	0.113	36.2	20.6	15.6
$9 \times 47 \times 2$	0.842	0.960	0.118	31.5	21.9	9.6
$9 \times 48 \times 2$	0.847	0.961	0.114	30.4	20.7	9.7
$9 \times 49 \times 2$	0.845	0.963	0.118	31.6	20.2	11.4
$9 \times 50 \times 2$	0.852	0.965	0.113	31.8	38.2	30.5
$9 \times 51 \times 2$	0.844	0.959	0.115	38.0	49.6	40.9
$9 \times 52 \times 2$	0.843	0.958	0.115	35.3	20.8	14.5
$9 \times 53 \times 2$	0.851	0.958	0.107	31.4	19.5	11.9
$9 \times 54 \times 2$	0.852	0.962	0.109	30.5	19.5	11.2
$9 \times 55 \times 2$	0.851	0.961	0.109	29.0	21.7	12.5
$9 \times 56 \times 2$	0.840	0.959	0.118	108.2	18.5	89.8
$9 \times 57 \times 2$	0.847	0.963	0.116	35.0	20.7	14.3
$9 \times 58 \times 2$	0.843	0.960	0.117	31.7	23.4	12.6
$9 \times 59 \times 2$	0.839	0.957	0.118	32.9	21.4	11.5
$9 \times 60 \times 2$	0.845	0.962	0.117	27.6	20.0	7.7

Table B-10: R^2, AAD% and geometric distance of the training and testing data for the cascade feedforward backpropagation neural network with two hidden layers used in case study 2

Neural network size	R^2_{train}	R^2_{test}	GD_{R^2}	$AAD\%_{tra}$	$AAD\%_{tes}$	$GD_{AAD\%}$
$9 \times 1 \times 1 \times 2$	0.667	0.833	0.166	49.7	38.9	10.8
$9 \times 2 \times 2 \times 2$	0.720	0.881	0.161	59.7	97.4	41.9
$9 \times 3 \times 3 \times 2$	0.739	0.903	0.164	45.7	49.4	6.6
$9 \times 4 \times 4 \times 2$	0.773	0.925	0.152	40.9	39.0	8.6
$9 \times 5 \times 5 \times 2$	0.777	0.923	0.146	38.9	49.7	22.4
$9 \times 6 \times 6 \times 2$	0.769	0.919	0.150	47.9	34.9	15.7
$9 \times 7 \times 7 \times 2$	0.813	0.933	0.119	67.2	71.9	73.3
$9 \times 8 \times 8 \times 2$	0.792	0.936	0.145	12906.9	49.8	12885.3
$9 \times 9 \times 9 \times 2$	0.789	0.927	0.138	48.5	30.5	21.9
$9 \times 10 \times 10 \times 2$	0.823	0.944	0.121	242.0	25.6	218.9
$9 \times 11 \times 11 \times 2$	0.804	0.949	0.145	60.1	25.7	36.1
$9 \times 12 \times 12 \times 2$	0.807	0.939	0.133	39.4	27.3	12.1
$9 \times 13 \times 13 \times 2$	0.829	0.949	0.119	35.8	19.3	16.6
$9 \times 14 \times 14 \times 2$	0.836	0.950	0.114	33.3	24.9	9.6
$9 \times 15 \times 15 \times 2$	0.853	0.968	0.114	37.3	30.1	21.9
$9 \times 16 \times 16 \times 2$	0.852	0.958	0.106	36.0	18.4	17.5

Table B-10 continued

Neural network size	R^2_{train}	R^2_{test}	GD_{R^2}	$AAD\%_{tra}$	$AAD\%_{tes}$	$GD_{AAD\%}$
$9 \times 17 \times 17 \times 2$	0.845	0.953	0.108	64.9	21.7	43.2
$9 \times 18 \times 18 \times 2$	0.880	0.966	0.086	26.3	47.7	28.7
$9 \times 19 \times 19 \times 2$	0.848	0.952	0.104	32.9	21.4	11.5
$9 \times 20 \times 20 \times 2$	0.886	0.973	0.087	26.5	17.0	11.3
$9 \times 21 \times 21 \times 2$	0.870	0.959	0.090	61.3	25.2	42.2
$9 \times 22 \times 22 \times 2$	0.893	0.972	0.079	26.3	16.6	10.1
$9 \times 23 \times 23 \times 2$	0.914	0.977	0.063	21.7	12.0	9.7
$9 \times 24 \times 24 \times 2$	0.888	0.974	0.086	29.6	15.5	15.2
$9 \times 25 \times 25 \times 2$	0.851	0.957	0.106	29.8	21.0	8.8
$9 \times 26 \times 26 \times 2$	0.905	0.977	0.072	21.5	15.0	6.5
$9 \times 27 \times 27 \times 2$	0.925	0.986	0.061	29.2	18.4	20.6
$9 \times 28 \times 28 \times 2$	0.901	0.968	0.066	21.7	16.4	5.4
$9 \times 29 \times 29 \times 2$	0.950	0.995	0.045	14.3	5.8	8.5
$9 \times 30 \times 30 \times 2$	0.891	0.975	0.085	40.0	12.3	27.7
$9 \times 31 \times 31 \times 2$	0.903	0.969	0.066	22.0	13.6	8.4
$9 \times 32 \times 32 \times 2$	0.915	0.983	0.068	21.7	10.3	11.4
$9 \times 33 \times 33 \times 2$	0.885	0.969	0.084	24.2	19.4	5.0
$9 \times 34 \times 34 \times 2$	0.899	0.970	0.072	21.6	12.4	9.2
$9 \times 35 \times 35 \times 2$	0.888	0.976	0.088	25.1	13.9	11.2
$9 \times 36 \times 36 \times 2$	0.890	0.973	0.083	24.4	66.2	52.7
$9 \times 37 \times 37 \times 2$	0.853	0.962	0.109	32.4	19.2	13.2
$9 \times 38 \times 38 \times 2$	0.905	0.972	0.067	30.2	12.5	17.8
$9 \times 39 \times 39 \times 2$	0.869	0.969	0.100	24.3	13.5	10.8
$9 \times 40 \times 40 \times 2$	0.859	0.962	0.102	27.0	20.6	7.3
$9 \times 41 \times 41 \times 2$	0.900	0.972	0.072	21.9	11.9	10.0
$9 \times 42 \times 42 \times 2$	0.900	0.975	0.075	22.3	11.4	10.9
$9 \times 43 \times 43 \times 2$	0.899	0.976	0.077	26.4	16.3	10.6
$9 \times 44 \times 44 \times 2$	0.883	0.966	0.083	32.6	15.2	17.5
$9 \times 45 \times 45 \times 2$	0.907	0.971	0.064	21.0	14.7	9.7
$9 \times 46 \times 46 \times 2$	0.952	0.996	0.045	13.7	4.9	8.8
$9 \times 47 \times 47 \times 2$	0.883	0.964	0.081	26.4	20.7	7.5
$9 \times 48 \times 48 \times 2$	0.909	0.984	0.074	20.9	11.1	9.7
$9 \times 49 \times 49 \times 2$	0.903	0.975	0.071	20.2	11.7	8.6
$9 \times 50 \times 50 \times 2$	0.920	0.984	0.064	19.0	9.8	9.3

Table B-11: R^2, AARD% and geometric distance of the training and testing data divided by randomly selecting data points where the data were obtained from Lashkarbolooki & Vaferi, et al., (2013) using one hidden layer for in case study 3

Neural network size	R^2_{train}	R^2_{test}	GD_{R^2}	$AARD\%_{tr}$	$AARD\%_{te}$	$GD_{AARD\%}$
$5 \times 1 \times 2$	0.867	0.869	0.006	55.2	66.3	11.8
$5 \times 2 \times 2$	0.926	0.928	0.003	87.5	112.3	26.3
$5 \times 3 \times 2$	0.971	0.974	0.004	24.4	25.4	3.0
$5 \times 4 \times 2$	0.980	0.982	0.002	18.1	16.2	2.0
$5 \times 5 \times 2$	0.992	0.993	0.001	11.0	9.0	2.0
$5 \times 6 \times 2$	0.990	0.992	0.002	11.0	9.9	1.1
$5 \times 7 \times 2$	0.990	0.991	0.001	12.0	10.4	1.9
$5 \times 8 \times 2$	0.994	0.995	0.002	14.1	15.7	2.8
$5 \times 9 \times 2$	0.995	0.996	0.000	8.6	7.7	1.3
$5 \times 10 \times 2$	0.990	0.997	0.007	16.4	16.9	6.8
$5 \times 11 \times 2$	0.998	0.998	0.001	11.8	13.8	3.4
$5 \times 12 \times 2$	0.995	0.997	0.001	8.5	5.2	3.3
$5 \times 13 \times 2$	0.996	0.997	0.000	6.2	5.0	1.3
$5 \times 14 \times 2$	0.996	0.996	0.001	15.2	17.4	5.2
$5 \times 15 \times 2$	0.997	0.998	0.001	5.6	4.6	1.2
$5 \times 16 \times 2$	0.997	0.999	0.001	6.4	4.3	2.4
$5 \times 17 \times 2$	0.997	0.998	0.001	11.0	4.1	7.0
$5 \times 18 \times 2$	0.994	0.996	0.001	9.7	7.1	3.2
$5 \times 19 \times 2$	0.996	0.997	0.001	5.4	4.5	0.9
$5 \times 20 \times 2$	0.996	0.996	0.001	8.9	8.9	1.4
$5 \times 21 \times 2$	0.997	0.998	0.001	7.8	5.7	2.3
$5 \times 22 \times 2$	0.997	0.998	0.001	6.4	5.0	1.8
$5 \times 23 \times 2$	0.998	0.998	0.001	5.8	4.4	1.5
$5 \times 24 \times 2$	0.998	0.999	0.000	7.5	4.1	3.4
$5 \times 25 \times 2$	0.997	0.998	0.001	17.5	14.4	9.2
$5 \times 26 \times 2$	0.996	0.997	0.001	24.6	7.5	18.8
$5 \times 27 \times 2$	0.997	0.997	0.000	5.9	5.8	0.9
$5 \times 28 \times 2$	0.996	0.997	0.001	24.8	7.2	18.8
$5 \times 29 \times 2$	0.997	0.998	0.001	11.8	12.7	4.5
$5 \times 30 \times 2$	0.996	0.998	0.002	6.4	4.1	2.4

Table B-12: R^2, AARD% and geometric distance of the training and testing data divided by randomly selecting data points where the data were obtained from Lashkarbolooki & Vaferi, et al., (2013) using two hidden layers for in case study 3

Neural network size	R^2_{train}	R^2_{test}	GD_{R^2}	$AARD\%_{tr}$	$AARD\%_{te}$	$GD_{AARD\%}$
$5 \times 1 \times 1 \times 2$	0.944	0.942	0.003	49.6	56.6	7.3
$5 \times 2 \times 2 \times 2$	0.991	0.993	0.001	12.9	11.5	2.7
$5 \times 3 \times 3 \times 2$	0.994	0.995	0.001	60.6	11.6	50.9
$5 \times 4 \times 4 \times 2$	0.997	0.998	0.001	6.2	4.6	1.7
$5 \times 5 \times 5 \times 2$	0.995	0.996	0.001	13.5	16.3	3.2
$5 \times 6 \times 6 \times 2$	0.997	0.997	0.001	22.5	5.6	16.9
$5 \times 7 \times 7 \times 2$	0.996	0.997	0.000	12.9	13.6	2.6
$5 \times 8 \times 8 \times 2$	0.995	0.997	0.001	9.4	5.2	4.1
$5 \times 9 \times 9 \times 2$	0.998	0.998	0.001	4.7	4.5	0.6
$5 \times 10 \times 10 \times 2$	0.997	0.997	0.000	5.1	5.2	0.6
$5 \times 11 \times 11 \times 2$	0.997	0.997	0.000	12.5	12.9	4.2
$5 \times 12 \times 12 \times 2$	0.996	0.997	0.000	7.4	4.0	3.5
$5 \times 13 \times 13 \times 2$	0.998	0.998	0.000	5.0	3.9	1.2
$5 \times 14 \times 14 \times 2$	0.998	0.999	0.001	5.4	3.7	1.7
$5 \times 15 \times 15 \times 2$	0.998	0.998	0.000	7.6	5.8	3.2
$5 \times 16 \times 16 \times 2$	0.998	0.999	0.000	7.2	7.1	2.4
$5 \times 17 \times 17 \times 2$	0.998	0.998	0.001	5.4	5.5	1.2
$5 \times 18 \times 18 \times 2$	0.998	0.999	0.001	7.9	7.8	1.6
$5 \times 19 \times 19 \times 2$	0.998	0.998	0.001	6.3	6.0	1.6
$5 \times 20 \times 20 \times 2$	0.997	0.998	0.001	5.6	5.5	1.0
$5 \times 21 \times 21 \times 2$	0.998	0.998	0.000	5.0	3.8	1.1
$5 \times 22 \times 22 \times 2$	0.997	0.998	0.001	5.6	3.6	2.0
$5 \times 23 \times 23 \times 2$	0.998	0.998	0.000	8.2	5.8	3.2
$5 \times 24 \times 24 \times 2$	0.998	0.998	0.000	10.8	13.9	3.1
$5 \times 25 \times 25 \times 2$	0.997	0.998	0.001	8.3	7.6	2.9
$5 \times 26 \times 26 \times 2$	0.998	0.999	0.001	12.3	5.8	6.9
$5 \times 27 \times 27 \times 2$	0.998	0.998	0.000	6.0	5.9	1.4
$5 \times 28 \times 28 \times 2$	0.998	0.998	0.000	46.0	10.5	40.3
$5 \times 29 \times 29 \times 2$	0.997	0.999	0.001	7.3	7.0	2.1
$5 \times 30 \times 30 \times 2$	0.998	0.998	0.001	12.6	5.0	8.7

Table B-13: *R^2, AARD% and geometric distance of the training and testing data divided by selecting complete binary systems where the data were obtained from Lashkarbolooki & Vaferi, et al., (2013) using one hidden layer for in case study 3*

Neural network size	R^2_{train}	R^2_{test}	GD_{R^2}	$AARD\%_{tr}$	$AARD\%_{te}$	$GD_{AARD\%}$
$5 \times 1 \times 2$	0.728	0.580	0.148	40.6	63.6	23.0
$5 \times 2 \times 2$	0.869	0.635	0.234	62.2	248.1	185.9
$5 \times 3 \times 2$	0.878	0.761	0.117	29.1	44.2	15.1
$5 \times 4 \times 2$	0.885	0.698	0.187	260.8	99.5	182.9
$5 \times 5 \times 2$	0.928	0.791	0.136	42.7	30.5	27.3
$5 \times 6 \times 2$	0.906	0.790	0.116	33.8	88.3	54.8
$5 \times 7 \times 2$	0.917	0.835	0.082	25.5	27.4	6.7
$5 \times 8 \times 2$	0.842	0.663	0.179	54.6	55.4	38.1
$5 \times 9 \times 2$	0.923	0.749	0.175	26.1	46.0	23.7
$5 \times 10 \times 2$	0.764	0.638	0.250	191.3	300.3	195.3
$5 \times 11 \times 2$	0.792	0.795	0.119	36.6	31.7	10.0
$5 \times 12 \times 2$	0.908	0.714	0.194	35.0	36.3	6.6
$5 \times 13 \times 2$	0.726	0.525	0.223	79.6	121.0	43.4
$5 \times 14 \times 2$	0.885	0.789	0.095	38.9	52.8	24.4
$5 \times 15 \times 2$	0.850	0.782	0.084	42.1	35.3	11.9
$5 \times 16 \times 2$	0.660	0.384	0.277	182.3	136.3	127.1
$5 \times 17 \times 2$	0.780	0.539	0.241	55.5	81.6	27.3
$5 \times 18 \times 2$	0.672	0.653	0.225	54.0	36.0	23.0
$5 \times 19 \times 2$	0.826	0.791	0.154	30.4	28.2	20.0
$5 \times 20 \times 2$	0.777	0.618	0.178	27.3	28.0	6.1
$5 \times 21 \times 2$	0.860	0.566	0.294	68.7	168.8	104.9
$5 \times 22 \times 2$	0.715	0.802	0.142	51.8	36.9	29.0
$5 \times 23 \times 2$	0.737	0.322	0.414	91.3	78.8	45.3
$5 \times 24 \times 2$	0.870	0.734	0.153	38.8	45.4	26.2
$5 \times 25 \times 2$	0.727	0.547	0.181	140.4	59.3	81.8
$5 \times 26 \times 2$	0.901	0.868	0.034	27.2	16.2	12.8
$5 \times 27 \times 2$	0.599	0.548	0.258	81.2	119.1	56.2
$5 \times 28 \times 2$	0.731	0.681	0.321	122.6	161.7	42.7
$5 \times 29 \times 2$	0.777	0.679	0.138	84.0	72.5	17.8
$5 \times 30 \times 2$	0.750	0.553	0.209	195.7	49.2	153.9

Table B-14: R^2, AARD% and geometric distance of the training and testing data divided by selecting complete binary systems where the data were obtained from Lashkarbolooki & Vaferi, et al., (2013) using two hidden layers for in case study 3

Neural network size	R^2_{train}	R^2_{test}	GD_{R^2}	$AARD\%_{tr}$	$AARD\%_{te}$	$GD_{AARD\%}$
$5 \times 1 \times 1 \times 2$	0.796	0.683	0.113	37.6	51.6	16.9
$5 \times 2 \times 2 \times 2$	0.928	0.769	0.160	42.3	42.7	21.6
$5 \times 3 \times 3 \times 2$	0.861	0.710	0.151	74.0	75.0	70.1
$5 \times 4 \times 4 \times 2$	0.901	0.791	0.110	48.7	25.8	24.9
$5 \times 5 \times 5 \times 2$	0.882	0.739	0.143	37.0	35.5	9.2
$5 \times 6 \times 6 \times 2$	0.839	0.730	0.109	70.2	70.6	50.0
$5 \times 7 \times 7 \times 2$	0.841	0.700	0.142	46.6	53.5	18.1
$5 \times 8 \times 8 \times 2$	0.632	0.593	0.149	66.9	45.4	21.5
$5 \times 9 \times 9 \times 2$	0.526	0.663	0.275	58.6	36.8	22.2
$5 \times 10 \times 10 \times 2$	0.894	0.763	0.132	17.9	16.8	1.5
$5 \times 11 \times 11 \times 2$	0.904	0.583	0.322	189.9	40.6	161.0
$5 \times 12 \times 12 \times 2$	0.622	0.346	0.300	141.1	205.5	86.1
$5 \times 13 \times 13 \times 2$	0.735	0.509	0.226	52.9	49.1	11.4
$5 \times 14 \times 14 \times 2$	0.925	0.772	0.153	20.6	23.1	4.6
$5 \times 15 \times 15 \times 2$	0.877	0.671	0.206	179.8	368.5	191.7
$5 \times 16 \times 16 \times 2$	0.791	0.739	0.116	61.0	45.6	21.7
$5 \times 17 \times 17 \times 2$	0.569	0.435	0.155	78.9	57.4	34.8
$5 \times 18 \times 18 \times 2$	0.747	0.572	0.299	70.4	68.5	32.0
$5 \times 19 \times 19 \times 2$	0.869	0.774	0.095	82.4	36.4	49.4
$5 \times 20 \times 20 \times 2$	0.470	0.558	0.378	70.7	61.6	29.3
$5 \times 21 \times 21 \times 2$	0.628	0.436	0.192	286.3	116.2	178.3
$5 \times 22 \times 22 \times 2$	0.562	0.342	0.251	47.7	48.2	5.4
$5 \times 23 \times 23 \times 2$	0.857	0.641	0.245	93.3	70.3	58.5
$5 \times 24 \times 24 \times 2$	0.685	0.460	0.226	209.3	586.1	442.4
$5 \times 25 \times 25 \times 2$	0.950	0.864	0.094	32.4	87.5	69.4
$5 \times 26 \times 26 \times 2$	0.901	0.746	0.169	34.4	28.5	13.8
$5 \times 27 \times 27 \times 2$	0.434	0.314	0.120	330.0	37.0	292.9
$5 \times 28 \times 28 \times 2$	0.571	0.317	0.256	41.9	39.6	9.0
$5 \times 29 \times 29 \times 2$	0.780	0.264	0.517	71.2	60.8	27.0
$5 \times 30 \times 30 \times 2$	0.799	0.790	0.061	35.2	31.0	12.6

Table B-15*: R^2, AARD% and geometric distance of the training and testing data divided by randomly selecting data points where the data were obtained from Vaferi, et al., (2018) using one hidden layer for in case study 3*

Neural network size	R^2_{train}	R^2_{test}	GD_{R^2}	$AARD\%_{tr}$	$AARD\%_{te}$	$GD_{AARD\%}$
$5 \times 1 \times 2$	0.672	0.686	0.014	34.7	34.4	0.6
$5 \times 2 \times 2$	0.926	0.927	0.002	17.4	17.1	0.5
$5 \times 3 \times 2$	0.958	0.958	0.002	16.8	18.3	1.9
$5 \times 4 \times 2$	0.957	0.958	0.002	13.7	13.9	0.9
$5 \times 5 \times 2$	0.978	0.980	0.002	23.2	24.7	1.9
$5 \times 6 \times 2$	0.981	0.982	0.001	9.3	8.7	0.6
$5 \times 7 \times 2$	0.990	0.990	0.001	6.4	6.2	0.3
$5 \times 8 \times 2$	0.992	0.993	0.001	5.7	5.7	0.1
$5 \times 9 \times 2$	0.993	0.994	0.001	5.3	4.8	0.5
$5 \times 10 \times 2$	0.994	0.995	0.001	5.0	5.0	0.3
$5 \times 11 \times 2$	0.995	0.995	0.001	4.3	4.1	0.2
$5 \times 12 \times 2$	0.994	0.995	0.001	5.2	4.2	1.0
$5 \times 13 \times 2$	0.995	0.995	0.001	4.7	4.4	0.3
$5 \times 14 \times 2$	0.995	0.996	0.001	4.2	3.9	0.3
$5 \times 15 \times 2$	0.995	0.995	0.001	4.9	4.4	0.5
$5 \times 16 \times 2$	0.996	0.996	0.001	3.6	3.4	0.2
$5 \times 17 \times 2$	0.995	0.996	0.001	4.0	3.7	0.2
$5 \times 18 \times 2$	0.995	0.996	0.001	4.3	4.0	0.2
$5 \times 19 \times 2$	0.997	0.997	0.001	3.4	3.2	0.3
$5 \times 20 \times 2$	0.996	0.996	0.001	6.7	4.9	2.6
$5 \times 21 \times 2$	0.997	0.998	0.001	3.0	2.5	0.5
$5 \times 22 \times 2$	0.994	0.995	0.001	5.0	4.8	0.4
$5 \times 23 \times 2$	0.996	0.997	0.001	3.3	2.7	0.6
$5 \times 24 \times 2$	0.996	0.997	0.001	4.6	3.4	1.2
$5 \times 25 \times 2$	0.997	0.998	0.001	3.4	2.7	0.7
$5 \times 26 \times 2$	0.996	0.997	0.001	6.6	3.2	3.4
$5 \times 27 \times 2$	0.996	0.997	0.001	3.4	2.9	0.5
$5 \times 28 \times 2$	0.996	0.997	0.001	3.7	3.3	0.4
$5 \times 29 \times 2$	0.997	0.998	0.001	3.1	2.7	0.4
$5 \times 30 \times 2$	0.997	0.998	0.001	3.7	2.7	0.9

Table B-16: R^2, AARD% and geometric distance of the training and testing data divided by randomly selecting data points where the data were obtained from Vaferi, et al., (2018) *using two hidden layers for in case study 3*

Neural network size	R^2_{train}	R^2_{test}	GD_{R^2}	$AARD\%_{tr}$	$AARD\%_{te}$	$GD_{AARD\%}$
$5 \times 1 \times 1 \times 2$	0.697	0.710	0.016	35.0	34.6	0.6
$5 \times 2 \times 2 \times 2$	0.942	0.945	0.003	16.4	16.1	0.3
$5 \times 3 \times 3 \times 2$	0.969	0.971	0.002	11.0	10.9	0.4
$5 \times 4 \times 4 \times 2$	0.987	0.987	0.001	7.4	7.3	0.2
$5 \times 5 \times 5 \times 2$	0.992	0.993	0.001	6.2	6.1	0.3
$5 \times 6 \times 6 \times 2$	0.994	0.995	0.001	4.9	4.6	0.3
$5 \times 7 \times 7 \times 2$	0.995	0.996	0.001	3.8	3.6	0.2
$5 \times 8 \times 8 \times 2$	0.995	0.996	0.001	4.6	4.0	0.7
$5 \times 9 \times 9 \times 2$	0.996	0.998	0.001	3.7	2.8	0.9
$5 \times 10 \times 10 \times 2$	0.996	0.997	0.001	4.5	3.6	0.9
$5 \times 11 \times 11 \times 2$	0.997	0.998	0.000	2.7	2.4	0.3
$5 \times 12 \times 12 \times 2$	0.996	0.997	0.001	3.7	3.1	0.6
$5 \times 13 \times 13 \times 2$	0.998	0.998	0.000	2.6	2.3	0.3
$5 \times 14 \times 14 \times 2$	0.997	0.998	0.001	3.2	2.8	0.5
$5 \times 15 \times 15 \times 2$	0.997	0.997	0.001	2.9	2.6	0.3
$5 \times 16 \times 16 \times 2$	0.997	0.998	0.001	2.8	2.2	0.6
$5 \times 17 \times 17 \times 2$	0.996	0.996	0.001	4.2	3.4	0.8
$5 \times 18 \times 18 \times 2$	0.998	0.998	0.001	2.3	1.8	0.5
$5 \times 19 \times 19 \times 2$	0.997	0.998	0.001	2.6	2.4	0.3
$5 \times 20 \times 20 \times 2$	0.998	0.999	0.001	2.3	1.6	0.7
$5 \times 21 \times 21 \times 2$	0.997	0.998	0.001	3.0	2.0	1.1
$5 \times 22 \times 22 \times 2$	0.998	0.999	0.001	1.9	1.5	0.4
$5 \times 23 \times 23 \times 2$	0.997	0.999	0.001	2.1	1.6	0.5
$5 \times 24 \times 24 \times 2$	0.997	0.998	0.001	3.1	2.5	0.6
$5 \times 25 \times 25 \times 2$	0.996	0.998	0.002	3.5	2.8	0.7
$5 \times 26 \times 26 \times 2$	0.998	0.999	0.001	2.1	1.5	0.5
$5 \times 27 \times 27 \times 2$	0.998	0.999	0.001	1.5	1.0	0.5
$5 \times 28 \times 28 \times 2$	0.998	0.998	0.000	2.6	1.9	0.7
$5 \times 29 \times 29 \times 2$	0.998	0.999	0.000	1.9	1.5	0.4
$5 \times 30 \times 30 \times 2$	0.998	0.999	0.000	1.7	1.3	0.4

Table B-17: *R^2, AARD% and geometric distance of the training and testing data divided by selecting complete binary systems where the data were obtained from Vaferi, et al., (2018) using one hidden layer for in case study 3*

Neural network size	R^2_{train}	R^2_{test}	GD_{R^2}	$AARD\%_{tr}$	$AARD\%_{te}$	$GD_{AARD\%}$
$5 \times 1 \times 2$	0.665	0.639	0.026	34.7	33.0	1.7
$5 \times 2 \times 2$	0.919	0.908	0.011	18.0	20.3	2.3
$5 \times 3 \times 2$	0.948	0.918	0.030	14.9	17.6	2.7
$5 \times 4 \times 2$	0.924	0.941	0.027	22.5	23.5	4.3
$5 \times 5 \times 2$	0.925	0.927	0.014	19.2	21.1	3.3
$5 \times 6 \times 2$	0.975	0.958	0.020	10.2	10.3	1.3
$5 \times 7 \times 2$	0.971	0.968	0.009	18.1	14.0	5.4
$5 \times 8 \times 2$	0.959	0.948	0.015	19.9	23.3	11.4
$5 \times 9 \times 2$	0.980	0.982	0.004	9.6	13.2	4.1
$5 \times 10 \times 2$	0.983	0.978	0.005	16.4	11.2	6.6
$5 \times 11 \times 2$	0.984	0.987	0.005	9.2	10.6	2.5
$5 \times 12 \times 2$	0.976	0.974	0.003	59.8	50.3	71.7
$5 \times 13 \times 2$	0.969	0.971	0.002	11.7	10.5	1.5
$5 \times 14 \times 2$	0.986	0.985	0.002	27.1	12.0	17.1
$5 \times 15 \times 2$	0.980	0.982	0.003	17.9	12.3	8.0
$5 \times 16 \times 2$	0.981	0.980	0.004	12.3	20.6	9.5
$5 \times 17 \times 2$	0.984	0.981	0.006	9.4	10.6	2.0
$5 \times 18 \times 2$	0.959	0.975	0.016	136.1	15.3	121.4
$5 \times 19 \times 2$	0.982	0.986	0.004	13.9	14.0	10.0
$5 \times 20 \times 2$	0.973	0.984	0.012	23.5	9.1	15.1
$5 \times 21 \times 2$	0.979	0.986	0.007	10.0	9.4	2.2
$5 \times 22 \times 2$	0.986	0.987	0.002	10.2	9.6	0.7
$5 \times 23 \times 2$	0.984	0.985	0.001	9.6	8.3	1.3
$5 \times 24 \times 2$	0.986	0.992	0.006	12.7	8.7	6.2
$5 \times 25 \times 2$	0.991	0.994	0.003	7.6	14.4	8.1
$5 \times 26 \times 2$	0.973	0.980	0.007	19.5	18.3	7.9
$5 \times 27 \times 2$	0.987	0.987	0.004	17.3	10.1	8.7
$5 \times 28 \times 2$	0.988	0.995	0.006	7.0	7.4	1.5
$5 \times 29 \times 2$	0.988	0.992	0.004	8.1	6.2	2.0
$5 \times 30 \times 2$	0.977	0.982	0.005	10.0	9.9	2.6

Table B-18: R^2, AARD% and geometric distance of the training and testing data divided by selecting complete binary systems where the data were obtained from Vaferi, et al., (2018) *using two hidden layers for in case study 3*

Neural network size	R^2_{train}	R^2_{test}	GD_{R^2}	$AARD\%_{tr}$	$AARD\%_{te}$	$GD_{AARD\%}$
$5 \times 1 \times 1 \times 2$	0.675	0.676	0.033	35.0	32.2	2.8
$5 \times 2 \times 2 \times 2$	0.878	0.871	0.019	21.5	19.3	3.3
$5 \times 3 \times 3 \times 2$	0.921	0.920	0.016	17.2	17.1	1.7
$5 \times 4 \times 4 \times 2$	0.966	0.943	0.025	12.9	13.8	2.1
$5 \times 5 \times 5 \times 2$	0.970	0.960	0.012	18.2	12.8	7.4
$5 \times 6 \times 6 \times 2$	0.958	0.959	0.010	14.4	13.4	1.5
$5 \times 7 \times 7 \times 2$	0.989	0.990	0.002	7.4	6.6	0.7
$5 \times 8 \times 8 \times 2$	0.983	0.986	0.003	8.9	8.3	0.9
$5 \times 9 \times 9 \times 2$	0.988	0.987	0.003	8.2	8.6	1.0
$5 \times 10 \times 10 \times 2$	0.981	0.983	0.003	9.4	8.8	0.8
$5 \times 11 \times 11 \times 2$	0.976	0.976	0.004	11.8	10.3	2.5
$5 \times 12 \times 12 \times 2$	0.989	0.991	0.002	8.0	18.0	10.1
$5 \times 13 \times 13 \times 2$	0.974	0.966	0.012	17.9	46.9	29.8
$5 \times 14 \times 14 \times 2$	0.991	0.995	0.004	5.9	10.5	5.6
$5 \times 15 \times 15 \times 2$	0.988	0.993	0.005	7.1	5.9	1.2
$5 \times 16 \times 16 \times 2$	0.993	0.995	0.003	4.9	4.2	0.7
$5 \times 17 \times 17 \times 2$	0.985	0.990	0.005	7.5	7.5	1.2
$5 \times 18 \times 18 \times 2$	0.989	0.993	0.004	6.9	6.9	0.7
$5 \times 19 \times 19 \times 2$	0.982	0.994	0.012	9.9	8.5	1.3
$5 \times 20 \times 20 \times 2$	0.986	0.994	0.008	7.5	5.8	1.7
$5 \times 21 \times 21 \times 2$	0.993	0.997	0.004	4.4	3.4	1.0
$5 \times 22 \times 22 \times 2$	0.989	0.995	0.005	5.3	4.7	0.6
$5 \times 23 \times 23 \times 2$	0.981	0.991	0.009	9.5	7.3	2.4
$5 \times 24 \times 24 \times 2$	0.993	0.996	0.004	7.4	4.1	3.3
$5 \times 25 \times 25 \times 2$	0.986	0.993	0.008	7.1	5.7	1.4
$5 \times 26 \times 26 \times 2$	0.991	0.995	0.004	5.2	4.6	1.0
$5 \times 27 \times 27 \times 2$	0.989	0.997	0.008	5.9	3.6	2.3
$5 \times 28 \times 28 \times 2$	0.977	0.988	0.011	54.8	8.5	46.3
$5 \times 29 \times 29 \times 2$	0.984	0.993	0.009	7.7	5.9	1.8
$5 \times 30 \times 30 \times 2$	0.985	0.989	0.004	7.4	6.4	1.0

Appendix D: Weights and biases of neural networks

Table D-1: Input-hidden layer weight and bias matrix for case study 1

j \ i	1	2	3	4	5	6	7	Bias
1	-0.56	-0.73	-0.02	0.77	-0.74	-0.08	0.28	-0.58
2	-0.35	-0.62	-0.65	0.73	0.37	0.55	-0.63	0.67
3	0.51	0.74	-0.89	0.88	0.17	0.52	0.43	0.93
4	-0.29	0.08	0.64	0.81	-0.02	-0.64	0.70	-0.87
5	-0.97	-0.34	-0.93	-0.64	0.45	0.91	-0.84	-0.01
6	0.64	-0.94	-0.63	0.37	0.88	0.76	0.90	0.47
7	0.94	-0.41	0.45	0.37	-0.92	0.18	0.29	-0.24
8	1.01	0.86	0.01	-0.87	-0.39	-0.94	-0.42	0.68
9	0.16	-0.13	0.65	0.58	0.07	-0.65	0.17	-0.59
10	0.14	0.57	-0.66	-0.33	0.52	-0.41	-0.81	0.99
11	-0.24	-0.79	0.70	-0.28	-0.49	0.10	-0.54	0.05
12	0.78	0.16	-0.40	-0.77	0.05	0.42	-0.34	0.62
13	0.64	-0.49	0.17	-0.47	-0.58	-0.93	0.73	0.69
14	-0.50	0.65	0.94	-0.20	0.88	-0.28	-0.75	-0.13
15	-0.05	-0.28	0.74	1.01	-0.40	0.14	0.48	-0.39
16	-0.90	-0.31	0.45	-0.30	0.33	-0.34	-0.40	0.64
17	-0.93	0.48	0.31	0.00	-0.20	-0.47	-0.81	0.43
18	0.69	-0.40	0.59	0.52	-0.22	0.13	0.66	-0.50
19	-0.77	-0.83	0.61	0.08	-0.19	0.62	0.50	0.41
20	0.06	0.15	-0.26	-0.35	0.19	0.86	0.49	0.29
21	0.63	-0.61	-0.98	-0.07	-0.40	0.67	-0.78	-0.20
22	0.30	0.84	0.12	0.34	-0.49	0.81	0.42	0.33
23	0.26	-0.13	-0.51	0.93	0.76	0.15	-0.09	-0.07
24	0.36	-0.07	-0.28	0.80	-0.84	0.90	-0.82	0.46
25	0.65	-0.78	-0.15	0.72	0.73	-0.92	0.17	-0.75
26	-0.13	0.86	0.25	0.50	0.66	0.45	0.65	-0.73

Table D-2: Hidden-hidden layer weight matrix for case study 1

i \ j	1	2	3	4	5	6	7	8	9	10	11	12	13
1	0.08	0.07	-0.58	-0.68	0.28	0.75	0.30	0.83	-0.51	-0.68	0.54	0.26	0.93
2	-0.19	-0.34	-0.08	0.33	-0.08	-0.01	0.42	0.45	-0.15	0.02	-0.22	-0.07	0.18
3	-0.34	0.10	-0.90	0.62	-0.47	-0.49	0.16	-0.74	-0.96	0.89	-0.09	0.39	-0.15
4	-0.56	-0.65	0.70	0.29	-0.43	-0.66	0.19	-0.60	-0.09	0.80	0.10	-0.38	-0.25
5	0.50	0.08	0.11	-0.12	0.84	0.75	-0.97	-0.19	0.27	-0.13	0.32	0.04	-0.95
6	0.44	-0.53	0.90	-0.47	0.69	0.80	0.47	0.49	0.26	-0.07	0.55	-0.31	-0.63
7	0.73	-0.10	0.40	0.17	-0.75	-0.55	0.36	-0.30	0.02	-0.39	-0.15	0.10	-0.19
8	-0.65	-0.52	-0.30	-0.38	-0.66	0.92	-0.94	-0.49	-0.17	-0.84	0.42	0.42	-0.53
9	0.60	0.71	0.30	0.65	0.29	0.04	0.27	-0.74	0.11	-0.11	-0.46	-0.27	-0.74
10	-0.75	-0.92	0.18	-0.33	-0.14	0.65	-0.70	0.58	0.13	-0.41	-0.70	-0.68	-0.09
11	0.05	-0.62	0.84	0.13	-0.02	0.90	0.28	0.06	0.48	0.98	-0.99	0.30	1.00
12	-0.62	0.79	0.86	0.81	-0.93	1.01	-0.30	0.15	-0.73	-0.17	-0.90	-0.33	0.09
13	0.26	0.55	0.20	-0.88	0.53	-0.29	0.27	-0.87	0.32	-0.18	-0.31	0.05	0.03
14	-0.68	-0.75	-0.33	0.37	-0.97	0.03	0.22	-0.16	0.68	-0.23	0.62	0.24	-0.37
15	0.80	-0.28	0.84	0.42	0.30	0.28	0.59	0.73	-0.45	-0.64	-0.16	0.37	0.14
16	0.52	0.09	0.91	0.90	0.80	-0.70	0.77	-0.21	0.53	-0.17	-0.71	0.85	-0.37
17	0.81	-0.72	0.57	0.92	0.86	-0.84	0.41	-0.13	-0.06	0.06	-0.41	-0.82	-0.92
18	0.71	0.12	0.78	0.63	-0.48	-0.49	0.14	-0.48	-0.65	-0.47	-0.72	0.02	-0.05
19	-1.01	-0.15	0.41	0.73	-0.28	-0.74	0.36	-0.48	0.52	0.33	0.66	0.20	0.41
20	-0.33	-0.25	0.85	-0.66	0.17	0.43	0.11	0.75	0.92	0.23	-0.10	0.47	0.42
21	-0.44	0.15	-0.66	-0.34	0.58	-1.00	-0.21	-0.89	-0.55	0.44	-0.82	-0.65	0.18
22	-0.72	0.70	-0.06	0.54	0.83	0.27	-0.63	0.39	-0.87	-0.54	0.92	0.09	-0.23
23	0.74	0.67	-0.06	-0.92	-0.66	0.92	-0.54	-0.43	-0.80	-0.05	0.94	0.38	-0.87
24	0.98	0.57	-0.09	-0.91	0.09	0.15	-0.75	0.22	0.58	-0.37	-0.44	-0.96	0.19
25	0.06	-0.69	0.46	0.98	-0.92	0.04	-0.59	0.52	-0.20	0.29	0.69	0.41	-0.47
26	0.09	0.24	0.00	-0.56	0.19	-0.69	-0.88	0.90	0.15	0.97	0.75	-0.24	-0.39
Bias	-0.42	0.57	-0.15	0.24	-0.63	-0.47	0.74	-0.77	-0.39	-0.53	-0.44	-1.01	-0.76

T

able D-2 *continued: Hidden-hidden layer weight matrix for case study 1*

i \ j	14	15	16	17	18	19	20	21	22	23	24	25	26
1	0.03	0.59	0.14	-0.03	-0.40	-0.15	-0.99	-0.47	0.21	0.87	0.16	-0.51	-0.46
2	-0.28	-0.08	-0.81	0.47	0.88	0.14	0.08	-0.03	0.97	0.36	0.98	0.65	0.42
3	0.57	-0.84	0.58	-0.52	-0.46	0.51	0.24	-0.12	-0.26	-0.20	-0.28	-0.18	0.90
4	0.50	0.36	-0.37	-0.84	0.70	-0.76	-0.24	0.89	0.07	-0.22	0.84	-0.91	-0.36
5	-0.44	0.64	-0.43	-0.84	-0.02	-0.08	-0.08	0.17	-0.28	0.01	-0.05	-0.70	-0.14
6	-0.28	0.88	-0.24	-0.46	-0.76	-0.77	0.64	-0.06	-0.92	-0.36	-0.08	-0.02	0.37
7	-0.48	-0.77	-0.28	0.57	0.23	-0.72	-0.83	-0.52	-0.18	0.92	0.89	-0.39	-1.01
8	-0.03	0.87	0.30	0.78	0.47	-0.32	-0.87	0.35	-0.57	0.76	0.23	-0.03	-0.16
9	-0.09	0.45	-0.20	-0.24	0.14	-0.81	0.64	-0.37	0.38	-0.01	0.73	0.52	0.23
10	0.76	-0.39	0.01	-0.14	0.32	0.87	-0.48	0.36	-0.20	-0.84	-0.35	0.60	0.74
11	0.55	0.07	0.86	0.04	0.71	0.34	-0.52	0.76	0.87	0.10	0.11	0.08	0.18
12	0.26	0.38	-0.15	0.67	0.02	0.16	-0.27	-0.30	-0.24	-0.22	0.22	0.64	0.48
13	-0.05	-0.24	-0.16	0.41	-0.44	-0.68	-0.97	-0.44	-0.12	0.18	0.65	-0.35	-0.17
14	-0.44	0.50	0.01	0.00	0.99	0.21	-0.22	-0.82	-0.70	-0.93	-0.15	-0.97	0.71
15	0.81	0.88	0.75	0.79	-0.03	0.25	0.62	-0.64	0.05	0.39	-0.88	0.66	0.33
16	0.32	0.75	0.86	-0.03	0.66	-0.43	0.56	0.94	-0.23	0.54	0.59	-0.33	0.16
17	0.45	0.99	-0.09	-0.84	0.46	-0.69	-0.22	0.24	-0.34	0.64	0.59	-0.26	-0.89
18	-0.60	-0.54	0.30	0.12	0.03	0.05	0.66	-0.14	0.51	0.78	0.34	0.59	0.23
19	0.66	-0.71	0.54	0.05	0.92	-0.48	-0.04	-0.59	-0.71	0.36	0.92	0.84	-0.18
20	0.36	-0.22	-0.30	0.86	-0.89	-0.83	-0.52	0.25	0.07	0.79	-0.22	-0.74	-0.59
21	0.45	-0.85	0.27	-0.93	-0.81	-0.90	0.55	0.67	0.76	0.71	-0.73	0.25	-0.06
22	0.48	0.03	-0.67	0.84	0.51	-0.85	-0.16	0.86	-0.33	0.31	0.28	-0.77	0.34
23	0.01	-0.85	-0.45	0.66	-0.82	-0.01	-0.93	0.20	-0.29	-0.24	0.77	-0.18	-0.49
24	-0.96	0.82	-0.56	0.53	0.25	0.10	-0.26	0.31	0.94	0.03	-0.68	0.84	0.37
25	-0.05	0.01	-0.17	0.47	-0.02	0.70	-0.14	-0.08	-0.41	-0.90	0.06	0.26	0.90
26	0.40	-0.71	-0.43	-0.64	-0.03	-0.42	-0.02	-0.71	-0.55	-0.75	-0.07	-0.86	-0.09
Bias	0.29	0.43	0.99	0.77	-0.95	0.43	-0.81	0.65	-0.91	0.29	0.31	0.39	-0.05

Table D-3: Hidden-output layer weight matrix for case study 1

i \ j	1	2
1	-0.75	0.51
2	0.57	0.36
3	-0.34	0.02
4	-0.71	-0.10
5	0.30	0.61
6	-0.76	0.30
7	0.35	-0.70
8	0.94	-0.78
9	-0.71	0.58
10	-0.69	-0.91
11	-0.93	0.25
12	0.87	-0.53
13	-0.76	0.30
14	-0.65	-0.50
15	-0.67	0.83
16	-0.09	-0.05
17	-0.53	0.78
18	0.53	-0.60
19	-0.47	0.68
20	-0.02	-0.19
21	-0.73	0.46
22	0.94	-0.87
23	-0.60	-0.63
24	-0.58	-0.42
25	0.58	0.12
26	0.10	0.22
Bias	-0.10	-0.84

Table D-4: Input-hidden layer weight matrix for case study 2

j \ i	1	2	3	4	5	6	7	8	9	Bias
1	-1.85	-1.19	0.27	1.27	-3.66	-1.10	1.96	3.31	-2.28	1.02
2	0.70	0.27	-2.18	3.34	-4.50	-4.00	-3.16	0.10	-4.68	0.95
3	3.29	3.78	2.49	1.90	13.36	-2.48	0.33	-0.11	-0.85	-0.88
4	3.16	1.36	-0.59	4.00	10.13	0.50	6.68	2.52	0.81	0.81
5	2.69	0.52	-2.14	4.45	-18.98	6.94	1.95	-1.80	0.24	-0.74
6	-5.92	-0.69	-2.36	4.91	4.66	-2.35	-0.11	1.09	5.44	-0.67
7	-0.43	2.36	1.87	-2.65	0.52	-4.06	-1.58	-1.32	4.45	0.60
8	-2.17	2.04	2.83	0.38	-0.86	2.39	0.16	0.71	-1.74	-0.53
9	1.45	5.93	-1.83	0.62	-3.30	-4.88	2.57	0.23	-5.88	0.46
10	6.98	3.10	4.32	-3.54	-0.78	-5.22	-2.07	0.09	-4.69	0.39
11	-1.25	0.12	1.13	-5.08	-5.25	6.16	0.15	-0.41	2.18	0.32
12	0.92	0.41	0.35	-2.02	3.57	-2.98	-3.18	-0.62	-3.90	-0.25
13	3.07	6.43	3.81	2.23	3.27	-6.11	0.33	-0.64	4.45	-0.18
14	4.51	-2.77	2.39	0.73	-1.58	4.05	6.00	1.19	2.83	0.11
15	-3.60	-0.81	-3.30	4.80	5.76	-4.74	-7.11	-2.20	-8.13	-0.04
16	-1.75	0.83	0.05	-1.38	2.11	0.69	-3.00	-1.57	-5.41	-0.04
17	3.48	-3.22	0.72	-3.78	-2.95	-0.01	-2.87	-3.20	-1.19	-0.11
18	-1.43	-4.63	0.25	-4.80	-0.35	-2.69	2.51	0.14	5.73	-0.18
19	-6.46	-4.69	0.81	4.89	-0.63	1.85	0.29	2.49	-2.19	0.25
20	1.90	-4.19	0.43	1.13	-5.53	1.58	0.53	-0.73	-4.07	0.32
21	-1.68	0.36	0.66	-1.47	-3.93	1.70	-18.57	-4.24	-23.46	0.39
22	-0.45	-3.52	-3.40	-0.79	-0.69	2.71	1.90	-0.84	3.77	-0.46
23	-6.45	-0.61	-0.64	0.06	-4.20	3.17	-1.54	0.47	-4.04	0.53
24	0.06	0.24	2.52	-3.16	-10.83	-0.70	-0.31	3.29	15.71	0.60
25	-5.60	3.59	0.03	2.94	2.03	-0.02	6.88	0.27	6.59	0.67
26	3.57	-1.20	-0.79	-0.45	1.25	6.94	-1.64	0.17	2.01	0.74
27	1.77	0.94	-0.66	1.98	-5.60	-8.69	-4.89	4.18	-1.76	0.81
28	-1.08	1.18	1.50	-4.49	0.71	-2.39	-4.67	0.11	-6.75	-0.88
29	-4.12	3.72	0.82	-0.98	-2.04	-1.30	0.96	-1.60	0.96	-0.95
30	2.28	-0.91	1.65	-1.11	-5.47	-1.87	1.38	-0.57	-0.79	1.02

Table D-5: Hidden-hidden layer weight matrix for case study 2

i \ j	1	2	3	4	5	6	7	8	9	10
1	-2.39	-3.58	-2.83	7.54	-3.53	1.68	-0.80	-0.66	4.20	-1.15
2	1.38	-0.79	0.70	1.45	3.73	0.57	-0.09	0.50	3.07	0.27
3	0.06	0.15	0.76	1.32	0.43	-0.10	-0.12	1.07	-1.47	-1.08
4	-0.18	-1.22	-1.08	-9.46	-5.28	2.32	1.68	3.53	3.40	-1.18
5	1.44	3.92	0.76	-0.61	0.72	2.45	-0.35	2.56	3.34	-2.30
6	1.23	1.14	0.43	1.65	0.86	-4.48	1.87	-0.43	3.74	1.25
7	-0.62	0.04	2.61	-3.15	0.69	-0.49	-4.20	-0.73	-0.91	1.11
8	2.65	2.13	2.07	0.44	-0.90	-0.98	4.80	-1.06	-0.71	-1.35
9	0.66	2.85	0.39	3.28	0.36	-3.79	-5.04	2.64	-0.05	0.91
10	-1.89	-1.61	1.83	-0.43	1.79	0.54	0.01	0.49	1.13	-0.11
11	-0.71	2.35	-1.15	-0.71	-1.00	-4.46	1.91	5.06	5.35	1.17
12	-2.18	-0.55	-2.26	1.85	0.27	-2.96	-1.41	-0.56	3.49	4.96
13	-0.38	-2.02	-0.83	1.13	7.63	8.00	8.12	-0.49	1.32	0.81
14	-0.46	1.87	0.65	-0.28	1.46	-0.46	-1.47	2.95	1.25	-3.37
15	-0.66	-0.60	1.09	1.71	-0.93	-2.42	1.51	-1.37	3.97	-0.72
16	1.73	-0.01	-0.21	3.43	0.35	1.34	1.69	-3.97	3.69	0.22
17	-0.84	0.87	1.15	-3.86	-1.28	-3.75	0.75	-0.64	1.57	-1.01
18	0.13	-2.09	-3.24	-1.69	-0.42	1.83	-0.19	-2.75	1.28	0.23
19	0.18	-0.39	1.73	1.51	2.10	-2.26	-0.07	-3.26	1.47	2.77
20	1.06	2.09	1.31	2.58	3.50	0.32	-0.48	1.74	2.94	-2.76
21	0.63	1.69	1.02	1.42	-6.18	-0.77	-2.56	3.40	4.86	-2.03
22	-0.64	-0.85	-0.13	-5.86	-3.02	2.46	-0.95	-0.16	1.99	-0.58
23	0.77	0.62	2.07	1.83	-0.28	4.84	-0.42	-0.10	-0.33	0.54
24	1.82	-0.08	0.19	-0.08	-0.09	-5.00	-1.47	-0.46	0.62	-1.41
25	0.19	1.00	2.63	-1.06	1.23	-3.38	1.46	-1.59	1.59	1.12
26	-5.07	-1.88	3.40	-2.09	-2.93	4.87	-1.45	-2.19	-3.89	-3.04
27	0.68	-1.69	-4.23	-2.65	1.77	1.93	2.07	2.32	-5.62	5.52
28	1.70	1.86	6.89	-9.09	-5.94	0.00	-1.11	0.87	8.80	5.38
29	-0.84	1.37	-1.84	-1.40	-0.26	0.50	-0.86	-4.85	-1.80	0.07
30	-1.99	1.05	-1.72	-0.27	4.06	-3.91	5.49	1.11	0.25	0.50
Bias	-0.58	-0.41	0.28	-0.31	-0.07	-0.34	0.20	-0.29	0.13	-1.46

Table D-5 continued

i \ j	11	12	13	14	15	16	17	18	19	20
1	0.52	2.86	-5.15	1.11	2.65	-0.20	-1.54	-4.07	-0.93	-1.72
2	1.32	-0.75	0.49	1.27	-3.09	1.07	1.57	-1.32	-2.18	-2.89
3	0.11	0.33	0.47	-0.41	-0.03	-0.03	0.53	1.21	1.39	0.95
4	3.82	1.87	6.32	1.05	1.44	0.83	4.35	0.80	-2.31	1.74
5	-6.39	-1.68	3.71	-2.62	0.39	-1.33	1.69	-1.26	-2.62	0.98
6	-0.17	1.55	1.59	-2.83	0.45	-3.74	-1.45	0.24	-0.66	1.95
7	2.27	-1.60	-2.39	0.07	2.93	-0.03	-1.73	-1.20	1.78	3.95
8	0.06	-4.10	1.57	-0.96	2.70	-0.61	-1.96	-8.59	1.04	2.63
9	0.58	0.06	6.81	-1.68	-0.41	1.62	-3.13	2.09	-0.34	2.81
10	2.16	1.30	-4.88	1.32	0.50	-0.31	-1.27	0.73	1.08	5.28
11	-1.83	2.51	-1.02	-2.87	0.91	-4.48	-1.58	6.33	0.75	-2.91
12	1.84	1.03	-1.21	2.85	-2.49	-2.83	2.51	3.57	2.09	-1.23
13	4.67	-9.38	0.72	-1.45	3.70	-5.77	-5.95	1.16	5.38	-1.10
14	0.42	0.50	3.15	-0.56	-0.72	2.27	0.29	-0.87	-3.24	-0.36
15	-0.31	-0.78	0.99	-0.65	1.90	-0.93	0.71	2.15	2.96	-0.49
16	-0.74	-0.63	-3.23	3.07	-0.99	0.32	1.77	3.62	2.65	1.40
17	-6.49	0.93	-1.46	0.59	2.79	3.80	-2.22	-0.64	5.51	-0.73
18	0.54	2.21	-1.82	1.86	-1.01	1.71	0.75	1.48	0.02	-0.19
19	0.79	1.01	-0.92	-3.62	-0.33	-0.67	-0.94	0.26	0.11	0.89
20	-2.01	-2.23	-4.16	-1.65	-6.01	1.21	-0.73	-1.74	-2.70	-0.18
21	3.68	-3.34	4.22	-3.19	-1.69	0.40	-0.46	2.18	-0.20	-2.28
22	-0.79	2.60	2.49	2.10	0.25	-2.45	0.30	0.50	-1.48	-1.94
23	-4.28	1.71	2.41	5.62	1.22	0.28	-1.72	-0.73	0.76	-4.85
24	-2.67	1.74	-3.82	1.20	0.53	2.97	2.82	-1.34	-1.10	1.07
25	-1.63	-0.84	-1.41	-0.32	0.97	1.18	-1.97	3.31	-2.79	1.45
26	-1.54	1.32	1.23	-0.86	0.15	4.68	3.96	2.67	-2.62	1.07
27	-2.16	-7.07	-2.97	0.99	1.09	0.93	1.84	-2.90	0.79	3.80
28	15.45	9.01	-3.86	6.76	-6.08	-7.88	-3.55	-0.98	-0.70	1.51
29	1.13	3.84	2.34	2.58	0.63	2.71	-0.10	-3.46	1.24	-2.03
30	-0.08	2.46	-2.89	2.44	1.07	-4.44	-0.78	2.05	1.98	-1.28
Bias	-0.89	0.21	0.82	0.16	0.01	0.99	-0.33	-0.37	-0.48	0.45

Table D-5 continued

i \ j	21	22	23	24	25	26	27	28	29	30
1	-2.41	-2.78	-0.74	-1.77	2.01	-0.21	-0.65	-1.23	1.73	-3.08
2	-1.97	-1.81	1.94	0.64	-2.19	4.49	-1.73	1.35	-1.69	-1.00
3	0.74	1.02	0.89	0.16	1.12	1.29	0.15	0.48	1.59	-0.06
4	-1.97	3.15	-3.25	-1.91	3.38	-0.62	3.00	-8.31	0.81	-1.98
5	1.98	-2.45	-0.04	-1.02	0.13	4.24	2.42	2.54	-3.12	0.85
6	-0.28	-1.36	-0.96	1.17	2.01	-0.14	-2.09	-3.47	-0.56	-1.72
7	-1.63	5.61	2.59	-0.98	-0.60	-5.07	0.93	-4.30	-0.90	-1.00
8	1.93	-1.27	-1.43	-1.12	-1.05	2.06	-0.67	1.18	-0.91	2.36
9	0.37	-2.62	-6.30	-2.04	0.47	-4.82	0.56	-0.59	0.40	0.15
10	0.61	-0.87	-4.08	1.18	0.92	4.36	1.56	1.05	-2.74	-0.48
11	3.22	-1.43	-2.62	-0.56	2.14	-3.00	1.88	-1.94	-0.16	2.30
12	-1.31	2.09	-2.54	0.49	-1.45	-1.08	-1.67	-2.17	-1.95	0.16
13	-15.40	-6.77	1.84	1.50	-2.24	0.97	2.90	-7.40	4.16	-1.32
14	2.74	3.07	-1.60	1.12	1.83	-0.26	-0.41	-0.99	-0.53	-1.61
15	2.82	-2.51	-0.11	1.84	0.33	0.01	-1.47	-6.49	-0.12	-2.42
16	-3.08	-0.39	-1.49	-0.16	1.04	-3.49	-2.24	0.68	3.81	-2.13
17	0.14	-0.30	1.77	-2.35	-0.64	0.27	-0.20	0.42	2.21	1.96
18	-0.34	1.45	1.54	2.75	-1.32	-1.54	0.51	-2.01	-0.42	0.35
19	1.87	2.76	-2.59	1.31	0.04	2.89	-0.85	3.49	-0.39	2.19
20	-3.17	3.34	2.81	1.43	5.49	-0.61	0.92	1.63	-1.43	-1.57
21	2.47	-0.20	-2.27	-1.09	3.79	-3.14	2.81	6.82	-4.68	0.13
22	-0.70	-1.41	-0.71	0.01	-0.42	5.42	-1.96	-2.63	1.58	1.90
23	0.96	4.53	-1.54	-1.41	-0.34	4.16	-2.03	-1.05	-1.55	-0.66
24	0.88	-1.14	1.39	0.04	0.59	-0.58	4.03	-0.28	-0.63	3.65
25	-5.65	-3.14	1.41	-0.29	3.91	-2.38	0.69	1.62	7.43	-1.60
26	-0.03	2.81	-2.27	-1.59	-1.47	-0.03	4.37	-0.04	0.47	-0.76
27	5.27	-2.84	-7.45	-0.57	-0.40	-1.04	1.57	1.21	5.63	1.53
28	6.96	2.20	1.75	-11.83	-5.65	-6.09	7.02	-1.42	3.10	1.18
29	1.07	-0.05	-0.05	-0.95	1.54	0.74	1.39	0.90	-1.09	-1.30
30	1.84	-1.51	-2.50	-0.95	-1.91	-3.43	3.02	-2.50	2.49	-2.33
Bias	-0.10	-0.02	-0.89	-0.84	-0.47	-0.15	2.05	0.37	-0.22	0.34

Table D-6: Hidden-output layer weight matrix for case study 2

i \ j	1	2
1	-0.01	0.23
2	0.26	0.01
3	4.11	3.19
4	-4.47	0.20
5	0.31	-0.06
6	-0.35	0.18
7	0.19	-0.10
8	0.36	0.11
9	0.22	-0.03
10	0.32	-0.23
11	0.38	-0.41
12	0.33	-0.08
13	0.01	-9.27
14	2.07	-1.00
15	-1.34	1.90
16	0.03	-0.25
17	0.01	0.12
18	-0.07	0.83
19	-0.25	0.14
20	-7.13	0.17
21	-0.03	0.42
22	0.22	0.02
23	-0.20	0.28
24	-0.05	0.01
25	0.38	-0.02
26	-7.29	0.04
27	0.06	0.20
28	0.00	-9.21
29	2.36	-0.24
30	-0.25	0.13
Bias	-1.03	-0.84

Appendix E: RK-Aspen parameters

The Antoine Equation can be used to determine vapour pressure at specific temperatures for various pure components:

$$\log_{10}(P_{vap}) = A - \frac{B}{T + C}$$

where P_{vap} is the vapour pressure, T is the temperature and A, C and C is the Antoine Equation Parameters, as listed in Table D-1:

Table E-1: Antoine parameters of pure components of different hydrocarbons

Compound	Temperature Range (K)	A	B	C	Reference
Pentane	268.8-341.37	3.9892	1070.617	-40.454	Osborn & Douslin (1974)
Decane	367.63 - 448.27	4.07857	1501.268	-78.67	Williamham et al. (1945)
Hexadecane	463.20 - 559.9	4.17312	1845.672	-117.054	Camin et al. (1954)
n-Butanol	295.8 - 391.0	4.54607	1351.555	-93.34	Kemme & Kreps (1969)
n-Octanol	293. - 353.	6.47682	2603.359	-48.799	Geiseler et al. (1966)
n-Dodecanol	376.54 - 437.61	4.84691	2057.697	-105.421	Ambrose et al. (1974)
Decanoic acid	426.0 - 460.3	2.4645	733.581	-256.708	Kahlbaum (1894)
Tetradecanoic acid	385.03 - 465.1	1.44788	685.976	-262.3	Hammer & Lydersen (1957)

Table D-2 lists η_m (with the same order of magnitude as found by Lombard (2015)) and the binary interaction parameters ($k^0_{a,mn}$ and $k^0_{b,mn}$) for binary systems containing CO_2 and a specific hydrocarbon, as obtained using Aspen Plus.

Table E-2: Polar factors for pure components and binary interaction parameters for different hydrocarbons

Compound	**Temperature (K)**	η_m	$k^0_{a,mn}$	$k^0_{b,mn}$	**Residual root mean square error (%)**
Pentane	311	0.1024	0.1344	-0.00476	23.51
Decane	344	0.0497	0.1015	-0.02771	19.51
Hexadecane	314	0.0233	0.085	-0.07291	133.7
n-Butanol	354	-0.2572	0.0692	-0.0281	22.62
n-Octanol	328	-0.443	0.0763	-0.05099	159.79
n-Dodecanol	393	-0.1744	-1.3589	-2.8313	580.82
Decanoic acid	393	-0.3383	0.0429	0.03114	88.27
Tetradecanoic acid	393	-0.2088	0.0645	-0.01511	111.24

It should be noted that $k^1_{a,mn}$ and $k^1_{b,mn}$ can also be regressed to obtain better results, as discussed in Section 2.1.4. Since the RK Aspen model is only used to compare the results of the ANN models, only $k^0_{a,mn}$ and $k^0_{b,mn}$ will be regressed.